TECHNISCHE UNIVERSITÄT MÜNCHEN

Lehrstuhl für Ökologische Chemie und Umweltanalytik

Unravelling the interactions of Boron with natural organic matter (NOM) on a molecular level

András Gáspár

Vollständiger Abdruck der von der Fakultät Wissenschaftszentrum Weihenstephan für Ernährung, Landnutzung und Umwelt der Technischen Universität München zur Erlangung des akademischen Grades eines

Doktors der Naturwissenschaften

genehmigten Dissertation.

Vorsitzender: Univ.-Prof. Dr. W. Huber

Prüfer der Dissertation:

1. Priv.-Doz. Dr. Dr. Ph. Schmitt-Kopplin
2. Univ.-Prof. Dr. Dr. h. c. H. Parlar
3. Univ.-Prof. Dr. I. Kögel-Knabner

Die Dissertation wurde am 22.07.2008 bei der Technischen Universität München eingereicht und durch die Fakultät Wissenschaftszentrum Weihenstephan für Ernährung, Landnutzung und Umwelt am 24.11.2008 angenommen.

To my beloved grandparents...

Acknowledgements

First of all I gratefully acknowledge Philippe Schmitt-Kopplin for his extraordinary enthusiasm that encouraged me all along my study, from the odd interview till the mind-boggling final touch.

I am also grateful to my nearest and dearest colleagues of "room 25" for their friendship, help, and discussion throughout the study.

I also wish to thank my colleagues of "BioGeoAnalysts" for providing an exceptionally pleasant and productive working atmosphere.

Special thanks are due to Agnes, who willingly shared her local expertise and greatly assisted in all matters.

The author gratefully acknowledges the

-German-Israeli Foundation for Scientific Research and Development (GIF) for financial support of this work. GIF Research Grant Agreement No. G-798-175.8/2003

-Deutsche Akademische Austauschdienst (DAAD) for travel support. No. D/06/29417

The dissertation was prepared from May, 1st 2005 to July 31st 2008 at the Institute of Ecological Chemistry at the Helmholtz Zentrum München National Research Center for Environment and Health in the Helmholtz Association in Neuherberg.

Publications

Articles

[I] A. Gaspar, M. Englmann, A. Fekete, M. Harir and Ph. Schmitt-Kopplin. *Trends in Capillary Electrophoresis-Mass Spectrometry 2005 - 2006. Review* Electrophoresis. 29, 66-79, 2008 (presented in the Introduction)

[II] A. Gaspar, M. Harir, M. Lucio, Ph. Schmitt-Kopplin. *Preparative Free-flow electrophoretic separation and off-line ESI-FTICR/MS analysis of Suwannee River Fulvic Acid.* Electrophoresis *(submitted)* (presented in Chapter 2.1.)

[III] A. Gaspar, E. V. Kunenkov, R. Lock, M. Desor, I. Perminova, Ph. Schmitt-Kopplin. *Combined utilization of Ion Mobility- and ultra high resolution-MS to identify multiply charged constituents in natural organic matter.* Rapid Communication in Mass Spectrometry (accepted) (presented in Chapter 2.3.)

[IV] A. Gaspar, M. Harir, M. Lucio, Ph. Schmitt-Kopplin. *Targeted borate complex formation as followed with electrospray Fourier transform ion cyclotron mass spectrometry: monomolecular model system and polyborate formation.* Rapid Communication in Mass Spectrometry 22, 3119-3129, 2008 (presented in Chapter 4.2.)

[V] A. Gaspar, M. Lucio, M. Harir, Ph. Schmitt-Kopplin. *Targeted and non-targeted borate complex formation as followed with electrospray Fourier transform ion cyclotron mass spectrometry: Novel approach for identifying borate complexes with natural organic matter* Analytical Chemistry (under revision*)* (presented in Chapter 4.3.)

M. Harir, M. Frommberger, **A. Gaspar**, D. Martens, A. Kettrup, M. El Azzouzi, Ph. Schmitt-Kopplin. *Characterization of imazamox degradation by-products by using liquid chromatography mass spectrometry and high-resolution Fourier transform ion cyclotron resonance mass spectrometry*. Anal. Bioanal. Chem. 389, 1459-1467 (2007)

M. Harir, **A. Gaspar**, M. Frommberger, M. Lucio, D. Martens, A. Kettrup, M. El Azzouzi, Ph. Schmitt-Kopplin. *Photolysis pathway of Imazapic in aqueous solution: ultrahigh resolution mass spectrometry analysis of intermediates*. J. Agric. Food. Chem. 55(24), 9936-9943 (2007)

M. Harir, **A. Gaspar**, M. Frommberger, D. Martens, A. Kettrup, M. El Azzouzi, Ph. Schmitt-Kopplin. *Photocatalytic reactions of imazamox at TiO2, H2O2 and TiO2/H2O2 in water interfaces: Kinetic and photoproducts study*. Appl. Catal. B-Environ. (in press)

Book Chapters

[VI] I. Perminova, **A. Gaspar**, N. Hertkorn, Ph. Schmitt-Kopplin. *Separation techniques as powerful tools for unfolding molecular complexity of natural organic matter and humic substance.* Biophysico-Chemical processes in environmental systems, IUPAC Series (accepted) (presented in the Introduction)

Posters and presentations

A. Gaspar, E.Kunenkov, R. Lock, M. Desor, I. Perminova, Ph. Schmitt-Kopplin: *Multiple charged constituents in Suwannee river natural organic matter,* 14th IHSS Conference, Sept. 15 - 19, 2008, Moscow (Presentation)

A. Gaspar, E.Kunenkov, R. Lock, M. Desor, I. Perminova, Ph. Schmitt-Kopplin: *Evidences of the existence of multiple charged constituents in Suwannee river dissolved organic matter,* 56th ASMS Conference, June 1 - 5, 2008 in Denver (Poster)

Kovács K., Sajgó Cs., Brukner-Wein A., Kárpáti Z., **Gáspár A.**, Tombácz E., Schmitt-Kopplin Ph.: *Preliminary results on molecular characterization of humic substances from thermal waters as an unexplored biogeosystem*, P32. 9th Conference on Colloid Chemistry (9CCC), October 3-5. 2007. Siofok, Hungary, Book of Abstracts p. 120 (Poster)

A. Gaspar, E. Belyaeva, M. Meuller, I. V. Perminova, F. Frimmel, M. Frommberger, N. Hertkorn, Ph. Schmitt-Kopplin: *Analysis of Suwannee river fulvic acid with ESI-ICR/FTMS after fractionation with free-flow electrophoresis and size exclusion chromatography*, First International Symposium on Ultrahigh Resolution Mass Spectrometry for the Molecular Level Analysis of Complex(BioGeo)Systems, 6-7 November, 2006, Neuherberg, Germany (Poster)

E. V. Kunenkov, A. S. Kononikhin, **A. Gaspar**, Ph. Schmitt-Kopplin, I. V. Perminova, A. V. Garmash, N. Hertkorn, I. A. Popov, E. N. Nikolaev: C*omparison of FTICR Data on the Suwannee river humic and fulvic acid*, First International Symposium on Ultrahigh Resolution Mass Spectrometry for the Molecular Level Analysis of Complex(BioGeo)Systems, 6-7 November, 2006, Neuherberg, Germany (Poster)

A. Gaspar, J. Junkers, Ph. Schmitt-Kopplin, N. Hertkorn: *ESI ICR FTMS and NMR analysis of Free-Flow Electrophoresis fractions of Suwannee river NOM*, 17th International Mass Spectrometry Conference, 27 Aug.- 1 Sept., 2006, Prague, Czech Republic (Poster)

A. Gaspar, M. Frommberger, J. Junkers, Ph. Schmitt-Kopplin, N. Hertkorn; *Molecular-level analysis of Suwannee river NOM derived from organic structural spectroscopy and fractionation studies*, 3rd Symposium on NMR spectroscopy in soil and geo sciences, 6-9 August, 2006 Freising, Germany, (Poster)

Abstract

Boron, known as micronutrient, is necessary for full-functionality of plants. B plays an important role in cell development, elongation and structural integrity of plant cell walls. However this type of role only favourable, if the available boron concentration in soil does not exceed the maximal tolerable level. If the concentration in the surrounded soil either exceeds or does not reach the well defined narrow band of the B level can result many types of malfunction.

Higher concentration of Boron might be discharged either from natural or anthropogenic sources. Beside the rare volcanic activities, the usage of seawaters, with the elevated B content, represent a common threat for plantation in arid countries, where water sources are limited. Unfortunately the elimination of B during the desalination process is rather challenging than plausible. Further problem is a continuous discharge of elevated B content from industrial and domestic processed water sources. These general sources might increase the level of B in soil and produce a toxic environment for the vegetation.

If natural organic matter is considered as inexhaustible and exploitable material that might and adsorb Boron, than the generally existing low cost-effective adsorbents could be replaced. For instance cheap composted materials with significant organic matter content, could be a possibility.

However the first step to find a proper organic matter, and beside the adsorption behaviour, is to understand on molecular level the mechanism of boron complexation with such a complex material. And based on the obtained results, the expected properties, that might preferentially favourable for B complexation, could be exploited by the screening of the adequate NOM.

Therefore in this thesis different type of analytical approaches were tested and introduced, either alone or in combination. Since the potentially applicable organic matters denote such a complexity, it was necessary to pay attention and describe the NOM constituents in detail. Since the complexity of these materials often hinders the analysis of a complex array of structures, prior, an electrophoretic separation was introduced. The application of such separation, is originated from the generally observed attribute of B complexation mechanism. B and its forms are tend to complex with hydroxyl and carboxyl groups in adequate forms and positions. And whilst electrophoretic separation is capable, to separate constituents based on functional groups, that are in negative operation modus, within these materials are mainly hydroxyl and carboxyl groups. Beside the expected separation

phenomena, further benefit was also experienced. Due to the separated constituents a wider range of constituents were revealed under the analysis, extending the number of the visualized molecules that were limited by the analytical method itself.

As a next step based on the gained information about the potential binding sites and their abundances and former B-complex identification via capillary electrophoresis, a reverse approach was tried, as a possible fast and descriptive method to characterize the B binding capacity of different NOMs with different origins. Polymers with immobilized Boronic acid on their surfaces were utilized in order to enable a fast and in a first step a qualitative method to differentiate between boron affinity of the different organic matters. However, by closer examination of the B-complex detection methodology, the obtained responses were difficult to interpret, hence capillary electrophoresis as a detection method was replaced with a direct and more informative detection method, namely mass spectrometry.

FT-ICR/MS with its mass accuracy and ultra high resolution enabled to identify dozens of complexes in a single run, however the observed number and abundances of the complexes were greatly depended from the instrumental and experimental settings. Nevertheless the utilization of such a mass accuracy and resolution enabled to identify and assign molecular formulae of B complexes in batch experiments. Not only with model compounds and in designed experiments, but also with natural organic matter were tested successfully. Based on the observed regularity by model compounds and B, which were derived from the properties of the B complex formation, general rules were set up to follow and assign complexes among thousands of constituents. With the developed search tool boron complexation tendencies could be revealed among the analyzed organic matters and therefore effective candidates with potential B retention can be assigned. The observed molecules and their position in van Krevelen plot are in good agreement with the gained results, derived from the polymer utilization. This search engine in combination with FT/MS might help in the near future to select and advise potential organic matter or even organic matter containing material that will be used for boron elimination from irrigation water not only in laboratory scale.

List of figures

List of tables

Abbreviations

AAS	Atomic Absorption Spectrometry
AEM	Average Electrophoretic Mobility
AES	Atomic Emission Spectrometry
AI	Aromaticity Index
APPI	Atmospheric Pressure PhotoIonization
ATP	Adenosine TriPhosphate
B	Boron
^{13}C-DEPT NMR	Carbon Distorionless Enhancement by polarization transfer
CE	Capillary Electrophoresis
CGE	Capillary Gel Electrophoresis
CID	Collision Induced Dissociation
CIEF	Capillary Isoelectric Focusing
CPMAS	Cross Polarization Magic Angle Spinning
CZE	Capillary Zone Electrophoresis
DAD	Diode Array Detector
DNA	DezoxyriboNucleic Acid
DOC	Dissolved Organic Carbon
DOM	Dissolved Organic Matter
EOF	ElectroOsmoticFlow
ESI-MS	Electrospray Ionization Mass Spectrometry
FA	Fulvic Acid
FFE	Free-Flow Electrophoresis
FT-ICR/MS	Fourier Transform Ion Cyclotron Resonance Mass Spectrometry
HA	Humic Acid
HP-IMAC	High Pressure Immobilized Metal Affinity Chromatography
HPLC	High Pressure Liquid Chromatography
HPSEC	High Performance Size Exclusion Chromatography
HS	Humic Substances
ICP-MS	Inductively Coupled Plasma Mass Spectrometry
IEF	Isoelectric Focusing
IR	Infra-Red Spectroscopy

KM	Kendrick Mass
KMD	Kendrick Mass Defect
MALDI	Matrix-assisted Laser Desorption/Ionization
MF	MicroFiltration
NACE	Non-Aqueous Capillary Electrophoresis
NADPH	Nicotinamide Adenine Dinucleotide Phosphate
NMR	Nuclear Magnetic Resonance
NOM	Natural Organic Matter
NTIMS	Negative Thermal Ionization Mass Spectrometry
PAGE	PolyAcrilamide Gel Electrophoresis
PCA	Principal Compound Analysis
pyrGC/MS	Pyrolisis Gas Chromatography Mass Spectrometry
Qq TOF	Quadrupole Time-Of-Flight Mass Spectrometry
Q-TOF IM/MS	Quadrupole Time-Of-Flight Ion-Mobility Mass Spectrometry
RNA	Ribonucleic Acid
RO	Reverse Osmosis
RP-HPLC	Reverse Phase High Pressure Liquid Chromatography
SDS	Sodium Dodecil Sulphate
SEC	Size Exclusion Chromatography
SRFA	Suwannee River Fulvic Acid
SRHA	Suwannee River Humic Acid
SRNOM	Suwannee River Natural Organic Matter
TIMS	Thermal Ionization Mass Spectrometry
TSP-MS	Thermal Spray Mass Spectrometry
UDOM	Ultrafiltered Dissolved Organic Matter
UF	Ultrafiltration
UV-VIS	Ultra-Violet Visible Spectroscopy

Table of contents

1. Introduction

Boron is an essential micronutrient for plants and its role is only favourable if its concentration in soils is within the tolerable levels. In arid and semi-arid countries, where water sources are limited, water desalination from oceans and seawater are often the rule and the main source of water for human consumption and agriculture. Even though high-end instrumentations (membranes) are utilized, boron concentration in irrigation water from seawater easily may exceed the tolerable limit for vegetation. Moreover if desalinated water is continuously used for irrigation, the boron concentration might increase in the soil, resulting a mobile boron fraction that is easily accessible for plant and may create toxicity.

Beside natural sources, anthropogenic impacts also contribute to contamination and to negative effects. Processed and unprocessed domestic and industrial water releases, might also the extreme suppliers of B in environment. Frequently used detergents as a good example, can contain up to 6000ppm of B and with this rewarded the "main threat" title. Without B-specific cleaning processes in waste water treatment plants these sources could be introduced into natural flows, and soils without any further decrease. If this reprocessed water also used for irrigation, similar toxicity problems arise.

Over the last two decades B-specific resins were developed to overcome this problem, however the operation (regeneration, etc.) of these are rather money and time consuming; cost effective alternatives are highly preferable.

Natural organic matter (NOM) known as an effective buffer against any chemical extremes, that is due to its various high affinity and binding capacity to a wide range of organic and inorganic compounds. Beside its prosperous complexity, natural organic matter is presented in “geo-systems” in such an enormous amount, that could make its applications more than cost effective. Additionally, Boron adsorption studies on different soil constituents (minerals, organic matter), has been already extensively investigated and modelled. These facts support the idea to apply natural organic matter for Boron removal. However to unravel the chemical composition and structures involved in interactions still remains a challenging task for analytical chemists.

Since the ultimate goal would be to highlight the potentials of a NOM based boron elimination, Hence in this dissertation the main focus was to set up a proper molecular-level characterization of boron complexation with organic matter and find a rather straightforward

way to identify complexes. In order to describe the boron retention properties of the selected organic matters, since those abundances might indicate the affinity properties of the selected organic matter. Nevertheless, the complexation mechanism is only described fully if reactions partners and their molecular-level properties are also fully detailed. Therefore boron and its various forms and a selected organic matter were investigated separately. To reach this goal, different way of realization could be emphasize, although with hopefully similar results.

In this study, mainly three possible approaches were involved (Figure 1). Initially a reverse method with utilization of commercially available immobilized Boronic acid functionalized polymers was tested, as a simple B affinity separation in combination with CZE detection. Than an up-scale electrophoretic method (FFE) was used in order to gain sizable fractions that B- binding properties of them could be analyzed in detail. And as a one-step method FT/MS technology was introduced. However these three main paths were extended with several side studies, like the description of polyborate formation, these contribute elementally to the complete view.

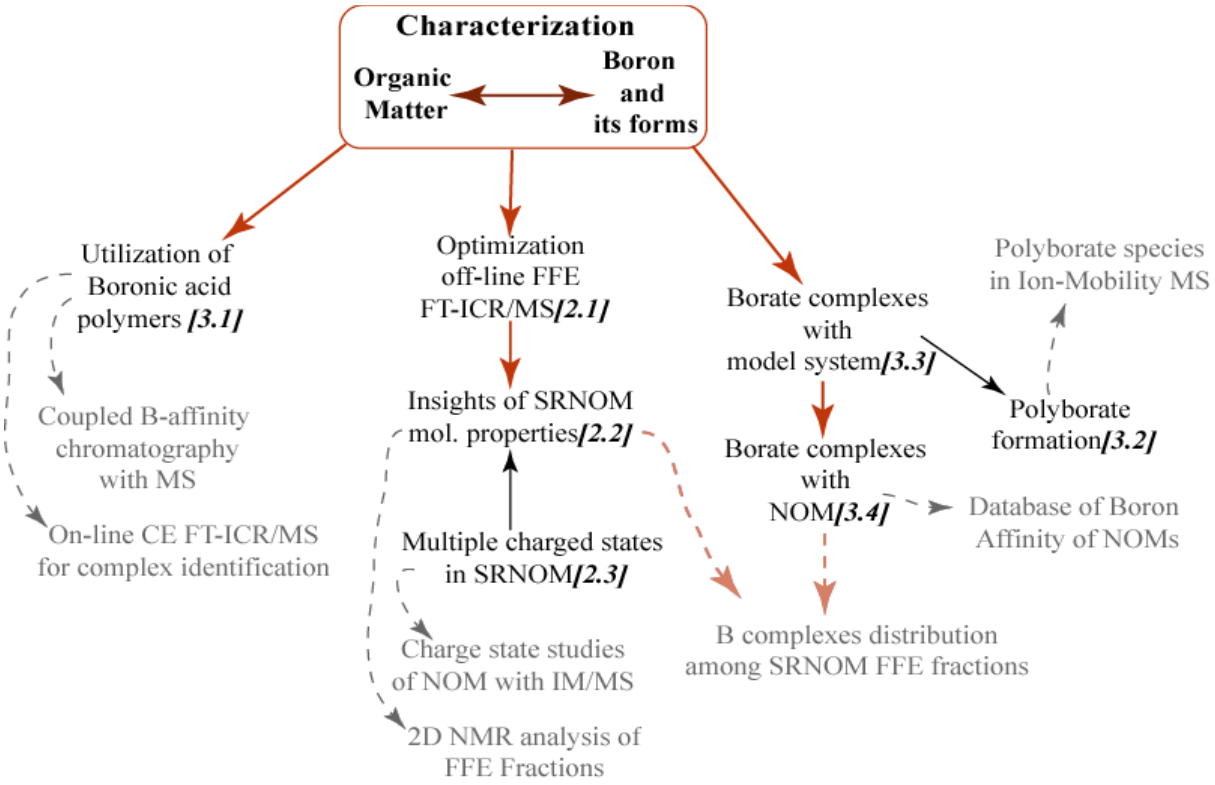

Figure 1: Proposed work-flow for the study of Boron complexation with natural organic matter. Beside the achieved parts (black), the potential future works were also marked (grey) The numbers in brackets sign the different chapters in the thesis.

1.1. Boron in the environment

With the possible exception of carbon, B has the most interesting and diverse chemistry of any element. Much of this interest arises from the electron deficiency of many of its compounds. This is due to the fact that boron possesses only three valence of electrons which, when incorporated in three bond pairs, leave a p-orbital unfilled in the valence shell. This type of bonding is particularly common in boranes, that play an important role in synthetic organic chemistry[1]. In spite of its importance, boron is not an abundant element and in the environment, as an ubiquitous element, always found covalently bound to oxygen.

Because of its property, boron is mobile and susceptible to fractionation in earth processes, as depicted in the boron cycle[2]. The distribution of boron can be segmented into the main principal earth reservoirs: the hydrosphere, essentially the oceans, the outer crust or lithosphere and the inner mantle. These reservoirs distribute only low concentration of borates (borax, ulexite, kernite, colemanite), high concentration exploitable ores are only rarely found (United States, Turkey and South America). In rocks B-concentration average about 10-20 mg B/kg. In sea water it can range from ca. 1-10 mg B/kg, while its concentration in fresh waters is 350 times lower. The oceans are the largest global reservoirs for boron, and in many studies have been shown that the boron concentration in the ocean has been constant for the last 10 million year. Most soils have low B content (<10mg/kg) but higher B content (10-100mg/kg) soils are usually associated with recent volcanic activities[3].

Boron is an essential micronutrient for organisms. Usually only soluble B is available to plants and this is usually lower than 10 % of the total soil B content. B availability is controlled by the interactions with the soil carbonates and oxides/hydrous oxides of Fe and Al. The B level in animal tissue averages ca. 0.3 mg B/ kg on dry weight basis[4] and this concentration vary with the boron concentration of the water supply. The B containing of plants mainly refers to their structural component in their cell wall[5,6]. Boron may be of importance form maintaining the structural integrity of plasma cell membranes. This function is likely related to stabilization of cell membranes by boron association with some membrane constituents. The initial proof of the essentiality of B in plants was published by Warrington[7], however the possible interactions with biomolecules remain largely unknown. Recent research on the complexation, isolation and characterisation of B complexes with polysaccharides and other diol containing molecules are outlined in Power et al[8]. Furthermore B plays a key role in development, cell elongation and structural integrity of dicotyledonous plant cell walls. The presence and distribution of boron-containing

compounds in vascular plants, marine algal species and microorganism was recently reviewed by Dembitsky et al[9]. Different enzymes of plants microorganisms, animals and humans could react with boron compounds resulting in stimulation, stabilization and/or inhibition. In case of inhibition, boron compounds frequently occupy the active site of the enzymes.

As an essential micronutrient its deficiency could cause also rapid inhibition of plant growth, releasing the inhibition of 6-phosphogluconate- and of glucose-6-phosphate dehydrogenases, resulting in increased phenols production[10,11]. B deficiency causes impaired membrane function as its primary effect. Symptoms of deficiency such as auxin and phenol built-up, as well as increased RNAase activity are secondary manifestation of the reduced ability of membranes to transport vital nutrients and metabolites. Further membrane functionalities like phosphate transport, where B is stated as important regulator, ATPase and NAD(P)H-dependent redox systems, were significantly reduced or inhibited with lower than sufficient B concentration.

The positive effect for normal plant growing is maintained only if the B concentration in the soil solution is maintained in a relatively narrow range[12,13].

Beside the natural and continuous discharge of B, through biogeochemical processes, from its natural reservoirs, the total anthropogenic mobilization is approximately 1.5 times higher than the total mobilized amount from the Earth's crust by rock weathering. However products like glass, fibreglass or ceramics are depicted as artificial deposits, but laundry bleaches, fire retardants, agricultural fertilizers, industrial and domestic discharges become abundant source of B[3].

If B is not sufficiently removed from wastewater during the common treatment methods, it may become toxic[13]. B accumulation occurs both naturally and through artificial means such as irrigation. Boron concentration in seawater averages 4.5 mg/liter and is slightly higher in the Mediterranean Sea. At these concentrations, B does not constitute a threat to human health but is highly toxic to many crops. Boron in neutral and acidic environments readily passes through the RO membranes. Without additional treatment, B in Mediterranean seawater after RO will reach 2 mg/liter, which is toxic for all but the most tolerant crops. Toxicity symptoms in orchards were observed after irrigation with effluent originating from desalinated municipal water in Eilat with ~1.2 mg/L B produced. Concentrations of 2 mg/liter B in irrigation water also caused reductions in yields in peanuts and tomatoes in the Negev region [14].

About five million ha of soils containing greater than 15 mg/kg B, above the threshold for normal plant growth, exist in southern Australia, corresponding to 30% of the region[1]. Up to 17% of the barley yield loss in this area was estimated to be caused by B toxicity. B toxicity in grapevine, with defined toxicity symptoms and evaluate growth, production, and B accumulation, was presented by Yermiyahu et al. [15]. The effect of excess B on grapevines (Vitis vinifera L. cv. Sugraone) was evaluated in a 4-year study in Israel's Jordan Valley. Vines were monitored for growth, yield, and B accumulation. Boron accumulation in leaves correlated with B toxicity symptoms that materialized as chlorosis and necrosis of leaves beginning at their margins, reduced leaf size, and reduced internodal distance between adjacent leaves. Boron accumulated in grapevine leaves linearly as a function of increased B in irrigation solution with time and with age of leaves. Both deficient and toxic levels of B can occur during a single growing season, since the range between toxic and deficient soil solution concentrations of B is smaller than any other nutrient element. Therefore and for many other examples, B became a major concern in arid lands, where the reuse of water is essential. Further notable problem in these countries, that during the desalination process, the utilized technologies, for instances membranes, are not able to retain boron, which might also increase the level of boron concentration in soils, if this water was used for irrigation.

To eliminate boron, specific resins were developed and applied however these are tend to be low cost-effective[16-18]. Therefore assign and characterize effective and cost-effective sorbents, such as organic rich organic humified matter (composts, peats) which denote similar boron specific retention, is necessary. In order to describe the properties and possible boron removal using such organic materials, the understanding of the B complex formation on a molecular level is on high demand[19].

[1] www.dwlbc. sa.gov.au/land/topics/rootzone/boron.html

1.2. Analytical approaches for boron speciation

The most common methods for determination of B concentration are spectrophotometric and plasma-source spectrometric methods. A number a spectrophotometric methods based on the use of specific reagents for the colour development are employed for B speciation. The most commonly used, and desirable for automation, is azomethine-H technique[20-22]. Flow injection (FI) spectrophotometric methods have been developed in the early nineties for directly introduced soil samples[23]. Atomic emission spectrometry (AES) and atomic absorption spectrometry (AAS) generally involve introduction of samples into flame, where elements of the sample are atomized. In case of AAS measurement free atoms of an element absorb photons, while the AES method measures the emission from the atomized and the excited species when they fall to ground state. These methods often require separation and preconcentration of B from the sample matrix for acceptable results. The B is measured as a volatile methyl borate, in case of AES as BO^{2-} radical[24]. Using plasmas as ionization sources and plasma sources analytical instruments (plasma-source-OES and MS) provide higher sensitivity and lower detection limit for B determination[24, 25].

For direct investigation of B complexation, beside UV absorption and conductivity changes measurements, capillary electrophoresis, NMR and mass spectrometry provide more sophisticated tools. NMR spectroscopy have been used also for provide evidence for the existence of boron complexes. ^{13}C, ^{1}H and ^{11}B NMR have been used either in conjunction with each other, or separately. The pH dependent stability of the different esters of boric acid and borate with glycol, glycolic acid, oxalic acid and glyceric acid[26], sugars and sugar acids[27] and other dihydroxy compounds[19, 28]have been studied in aqueous medium[26]. General rules of thumb: ester of boric acid and borate in aqueous medium show the highest stability at a given pH where the sum of the charges of free esterifying species is equal to the charge of the ester. ^{11}B NMR also enables the distinction and direct identification of a variety of borate esters and simultaneously the determination of the corresponding association constant[29]. Moreover, ^{11}B NMR also a useful and accurate technique, to determine stability constants and thermodynamic parameters ($\Delta H°$ and $\Delta S°$) at variable temperatures[30].

The formation of borate esters of various mono- and disaccharides in aqueous condition and their stability constants were also studied by ^{11}B and ^{13}C NMR spectroscopy[31]. In case of linear and cross linked polysaccharides (Dextran), four different borate complexes were reported, where the borate was bounded to α, β diols and α γ diols

glucopyranoside residues[32]. Boron as $[B(OH)_4]^-$ also reacts in aqueous solution with triols R-C$(CH_2OH)_3$ forming various amount of mono-chelate, bis-chelate, and cage structures which were identified and measured by ^{13}C, ^{1}H and ^{11}B NMR spectra[33]. Normally B forms a five member rings with 1,2 diols, but in a case of 1,3 diols the complexation results a six member rings (Figure 2) [34].

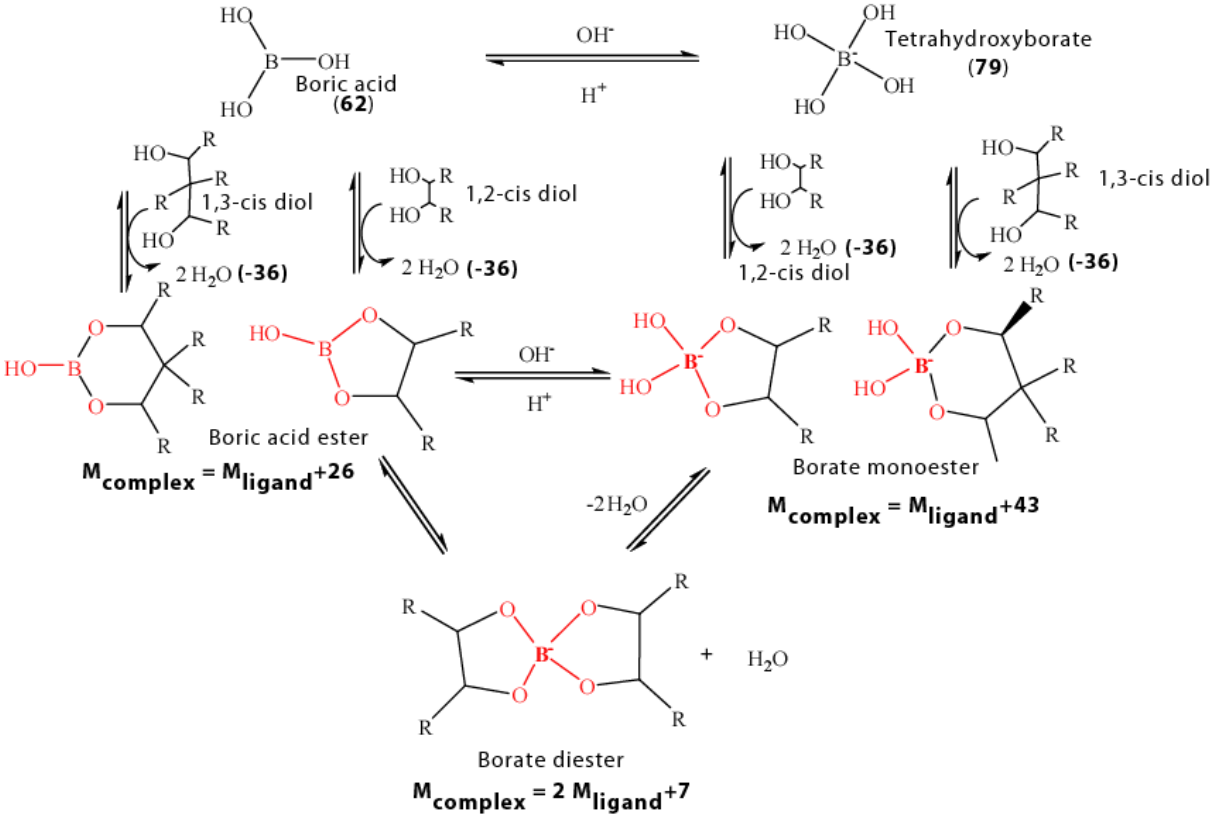

Figure 2. pH-dependent equilibrium between boric acid and borate ion and proposed pathways of complexation at low B concentration with their occurred mass changes during complex formation.

The equilibrium (Figure 2) between the trigonal boric acid ($B(OH)_3$) and the tetrahedral tetrahydroxyl-borate ($B(OH)_4^-$) anion is very sensitive to pH; indicated e.g. by large variation in the chemical shift of a single averaged ^{11}B NMR resonance representing the two rapidly interconverting species [35].

Both forms are known to complex diol groups of the proper geometry in cyclic and non-cyclic polyhydroxy compounds [36]. Five-membered ring complexes with 1,2-diols or six-membered rings with 1,3-diols give bidentate esters, also called the monocomplex (BL^-), as well as the spiranes or tetradentate esters (dicomplex BL_2^-). Depending on the pH hydroxycarboxylic acids and dicarboxylic acids can be involved in the formation of the

complexes as well [26,29]. According to the charge rule complexes formed with boric acid are less stable at higher pH than the complexes formed with tetraborate ions[37].

Fundamental characteristics of borate –cis-diol containing biomolecules complex were shown for different purposes[38,39]. Mass spectrometry, as a superior method based on its ability was also used for examining borate complexation 16 different nucleotides, where the authors demonstrated the stability of the borate-nucleotide complex in different charge and phosphorilation state[40,41]. MS has been also used in studies of boric acid complexes of polyols and carbohydrates using thermospray mass spectrometry (TSP-MS) [42] and MALDI[43] and coordination-ionspray MS[44]. Negative thermal ionization mass spectrometry (NTIMS) was applied to analyze the boron isotopic composition of natural waters[45]. How an ESI-MS can become an alternative technique to ICP-MS and TIMS was showed by Moraes M.C.B. et al[46]. Although they converted all boron species to BF_4^-, the isotope patter of those is equivalent to the isotope pattern of the boron atom, with relatively free-off interference spectrum.

The various B species in solution (1,2 and 1,3 diols; BL^-, BL_2^-) can be determined and quantified by ^{11}B NMR spectroscopy for a wide range of natural isolates and ligands: low molecular weight aliphatic acids, polyhydroximes, phenols, carbohydrates or higher polymeric polyols like agar or polyvinyl alcohol. The relative concentration of B species depends on the borate/ligand ratio and the pH of the solution [19].

Borate complexation induced changes in the charge-to-mass ratios of the ligands has been already used in the early 1950´s to determine the configuration of carbohydrates [36], or to selectively separate proteins by means of electrophoretic techniques (zone and gel electrophoresis). The routine analysis of carbohydrates and oligosaccharides with CZE is also based on these properties [27]; borate not only induces the formation of charged and mobile complexes from uncharged ligands, like sugars catechols an catecholic proteins, (thereby increasing the selectivity of their separation), but also significantly enhances the UV-absorbance, facilitating on-line UV detection.

1.3. Reactions of boron with soils

The Boron concentration in soil solution is generally controlled by the B adsorption reactions, as the amount of water soluble B available for plants uptake. Plants respond only the B activity in soil solutions and the B that was adsorbed by the soil surfaces is not perceived as toxic by plants [47, 48]. Factors that affecting B availability and extent of B adsorption in soils are solution pH, soil texture, moisture and temperature.

With increasing soil solution pH, B becomes less and less available to plants. Boron uptake by plants at identical water soluble B content was significantly greater at lower soil solution pH[49]. Boron adsorption by soils increased as a function of the solution ph in a range of pH 3 to 9 and decreased in the range of pH 10 to 11.5 [47,48]. Because coarse textured soils often contain less available B then fine textured soils, B deficiency often occurs in plants growing in sandy soils. At identical water soluble B concentration, plant B uptake was greatest for the most coarse textured soils[49]. Furthermore B adsorptions is also positively correlated with soil clay content. The correlation was specifically significant between clay minerals like kaolinite, montmorillonite and chlorite. The B availability generally decreases as soils dry, making B deficiency in plants more likely[50]. An increased B adsorption due to the temperature might be indirectly influenced, since soil temperature has a clear effect on soil moisture.

Boron adsorbing surfaces, like oxides, clay minerals, calcium carbonate and organic matter have been also investigated in numerous studies[51,52]. The mechanism of B adsorption on aluminium and iron oxide minerals is considered to be a ligand exchange with reactive surface hydroxyl groups. Anions adsorption on mineral surfaces produces a shift in the point of zero charge (PZC) of the mineral to a more acidic pH value [52]. Pressure jump relaxation experiments indicated that B adsorbs as an inner-sphere surface complex on aluminium-hydroxide via ligand exchange of borate with surface hydroxyl groups [53]. Boron adsorption on clay minerals is considered to be a two step process. Initially, B adsorbs onto the particle edges, subsequently migrates, and incorporates structurally into the tetrahedral sites replacing structural silicone and aluminium. The mechanism of the B adsorption step is considered to be a ligand exchange with the surface hydroxyl groups on the clay particle edges [52].

Organic matter is an important soil constituent affecting the availability of B. Adsorbed B and its adsorption maxima were highly significantly correlated with organic

carbon content[54]. Boron adsorption on mineral soil increased with increasing additions of composted organic matter [55,56]. Adsorption on a soil humic acid increased with increasing pH up to a maximum near to 9 and decreased with increasing pH above 9. Boron adsorption on composted organic matter occurred rapidly, reaching equilibrium after three hours and increased with increasing solution ionic strength. Mono-chelated and bis-chelated B-diolcomplex formation is a possible mechanism for B sorption by organic matter.

1.4. Non-hyphenated analytical approaches for characterization of NOM

Natural organic matters (NOM) are presented in terrestrial and aquatic ecosystems and they play a fundamental role in the environment. Natural organic matters are complex biogeochemical non repetitive materials existing in such a vast amount, that their quantity easily exceed the amount of functional biomolecules[57-59]. During diagenesis, they continuously undergo reformation, degradation, governed by the fundamental restrains of thermodynamics and kinetics, resulting the extreme intricacy. The natural diversity of these complex organic materials denotes high variability and density of binding sites, which enable them to behave as natural buffer against environmental and chemical extremes. Furthermore natural organic matter defines the bioavailability and cycling of organic and inorganic nutrients and pollutants[60-63], making the molecular level understanding of such supermixtures essential.

Soluble extracts of NOM can be recovered from soils and sediments by well-established alkaline extraction protocols, and these are referred to as humic substances (HS). These reference NOM samples contain not only the hydrophobic and hydrophilic acids but also other soluble organic solutes that are present in natural waters[2]. NOM that is present in natural waters, namely dissolved organic matter (DOM), is operationally defined as the fraction that will pass through a filter of a nominal pore size (0.45 microns).

Despite the continuous development of sophisticated analytical techniques, like FT-ICR/MS with high sensitivity and low detection limit, direct analysis of organic matters remain limited. Since their concentration in dissolved form compared to the inorganic content, especially in marine environment, is very low. Therefore for further detailed studies of dissolved organic matter (DOM) either originated from fresh water or from marine water, it is advantageous to be able to isolate DOM from water and remove the disturbing inorganic

[2] http://www.ihss.gatech.edu/

content. The inorganic salt content can also cause further problems by the isolation and concentration procedure [63, 64].

The most common methods for isolation and fractionation of DOM are: adsorption on XAD resins, where DOM is extracted from water, ultrafiltration (UF), nanofiltration (NF) and reverse osmosis (RO), where water is removed from the DOM. Beside the existing method, the working group of Perdue has also employed reverse osmosis coupled to electrodialysis to concentrate organic matter from marine water sources[65-67]. Reverse osmosis (RO) enable to concentrate organic matter from fresh water, however beside this process, the co-concentration of some inorganic salts (sulphuric acid and silicic acid (H_4SiO_4)) also takes places. Unfortunately the presence of these acids leads to an overestimated carboxylic and phenolic content value. If Electrodialysis (ED) was coupled to RO the content of these acids could be removed dramatically, resulting a low ash containing material with an average loss of 3% of the total organic carbon. The technology of RO coupled to ED, known as mild isolation technology, has the advantages of avoiding pH manipulation, no utilization of organic solvent and high yield of organic carbon content. Therefore the coupled RO/ED process, that is a fast method of isolation of large quantities of relatively unfractionated, low-ash NOM from waters, could substitute the other common isolation methods [64].

Individual compounds within the mixture, such as simple sugars, fatty acids, carbohydrates, peptides, often called as non-humic substances, usually preserve their reactivity and could be characterized individually[68-70]. Beside these compounds Humic Substances are rather complex, sometimes highly altered mixture, which characterization is challenging. HS can be further classified into humic acids (HA), fulvic acids (FA), and humin. HA is base-soluble and acid-insoluble, FA is soluble across the entire pH range, and humin is insoluble across the entire pH range. Isolation of HA and FA is typically achieved with a simple acid/base extraction procedure [71].

The enormous complexity of NOM derives from numerous biogeochemical processes resulting a wide variety of components with numerous physical and chemical properties. During diagenesis, they continuously undergo reformation, degradation, governed by the fundamental restrains of thermodynamics and kinetics, resulting the extreme intricacy. The natural diversity of these complex organic materials denotes high variability and density of binding sites, which enable them to behave as natural buffer against environmental and chemical extremes and additionally, NOM is a major source of carbon not only to the oceans but plays a pivotal role in the global carbon cycle [57,63]. Therefore an improved understanding of its composition is on high demand.

However numerous attempt were done in order to unravel the complexity of such a material [72-75], the proper characterization of such system is feasible only if minimal–invasive sampling techniques[76-78]and several high-end analytical techniques are combined, since generally applied methods, such as elemental composition analysis, UV-Vis and IR spectroscopy describe them only with averaged characteristic[79,80].

1.4.1. Elemental and functional group analysis

1.4.1.1. Elemental composition analysis

The elemental composition represents the most fundamental characteristic of organic compounds and can be determined with good precision [63,81]. The content of C, H, O, N, S and ash content provides essential information on the origin of the sample [82]. Rice and MacCarthy have compiled from the literature elemental data (C, H, O, N, S, atomic H/C and O/C ratios) for humic acids (410 samples), fulvic acids (214 samples) and humin (26 samples), isolated from environments all over the world, and analyzed statistically. The large data base showed statistically significant differences between the various humic substances. However they found the standard deviation for carbon content significantly low and therefore they suggested an optimum composition for humic substances in nature.

Determining the elemental composition of a discrete chemical compound is a first step to obtaining its molecular formula; this, in turn, is critical for determining its structural formula. However, in the case of non-stoichiometric materials such as coal, kerogen and humic substances, the concept of even a net molecular formula is extremely limited, and a unique, structural formula does not exist for these materials. Nevertheless, elemental analysis is a useful tool for characterizing non stoichiometric mixtures such as humic substances. Because humic substances are non-stoichiometric materials they must be characterized in terms of their average properties.

The H to C ratio (H/C) is an indicator of the amount of saturation of C atoms and the degree of aromaticity. The lower the ratio, the higher the amount of unsaturated structures[83], however Perdue [84] has pointed out that the total unsaturation of a humic material cannot be obtained solely from the H/C ratio. In addition to unsaturated forms of carbon the *H/C* ratio is also a function of unsaturation present in functional groups, primarily carboxyl and carbonyl groups, with lesser contributions from other miscellaneous forms of

unsaturation. The *H/C* ratio thus appears to be a qualitatively useful parameter for comparing the aromaticities of humic materials.

The O to C ratio (O/C) is assumed to indicate the carbohydrate content and degree of oxidation. The O/C values for wastewater effluent samples are slightly lower than the values for brown water. N/C values are higher for water derived from microbial active sources (wastewater) than for those systems with higher plant material. For samples showing a considerable ash content, the O/C ratio is often high[85]. Therefore, in relation to DOM composition, only C and H values are of importance. For samples showing relatively high ash contents (>80%), the H/C ratio also is questionable. Plot, so called "van Krevelen" enables another view to differentiate the elemental compositions of organic matters, humic and fulvic acids. Based on the origin the median elemental compositions occupy different regions in the van Krevelen plot. The theoretical location, defined by lipids, lignins and sugars might delimit the possible compositions of all biomasses, however the general observed ratios are beyond the pale. For instance, aquatic organism do not contain lignins, they would tend to occupy a smaller region, defined by lipids, proteins and sugars, however the continuous conversion of biomass to organic matter realign the occupied location in the diagram. Therefore such a presentation, which will be detailed later, is a powerful tool to follow alteration processes. Hence beside the median elemental composition, the elemental ratios of individual constituents could be also plotted, this type of visualization can be also utilized during the FT-ICR/MS data interpretation.

1.4.1.2. Potentiometric titration

Among the determined elements, heteroatoms like O, N and S contribute to functional groups that are resulting multiple acid-base equilibriums. The acid-base properties of a humic substance is interesting since these substances contribute to the acid base balance of the natural waters and greatly influence the metal binding properties. The abundances of carboxyl and phenolic functional groups are often considered as the main contributors and can be determined by potentiometric titration [86] [87] [88]. Methodologically, titration approaches could be divided into indirect and direct titrations. Though the simplicity of the indirect method, direct titration provide much detailed thermodynamically description of the proton binding of the humic substances [84, 89-91]. Unfortunately, the lack of distinct points in the titration curves of humic substances and the overlap of wide range of pKa values of acidic groups make it impossible to quantify the separate contributions of the carboxyl and the

phenolic groups to the total acidity. To overcome this problem, either empirical rules were often applied, or numerical models were fitted to the titration data. Assuming that all the carboxyl groups are titrated by pH 7 and the one half of the phenolic type functional groups between pH 8-10. On the other hand, fitting models that might estimate correctly the phenolic-to-carboxyl ratio, is a hard task and often yield confusing results.

Results, derived from ^{13}C NMR, yield commonly a signal peak at a chemical shift of 170 – 175 ppm that might derive from carboxyl groups (COOH), esters (COOR) and/or amides. Comparing the observed results and the data obtained by titration for carboxyl groups and amino acids provided similar values for samples from natural aquatic systems therefore might indicating that the concentration of ester groups is low in the isolated HS. In case of anthropogenically influenced humic substance, the contents of peptide and acidic functions obtained by titration and hydrolysis are higher than results from NMR analysis. Parallel, these samples have characteristically high levels of S and inorganic compounds and contribute to the proton capacity determined by titration. With the S levels obtained by elemental analysis, a maximum concentration of HSO_3-R can be calculated and converted to acidic proton concentrations. These concentrations must be subtracted from the titration data in those instances where carboxylic acids are to be quantified [88].

1.4.1.3. Spectroscopic characterization

1.4.1.3.1. UV-Vis

UV-Vis absorption is commonly accepted as conventional and versatile tool for the characterization of organic matter in natural waters[92]. The spectra are commonly broad, do not exhibit any obvious features and monotonously decrease with increasing wavelength with a typical characteristic from 200 nm up to 800 nm. The obtained spectra have usually poor resolution. However the so obtained spectra have usually much lower intensities than humic substances alone, for quantification of the NOM concentration in water samples, the denoted absorbencies at 254 nm (UV) and 436 nm (VIS) are frequently used in combination with the total organic carbon content. Absorption of light by HA in the UV range is caused by re-electrons and reflects aromatic and carboxylic electron systems as well as their conjugates. On the other hand, functional groups with quinoide structures and keto-enol systems are more responsible for the absorption in the visible range. Furthermore, the calculated so called

"Specific absorbance values" at certain wavelengths ($SUVA_{254}$) can be used to describe the composition of water in terms of hydrophobicity and hydrophilicity[93].

Normalization of the absorbance based on the mass concentration of TOC (specific values: A(254 nm)/ TOC)) is most useful for comparing different samples. Because the presence of chromophores constituents particularly in the UV region, strong absorption used to observed, though pH changes might influence the observed absorbencies[94,95] usually with an decreased absorbance as solution pH decreases. Although the observed spectra are generally broad and featureless, the absorption intensities significantly varied among the NOM samples, depending on their different origin, enabled ranking and distinguishing between the samples. For the spectral differentiation often the ratios of prominent absorption wavelengths were used, which might indicate the degree of condensation of the aromatic carbon network (E_{465}/E_{665}) [96].

1.4.1.3.2. IR

Infrared spectroscopy has been widely used for gross characterization of humic-type constituents and can provide valuable information on the structural and functional properties of NOM, e.g. oxygen-containing functional groups, occurrence of protein and carbohydrate moieties and relative proportions of aromatic versus aliphatic moieties[97]. However, the unambiguous assignments of different spectral bands are not possible for humic-type very heterogeneous organic material, since the significant overlapping of individual absorptions at different vibrational modes by different functional groups. Though prosperous attempts were done to increase resolution by FTIR DRIFT method [96, 98-100].

1.4.1.3.3. NMR

The most powerful and information-rich spectroscopic method for structural characterization of HS is definitely the NMR methods. Several reviews have been published describing the application of NMR to structural investigations either in solid- or liquid-phase (e.g.[64, 72, 75, 101-105]).

Beside the generally applied ^{1}H NMR, ^{13}C NMR, techniques[106-108], in addition, ^{15}N and ^{31}P NMR methods[105,109-113] and Zang et al. [114]. were used. For certain purposes, like investigation of interactions of metals, B, etc. with HS further NMR techniques have been also utilized [19,115]. In case soil organic matter, that is rarely soluble of solid-

state NMR has an important advantage over liquid-state NMR[105,116,117]. Some other advantages are that the technique is non-destructive hence the sample remain unaltered, and the spectra are not affected by the applied solvent and the samples can be analyzed at variable, especially low, temperatures. This allows examination of the molecular mobility, which aids in structural characterization

Multidimensional NMR techniques can be used to resolve contributions that overlap strongly in a 1D NMR experiment[106]. Combinations of these techniques, such as Total Correlation Spectroscopy (TOCSY), Heteronuclear Multiple Quantum Coherence (HMQC), Heteronuclear Single Quantum Coherence (HSQC), Heteronuclear Multiple Bond Correlation (HMBC), and Nuclear Overhauser Effect Spectroscopy (NOESY), have been successfully used for identifying the predominant structures in humic substances obtained from diverse sources[118-122]. Recent studies have shown the application of three dimensional (3-D) NMR spectroscopy for HS characterization[123]. The advantage of the additional dimension is given in the increased spectral dispersion compensating overlapping signals observed in 2-D spectra. Although the time involved in collecting and handling the enormous data set is long, the authors are confident that this technique will lead to improved resolution [123].

1.4.1.3.4. Fluorescence

Since NOM, specially DOM, samples have chromophoric (light absorbing) and fluorophoric (light emitting) moieties, the analysis of them with rather sensitive fluorescence spectroscopy has great potentials[124, 125]. Fluorescence excitation-emission matrix (EEM) has became increasingly widespread due to the potential to interpret organic matter fluorescence properties and high instrument sensitivity. The fluorescence in different spectral regions is associated with different types of functional groups, therefore, DOM samples, may have their own characteristic EEMs [126-129]. More importantly, unlike UV/visible absorption, the intrinsic fluorescence of humic substances contains information about their dynamic properties related to their intra- and intermolecular interactions functional groups, conformation, and heterogeneity[130, 131].

1.4.1.4. Mass Spectrometry (MS)

When NOM is characterized, elemental analysis, spectroscopic and other methods often do not give information about specific components but instead average descriptors of the bulk material. However these type of methods are essential to describe different functional groups or follow structural changes, the problem of distinguishing changes on molecular level remained unresolved. The continuous development of ionization and detection technologies in mass spectrometry enabled to apply also this method to characterize complex mixtures, such as natural organic matter. Laser desorption (LD), electrospray ionization (ESI) and atmospheric pressure photo ionization (APPI) are ionization technique, enabling almost fragmentation-free ionization without derivatisation of a whole range of structures. Beside the ionization developments, the expansion of the available resolving power and mass accuracy also contributed to the spreading of the application of this method for dissolved organic matter.

Electrospray ionization (ESI) technology was utilized for the first time by McIntyre et al. to analyze organic materials found in drinking water[132]. Although the low resolution capability of triple-Quadrupole mass spectrometer, the authors were able to identify series of peaks with 14 and 2 Da mass differences within the observed spectrum, that showed distribution from 200 to 700 Da with a maximum at around 350 Da. Based on the obtained results, they proposed a further utilization of electrospray-ionization technique, however in combination with mass spectrometry with more accuracy and resolving power. Thereby the authors highlighted the advantage over other techniques, like pyrolysis-MS.

Using ESI, enables to analyze constituents of humic substances without further derivatisation. This is because electrospray ionization takes place at atmospheric pressure, ionizes a wide range of polar, hydrophilic molecules and can be operated in positive and negative mode[133-136]. Multistage tandem ion-trap mass spectrometry, coupled to electrospray ionization was also utilized in order to investigate fragmentation pathways and propose possible structures for certain individual fulvic acid molecules[137]. Although the obtained results, the authors also pointed out the potential benefit of ES ionization combined with high-resolution mass spectrometry. Quadrupole coupled to time-of-flight mass spectrometry (QqTOF-MS) with electrospray were used beside high resolution MS to screen a series of humic and fulvic acid samples[138]. The authors used this technique to provide with a rapid means of examining qualitative differences among the samples. Independently the applied detection method they pointed out possible concerns about the applied ionization

technology. The concerns about the observed molecular weights and their distribution, furthermore the differences in the ionization efficiencies might only allow qualitative data interpretation.

Although the low resolution instruments are able to describe trends and differentiate samples with different origins, NOM samples, with more than 10 peaks per nominal mass, require higher resolved spectra over the above described mass range (Figure 4). The needed high resolving power, up to the present can only be achieved with the utilization of Fourier Transformation Ion Cyclotron Resonance Mass Spectrometry (FT-ICR/MS) [139,140] or LTQ Orbitrap, that combines a linear ion trap with radial ejection and an orbitrap mass analyzer[141,142]. In FT-ICR mass spectrometers, ions subjected to strong magnetic fields move in circular orbits (ion cyclotron motion) within a cell. Circulating ions have specific ion cyclotron frequencies defined by their mass-to-charge ratios. After excitation to increase the spatial excursions of these orbits and bring the ions into phase at time zero, these frequencies can be recorded as time domain signals as the excited ions in extended orbits circulate across signal detecting plates and their orbits return to a random state. The diminishing time domain signals can be digitized and processed into frequency domain signals by Fourier transformation(Figure 3/b). The frequencies can be converted to mass-to-charge ratio [140]. Since frequencies can be measured very precisely, FT-ICR MS is known for its ability to achieve very high mass resolution. The mass resolving power increases linearly with the increasing magnetic field strength[143]. In Orbitrap, mass-to-charge ratio is derived from the frequency of harmonic ion oscillations *along the axis* of the field (Figure 3/a). The Orbitrap mass analyzer is an electrostatic trap wherein tangentially injected ions rotate around a central electrode, being confined by applying an appropriate voltage between the outer and central electrodes. Mass analysis is based on image current detection of frequencies of axial oscillations. Therefore, its extent of mass accuracy is limited by the same factors as FT-ICR.

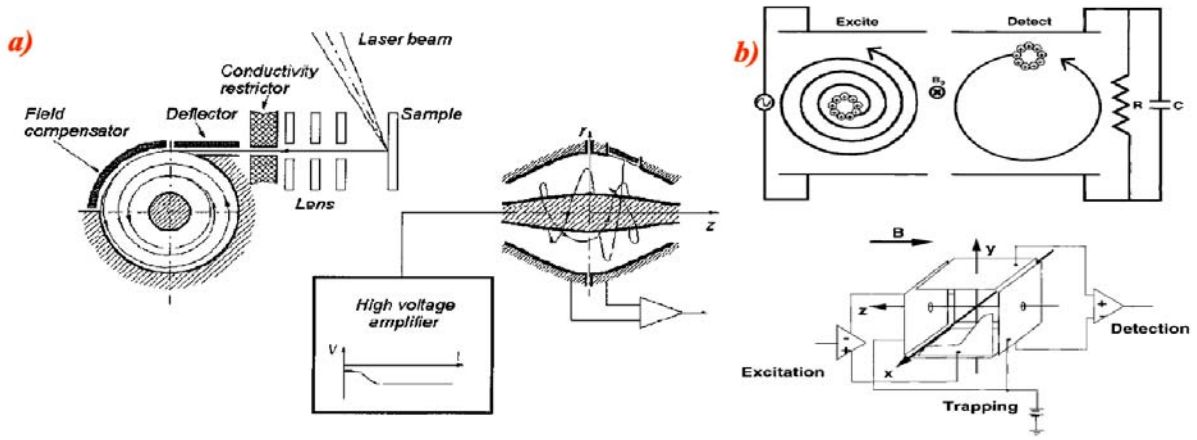

Figure 3. ***a)*** *Schematics of the experimental setting in Orbitrap [adapted from [141]]* ***b)*** *excitation and detection in the ICR cell [adapted from [140]]*

These type of mass analyzers enables the resolving power of 100-200 000 and over 300 000, in case of LTQ-Orbitrap and FT-ICR respectively [142], that enables direct molecular formulae assignment (Figure 4). However formula assignment only from mass data might result several formulae for the same molecular mass. Therefore sensitive chemical constrains have to be applied parallel in order to achieve valuable results[79, 144-147].

Because the so obtained information is extremely complex, the direct interpretation of spectra, derived from NOMs, is not possible. Since the molecular formulae can be determined for the correspondent masses, the obtained formulae can be further used and visualized in various ways.

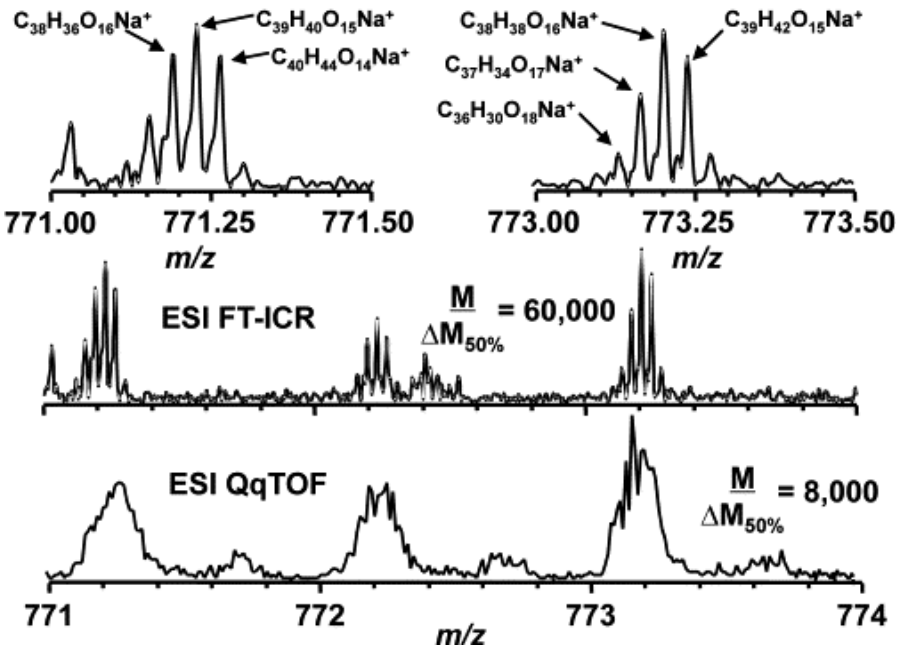

Figure 4.Comparison of expanded spectra derived from ESI Qq-TOF (bottom) and 9.4 T FT-ICR/MS (middle). [Adapted from [138]]

van Krevelen (1961) developed a graphical method to study the coalification process in which the atomic hydrogen/carbon (H/C) ratio is plotted as a function of the atomic oxygen/carbon (O/C) ratio. This type of plot, now generally known as a van Krevelen diagram, is often used for the classification of coals and kerogens[83]. A frequent application of the van Krevelen diagram is to illustrate the changes in elemental compositions that occur during the alteration of organic geochemicals in a geologic environment; e.g. H/C and O/C ratios have been used to follow the effects of diagenesis on humic substances. van Krevelen diagrams have also been used by various workers to illustrate compositional differences between humic acids and fulvic acids, and also to show variations in humic substances as a function of source. One of the major benefit of plotting molecular formulae in van Krevelen diagram is the direct structural information about the individual constituents and the potential of classification of them into compound classes (lipids, lignin, condensed hydrocarbons, aromatics, etc.)[148]. However it has to always keep in mind, that these assigned formulae and their occupied spots in the van Krevelen diagram are not necessary denote one unique chemical structure but possible superposition of isomers[79].

Further data evaluation and visualization, with so called Kendrick plot[149]might be useful, because of the increasing number of the false molecular formula assignments at high m/z values up to 1000 m/z. The Kendrick mass defect (KMD) plot acquits the obtained masses into homologous series of compounds within a sample. A homologous series is a series of m/z values that differ only by the exact mass of a certain functional group, such as a CH_2 or OH group. KMD converts the nominal mass of a CH_2 to exact mass by the m/z value from the mass spectrum resulting the Kendrick mass (KM), then KMD is calculated by subtracting the Kendrick mass from the observed nominal mass [150].

As the KMD plot is not as descriptive as the van Krevelen, KMD could be also used, in combination with the van Krevelen, as a safety filter. Kim et al. [151] also suggested combined method applying Kendrick mass defect analysis to peaks on trend lines identified using van Krevelen diagrams. This approach permitted them to find some prevalent differences between different ions in ultrahigh-resolution mass spectrum of DOM and to find some small characteristic structural fragments like CH_2O, C_2H_2 and C_2H_4. Studying such prevalent differences seems to be promising because it may has a potential to give a lot of useful information for complex object. Kunenkov et al. developed a data processing software which is capable of revealing additional structural information from a statistical analysis of the internal data structure of a complex spectrum. To do so, the raw spectrum is subjected to statistical analyses, in which pair-wise mass differences between all peaks in a spectrum were

calculated, and the results were plotted as mass difference appearance probability versus mass difference (Total Mass Difference Statistics, TMDS) [152].

Fievre et al. [153] used for the first time ESI combined with an ultrahigh resolution FT–ICR mass spectrometer to evaluate the molecular weight distribution of humic and fulvic acids isolated from the Suwannee River. The authors also compared the outcome of laser desorption (LDI) and electrospray ionization (ESI) coupled to FT-ICR/MS. The results suggested a possible fragmentation by LDI, since the higher-mass species disappeared from the spectrum. Parallel they denote electrospray ionization as a potential tool for determining individual compounds that could be the building blocks of humic substances. Recently chip-ESI in combination with APLI (atmospheric pressure laser ionization) [154] was hyphenated to FT-ICR/MS in order to ionize and analyze polar and non-polar aromatic compounds simultaneously. Since humic substances also contain also aromatic and polar compounds, this combined ionization technique could be useful to cover a wider range of ionisable constituents.

Since than numerous attempt were made to describe these immensely complex systems with ambiguous results [64,79,145,147,148,150,155-160]. The presented results generally describe FT-ICR/MS as an appropriate tool for characterizing natural organic matter with different origin. In some cases the main goal is even to compare the differences, originated from the different sources[156,161]. Molecular formulae determination and classification of the constituents is one of the major topic. Based on the assignment with the different visualization and grouping methods different building blocks and potential chemical structures could be assigned individually. Based on the measurements these materials generally denoted mainly as singly charge-state compounds, although this statement is often due to the parameter settings and a deviation in the potential ionization efficiencies [147,148, 153,162].

Laser-desorption FT/MS was also introduced to determine the molecular weight distribution of well characterized fulvic acid samples. The authors reported slightly lower average molecular weight compared to gel filtration chromatography (GFC) or vapour pressure osmometry (VPO), however they confirmed that LD is capable of desorbing an ionizing intact molecules without fractionation, if low laser energy was applied[163]. Laser-desorption was also utilized to analyze possible aggregates of humic acids [164].

However not only the sample complexity makes the analysis difficult and the results hard to interpret, but the applied settings have also tremendous effects[162, 165, 166]. Self-estereification, in presence of methanol is often neglected, however it has shown that

carboxylic acid self-catalyzes its esterification with methanol solvent [165]. Furthermore parameter settings, spray solution composition, sample preparation could completely change the shape of the observed spectra.

Since Hydrogen/deuterium (H/D) exchange mass spectrometry was a possible way to study protein structure and dynamics [167], Hydrogen/deuterium exchange was tried also to study the structure of fulvic acid and its interactions with metal [168, 169].

1.4.2. Identification of basic structures of NOM

Since organic matter in soils, is a complex mixture of substances that formed largely by microbial degradation of plant tissues and in oceans, bacteria are the main contributors to the dissolved nitrogen, major constituents, peculiar for living organism, is considered as a part of the organic matter[70,73,170-172]. The main classes of chemical compounds, derived from plants are cellulose, hemicellulose, phenolic compounds such as tannins and lignin, water-soluble compounds such as sugars, amino acids and aliphatic acids, ether- and alcohol soluble compounds such as fats, oils, waxes, resins and pigments, and proteins. Compounds that arise from microbial constituents may include lipids, carbo- hydrates, proteins, melanins and other polyketides. Accordingly, lipids, proteins and sugars can provide some insight into the level of heterotrophic activity in natural waters. Several percent of the organic matter can be attributed directly to lignins, lipids, proteins, and sugars, which are found in waters both as their chemically bound forms and as their free forms. Mostly, these constituents of DOM exist as chemically bound forms, from which their respective monomers (lignin-derived phenols, simple carboxylic acids, amino acids, and monosaccharides) can be liberated by vigorous hydrolytic and/or oxidative degradation.

Therefore targeted analysis of such constituents is reasonable and within a frame of an exchange scholarship, neutral sugars and amino acids were also investigated.

1.4.2.1. Hydrolysis, determination of monosaccharides

Hydrolysis by acids, bases or enzymes was used to obtain information on the building units of complex biogenic matter [68,173-175]. Powerful methods have become available to identify amino acids, carbohydrates and fatty acids in low concentrations of μg/L by HPLC methods. Studies of several reference samples[173] showed that monosaccharides, like pentoses, hexoses, deoxycarbohydrates and aminosugars make up to 8 mass percent of the

organic carbon (OC) of FA and HA, whereas the values for non-humic substances (NHS) were significantly higher. Glucose, galactose, mannose and xylose were predominantly found. Data gained by ^{13}C NMR show that up to 30% C is involved in carbohydrate structures. The NMR values are significantly higher than those gained from hydrolysis measurements. Typical ^{13}C NMR signals of carbohydrates arise at 70 and 103 ppm (TMS scale), however an exact determination is not possible due to strongly overlapping signals in the O-alkyl range. N-acetylated carbohydrates and chemically modified carbohydrates show distinct NMR signals, but they will not be detected with the chemical method. Thus, the absolute concentration of carbohydrates is expected to be higher than the amount of identified hydrolyzed carbohydrates.

Carbohydrates are major components of marine organic matter and therefore understanding the sources, transformations, and fates of carbohydrates in the marine environment can provide insight into the overall cycling of photosynthetically produced organic carbon. There have been several studies on the production of dissolved carbohydrates by marine phytoplankton and their consumption by marine heterotrophs. However, there are relatively few comparative studies of the molecular composition of carbohydrates in marine and freshly produced phytoplankton DOM. A relatively large fraction (30% of DOC) can be isolated from seawater for chemical characterization using tangential-flow ultrafiltration with 1000-Da cut-off membranes[76]. Samples from different ocean basins indicate that polysaccharides comprise a major fraction of ultrafiltered DOM (UDOM) in surface waters [68-70]. Molecular-level characterization of aldoses in UDOM indicates little spatial variability in molecular composition[68,70].

1.4.2.2. Hydrolysis, determination of amino acids

Amino acids (AA) occur in aquatic environments either in a free status, likely as dissolved free individual compounds as part of natural polymers such as peptides and proteins and in living cells. AA are also important carbon and nitrogen nutrients for many aquatic microorganism, primarily for bacteria and algae resulting high AA content in these organisms. Therefore the main suppliers of AA into aquatic environments are the primary producers such as algae and higher water plants, i.e., macrophytes. Bacteria are considered major sinks for AA. In addition NOM from catchments, runoffs and precipitation can also import AA, which can be bound to many different kinds of organic compounds. Two important classes of amino acid pools exist in the NOM pools: dissolved free amino acids and combined amino

acids[176]. Jahnel et al. [173] showed that 17 proteinogenic amino acids (AA) can be released by a hydrochloric acid treatment and with proteolytic enzyme *pronase E*. Although the total amount of AA carbon related to the total DOC is low (samples investigated in the study: below 5%), the percentage of AA-derived N related to the total N content can account for 4% for groundwater fulvic acids (FA) up to 30% for soil humic acids (HA) [177]. From ^{15}N NMR, data for the same set of samples show that up to 90% of N is attributed to amide nitrogen. However, it must be kept in mind that the exact determination of its peptide content based on ^{15}N NMR data is not possible due to overlapping signals in the amide range (peptide and other amide nitrogen, like N-acetylic groups). Therefore, NMR data provide an estimate of the maximum amount of these structural fragments.

Amino sugars were also determined in natural samples, including seawater, using high-performance anion-exchange chromatography with pulsed amperometric detection and a new off-line sample cleanup procedure. The observed detection limits for amino sugars were between 1 and 4 nM with the S/N 3, allowing for the first time quantification of amino sugars in seawater without pre-concentration. However, acid hydrolysis-induced racemization compromises accurate determination of enantiomeric amino acid compositions.[174, 178]

1.4.3. Electrophoretic Separation of NOM

Electrophoresis plays a key role as analytical or preparative technique in the characterization of natural organic matter because it gives information about the behaviour of these molecular mixtures in controlled solution conditions depending on both the size and the charge distribution frequency of the analytes in the complex mixture.

The goal of most of the electrophoretic studies going on NOM over the years has been fractionation, often directed toward specific biomolecules (e.g., polysaccharides, N-containing compounds, enzymes) potentially present in the mixtures. Methods were mainly concentrating on the analysis of humic brand of materials (alkali extracts of soils) and in most of the cases, electrophoresis was used as fingerprinting method rather than a method to study quantitatively the structural characteristics of NOM such as molecular size or charge. Since the early years of electrophoretic separations of humic substances the main goal most of researcher was to obtain as much "bands" as possible such as they were experienced with the biomolecules. These bands were in most of the cases attributed to humic fractions having similar electrophoretic mobility. Even though possible interactions of the humic substances with buffer components or separation matrices leading to artefacts were proven already in the early 1950; For example Stevenson stated in 1953 that the associations of humic molecules could interfere with the separation process [179]; these facts were often neglected over the years.

Relevant literatures were reviewed in electrophoresis[180], capillary electrophoresis[181-184], classical electrophoretic techniques for the characterisation of humic substances [185, 186].

1.4.3.1. Zone electrophoresis

In free solution, the electrophoretic mobility (*i.e.*, μ_{elec}, the particle velocity per unit applied electric field) is a function of the net charge, the hydrodynamic drag of a molecule and the properties of the solutions (viscosity, present ions - their concentration and own mobility). It can be expressed as the ratio of its electric charge Z ($Z = q.e$, with e the charge if an electron and q the valance) to its electrophoretic friction coefficient. Different predictive model were demonstrated involving the size, the flexibility and permeability of the molecules or particles.

Henry´s theoretical model of 1931 [187] of μ_{elec} for colloids can be combined with the Debye-Hueckel theory predicting a linear relation between the mobility with the charge Z. For

small molecules (metabolites, monomers and small oligomers) the mobility equation may be empirically approached with the Offord model (linear relation to charge to size ratio, the charge being obtained directly from the ionization constants and the size being approached with the molecular mass exponent a factor α) (see [188]).

$$\mu_{elec} = a \cdot \frac{eZ}{M^{\alpha}}$$

M is the molecular mass; a and α are two constants determined experimentally and can vary as a function of the class of chemical compounds (DNA, peptides, organic acids) [189].

This empirical concept is well accepted and was adapted to simulate with enough precision the separation of various types of analytes such as DNA fragments, peptides up to proteins[190], enabling the optimization of their separation or the assigning chemical structures and properties. Although, from oligomers to polymers, the theoretical and empirical approaches often involve a polymerisation degree (N, number of monomer units) into their models [183]; this approach yields exact results but is not applicable in a general manner to polydisperse polyelectrolytes such as NOM. In the lower nanometer range of polymers to lower micrometer for living organisms or their fractions (bacteria, mitochondria, cells and cell wall fractions), the solution of the mobility of charged particles can also be approached as a solution of the Poisson–Boltzmann equation expressed in spherical coordinates for the distribution of ions around the sphere and the consequent potentials, coupled with the equations for force as a result electroosmotic flow [191].

Hard sphere or cylinder models [192-195] permeable Donnan gel phases [196, 197], branched[198] or linear [199] polyelectrolytes models were proposed for NOM. Here the different models must be differentiated in detail, i.e. impermeable hard spheres, semi permeable spherical colloids ([197, 200] or fully permeable electrolytes. Latest developed model by Duval et al. applied to NOM involves an electrokinetic model for a soft particle taking account of a hard (impermeable) core and a permeable diffuse polyelectrolyte layer [201]. The model proposed by Duval certainly is the most appropriate for humic substances.

1.4.3.2. Capillary Zone Electrophoresis

The main advantage of capillary electrophoresis is the simple instrumentation consisting of a high-voltage power supply, two buffer reservoirs, a fused silica capillary and a detector. The basic set-up is usually completed with enhanced features such as multiple

injection devices, autosamplers, sample and capillary temperature controls, programmable power supplies, multiple detectors, fraction collection and computer interfacing.

Capillary electrophoresis separation is performed in a flexible fused silica capillary tube that is filled with an appropriate buffer solution of defined pH and ionic strength (aqueous / non aqueous). A small volume of sample (lower than 3-4% of the column volume to keep the separation efficiency) is introduced hydrodynamically (or less often electrokinetically) into the capillary to which an electrical potential is applied (Figure 5).

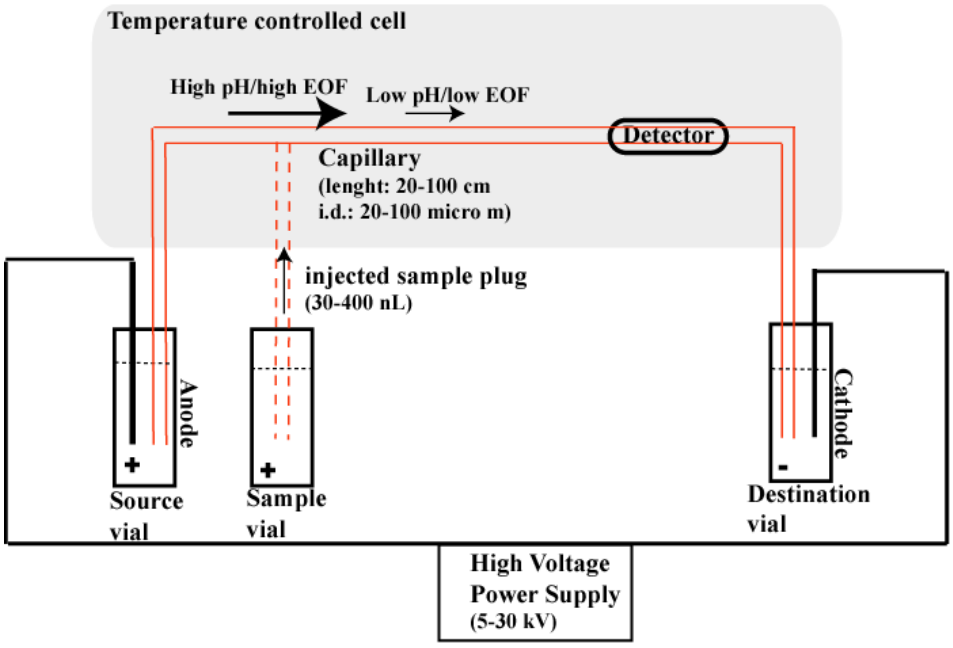

Figure 5. Simple setup of capillary electrophoresis (the potential setup is illustrated as generally used for NOM).

Charged species of the sample exhibit different effective electrophoretic mobilities (field strength reduced velocities) and are thereby separated. Detection may possible with UV-Vis, laser induced fluorescence, electrochemistry, conductivity or mass spectrometry. Different techniques are possible as a function of the type of capillary column relative to the buffer, allowing separation of charged, neutral, polar or hydrophobic analytes. Compared to chromatography, the main differences in CE are the technique of injection into the capillary and the means by which the sample is driven through the column that is not hydrodynamically pumping but instead electroosmosis[184,202]. This elementary process in CE, the electrically driven pump as a direct consequence of the surface charge on the walls of the uncoated fused silica capillary. The capillary surface carries silanol groups (pK_a 3-5) that ionize as a function of the pH of the separation buffer[203]. The dissociation of SiOH groups to SiO^- produces a negatively charged surface on which an electrical double layer is established at the solid/liquid interface to preserve electroneutrality. The counterions and their associated

solvating water molecules migrate in the electric field producing a flow of solution towards or against the detector called *electroosmotic flow (EOF)*, which is directly dependent on the chemistry of the separation buffer, its viscosity η and its dielectric constant ε (especially important in the non aqueous mode – NACE). An increase of the ionic strength can for example decreases the zeta potential and in consequence decrease the EOF. Strongly adsorbed ions will have the same effect. Coating systems (such as neutral or charged polymers) can chemically alter the surface and also regulate the EOF if needed for a separation.

Capillary zone electrophoresis (CZE) is the basis of separation within all above CE-techniques. By changing the separation buffer system based on the setup of CZE, optimized interactions with of the sample with some buffer constituents allow an increased selectivity in the separation of the charged or neutral analytes. CZE allows the separation of anions and cations as a direct function of their charge density (effective charge to size ratio) (Schmitt et al., 1997). The addition of solvents to the running buffer up to 100% in nonaqueous buffers (non-aqueous CE - NACE), can additionally allow specific selectivity and increased solubility for some analytes and is mostly used for pharmaceuticals or plant secondary metabolites[204]. The selectivity is governed by their effective charge and thus by the separation buffer pH and the electroosmotic flow (EOF). This method was the most freuently used with NOM.

1.4.3.3. Isoelectric focusing

Isoelectric focusing (IEF) was introduced for biochemical separations in the 1960ies [205]. The separation is carried out in a pH gradient, created by the addition of zwitterionic substances called ampholytes to the separation solution or integrated into the gels (analytical agarose, sephadex or polyacrilamide gels); the analytes migrate in the solution or in the gel matrix to the pH where their positive charges balance their negative charges (isoelectric points (pI)). IEF in gels of humic substances generates a series of regular bands in different isoelectric point domains, extending from a more diffuse area of increasing colour when going through lower pH (anode) to higher pH values (cathode). Although the results obtained with the IEF technique in gel with HS are extremely dependent on the experimental conditions[206], IEF in gels was one of the most used classical electrophoretic techniques for the fingerprinting of NOM (for example, to follow the humification processes)[207]. It was used to fingerprint HS from different soils, composts[206,208,209], fulvic and humic acids[210] and to differentiate phenoloxydase products[207]. It was also used to follow the humification processes [207-209,211-214].

With a median nitrogen content around 2% [63], NOM may contain only limited amount of free positive charge (amino acid and peptide bonds play a minor role) which could be involved in charge neutralization and responsible for band formation. In solution IEF, only limited amount of carbon from the original sample will be found in the pI range > 4; the flocculation of around 60% of the carbon, occurred at pH value <4 [215].

Preparative solution isoelectric focusing can be performed in order to fractionate NOM (sample load up to 50 mg); the harvested 20 fractions were characterized with UV-Vis spectroscopy, gel permeation chromatography and capillary zone electrophoresis (CZE) and showed the distribution of the molecular weight of the focused fulvic fractions in the created pH gradient. CZE of the obtained fractions showed a series of sharp peaks that resulted from the disaggregation of the colloidal NOM after interaction with the ampholites and moreover even some signals could be observed in the cationic range [202, 215]. In column borate complexation was also used in CZE to compare the harvested fractions by fingerprinting. Only 32% of the total FA did not precipitate with the ampholites, that were employed and this FA fraction was mainly composed of low-molecular-weight compounds as was shown with CZE. Parallelisms were found in the distribution (at least 3 individualized fractions) of the low pH-focused NOM fractions in the preparative IEF compared to CIEF. Due to the interactions between the NOM and the ampholites, this method found only limited application, especially when the fractions needs to be analyzed with mass spectrometry or NMR spectrometry.

1.4.3.4. Capillary gel electrophoresis

Separations on agarose or polyacrilamide gels are also over 100 years old. Many interesting developments occurred about 30 years ago, when was realized that these supports were ideal for the separation of proteins in denaturing agents such as urea or sodium dodecyl sulfate (SDS): polyacrilamide gel electrophoresis (PAGE) was born. In terms of the separation of bands (fingerprinting without possible structure information), the PAGE approach certainly yields good results but a direct correlation in terms of structural characteristics is difficult because of specific interactions with the buffer/gel components. The separation is certainly caused by chemical interactions between fractions of the NOM and polyacrilamide, urea, SDS or buffer constituents that depend on the sample structure. Trubetskaya and Trubetskoj [216-219] have showed that this approach using complexing buffers may still be used; recent findings have shown that most fluorophores and a large

proportion of photoinductive chromophores are located in the low mass fractions of soil humic substances and such a distribution of photochemically active constituents may be characteristic across different soil types [220].

Capillary gel electrophoresis (CGE) has historically been developed for the separation of proteins and DNA fragments and this technique is used to sequence the Genomes. In the presence of anionic detergents such as sodium dodecylsulfate (SDS) proteins get a homogeneous charge density and in the presence of sieving medium the CGE migration times can directly be correlated to size. SDS however can not be used with NOM because strong interactions alter the electropherograms significantly [186]. When comparing systems with different charge density the linear relation between the mobility and size [221] is not verified anymore and only the variation in effective mobility in presence of the gel is correlated to the size. A physical gel composed of 0.3% methylcellulose in a 25mM carbonate buffer pH 9.3 was shown as possible separation medium for NOM in CGE. From all tested gels, the polar polysaccharides were found the best for the separation of NOM; the interactions are minimized but can never be suppressed.

1.5. Hyphenated analytical approaches for characterization of NOM

1.5.1. Hyphenated liquid chromatography techniques

1.5.1.1. SEC-ESI/MS

Electrospray ionisation combined with SEC is a potentially prevailing technique for the molecular size determination and characterisation of HS at the same time [222-225]. The SEC separation offers a possibility to interpret the highly complex spectra, obtained from high resolution MS, equipped with soft ionization techniques, for instance electrospray ionization. Especially if the compatibility of ESI and eluents favourable for the SEC of HS can be improved. The apparent ability of HS to produce both positive and negative ions offers additional possibilities for structural determinations. More efficient methods to suppress the formation of multiply charged ions in favour of singly, or moderately, charged species are greatly needed to allow unequivocal molecular weight determinations[226]. Investigations of humic (HA) and fulvic acid (FA) fractions with ESI-MS found lower mass distributions for humic acids (300–1200 Da) compared to size exclusion chromatography (1000–100,000) [227]. Therefore, new questions arise as to whether there are colloidal aggregates responsible for the higher masses found by previously-applied methods like SEC, or whether there is a more selective ionization in ESI responsible for the recent findings. The latter would mean only a specific portion of HS can be ionized by ESI. A reason for this may be the selective ionization due to the different ionization efficiencies of different compounds in ESI.

As in biological applications ESI-MS may be suited to detect non- covalent interactions of dissolved species in aqueous samples. This type of ionization may assure the existence of certain aggregated supra-structures which was supported by SEC, but not detected in MS where the observed average masses support the low molecular weight molecules. It is interesting to note that ionization experiments on poly(carboxylic acids) indicated a low-molecular weight of ESI-MS (about 330 in the positive ion mode and of about 280 in the negative ion mode), although the observed mass distribution of this standard was 2000 Da [137]. On the other hand, a first indication that ions generated by ESI are at least partially representative of the entire sample is that elemental composition values of combustion agree well with data obtained from ESI. Ultrahigh resolution electrospray ionization Fourier transform ion cyclotron resonance mass spectrometry (ESI-FT-ICR-MS) is

a promising technique for advanced structural and chemical characterization of natural organic matter [79, 150, 159].

1.5.1.2. LC-NMR

Separations using reverse phase (RP) liquid chromatography are potentially more powerful as samples can be studied without derivatization. Numerous attempts have been made to separate NOM, and while most studies exhibit some degree of separation, to date the complete separation of a NOM sample has not been accomplished. Even only partial separation is possible, it is worth to hyphenate a separation method with structure information oriented analytical applications. Liquid chromatography combined with nuclear magnetic resonance and preliminary studies with solid phase extraction were conducted on NOM isolated from freshwater and soil [228].

1.5.2. Hyphenated gas chromatography techniques

1.5.2.1. Pyrolysis GC/MS

Pyrolysis GC/MS involves chromatographic separation of pyrolysis products into single components and so mass spectral data obtained for each component. The interpretation of the data requires a detailed knowledge of the pyrolysis behaviour of the compounds; since secondary reactions inevitably modify the original compound, the pyrolysis data are susceptible to bias. For example, pyrolysis of cellulose results in carbonyl compounds, acids, furans, pyranones, anhydrosugars and phenols. Fatty acids may be decarboxylated under the pyrolysis procedure, especially in the presence of mineral soil that may have a catalytic effect on such reactions. Thus mainly alkanes and alkenes can be identified in the pyrolysates obtained from soils, with only minor occurrence of fatty acids [229]. Nitriles found in soil pyrolysis could originate from the reaction of long chain fatty acid with some nitrogen derivatives present in the soil [230]. The pyrolysis of polar macromolecular materials is well known to produce volatile polar products, only some of which can be chromatographed; very polar products remain attached to the column, undetected and unquantified. Pyrolysis with tetramethyl ammonium hydroxide (TMAH) derivatizes polar compounds to less polar products, which are more amenable to chromatographic separation. This procedure avoids decarboxylation and produces methyl esters of carboxylic acids and methyl ethers of hydroxyl groups[231,232]. This already multi-dimensional technique in combination with cross

polarization magic angle spinning (CP-MAS) ^{13}C-NMR provided chemical information on the chemical composition of soil organic matter[233].

The combination of pyrolysis in the presence of methylating agent (TMAH), non destructive techniques, like XANES (X-ray Absorption Near-Edge Structure) and XPS (X-ray Photoelectronon Spectroscopy) allows to characterize polar moieties and sulphur functionalities at the same sample. The combination of these different approaches allowed a more complete understanding of the organic sulphur structures in the leonardite coal. In agreement with previous studies, the results showed that oxidized sulphur functionalities, such as sulphonate and sulphate, represent the major forms of sulphur in leonardite coal. The organic matter in coals contains significant amounts of oxygen, sulphur and nitrogen heteroatom incorporated in various functionalities (e.g. carboxylic group), which vary in abundance depending on the specific conditions of the coal-beds. Nuclear microprobe analysis (NMA), which is a non-destructive technique, allows to detect and quantification of all elements of the periodic table located on the solid surface with large spatial resolution. The technique provides an evidence of a strong affinity with the smallest HA colloids of numerous trace elements[234].

1.5.3. Online hyphenated electrophoretic techniques

Capillary electrophoresis (CE) is a relatively non-perturbing method that allows the electrophoretic separation of small molecules, polymers or macromolecules in various modes of separation using aqueous or non-aqueous buffers with coated or uncoated capillary columns. The combination of CE online with mass spectrometry provides a very powerful analytical system, characterized by its high resolution capability and detection sensitivity [235]. Additionally, the small volume of the analyte used in CE techniques allows the analysis of cellular components. For polydisperse mixtures, such as NOM, hypenation could provide insights into the distribution of charge density at specified pH and ionic strength. For correct interpretation of the CE_ESI/MS results of NOM an independent understanding of the behaviour in both CE and ESI/MS is necessary and be aware of any art factual signals, for this reason the use of CE with NOM and humic substances were reviewed [186].

A possible use of CZE-ESI/MS for the characterization of Suwannee River NOM was presented by Schmitt-Kopplin [236]. In a first step the ESI interface conditions were optimized with model compounds and the behaviour of different oligomers were investigated. However the used model compounds during the optimization (trimellitic acid and phthalic

acid) are multiply charged in solution but are only single-charged after electrospray, testing the charge retention under the ionization conditions, higher molecular mass oligomers (polycarboxylic glycyrrhizic acid) were also injected, resulting doubly charged detected peaks. High-molecular-mass humic substances presenting multiple charges in solution could thus also bear multiple charges after separation and ESI with a high probability. To test this hypothesis, several oligomers(polyelectrolytic polystyrene sulfonates (PSS) and polyacrylic acid (PAA)) were separated as multiply charged anions in CZE and detected in ESI-MS. The results showed that actually, it is possible to detect multiple charged states with this approach. The analysis of NOM confirms that molecules smaller in average and more charged are present in the high mobility region of the hump and that higher m/z are found in the low-mobility range of the colloidal charge density distribution, which was already suggested [186].

1.5.4. At line hyphenated free flow electrophoretic (FFE) techniques

Since the surface properties (charge density) of these natural complexes influence their environment, like buffering capacity or specific binding an ion pollutant in natural systems like groundwater or soil, separation and analysis based on these properties are highly favourable. Thought electrophoretic separation methods are also available, when detection methods, like MS, are not on-line hyphenated, for further possible off-line analysis, the provided sample amount would not be sufficient. To overcome this problem, an upscale method, in mL range, is available in electrophoretic separation, namely free-flow electrophoresis. The behaviour of the fulvic acid were described by the CZE profiles and mobility distributions, obtained from the fractions separated by FFE[237]. The FFE approach enables new possibilities for the structural investigation of humic materials with other analytical characterization techniques (chromatographic and spectroscopic such as nuclear magnetic resonance spectroscopy). Further advantage of these obtained fractions, that they can be conserved, avoiding certain rearrangement by the time, and the different fractions, beside off-line investigation, can be a base of different interaction studies, revealing the responsible reactive parts of these highly altered mixtures in nature like NOM. To follow the FFE separation, the fractions can be analyzed offline by FTICR MS, and the obtained spectra visualized by van Krevelen diagram to evaluate the NOM composition and structure.

Electrophoretic separation and so an up-scaled form of it, enables a non-surface influenced separation, where the result of the separation is directly linked with the acidity of

the sample. Since carboxylic acids and phenolic acids are known as the main contributors to the general functional groups of natural organic matter, such a separation has clear advantage compared with other separation methods. Furthermore an up-scaled separation also enables to produce samples in a sizable amount, which allow different analysis on the same set of sample. Therefore in the upcoming chapters this hyphenated system will be optimized and used.

2. Characterization of NOM

2.1. Optimization a charge density fractionation of NOM

To interpret and characterize vastly complex mixtures, prior a preparative at-line free-flow electrophoresis (FFE) was utilized to gain sizable amount of fractions. In order to gain valuable results the electrophoretic separation and the applied analytical method (FT-ICR/MS) were optimized and harmonized.

2.1.1. Introduction

The level of intricacy in the analysis of large molecules and of mixtures can be classified according to their polydispersity and heterogeneity. The structures of complicated, but monodisperse, natural products and biopolymers are readily accessible (provided that sufficient amounts of materials are available) by a combination of analytical methods, which primarily rely on NMR spectroscopy and mass spectrometry. Supramolecular structures, composed of (modified) biopolymers aligned in aggregates, which are supported and defined by weak interactions, require a more elaborate characterization, which requires an adequate definition of covalently bonded molecules and of their non covalent interactions.

Currently, the molecular level structural analysis of natural organic matter (NOM) or humic substances (HS) is primarily focused on the definition of the covalent bonds. In an ongoing evolution, future high quality structural analyses of NOM/HS will have to provide a characterization of individual molecules and a description of the extent and mechanisms of their interactions. Complementary organic structural spectroscopy of NOM in conjunction with fractionation creates data sets of high information density. The nature of alterations within a range of closely related NOM fractions is a response on a incremental change of "environmental" properties within the separation column (and thus a measure of NOM function under that specific conditions). These conversions can be assessed via in-depth structural analysis and linked to molecular composition and structure. Moreover the combinations of independent analytical approaches have the wealth of inherent multivariate profiling capabilities with a potential and richness of fundamental advanced knowledge and understanding of NOM.

HPLC coupled efficiently to structure-selective spectroscopic detection might also permit a better description of detailed chemical and structural properties of HS. Although HPLC offers structure-dependent separation, the obtained information strongly depend on the extent of recovery from the chromatographic column. This recovery, which might generally driven by the pore size of the stationary phase and the applied solvent gradient was revised by Woelki et al. [238]. Liquid chromatography was also utilized to fractionate humic substances based on their affinity for immobilized copper(II) ion, in order to describe the general role, bioavailability of trace metals in natural aquatic environment. The obtained results also suggest that combined chromatographic measurements, such as HP-IMAC, HPSEC and RP-HPLC, yield significant information regarding the properties of different fractions among the HS [171, 239]. Combine LC with tools that can provide molecular level information might overcome the general problem of co-elution or partial separation if separation of numerous compounds is desired. Hence LC-NMR and LC-SPE-NMR hyphenations were tested to study NOM, isolated from freshwater and soil [228]. The authors describe preliminary applications of such coupled methods with aware of the predicted relatively poor separation efficiency of the vast samples, however certain attempts (like application of ion-pair reagent to avoid the formation of aggregates) were done to unravel the complexity of NOM.

As size exclusion chromatography (SEC) is one of the most powerful tool for the determination of the molecular weight distribution of macromolecular compounds, this technique was also applied to describe the complexity of humic substances, however the separation conditions influence the results unambiguously [240]. Since the generally recorded molecular weights for humic substances cover a wide range, defining the origin of this phenomena and general descriptors to discriminate between HS samples is crucial [241, 242]. The ability of SEC coupled to mass spectrometry was also tested [223, 224]. Based on the obtained results three fractions were distinguished from low molecular weight to high molecular weight and characterized by mass spectrometer.

Capillary electrophoresis methods and on-line coupling with mass spectrometry, were shown to be ideal to investigate structural properties of charged macromolecules (for more details please see the reviews of Schmitt-Kopplin et al. and Gaspar et al. [184,243,244]). Different capillary electrophoretic techniques were tested and used on NOM with various origins over the last decade [19,28,186,236,245] with a promising future aspect.

Free-flow electrophoresis (FFE), since its method was described, it was used for peptides, proteins membranes biological particles and for small ions[246]. As zone electrophoretic techniques allow a separation of NOM on the basis of their own chemical

surface properties (charge) and configuration (size) under different solution conditions without interaction with an active phase such as in liquid chromatography, the up-scale version of capillary electrophoresis, namely free-flow electrophoresis was also applied in order to separate humic substances [247].

The wealth of inherent multivariate profiling capabilities is of adequate potential and richness to fundamentally advance knowledge and understanding of NOM/HS. These extended applications can provide alternative interpretations and the combination of them advocate molecular composition and structure information. In this chapter, the significance of the outlined complementary approach to HS characterization on the example of Suwannee river FA was demonstrated.

This chapter was prepared, based on the article ”*Preparative Free-flow electrophoretic separation and off-line ESI-FTICR/MS analysis of Suwannee River Fulvic Acid”***[II]**

2.1.2. Instrumentation

2.1.2.1. FFE

The FFE fractionations were performed in an Octopus PZE free-flow electrophoresis device manufactured by Dr. Weber GmbH (Kirchheim, Germany). The FFE device used in these experiments has a vertical separation chamber with a length of 500 mm, a width of 100 mm and a thickness of 0.5 mm, resulting in a total chamber volume of 25 mL which was tempered to 15°C. Separation buffer after the calibration was 2.5 mM ammonium bicarbonate. The electrodes were separated from the electrophoretic chamber by filter membranes (electrode buffer: 500 mM ammonium bicarbonate (pH 9.2), 1 L per electrode). The separation medium was continuously pumped into the bottom of the chamber (950 mL/h) with a laminar flow profile in the chamber. The analyte was also continuously pumped (2 mL/h) at the bottom of the chamber (applied sample concentration was: 20 mg/mL), and it migrated to the top according to the separation medium speed (vertical direction) and to their electrophoretic mobility (horizontal direction). After reached an array of outlet tubes (every 1.06 mm, 96 fractions in all) at the top of the chamber the separation media and the sample were collected in tray which contains 96 wells, with UV applicable bottoms, ready for further raw characterization with UV spectrophotometer.

First the FFE system was optimized followed by the fast UV measurements to enhance the separation, based on the sample mobility and centre it not to exceed the dimensions of the

separation chamber. After the optimization procedure the obtained settings were used for the final separation. The acquired fractions were analyzed separately by direct infusion FT/MS.

2.1.2.2. UV-Vis spectrophotometer

UV-visible spectra of the fractions collected from the Octopus were recorded on Bio-Tek kc-Junior micro plate reader at 254 and 214 nm.

2.1.2.3. ESI-FTICR/MS

High-resolution mass spectra were acquired on a Bruker (Bremen, Germany) APEX Qe Fourier transform ion cyclotron resonance mass spectrometer, equipped with a 12 Tesla superconducting magnet and an APOLLO II electrospray source. For negative electrospray, acetonitrile was used. Samples were introduced into the micro-electrospray source at a flow rate of 120 µl/h (by final optimized FFE separation). The nebulizer gas pressure was set to 20 psi, and a drying gas pressure to 15 psi (@ 250 °C). Spectra were externally calibrated on clusters of arginine (10 mg/l in methanol); calibration errors in the relevant mass range were always below 0.1 ppm. The spectra were acquired with a time domain of 1 megaword with a mass range of 150 –1000 m/z. The spectra were zero filled to a processing size of 2 megawords. Before Fourier transformation of the time-domain transient, a sine apodization was performed. By FT/MS optimization only the non-instrument dependent parameters were took into account, namely the concentration of the applied samples, ionic strength of the buffer and the infusion flow rate, hence these parameters are crucial if in an off-line FFE-FT/MS approach the instruments need to be harmonized. All internal parameter like ESI voltage, mass filtering by Quadrupole, excitation parameters, etc. were formally optimized for SRFA (result not shown here), and those parameters were applied for this approach.

2.1.2.3.1. Calculation

For simple and robust data presentation by electrophoretic data, the vial number based x-axis vs. UV signal was transformed into the corresponding effective mobility-scale (μ_{eff}-scale) versus detection signal electropherogram. With the new scaling, the obtained electropherograms are more representative and the comparison of complete

electropherograms is directly possible [248]. The procedure of the separation window calibration was applied from [247].

The obtained mass spectra were calibrated internally with the generally occurred fatty acids and the calibrated FT-ICR spectra were exported to peak lists at a signal to noise S/N=2. From the exact masses, possible elemental formulas were calculated for each peak in batch mode by a software tool written in-house. The generated formulas were validated by setting sensible chemical constraints (N rule, O/C ratio ≤ 1, H/C ratio $\leq 2n + 2$, element counts: C $\leq$ 80, H unlimited, O $\leq$ 60) in conjunction with an automated theoretical isotope pattern comparison.

2.1.3. Optimization of the FFE separation

In previous work of Junkers et al. [247] the followed optimization was already described, however in our approach it is not directly applicable, since the used buffer namely sodium carbonate, is low volatile, therefore not compatible with the separation followed FT/MS measurements. Hence the similar optimization procedures were conducted here also.

2.1.3.1. Buffer adjustment and calibration of the separation window

As new buffer was introduced into the FFE separation, the system calibration and the separation window adjustment were necessary. Three different level of separation buffer concentration were tried (5, 2.5, 1 mM Ammonium bicarbonate, pH 9.2 (adjusted with ammonium hydroxide (25V/V%) in conjunction with 500 mM electrode buffer as a system installation requirement. As an upper constrain of the separation buffer concentrations, the fact that high ionic strength might hinder the further off-line MS application, and as lower limitation the sufficient buffer capacity were considered. The effect of the various electrode buffers also resulted differences in the separation efficiency, however the concentration, mentioned above, was found preferentially better than if the concentration was lowered (results not shown here). Beside the applied buffer concentration, its flow rate was also varied, in order to maximize and centre the separation. These adjusted rates of the separation buffer were: 1.2(1146mL/h), 1.0(955mL/h), 0.8(760mL/h) (settings before the brackets are referring to the system set-ups). The sample (SRFA) was injected into the system with the concentration of 20 mg/L and flow rate of 2mL/h. The applied high concentration was

necessary while the calculated dilution might reach the 500 folds of the injected concentration (the concentration at the main fractions containing wells might not exceed the 40 µg/L concentration). Additionally the obtained fractions were further diluted during the FT/MS analysis. The calibration was followed with UV-Vis detector at 254 nm (Figure 6.).

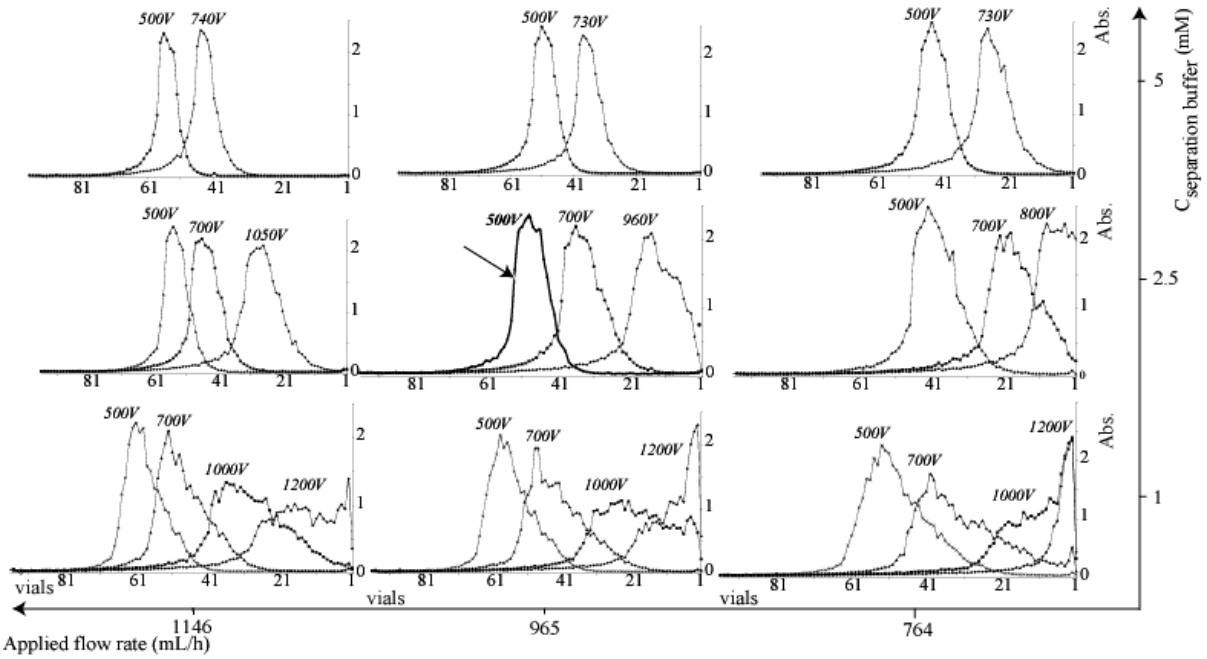

Figure 6. Summary of the FFE separation of SRFA under various conditions. Two dimensional parameter-matrixes were set up to gain good fractionation and still preserve the capability of an off-line analysis with the mass spectrometer. In nine different $c_{separation\ buffer}$ *(mM)-Applied flow rate (mL/h) settings the applied separation voltage was also adjusted to tune the separation. After the separation settings were set and the fractionation is stabilized, the fractions were collected in UV-VIS reader plate with 96 wells to follow the effect of the settings. The absorbance measurements were conducted at 254 nm. The optimum (highlighted with bold) was selected for further application since, its peak shape and centred position in the separation chamber. However broader separation curve assumes better fractionation, it should be noted that these UV-Vis spectra slightly mislead the interpretation of the sample distribution along the separation chamber, since the formally observed Carbon content, as many of the SRFA constituents are not UV-active [247]. However to follow the effect of the settings rapidly absorbance measurements had been sufficient with the above mentioned remarks. For the further analysis the parameters of 500 V separation power, 2.5 mM separation buffer at flow rate of 965 mL/h were applied.*

The conversion of vial numbers into effective mobility scale was described in details in [247]. Briefly, after the essential parameters (Voltage, buffer flow rate and buffer ionic strength) were optimized, these settings were used to verify the behaviour of model compounds (benzoic acid (-0.0186 cm^2/Vmin), phthalic acid (-0.030 cm^2/Vmin), trimellitic acid (-0.038 cm^2/Vmin) and pyromellitic acid (-0.042 cm^2/Vmin) within these conditions and their effective mobilities, which were described formally with CZE system. Based on the

obtained FFE separation of these model compounds and their mobilities correlation could be set up between the effective mobility and the vial numbers (Figure 7.).

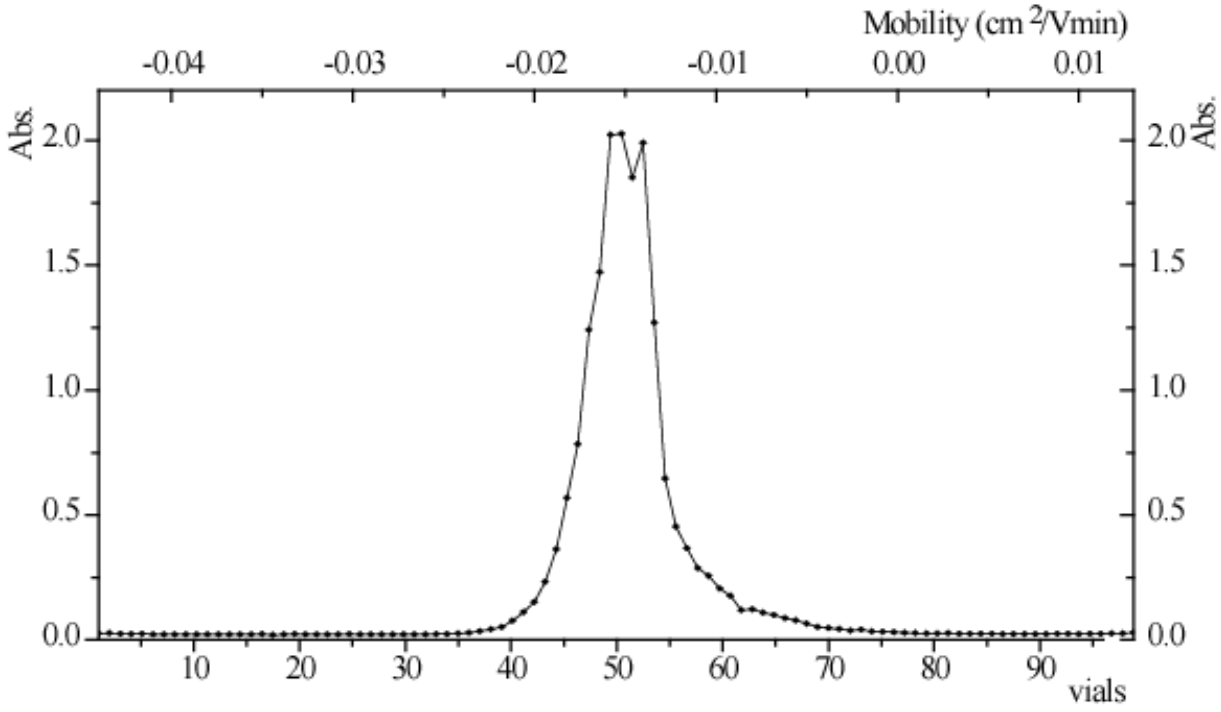

Figure 7. Calculated effective mobility of the obtained fractions over the separation chamber. For details see ref. [247]

2.1.4. Optimization of the FT-ICR/MS settings

Spray solution composition, pH (background electrolyte ionic strength) and infusion flow rates are mainly responsible for the main derivation during analysis of the very same sample. Different organic solvent and their different composition with other solvents for example water were also investigated[236]. Here we conducted an experiment which dedicated to reveal the correlations between buffer concentration (ionic strength) ESI-spray (direct infusion) flow rate and the sample concentration. The dimensions of the experiment were planned to fit with the applied conditions of the FFE fractionation.

Ammonium bicarbonate buffer, similar which was used in FFE separation at three different concentrations with three different flow rates was injected. The initial concentrations were 20, 10 and 5 mM of ammonium bicarbonate, which were diluted 5 folds with acetonitrile before injection resulted 4, 2.5 and 1 mM injected buffer concentration. The applied electrospray infusion flow rates were 30, 60 and 120 μL/h. The applied lowest flow rate caused instability

in the electrospray; hence the results from these settings were not considered as reliable data therefore further applications were avoided. Since the provided concentrations in the FFE fractionations are relatively hard to predict (correlated with the separation efficiency), the tested SRFA initial concentration (before dilution with organic solvent) in the electrospray was over the range of 50-500µg/L. As organic solvent, acetonitrile was used with the dilution of five folds to provide the electrospray stability. The frame of the optimization experiment, including the obtained number of peaks, as a primary indicator of the different settings effect is detailed in Figure 8.

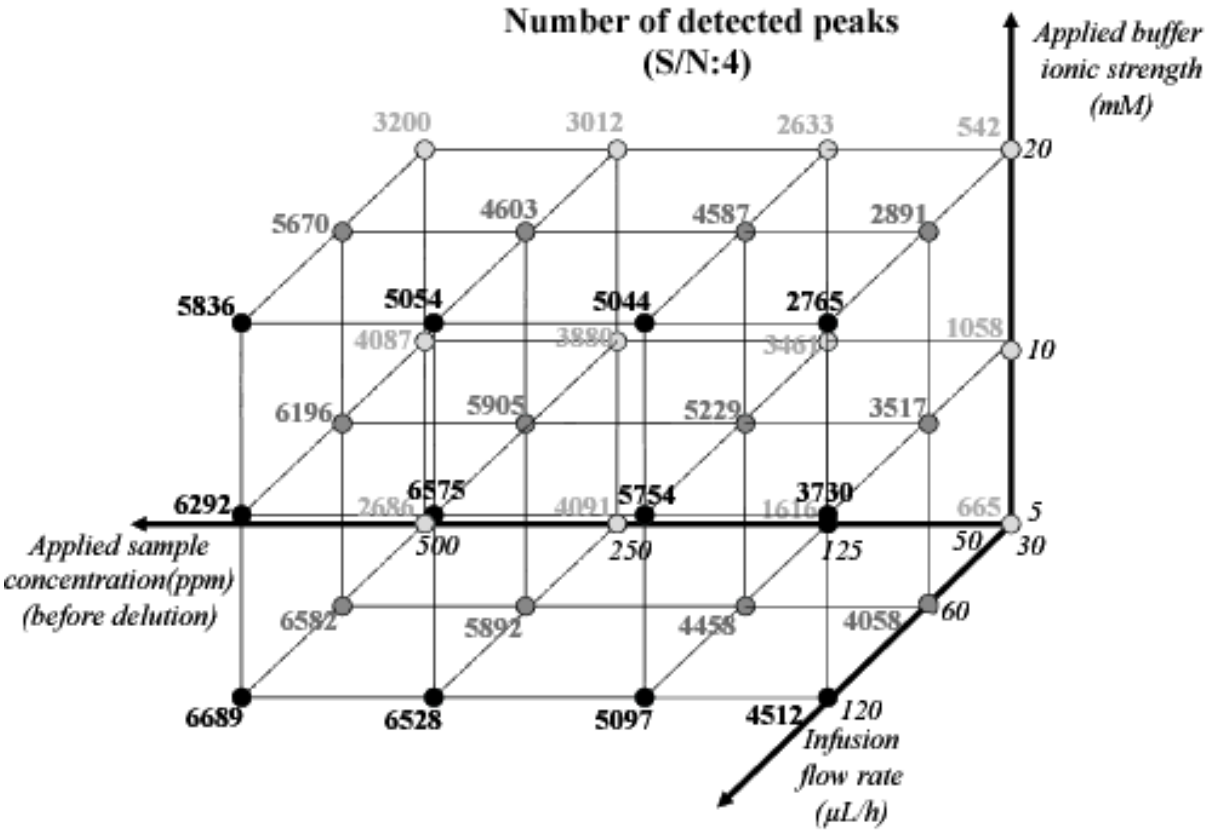

Figure 8. Three-dimensional MS experiment with different external (not instrument dependent) parameters, like infusion flow rate, buffer ionic strength and sample concentration settings. The range of these parameter were set to correspond with the FFE fractionation parameters in order to enable the direct analysis of the obtained fractions. Additionally the infusion flow rate was also investigated to define the lowest applicable value. As a result 36 different combinations of settings were measured, with identically 500 scans per run. The obtained number of peaks (at S/N:4) were highlighted (with light-, dark-grey and black coloured) .

Considering the complexity of the experiment, in three different correlation levels were separated for detailed and comprehensive evaluation. These were: applied sample concentration vs. infusion flow rate, buffer ionic strength vs. applied sample concentration

and buffer ionic strength vs. infusion flow rate, respectively. The obtained number of peaks at each settings were extended with interpolation, resulting a continuous matrix, generated in Origin version 7.5Pro (OriginLab Corporation, Northampton, MA USA), which were used for further visualization, with the assumption that the effect of the parameter settings are incessant within the measured level of parameters. The summarized results are shown in Figure 9.

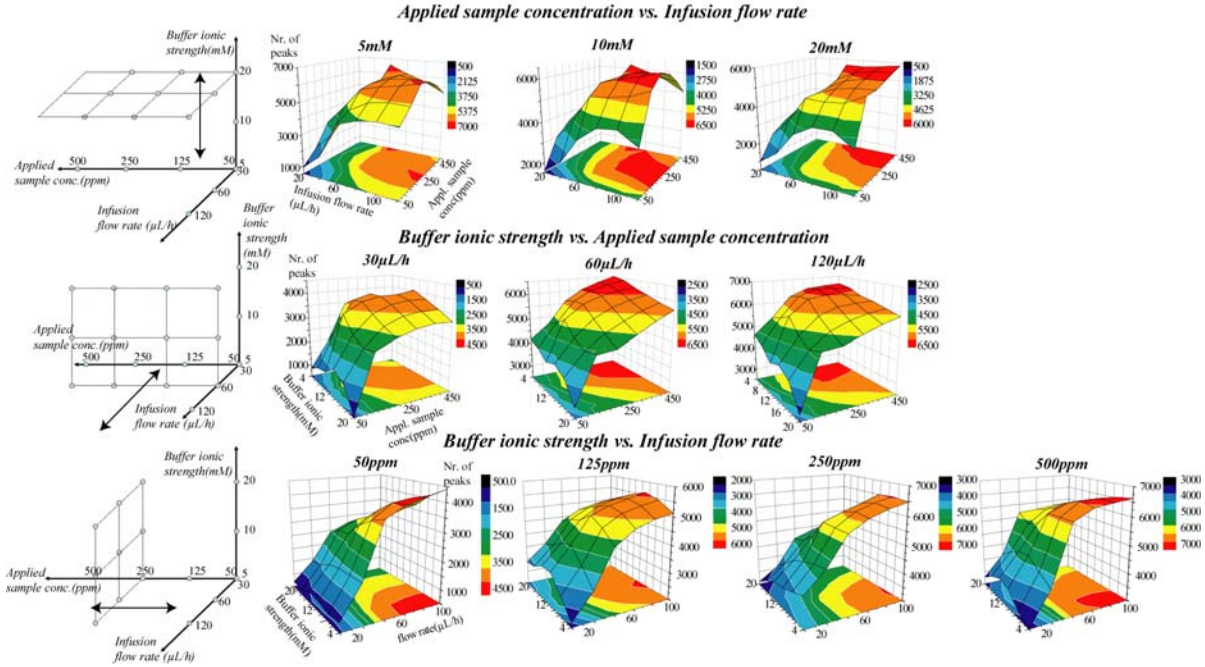

Figure 9. Segregated presentation of the effect of the settings, obtained from 3-D optimization experiment. Assuming that that the effect of these parameters continuous and considering the obtained results (number of detected peaks (Fig. 8.)) only as members of a possible continuum of the 3D frame, interpolation were done by Origin 7.5 program. The obtained incessant matrix was plotted in three different levels; where in each case one setting parameter was fixed.

Overall it could be asserted that the analysis of aqueous complex matrices, the relatively low and volatile buffer concentration is desired. If the concentration of the applied buffer could be lowered, enables to analyze diluted samples. This might be evitable if the sample itself immensely complex and the ion suppression within the probe is not predictable. In our experiments the use of lower than 10mM of ammonium bicarbonate buffer result already higher number of detected peaks, which indicates indirectly efficient ionization.

However it is preferable to decrease parallel the analyte concentration to avoid self assembled dimers which might also affect the number of detected peaks [249]. Additionally the infusion flow rate was also investigated to define the lowest applicable value. In certain cases (preferentially the side fractions in the FFE separation, where beside the low sample

concentration, (relative carbon content) the buffer is predominant it might be useful to decrease the flow rate instead of dilute the sample further to achieve better signal to noise ratio regarding to the sample (allow less ion into the source). The flow rate might be a flexible parameter to change, though in our experiment, under 40µL /h signal instability might occur, hence preferentially it has to be kept above this rate.

2.1.5. Analysis of SRFA

After the optimization procedures, the final settings were used for the sample separation and analysis of the collected fractions. The array of the FFE separation outlet was collected in 96-well microplate and thirteen wells were chosen for direct FT/MS analysis. Before the infusion samples were diluted with acetonitrile without further buffer adjustment. In this article five, the most prominent fractions were highlighted in order to reduce the size of the data (Figure 10).

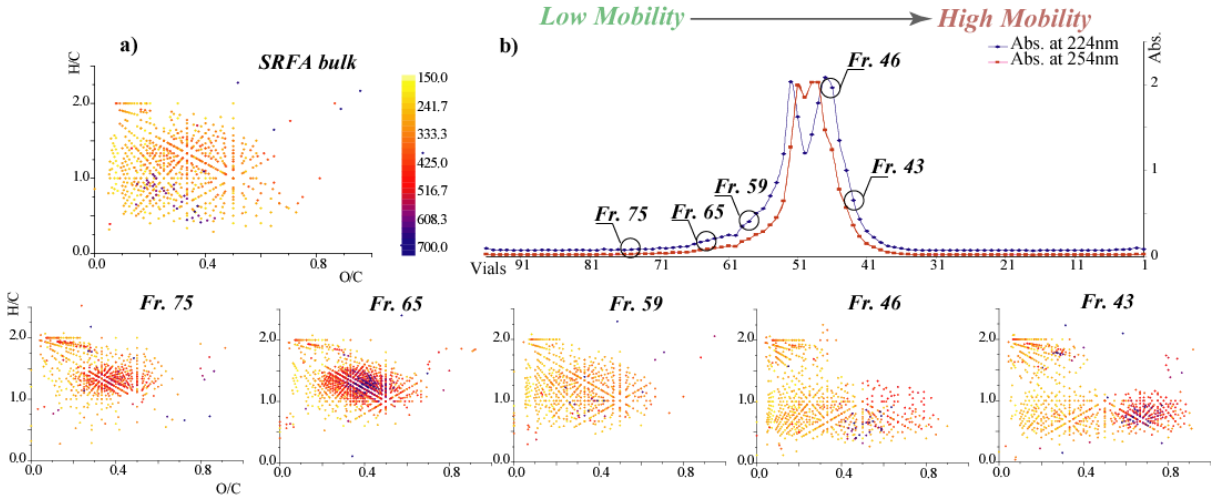

Figure 10. ***a)*** *Molecular elemental ratios for SRFA bulk (25 µg/L) obtained with single infusion negative-ESI/MS with 500 scans. The assigned formulas were introduced into van Krevelen diagram, colour-coded based on the masses of the formulas.* ***b)*** *UV spectra of SRFA at 214nm and 254nm obtained by FFE fractionation. The highlighted vials were diluted with acetonitrile and measured with direct infusion ESI-MS. The van Krevelen plots of the selected fractions represented here with mass based colour-coding.*

The simplified dataset represent the general expectation, namely that FFE separates SRFA constituents according to charge, shape and size characteristics. The obtained separation UV profile and the chosen vials showed in Figure 10/b, where due to the FFE setting, the effective mobility increases in inverse proportion to the number of vials, hence low mobile (relative high molecular weight and low charge density/neutral) molecules will

present towards the cathode and high mobile constituents (with higher charge density and/or lower molecular weight) proceeding towards the anode. In our experiment to follow the expected separation the obtained masses were converted into feasible molecular formulas with an in-house developed software. The observed tendency in the so called van Krevelen diagrams (Figure 10) met the general expectations and the loci of the average H/C and O/C ratios continually shifted from the relatively low O/C and high H/C ratio (fraction No.75 (H/C=1.2;O/C=0.3)) region towards higher O/C and lower H/C values (No.43 (H/C=0.75;O/C=0.7)), when proceeding from lower to higher mobility. Beside the common description, this general tendency can be detailed further if colour-coded representation is enabled. Mass dependent scaling, in third dimension, allows distinguishing between mass or charged driven cases within the high mobile fraction alone. In fraction No. 43 (assigned as high mobile fraction) the assigned molecular formulas could be subdivided into an oxygen-rich and an oxygen-depleted region in the van Krevelen plot. With relative high O/C and low H/C ratios, in contrast with their high molecular weight (see colour scale at figure 10/a) these molecules denote the similar effective mobility as the lower molecular weight but oxygen-depleted constituents. The calculation of their aromaticity index (AI) [144] and their position in van Krevelen plot could result a possible conclusion that the structures of these molecules are rather aromatic (single or multiple rings) with phenolic type hydroxyl functional groups. However they are depleted in possible charge carrying functional groups (respectively to our FFE separation settings (and pH: 9.2) these are negative charged side groups), since their calculated elemental atomic ratios suggest this assumption, their high mobilities could be attributed to their low molecular weight. In contrast to these higher mobile compounds the low mobile fraction (Fraction No. 65 and 75) indicate uniform mass and composition of elemental ratios.

Compared the generated plots with the plot obtained from the direct analysis of the SRFA bulk (Figure 10/a) it is interesting to note that a relative bigger area is covered if the obtained fractions were overlaid into one van Krevelen diagram(Figure 11/b).

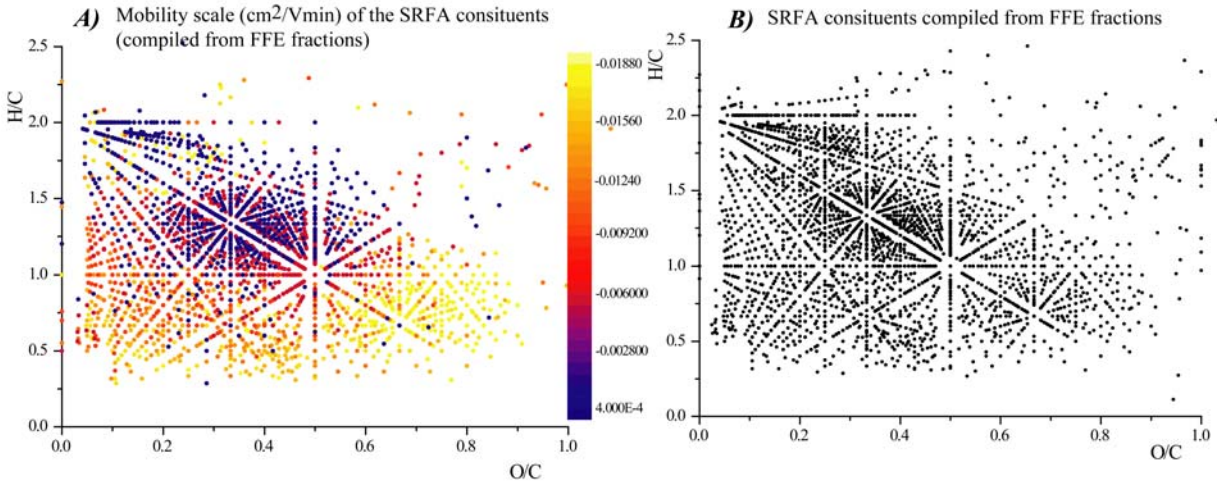

Figure 11. ***a)*** *Molecular element ratios for all assigned ions from the combined fractions colour-coded with their effective mobilities (cm^2/Vmin)* ***b)*** *element ratios plot of SRFA constituents compiled from the obtained FFE fractionation.*

On one hand, this result also supports the original idea, that multi-level characterization and structural analysis of such a vast compositional space like NOM [79] is crucial for a better understanding, since a separation procedure might hinder ion suppression due to the analyte complexity itself (Figure 12.). And on the other hand, a carefully implemented separation (considering possible side effects) step provides extra information referring to the molecular properties.

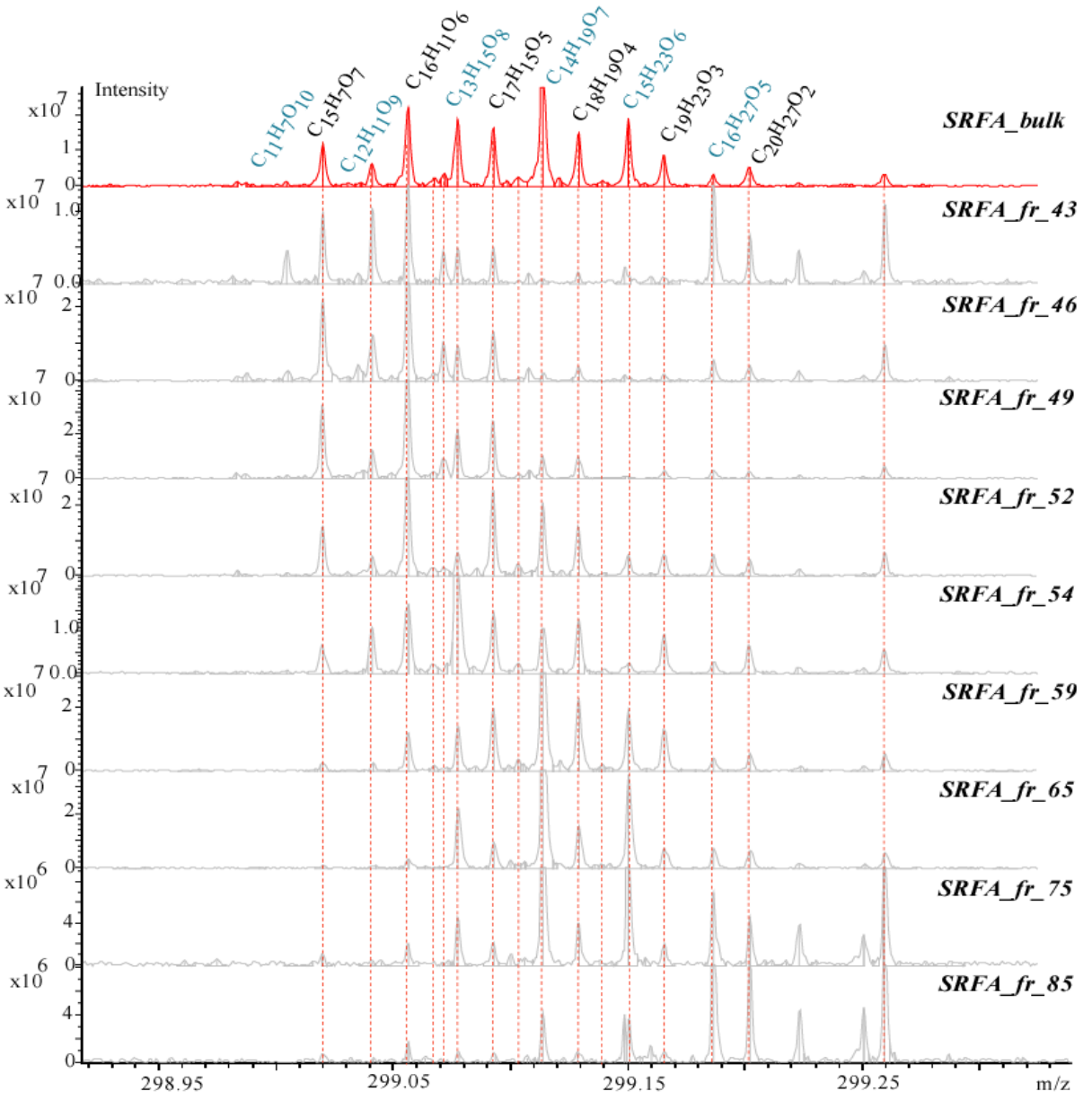

Figure 12. List of FT mass spectra of the nominal mass 299 m/z in which the C,H,O-ions observed. SRFA bulk (coloured with red) and the selected FFE fragments (coloured with grey). The effect of the FFE fractionation results: ***i)*** *continuous allocation of dominant ions from oxygen depleted molecules to oxygen-rich constituents as proceeding to higher mobile FFE fractions;* ***ii)*** *among the assigned constituents the fractions reveal more ions.*

2.1.6. Conclusion

Beyond that, natural organic matter (NOM) is well known to provide an analytical challenge which mainly due to its physical and chemical complexity and versatility, additionally molecular level composition of complex mixtures obtained by ESI-FT-ICR/MS, often leads to such an enormous dataset which might results difficulties during its interpretation. Various ionization sources and mass spectrometers have been utilized for these environmental samples, and emphasize particularly electrospray ionization coupled to ultrahigh resolution Fourier transform ion cyclotron resonance mass spectrometry which has succeeded in the extensive characterization of NOM. Although the exploitation of this unique approach, it is suggested further pre-separation before the analysis in order to gain enhanced dataset. Introducing extra separation results a multi-dimensional approach. Hereby, free-flow separation as an up-scale electrophoretic method was presented and the non-instrument dependent parameters (buffer ionic strength, applied sample, etc.) were harmonized to a possible off-line approach. Since an electrophoretic method separates mixtures based on their charge density and/or their masses without interaction with any surface, FFE has proven its competent as a possible separation technique before the FT/MS run. Beyond the obvious instrument-dependent separation effect (which were presented in this case as charge and mass distribution), a secondary consequence was also observed. The compilation of such fractions represents higher resolved spectra, with higher number of assigned molecular formulas which might led to a better molecular level understanding of mixtures with such a vast complexity.
In the following, FFE fractionations will be characterized further with different analytical approaches like NMR, in order expand the characterized range of substances, that were narrowed by the selectivity of the applied ionization-dependent direct infusion mass spectrometry.

2.2. Molecular characterization of NOM charge density fractions

2.2.1. Introduction

Herein, the characterization of SRNOM was described with different analytical approaches in order to gain further information and able to crosslink the observed results. Preliminary, electrophoretic separation was applied, considering the formally presented settings. To warrant sufficient quantity, long term separation was conducted. The obtained fractions were freeze-dried and spread for the different approaches.

Elemental composition-, amino acid-, and neutral sugar analysis were conducted beside spectroscopic and spectrometric approaches. With the help of the elemental composition analysis, general mass balance was able to set up in order to monitor the organic carbon distribution among the obtained fractions. Though carbohydrates are well known constituents in oceanic organic matter, released in large amounts by growing phytoplanktons, in other surface waters free carbohydrates might be good indicators for alteration state.

Microbes, like bacteria are tend to be the major sources of dissolved organic matter in oceans and amino acids, as constituents of organic matter, have been used to estimate the part of the contribution of bacterial origin in these materials. Bacterial membranes are considered the main sources of amino acids, that are components of the interpeptide bridge in peptidoglycan and contribute the overall rigidity of the cell membrane. Direct amino acid analysis only possible through strong acidic hydrolysis, since amino acids are linked through amide and glycoside bonds. Therefore to obtain a general view on amino acid content and its electrophoretic mobility behaviour, acid-induced hydrolysis followed with liquid chromatography was applied.

As in the former chapter was already suggested, NMR and high resolution MS, as comprehensive and in organic matter characterisation well-known powerful techniques, were utilized.

2.2.2. Methods and Experimental Settings

2.2.2.1. Free-Flow Electrophoretic separation

Fractions, for further analysis, were obtained on an Octopus PZE free-flow electrophoresis device manufactured by Dr. Weber GmbH (Kirchheim, Germany). The dimensions and operations settings of the separation and the instrument were detailed formally in Chapter 2. To obtain the fractions, the formally optimized settings were utilized. After the sample was introduced and the separation has reach its equilibrium, from array of outlet tubes samples were collected in tray which contains 96 wells for further UV analysis. Based on the denoted spectrum at 254 nm (Figure 13), the 96 tubes were grouped and the effluents were pooled in 11 different bottles. These pooled samples were freeze-dried and stored for further analysis.

2.2.2.2. Elemental composition analysis

The organic carbon and nitrogen contents of dried fractions were measured using a Carlo Erba 1108 CHN analyzer.

2.2.2.3. Neutral sugar analysis

Neutral sugars were analyzed according to Skoog and Benner [68, 174, 175] with modifications. Briefly, samples were hydrolyzed in 1.2 mol L^{-1} sulfuric acid and neutralized with a self-absorbed retardation resin (Kaiser and Benner 2000). After desalting with a mixture of cation and anion exchange resins, neutral aldoses were isocratically separated with 25 mM NaOH on a PA 1 column in a Dionex 500 system with an amperiometric detector (PAD). Chromatography of all neutral sugars was carried out at a flow rate of 1 ml min^{-1} under standard conditions. The following detector settings were used: E_{DET}=0.05 V (t_{DEL}=200 ms, t_{INT}=200 ms), E_{OX}=0.75 V (t_{OX}=200 ms), E_{RED}=-0.15 V (t_{RED}=400 ms).

2.2.2.4. Amino acid analysis

Enantiomeric amino acids were separated on a Licrospher 100 RP18 (250x4 mm, 5 µm) with a guard column (5x4 mm) after in-line derivatization with o-phthaldialdehyde/N-

isobutyryl-L-cysteine (OPA/IBLC) or o-phthaldialdehyde/N-isobutyryl-D-cysteine (OPA/IBDC) at 20 °C. The system was an Agilent HP 1100 system with an auto sampler and fluorescence detector controlled by HP Chemstation software. Samples were hydrolyzed with 6 M HCl in sealed ampoules for 20 h at 110°C. After hydrolysis, dry and neutral samples were dissolved in 100 µL water and 5 µL of L-glutamic acid-methyl-ester, the internal standard, was added. Vigorous vortexing usually dissolved the entire dried residue in the micro-inserts. Insoluble particles were removed by centrifugation and the sample was carefully transferred to a new micro-insert if necessary. To facilitate separation of enantiomeric amino acids a second chiral center was introduced by derivatization with IBLC and IBDC. Samples were run with both reagents, which allowed for correction of co-eluting peaks. Usually 30 µl of sample and 20 µl of IBL(D)C reagent were drawn into the sample loop and mixed inline for 2 min. After injection, the gradient program was started. For samples with >500 nM individual amino acids, 10 µl of sample were mixed with 10 µl of 0.5 M borate acid buffer (pH=9.5) and 10 µl IBL(D)C reagent. Samples were run alternating first with OPA/IBLC then OPA/IBDC.

Method program and gradient: Phase A was 40 mM potassium di-hydrogen phosphate adjusted to pH 12, phase B was methanol : acetonitrile (13:1 v/v); linear gradient 100 % A initial to 61 % A at 50 min, 46% A at 72 min and 40 % A at 80 min; then 100 % A at 85 min until 87 min. Total run time was 87 min. The flow rate was 0.9 mL min^{-1}. Excitation was set at 350 nm and emission of OPA derivatives was recorded at 420 nm[178].

2.2.2.5. FT-ICR/MS

Fractions were dissolved in methanol directly before the analysis and the pH were adjusted to 9.0 for each fractions with ammonium hydroxide. Ultra-high resolution mass spectra were acquired with a Bruker APEX Qe Fourier transform mass spectrometer (FT-ICR/MS) equipped with a 12 Tesla superconducting magnet and an Apollo II electrospray source. The samples were injected with direct infusion with the flow rate of 2 µL/min. The spectra were obtained in negative mode with the number of data points per measurements of 4 MW(time domain size) with the typical resolution of 5 $*10^5$. 512 scans were collected for each fraction.

2.2.2.5.1. Molecular formulae assignment

The spectra were externally calibrated on arginine clusters and then internally recalibrated with fatty acids. Once the exact masses of the molecules had been determined, their molecular formulae were batch-calculated by a software tool, written in-house. Following chemical constrains were applied: the maximum number of elements C,H unlimited, O(50) tolerance of mass error by ^{13}C isotope search ≤ 0.5ppm. The generated formulas were validated by setting sensible chemical constraints (N rule, O/C ratio ≤ 1, H/C ratio ≤ 2n + 2, element counts: C ≤ 80, H unlimited, O ≤ 60) in conjunction with an automated theoretical isotope pattern comparison.

2.2.2.6. NMR Spectroscopy

All experiments in this study were performed by N. Hertkorn, on a Bruker DMX 500 spectrometer at 303 K. About 10-30 mg SRNOM sample dissolved in about 250 µl 0.1 N NaOD for ^{1}H NMR, ^{13}C NMR and 2D NMR spectroscopy was transferred under exclusion of air into (then) sealed 3 mm capillary NMR tubes. The reference for ^{1}H NMR was $(H_3C)_3Si$-CD_2-CD_2-COONa (-0.14 ppm) and for ^{13}C an external reference (CH_3OH in D_2O: 49.00 ppm) was used. All proton detected NMR spectra were acquired with a 5 mm z-gradient $^{1}H/^{13}C/^{15}N$ TXI cryogenic probe using 90° excitation pulses (90°(^{1}H) = 8.3 µs; 90°(^{13}C) = 19 µs). 1D ^{1}H-NMR spectra were recorded using the first increment of the presat-NOESY sequence (solvent suppression with presaturation and spin-lock, 5.0 s acquisition time, 10.0 s relaxation delay, 64-80 scans, 1 ms mixing time, 1 Hz exponential line broadening). ^{13}C-NMR spectra were acquired with a cryogenic 5 mm $^{13}C/^{1}H$ dual probe (90°(^{13}C) = 9.75 µs), using a spin-echo sequence (10µs delay) with inverse gated WALTZ-16 decoupling (14 s relaxation delay; several ten-thousands of scans each from about 1-3 mg SuwNOM sample) with an acquisition time of 1 s and an exponential line broadening of 35 Hz.

The one bond coupling constant $^{1}J(CH)$ used in 1-D ^{13}C DEPT and 2D $^{1}H,^{13}C$ DEPT-HSQC spectra was set to 145 Hz [DEPT-HSQC NMR spectra were acquired with 320 scans and 312 increments]. Carbon decoupled $^{1}H,^{13}C$-HSQC NMR spectra were acquired under the following conditions: ^{13}C-90-deg decoupling pulse, GARP (70µs); F2 (^{1}H): acquisition time: 183 ms at spectral width of 5482 Hz, $^{1}J(CH)$ = 150 Hz, 1.82 s relaxation delay; F1 (^{13}C): SW = 22637 Hz (180 ppm); number of scans(F2)/F1-increments (^{13}C frequency). HSQC and DEPT-HSQC spectra were calculated to a 2048 x 512 matrix with exponential line

broadening of 30 Hz in F2 and a shifted sine bell (□/6) in F1. Gradient. but not sensitivity-enhanced, sequences (1 ms length. 450 μs recovery) were used for all proton detected spectra.

2.2.2.6.1. Analysis of NMR spectra

NMR integrals were measured manually from printed spectra. Difference NMR spectra were obtained using XWinNMR 3.0 software from spectra rather than from FIDs. Bucket analysis (Brindle. et al., 2002) was performed on the experimental and edited ^{13}C NMR spectra; these were decomposed into 250 equidistant integral segments with 1 ppm bandwidth. ranging from 0-220 ppm (Figure 17). Linear combination of DEPT-45. 90. and 135 ^{13}C NMR spectra produced edited sub-pectra of methane, methylene and methine carbon; the H/C ratio of the protonated carbon atoms was computed from bucket analyses: the difference of DEPT-45 spectra (showing all protonated carbon atoms) and the sum of the individual edited spectra was minimized.

2.2.3. Up-scaled electrophoretic fractionation

Electrophoretic separation, obtained on a FFE system yielded 96 fractions, that were separated based on their denoted mass and charge conditions. The basic set up of such an instrument results a homogenous electric field between the electrodes (horizontal), and according to the separation medium speed (vertical direction) and to the electrophoretic mobility (horizontal direction), molecules migration towards the anode (in negative mode). The effective mobility increases in inverse proportion to the number of vials, hence low mobile (relative high molecular weight and low charge density/neutral) molecules will present towards the cathode and high mobile constituents (with higher charge density and/or lower molecular weight), proceeding towards the anode. The similar phenomena were observed during the separation of SRNOM sample (Figure 16.). In laminar flow, in absence of the electric potential, a narrow band was observed and collected in sample vials 82-84. If the electric field was applied, the formally observed narrow band of sample was spread and moved towards the anode. The adjacent wells were pooled into 11 different fractions (Figure 13.) based on the denoted UV spectra. Grouping based on the mass balance of the fractions was not taken place, resulting unfortunately a lack of dried material from fraction 1,2,3,4 and 11.

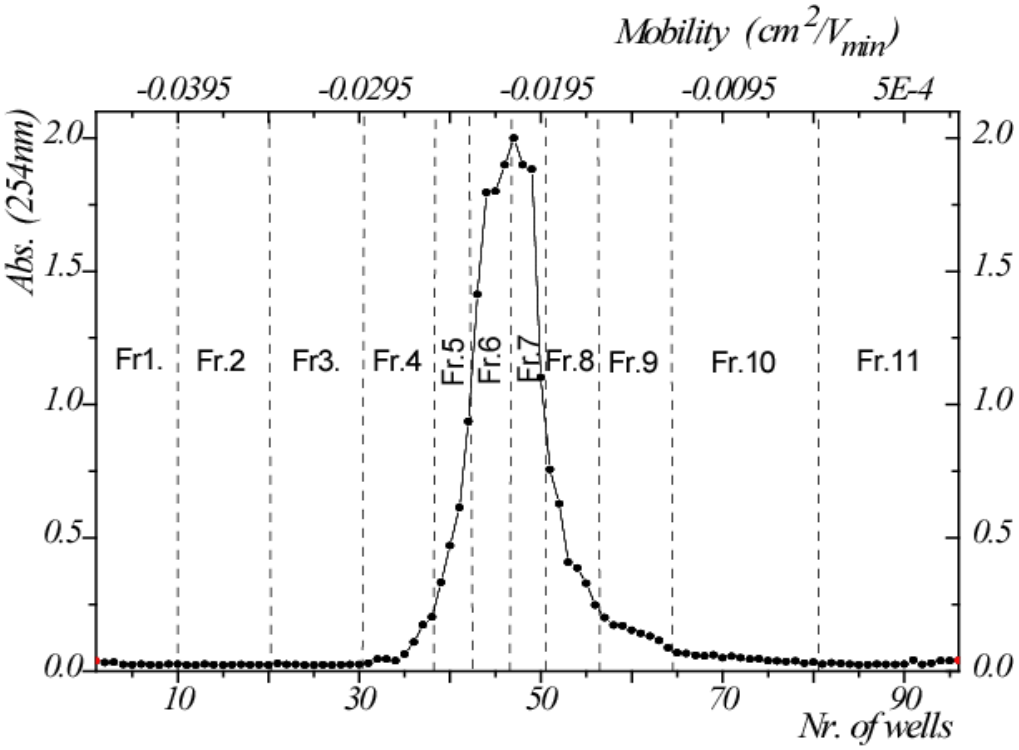

Figure 13. Pooled fractions of Suwannee river NOM (SRNOM) via free-flow-electrophoresis.

2.2.4. Elemental composition

Elemental composition of the bulk and the fractions, derived from elemental analyzer, has show in table 1. The results, obtained from the bulk material, were in agreement with the generally described values for these type of samples, but the fractions showed strong deviations in nitrogen content and therefore in C/N ratios. This artefact could be explained with external nitrogen contamination. During the separation process, ammonium bicarbonate buffer was applied as separation media, since from the earlier optimization experiments this volatile buffer showed good hyphenation properties with the ms approach. Although low concentration of buffer was applied, evidently after the freeze-drying process nitrogen still remained in the sample. Most probably was in salt form.

However for further calculations, like mass balances or yields, the carbon content carried valuable information. From figure 13., fractions 5-10 were considered as the main fractions, containing most of the separated bulk material.

Sample ID	wt (mg)	wt C (mg)	wt N (mg)	wt% C	wt% N	C/N
SR NOM	0.653	0.311	0.01	47.67	1.5	37
FR2	0.542	0	0	-	-	-
FR3	0.272	0.047	0.023	17.44	8.47	2.4
FR5	0.612	0.24	0.048	39.24	7.84	5.8
FR6	0.491	0.209	0.034	42.66	6.97	7.1
FR7	0.571	0.258	0.033	45.27	5.84	9
FR8	0.52	0.238	0.028	45.83	5.47	9.8
FR9	0.726	0.309	0.04	42.61	5.48	9.1
FR10	0.909	0.351	0.059	38.63	6.45	7
FR11	0.988	0.126	0.009	12.71	0.92	16

Table 1. Results of the elemental composition analysis. The measured carbon and nitrogen content, were given in mg (3rd and 4th columns, respectively), which were obtained by the burning of the weighted samples (2nd column).

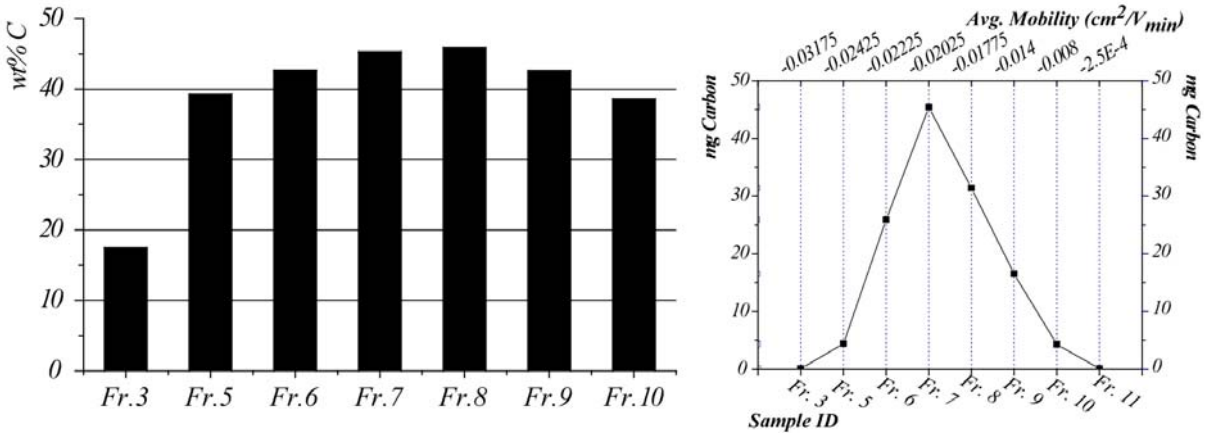

Figure 14. carbon content of the SRNOM FFE fraction in percentages (left) and in mg confronted with the average electrophoretic mobility(right).

The general mass balance (Figure 14.) of the fractionation was also calculated in order to have information about the yield of fractionation (Table 2.). The weight percentages were used in combination with the used and remained weights. The so calculated yield was almost 80% percent in weight and 73% in carbon content, respectively. The observed loss might due to the general fact that directly after the bulk material was dissolved and introduced to the system, 30 minutes waiting time was applied, in order to start the fraction collection, after the

system reached its equilibrium. Furthermore sample transfer and handling might also cause sample loss.

Sample ID	wt% C	CHN analysis (mg)	Nat. sugars (mg)	AA analysis (mg)	Residues (mg)	Sum	mg C
SR NOM	**47.67**	0.653	0.58	1.46	366	368.7	175.7
FR2	**-**	0.542	0.62	0.53	0	1.7	
FR3	**17.44**	0.272	0.42	0	0	0.7	0.1
FR5	**39.24**	0.612	0.62	1.82	8.1	11.2	4.4
FR6	**42.66**	0.491	0.53	1.65	58.12	60.8	25.9
FR7	**45.27**	0.571	0.92	1.36	97.5	100.4	45.4
FR8	**45.83**	0.52	0.69	1.79	65.5	68.5	31.4
FR9	**42.61**	0.726	1.28	1.56	35.2	38.8	16.5
FR10	**38.63**	0.909	0.64	0.78	8.8	11.1	4.3
FR11	**12.71**	0.988	0	0	0	1.0	0.1
					sum(mg):	**294.1**	**128.2**
					Yield of fractionation(%):	**79.8**	**73**

Table 2. general mass balance of the fractionated and the original samples. The carbon contents for each fractions and the original samples (last column) were given as the multiplication of masses and their relevant wt% of carbon, obtained by FFE fractionation. The general yield of fractionation was almost 80% (73% for C content).

2.2.5. FT-ICR/MS

For direct infusion FT/MS analysis, samples were diluted with methanol and injected without further modification. Fr Nr. 5-10 and the bulk SRNOM were analyzed and the results, derived from mass spectra, were converted into molecular formulae. These were plotted in van Krevelen diagrams (Figure 15. and 16.).

The molecular formulae, derived from the obtained mass spectrum of the bulk material, cover a relative wide region in the van Krevelen diagram, denoting a complex array of constituents within the sample (Figure 15.).

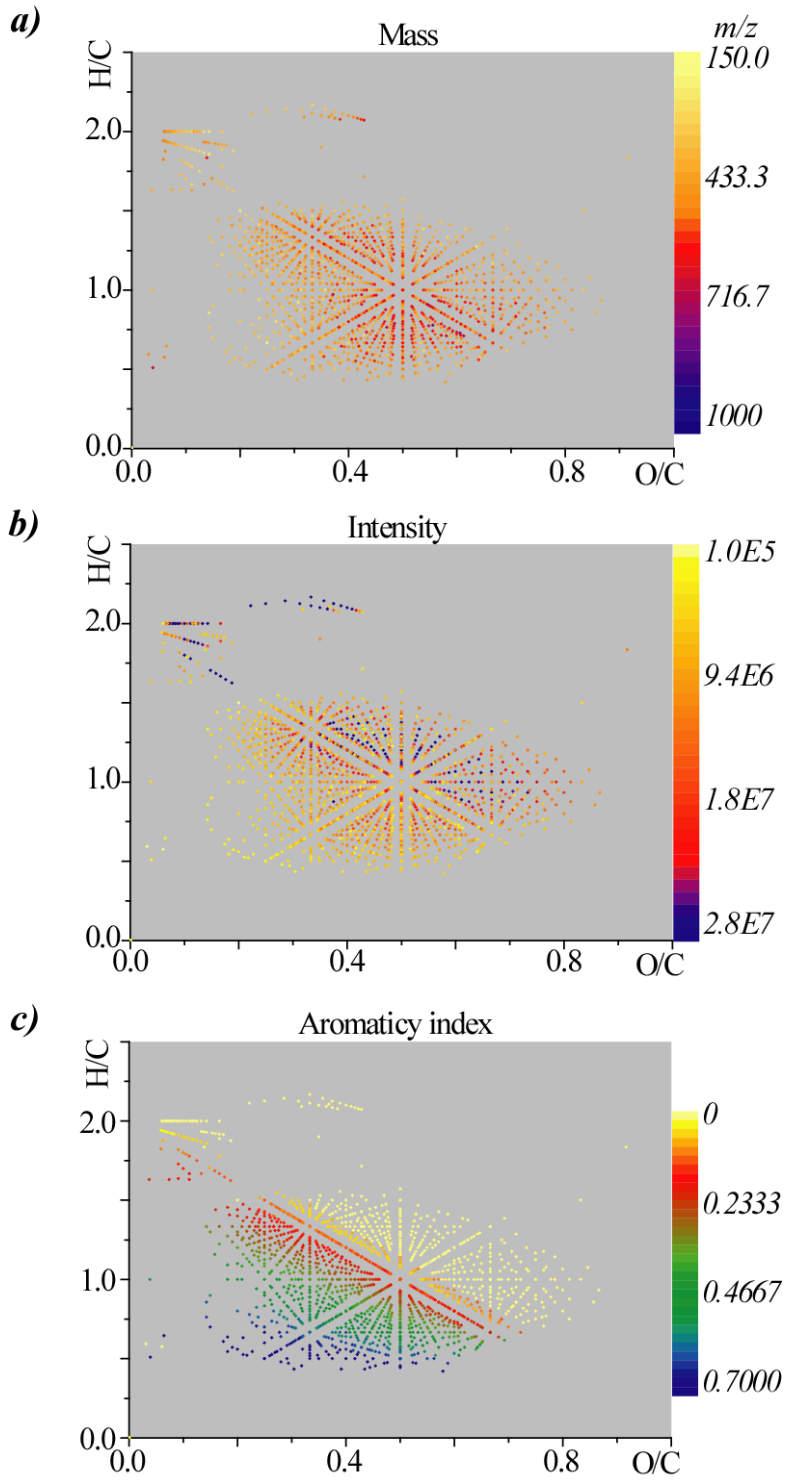

Figure 15. van Krevelen diagrams of the non-fractionated SRNOM derived from 12 Tesla ICR-FT/MS analysis. ***a)*** *Colour-coded by their denoted masses (m/z);* ***b)*** *intensity distribution;* ***c)*** *Aromaticity-index[144];*

The converted dataset represent the general expectation, namely that FFE separates SRNOM constituents according to charge, shape and size characteristics. Due to the FFE setting, the effective mobility increases in inverse proportion to the number of vials, hence

low mobile (relative high molecular weight and low charge density/neutral) molecules will present towards the cathode and high mobile constituents (with higher charge density and/or lower molecular weight) proceeding towards the anode. The observed tendency in the pooled fractions in the van Krevelen diagrams (Figure 16) met the general expectations and the loci of the average H/C and O/C ratios continually shifted from the relatively low O/C and high H/C ratio (fraction No.10 (H/C=1.3;O/C=0.4)) region towards higher O/C and lower H/C values (No.5 (H/C=0.7;O/C=0.7)), when proceeding from lower to higher mobility. Beside the common description, this general tendency can be detailed further if colour-coded representation is enabled.

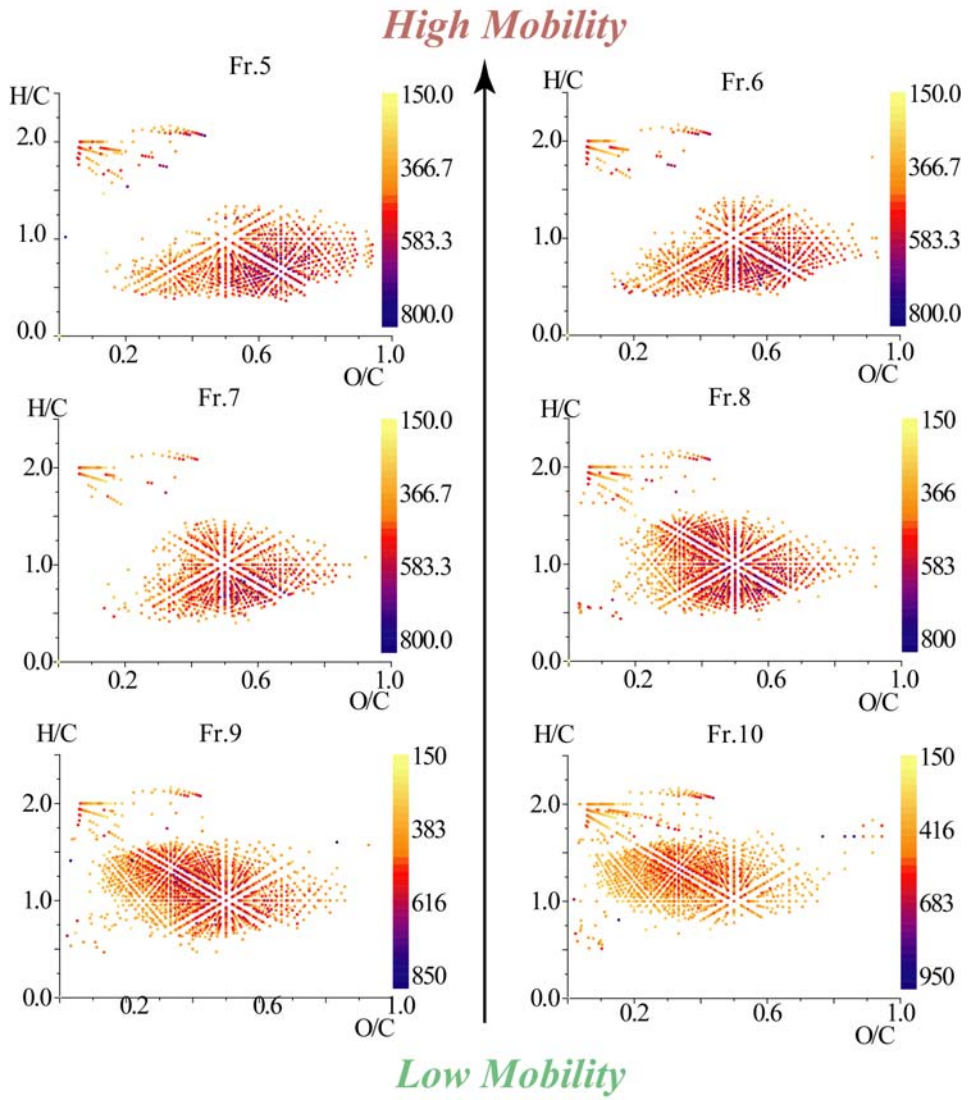

Figure 16. van Krevelen diagrams of the fractionated SRNOM samples.

Mass dependent scaling, in third dimension, allows distinguishing between mass or charged driven cases within the high mobile fraction alone. In fraction No. 5 (assigned as high

mobile fraction) the assigned molecular formulas spread over the regions, depicted as an oxygen-rich and an oxygen-depleted, in the van Krevelen plot. With relative high O/C and low H/C ratios, in contrast with their high molecular weight (see colour scale in Figure 16) these molecules denote the similar effective mobility as the lower molecular weight but oxygen-depleted constituents. Their position in van Krevelen plot could result a possible conclusion that the structures of these molecules are rather aromatic (single or multiple rings) with phenolic type hydroxyl functional groups. However they are depleted in possible charge carrying functional groups (respectively to our FFE separation settings (and pH: 9) these are negative charged side groups), since their calculated elemental atomic ratios suggest this assumption, their high mobilities could be attributed to their low molecular weight.

2.2.6. NMR

Eleven fractions of SRNOM were obtained; however, only SRNOM fractions 6 through 10 were obtained in sufficient quantity to warrant a full scale NMR analysis. From these five fractions and the non fractionated sample, one-dimensional ^{1}H NMR as well as (standard and multiplicity-edited) ^{13}C NMR spectra have been acquired (Figure 17) and the section integrals computed (Tables 3 and 4 and Figure 18; i.e. visual display of tables 3 and 4).

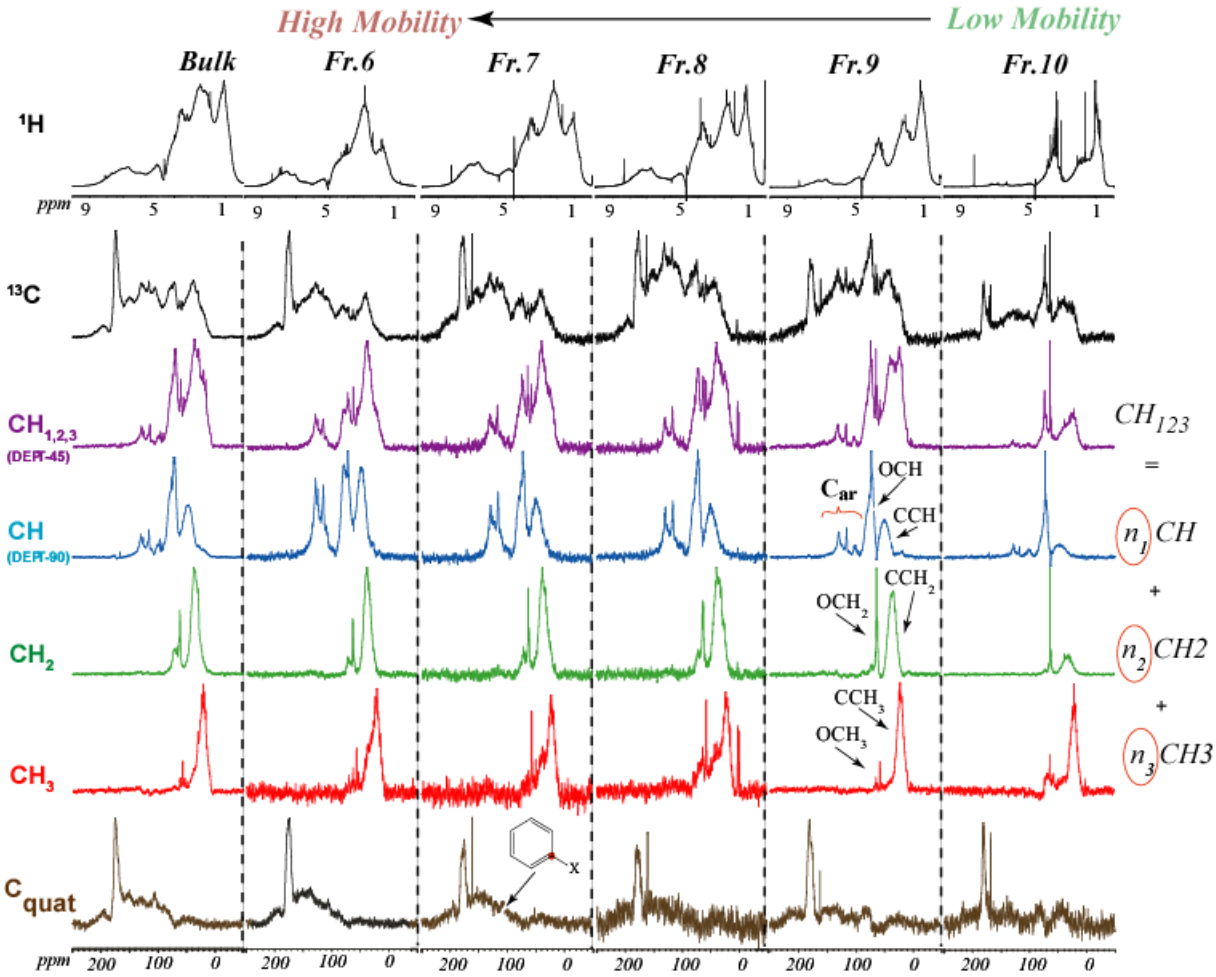

Figure 17. NMR spectra of SRNOM fractions 6-10 and the non-fractionated sample (left): ^{1}H (top), ^{13}C (second from top), DEPT-45 (purple, depicting CH_{123}), edited ^{13}C NMR spectra (blue: CH, green: methylene CH_2; red: methyl CH_3), and QUAT ^{13}C NMR spectra (bottom, black), depicting quaternary carbons only. The spectra were rescaled, therefore they do not represent the differences in the intensities.

SAMPLE	6.0 - 10.0	4.7 - 6.0	3.1 - 4.6	1.95 - 3.1	0.5 - 1.95
Fr. 6	13.38	4.52	22.42	38.88	20.80
Fr. 7	13.70	5.94	24.84	30.86	24.66
Fr. 8	12.44	4.50	23.60	28.11	31.35
Fr. 9	8.58	3.36	19.40	27.46	41.20
Fr. 10	3.17	2.34	28.36	14.01	52.12
SRNOM bulk	10.09	5.5	23.67	30.28	30.46

Table 3. ^{1}H NMR section integrals of SRNOM fractions [δ(^{1}H) / ppm]. General assignments for the 5 major regions of the ^{1}H-NMR spectra are as follows: ***(1)*** *0.5–1.95 ppm range, where protons on methyl and methylene carbons are directly bonded to other carbons often represent methyl groups terminating aliphatic units, but the hydrogen bound to saturated carbon with heteroatoms at least three bonds away;* ***(2)*** *1.95– 3.1 ppm range, protons on methyl and methylene carbons bound to functionalized carbon atom (carboxyl-,carbonyl- and keto groups) ,heteroatoms are two bonds away from the H;* ***(3)*** *3.1–4.6 ppm, protons on methyl, methylene, or methyne carbons directly bonded to O or N, including carbohydrate and amino acid protons;* ***(4)*** *4.7-6.0 ppm range, acetal and* ***(5)*** *6.0–10.0 ppm range, where protons attached to unsaturated carbons and aromatic protons, known as olefinic and aromatic region.*

SAMPLE	187 - 220	167 - 187	145 - 167	108 - 145	90 - 108	47 - 90	0 - 47
Fr. 6	4.08	19.55	11.36	25.46	9.27	17.73	12.55
Fr. 7	6.69	16.48	11.72	25.46	8.70	17.03	13.92
Fr. 8	3.60	12.43	12.15	27.00	9.72	23.40	11.70
Fr. 9	3.60	10.01	7.81	21.52	9.51	29.53	18.02
Fr. 10	1.83	11.93	6.42	18.35	7.34	31.65	22.48
SRNOM bulk	2.73	14.36	11.09	22.27	9.10	22.09	18.36

Table 4. ^{13}C NMR section integrals of SRNOM fractions [δ(^{13}C) / ppm]. The following major spectral bands were identified and integrated: ***(1)*** *0–47 ppm, representing mainly aliphatic or paraffinic carbon chains, primary aliphatic amines and some α-carbons of amino acids;* ***(2)*** *47–90 ppm, representing carbon atoms bound to one or more heteroatoms, primarily methoxyl (OCH3) groups, secondary aliphatic amines, and aliphatic ethers, the upper section often denoted as the "carbohydrate region";* ***(3)*** *90–108 ppm range for carbohydrate RC–OH or RC–OR functional groups, anomeric carbons of carbohydrates;* ***(4)*** *108–145 ppm range, as a result of resonance from aromatic carbons;* ***(5)*** *145–167 ppm range, representing the phenolic groups, O/N substituted sp^2-carbons;* ***(6)*** *167–187 ppm range, corresponding to carboxylic, carbonyl, amine, and ester carbons in NOM.* ***(7)****187-220 ppm range, carbonyl groups, ketones and aldehydes.*

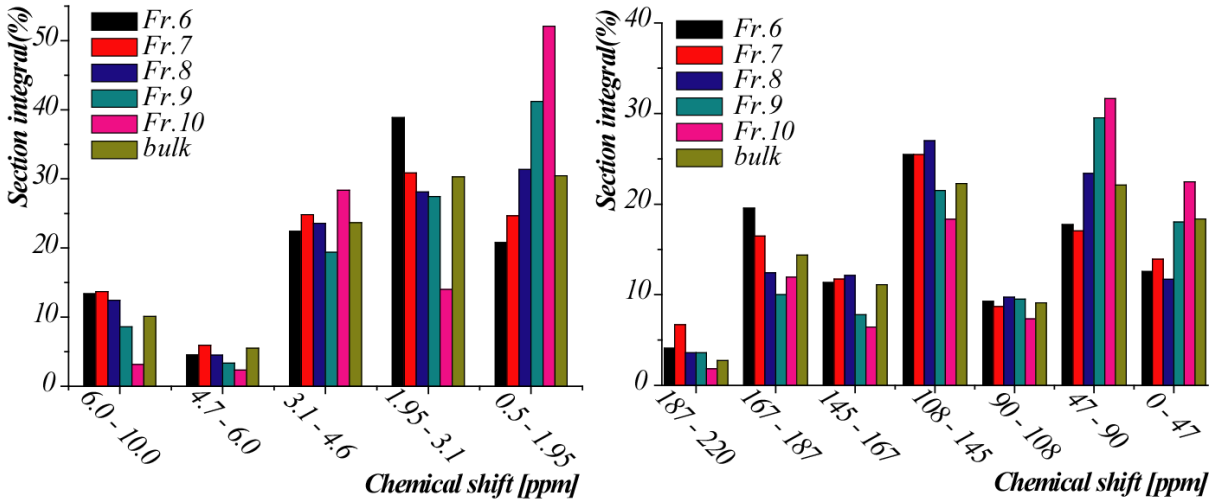

Figure 18. ^{1}H (left) and ^{13}C NMR (right) section integrals of SRNOM fractions

Identical samples were initially used for the acquisition of ^{1}H and ^{13}C NMR spectra. The rather sizable concentration required to achieve decent signal-to-noise ratio in ^{13}C NMR spectra led to appreciable line broadening in the ^{1}H NMR spectra. Therefore, separate ^{1}H NMR spectra with improved resolution have been later reacquired from dilute solutions of SuwNOM.

The inter-pulse delay in the ^{13}C NMR spectra (d1+aq = 15sec) at considerable digital resolution (aq = 1 sec) was sufficiently long to depict near quantitative relationships between NMR section integrals and occurrence of fundamental structural units.

At first glance, the NMR section integrals and line characteristics of the SRNOM fractions cover a sizable bandwidth of properties in both ^{1}H and ^{13}C NMR spectra, while the NMR spectra of the non-fractionated SRNOM represent near average values (Figure 18.).

As deduced from proton and carbon NMR spectra, the content of aromatic units is near constant in SRNOM fractions 6-8 and decreases considerably through out the fractions 9 and 10. The content of singly oxygenated (O-CH) groups stays near constant throughout SRNOM fractions 6-10 according to both proton and carbon NMR spectra. Strong intensity alterations occur in the aliphatic section, which is here divided into two regions, the "purely aliphatic region", comprised of **HC**-C-C units (i.e. heteroatoms are at least three bonds away from either protons ^{1}H NMR and carbons ^{13}C NMR) and the "functionalized aliphatic region", which is comprised of, e. g., **HC**-C-X units with X = O, N, S, including (δ -carbonyl protons in various chemical environments).

The proton NMR spectra indicate a strong increase in the purely aliphatic region and a similar extent of decrease in the region of functionalized aliphatics when proceeding from

SRNOM fraction 6 to 10. In carbon NMR, the upfield section [$\delta(^{13}C)$: 0…47 ppm], which comprises both types of "pure" and "functionalized" aliphatics ranges near constant from SRNOM fractions 6 – 8 and increases through SRNOM fractions 9 and 10, just opposite the trend observed in aromatic contents.

The average acidity as derived from the carbonyl-derivative section integral in the ^{13}C NMR spectra [$\delta(^{13}C)$: 167-187 ppm] near continually decreases from SRNOM fraction 6 through 10. The quantity of carboxylic carbon necessarily correlates with that of C- δ because of direct chemical bond between COOH and C- δ; the respective δ -carbon atoms "by definition" are functionalized. The increase of both carboxylic content and aliphatic functionalization deduced from NMR data is expected to directly affect the migration behaviour of SRNOM in free flow electrophoresis, in which separation is most likely governed by COOH-occurrence and extent of carboxylic dissociation.

More in-depth compositional relationships among these samples can be derived from analysis of NMR bucket integrals. For similarity assessment of proton NMR spectra, 100 buckets with 0.1 ppm width were used in the range of $\delta(^{1}H)$ = 0…10 ppm under exclusion of the residual HDO resonance; for ^{13}C NMR spectra, 250 buckets with 1 ppm bandwidth each were used, ranging from $\delta(^{13}C)$ = 0…250 ppm perform bucket analysis.

	basic unit	C=O	COOH	C(ar)-O	C(ar)-H	OC(H)-O	HC-O	CH_2	non-corr. for CH_123
H/C ratio		**0**	**1**	**0**	**1**	**1**	**1**	**2**	
	Fr. 6	0	19.55	0	25.46	9.27	17.73	25.1	**0.9711**
	Fr. 7	0	16.48	0	25.46	8.7	17.03	27.84	**0.9551**
	Fr. 8	0	12.43	0	27	9.72	23.4	23.4	**0.9595**
	Fr. 9	0	10.01	0	21.52	9.51	29.53	36.04	**1.0661**
	Fr. 10	0	11.93	0	18.35	7.34	31.65	44.96	**1.1423**
	SRNOM bulk	0	14.36	0	22.27	9.1	22.09	36.72	**1.0454**
	basic unit	**C=O**	**COOH**	**C(ar)-O**	**C(ar)-H**	**OC(H)-O**	**HC-O**	**CH_2**	
O/C ratio		**1**	**2**	**1**	**0**	**2**	**1**	**0**	
	Fr. 6	4.08	39.1	11.36	0	18.54	17.73	0	**0.9081**
	Fr. 7	6.69	32.96	11.72	0	17.4	17.03	0	**0.858**
	Fr. 8	3.6	24.86	12.15	0	19.44	23.4	0	**0.8345**
	Fr. 9	3.6	20.02	7.81	0	19.02	29.53	0	**0.7998**
	Fr. 10	1.83	23.86	6.42	0	14.68	31.65	0	**0.7844**
	SRNOM bulk	2.73	28.72	11.09	0	18.2	22.09	0	**0.8283**

Table 5. H/C and O/C ratios of seven fundamental NOM building blocks found in SRNOM fractions 6-10 and non-fractionated SRNOM.

A ^{13}C NMR-based reverse mixing model was used to compute the elemental H/C and O/C ratios of SRNOM fractions 6-10 and non-fractionated SRNOM.

Seven regions of chemical shift were attributed to fundamental building blocks with given H/C and O/C ratios as proposed in Table 5. In the basic version of the mixing model (uncorrected for carbon multiplicity), the transition from SRNOM fraction 6 through 10 continually decreases the O/C ratio; the H/C ratio increased from SRNOM fraction 8 through 10 and remained nearly constant in fractions 6-8.

Depiction of the H/C and O/C ratios in a van Krevelen diagram (Figure 20.), indicates rather continual trajectory and smooth fractionation of SRNOM.

Comparing these calculated results with the van Krevelen diagrams, obtained from FT-ICR/MS measurements, denote visible similarities. The observed continuous changes in

the loci (Figure 16.) are in good agreement with the here calculated basic reverse mixing model.

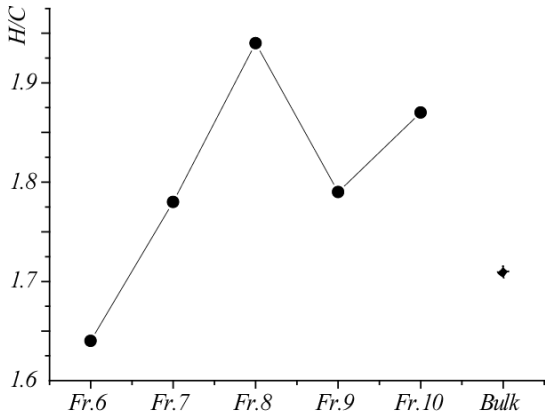

	n1-CH	n2-CH2	n3-CH3	H/C ratio
Fr. 6	51	68	45	1.64
Fr. 7	44	68	66	1.78
Fr. 8	37	64	93	1.94
Fr. 9	46	58	75	1.79
Fr. 10	40	66	81	1.87
SRNOM bulk	49	62	60	1.71

Figure 19. H/C ratio of protonated carbon as derived from ^{13}C DEPT NMR spectra

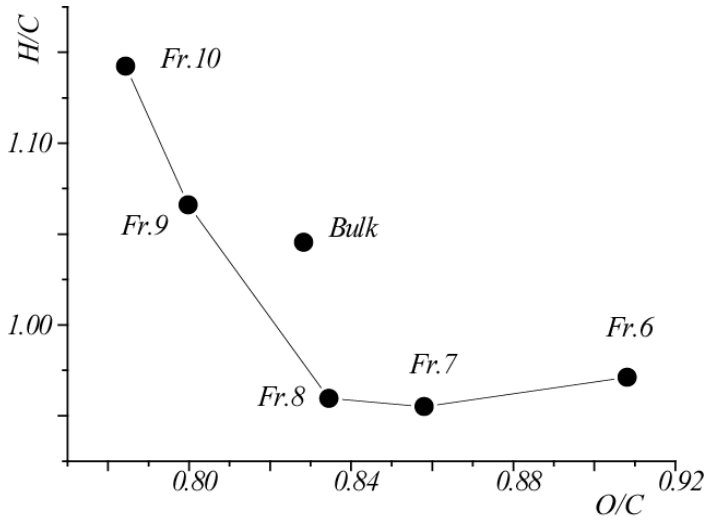

Figure 20. O/C and H/C elemental ratios as derived from ^{13}C NMR spectra according to a basic reverse mixing model

The average H/C ratio of the protonated carbon atoms in the SRFA fractions was computed from linear combination of ^{13}C DEPT NMR spectra and found to increase through SRNOM fractions 6-8, decreasing in fraction 9 and again, modestly, increasing in SRNOM fraction 10. Aliphatic branching, which determines the bulk of the hydrogenation in excess of methylene (cf. Figure 21.-23) provides a key means to assess the origin and diagenesis of SRNOM. However, aliphatic branching appears not relevant in directing the separation behaviour of SRNOM fractions. Accordingly, direct relationships between SRNOM migration in FFE and aliphatic branching are not expected and the observed, non continual variance in the aliphatic branching within consecutive SRNOM fraction follows expectations.

The extent of (average) protonation (Figure 19.) of carbon can be used to correct the elemental H/C ratio as observed in Figure 20.

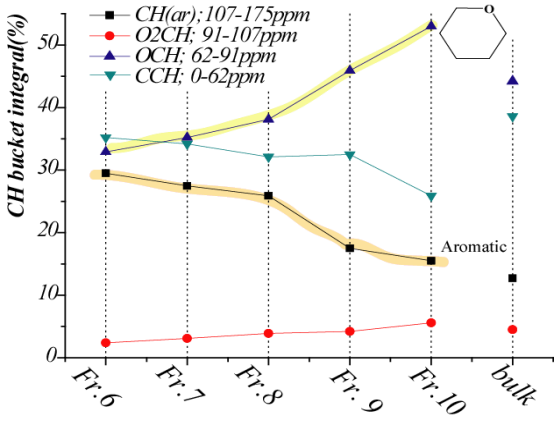

	CH(ar); 107-175ppm	O2CH; 91-107ppm	OCH; 62-91ppm	CCH; 0-62ppm
Fr.6	29.5	2.4	32.9	35.2
Fr.7	27.5	3.1	35.2	34.2
Fr.8	25.9	3.9	38.1	32.1
Fr.9	17.5	4.2	45.9	32.5
Fr.10	15.5	5.6	53	25.9
Bulk	12.7	4.5	44.2	38.6

Figure 21. ratio of $C_{ar}H$ [$\delta(^{13}C)$: 107-175 ppm], O_2CH [$\delta(^{13}C)$: 91-107 ppm], OCH [$\delta(^{13}C)$: 62-91 ppm], and C-CH [$\delta(^{13}C)$: 0-62 ppm] chemical environments in SRNOM fractions.

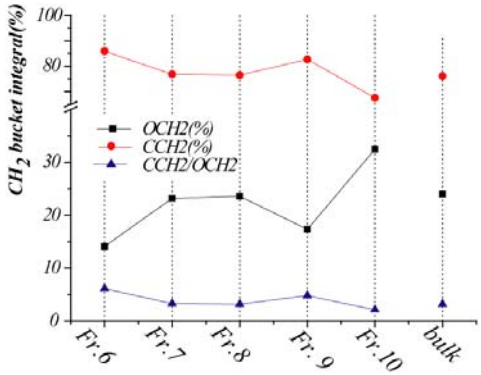

	OCH2(%)	CCH2(%)	CCH2 / OCH2
Fr. 6	14.1	85.9	6.1
Fr. 7	23.2	76.8	3.3
Fr.8	23.6	76.4	3.2
Fr.9	17.3	82.7	4.8
Fr.10	32.5	67.5	2.1
Bulk	24	76	3.2

Figure 22. ratio of O-CH_2 [$(\delta^{13}C)$: 50-100 ppm] and C-CH_2 [$(\delta\ ^{13}C)$: 0-50 ppm] chemical environments in SRNOM fractions

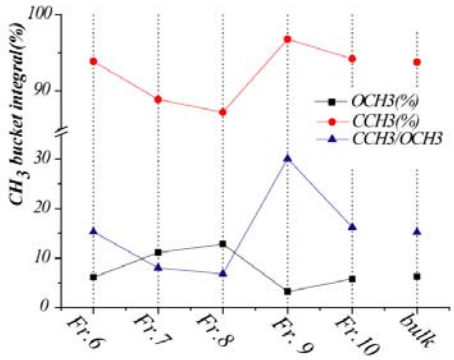

	OCH3 (%)	CCH3 (%)	CCH3 /OCH3
Fr. 6	6.1	93.9	15.3
Fr. 7	11.1	88.9	8
Fr. 8	12.8	87.2	6.8
Fr. 9	3.2	96.8	30.1
Fr. 10	5.8	94.2	16.2
Bulk	6.2	93.8	15.2

Figure 23. ratio of O-CH_3 [$(\delta^{13}C)$: 50-60 ppm] and C-CH_3 [$(\delta^{13}C)$: 0-50 ppm] chemical environments in SRNOM fractions.

2.2.7. Neutral sugar analysis

During the electrospray ionization, results, derived from FT/MS, has not shown any significant sugar-type constituents in the van Krevelen plot. Since these should have been located around the region with elemental ratios of 1;2 (O/C;H/C). Therefore individual sugar analysis was considered as a possible further analytical approach.

The following neutral aldoses were measured herein: glucose, galactose, mannose, fucose, xylose, rhamnose, arabinose. The beside the bulk material Fraction 3, 5-10 were analyzed and the obtained results shown in Figure 24.

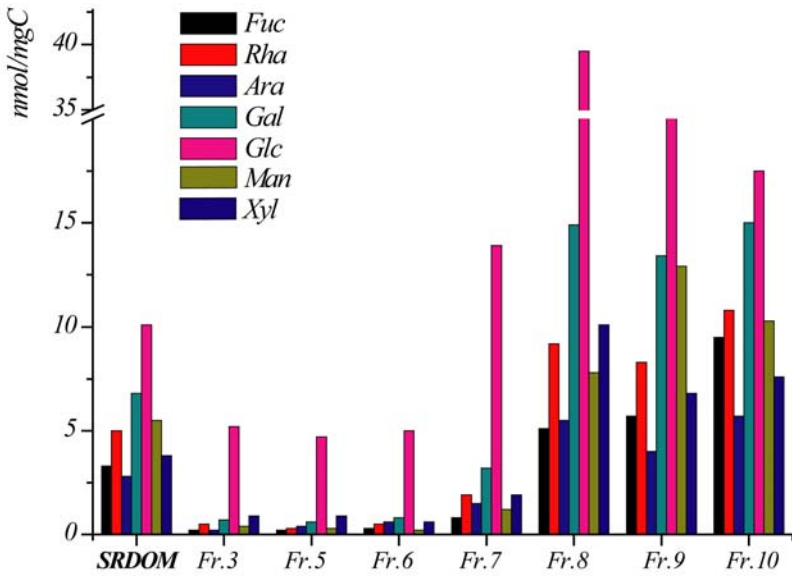

Figure 24. The neutral sugar content of the bulk and the fractions.

The first and most remarkable observation was, which derived from the bulk material, that neutral sugars comprised only a trace amount of the organic carbon. Since sugars were always an important and easily assumable nutrient for living organism, the presence or absence of these nutrients might refer of the state of alteration. Therefore the obtained results denote a higly altered material, that were exposed to significant microbial degradation.

The presented concentrations overall the fractions were tend to be higher then the bulk material itself. However after the calculated mass balance was taken into consideration, this contradiction could be solved. Though hereby it has to be noted, that the calculated balance showed over 103 % yield for sugars, and 73,8% for amino acids (Table 2.). The obtained high recovery of neutral sugars indicates a potential contamination of the samples. During the sugar analysis blank samples were applied parallel to indicate any non-sample related sugar

contamination. These samples showed no sugar signals, therefore the potencial contamination, preferentially glucose, might be originated from the separation and the sample handling. However the experienced extra amount of sugar seemed not to influence the overall tendency and therefore the results allow to describe possible tendencies.

The overall distribution of neutral sugars in the fractions shows typically a direct correlation with the low mobile fractions. NMR results (Figure 21) also support the occurred trend by the neutral sugar analysis. The lack of mobility and significant absorbance at 254 nm could be explained with possible oligosaccharides (i.e. liposaccharides) structures.

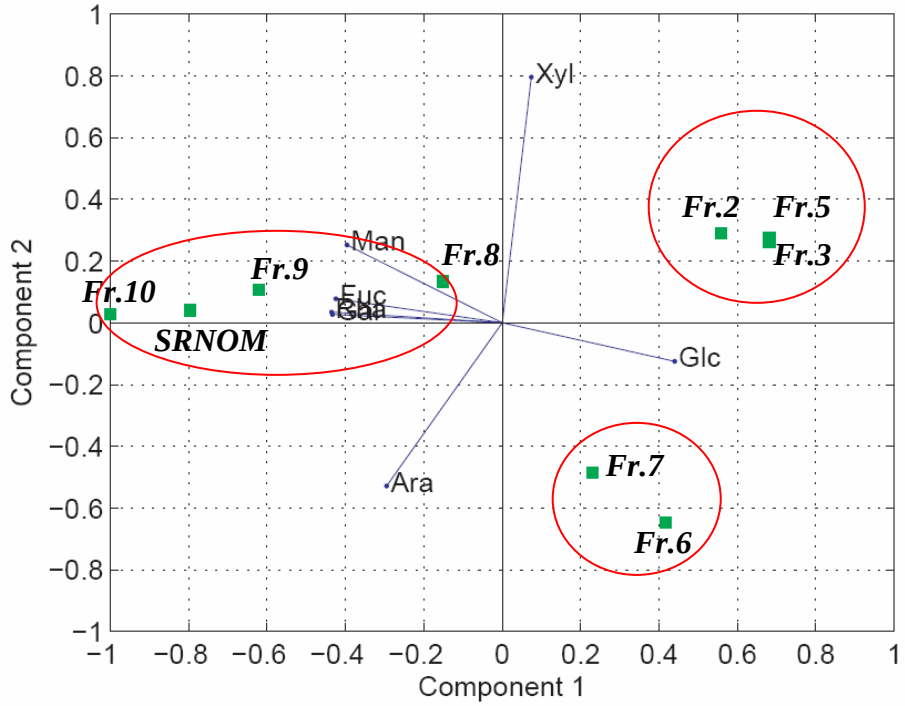

Figure 25. PC analysis of the bulk and fractionated SRNOM samples.

Principal compound analysis (PCA) of neutral sugars were also conducted (Figure 25). Mainly, three homogeneous groups were mainly distinguished. In relation with the first component the group Fr.8-10 and the bulk, are negatively correlated with the rest, the rule of fucose, mannose and galactose are relevant for this group. Hereby it has to be noticed that fractions with lower electrophoretic mobilities, show direct similarities with the bulk, non-separated organic matter. This type of differentiation was also observed in case of amino acid analysis (Figure 27). Fractions, depicted with higher mobilities, (Fr. 2,3,5) correlated positively and have rather a slight relevancies with xylose, than glucose. However these fractions contribute relatively low organic carbon.

2.2.8. Amino acid analysis

Fifteen amino acid were analyzed in the fractions and the bulk sample in order to describe a possible trend in distribution of these compounds in electrophoretic separation (Figure 26). In case of neutral sugars analysis, the obtained results showed that the target compounds are mainly denote low electrophoretic mobility and remain with the low mobile fractions. Oppositely to neutral sugars, amino acids have not shown specific distribution, but they were spread all over the fractions, though the observed concentrations were slightly increased towards the lower mobile fractions.

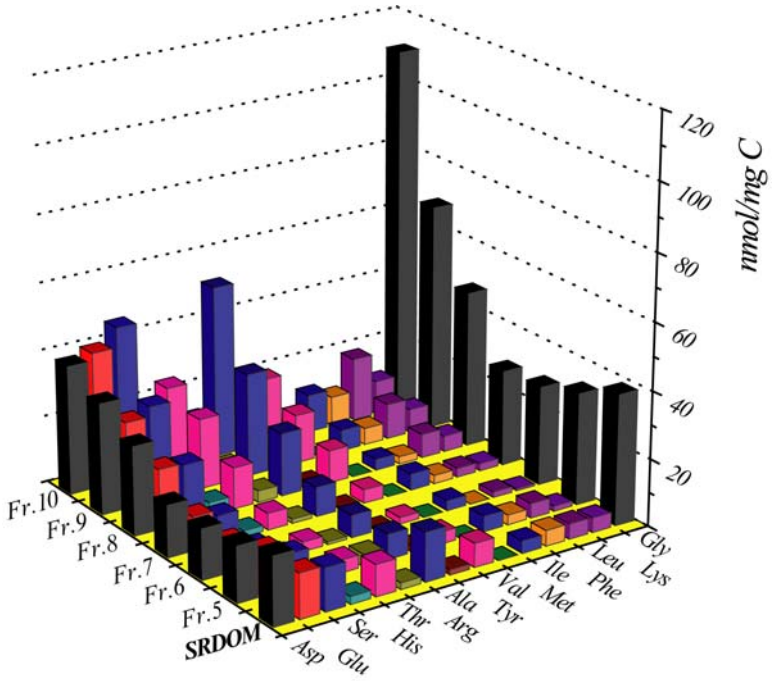

Figure 26. Amino acid content of the bulk and the fractionated materials.

Aspartic-, glutamic-acid, serine, alanine and glycine were the most abundant amino acids in the bulk material and this trend was also observed in the fractions. The general concentration was also slightly decreased as the electrophoretic mobility was decreased. Results, derived from principal component analysis, differentiate also between the lower and the higher mobile fractions. The bulk material showed closer relation to fractions 8, 9 and 10 than to fractions 5-7.

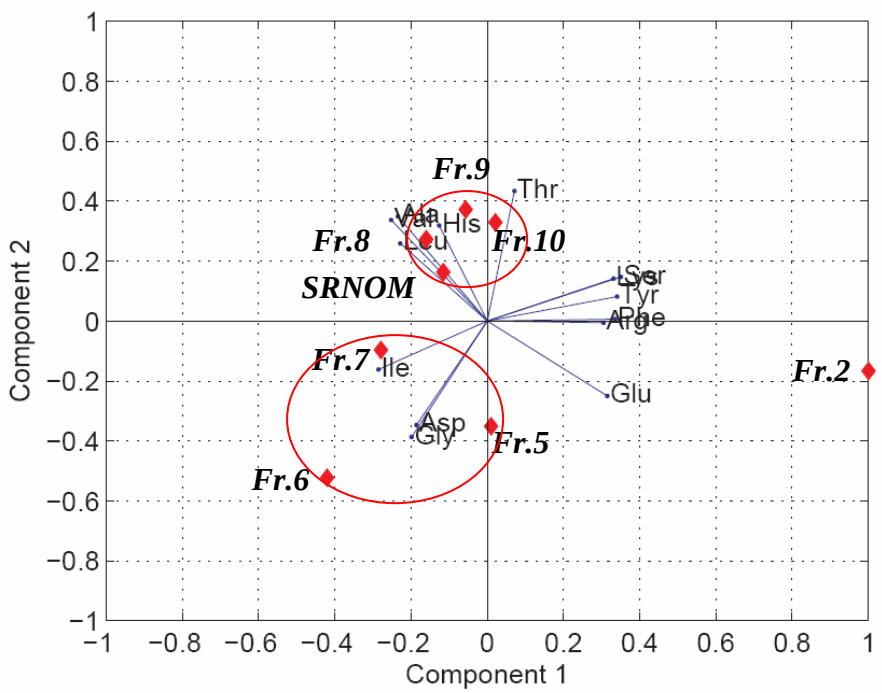

Figure 27. PC analysis of the bulk and the fractionated sample.

The obtained and calculated amino acid and neutral sugar content of the bulk and the separated fractions were summarized in Figure 28 and Table 6. Interpretation, based on Yield, enables to visualize the ratio of carbon atoms that are involved in amino acids or neutral sugars, as building blocks, relative to the other carbon atoms within other constituents of the fractions. Since the examined material is a surface water, the yield percentages of the bulk material are in agreement with the general expectations. The obtained organic matter from river waters usually depicted as highly altered materials, with enough dissolved oxygen to enable anaerobic metabolism. Therefore with relative low neutral sugar content.

Hereby it has to be noticed that within the observed yield distribution among the bulk and the fractionated samples does not reflect the mass balance. The yield stands for ratio within the sample and a powerful tool to compare different set of samples and follow possible changes. To obtain mass based distribution the amount of the observed constituents has to be combined with the relevant yield.

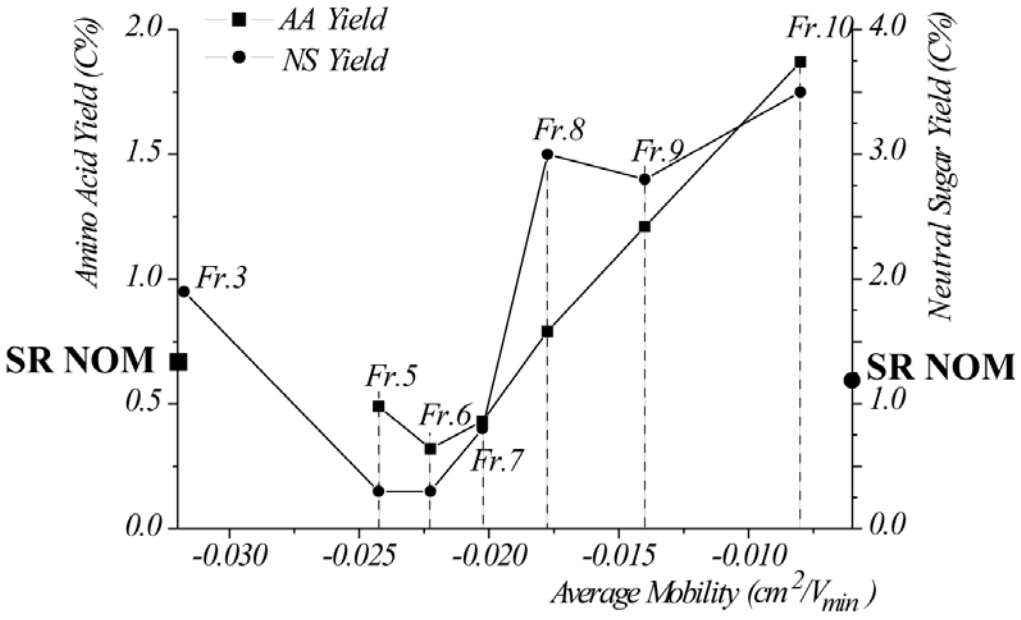

Figure 28. amino acid and neutral sugar yield of the bulk and the fractionated samples.

	mg C	***AA yield (%C)***	***nmolC as aminoacid***	***Distribution (%)***	***NS yield (%C)***	***nmolC as sugars***	***Distribution (%)***
SRNOM	175.7	0.6	**112.2**		1.1	**198.5**	
FR2		0.0	**0.0**	**0.0**	0.0	**0.0**	**0.0**
FR3	0.1	0.0	**0.0**	**0.0**	1.9	**0.2**	**0.1**
FR5	4.4	0.5	**2.1**	**1.9**	0.3	**1.5**	**0.7**
FR6	25.9	0.3	**8.2**	**7.3**	0.3	**7.9**	**4.0**
FR7	45.4	0.4	**19.7**	**17.5**	0.8	**37.8**	**19.0**
FR8	31.4	0.8	**24.9**	**22.2**	3.0	**95.4**	**48.1**
FR9	16.5	1.2	**19.9**	**17.8**	2.8	**46.5**	**23.4**
FR10	4.3	1.9	**8.0**	**7.1**	3.5	**15.0**	**7.6**
		Sum:	***82.8***	***Recov.: 73.8%***	*Sum:*	***204.3***	***Recov.: 102.9%***

Table 6. calculated amounts (nmol) of amino acids and neutral sugars and their distribution within the fractionated samples. The amino acid and sugar contents of the bulk material (corrected with the yield of the fractionation) were taken as 100%. The recovery of amino acids and neutral sugars were 74% and 103% respectively.

Different, but also information-rich representation might be, if the distributions of the involved carbons were plotted (Figure 29). In both cases (amino acids and sugars) the distributions followed a Gaussian-like curve, with the maximum of calculated amount of carbon in the fraction 8. Considering the fact that, fractions 8-10 were depicted with lower electrophoretic mobilities, it might be stated that, these building blocks are tend to remain with the lower mobile constituents. This could be explained with the assumption that, neutral

sugars and amino acids not existing in free, but in bounded forms. However the yield of both cases was increased in fractions 3-5 (Figure 28.), denoting also possible free constituents, though the calculated masses are not significant in these fractions (Figure 29).

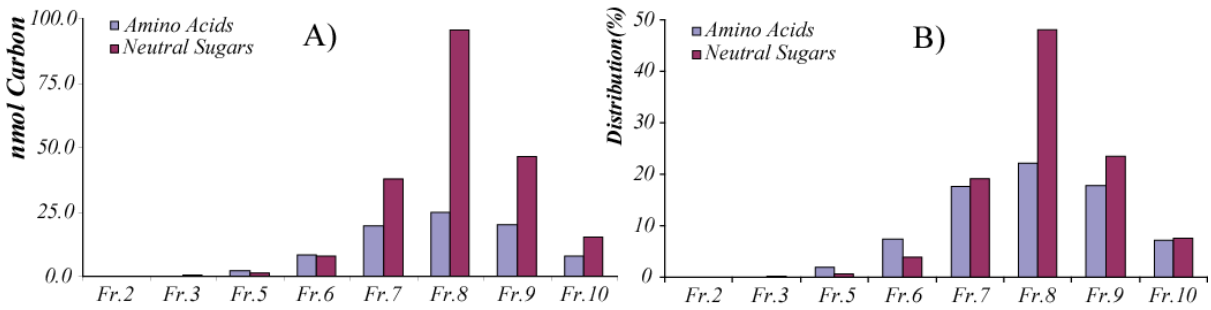

Figure 29. calculated amounts (nmol) of amino acids and neutral sugars ***(A)*** *and their distribution* ***(B)*** *within the fractionated samples.*

2.2.9. Conclusion

Hereby, the obtained fractions, derived from the up-scaled electrophoretic separation, were analyzed extensively by versatile analytical approaches. The samples were collected continuously in sizable amount to supply the different methods. To have a general idea of the carbon distribution within the fractions elemental analysis was conducted. Beside carbon, nitrogen content was also measured and it has revealed that during the separation and the sample handling process nitrogen might remain in the samples. Neutral sugar and amino acid analysis were also done, in order to extend the obtained view on possible constituents in FT/MS. Mass spectrometry, although it unsurpassed resolution and accuracy is only able to cover a certain part of the compounds within the sample. Since the result of analytical approach is really depend on the ionization methodology, external sugar and amino acid analysis might be a possible extension. However, due to the sample these compound only contribute to the total sample in low level.

^{1}H and ^{13}C NMR measurements were also done, where based on the obtained data the formally estimated impact of an electrophoretic separation appeared. Corrected results distinguished among the samples, and clearly described the separation from aliphatic compounds with low oxygen content to unsaturated and oxygen rich structures. NMR results showed a clear incensement in aromaticity and carboxyl functionality, which was in direct proportion with the observed mobility. While FT/MS results clearly distinguish between oxygen depleted aromatic compounds and constituents with abundant carboxylic functional groups. These highlighted results clearly support that original idea, that emphasize a need for

combination of complementary analytical methods. On the other hand a multidisciplinary platform for sample and /or separation description offers a needful basis to understand better organic matter and its composition.

2.3. Multiply charged constituents in NOM

Natural organic matter as complex biogeochemical non repetitive material was investigated with Ion Mobility/MS and ultra-high resolution FT/MS in approaches order to unravel the existence of multiply-charged state constituents. Hereby the potential molecular formulae (derived from FT-ICR/MS) of these double-charged species were described and assigned and the existence of these species were confirmed via Ion-Mobility MS.

2.3.1. Introduction

Intensive mass spectrometric information are presented here, using a 12 Tesla FT-ICR/MS and for the first time, for this purpose, a Q-TOF-IM/MS combined to integrated mathematical data analysis. FT-ICR/MS measurements give sufficient mass accuracy and resolution even in broad-band mode[250], enabling exact molecular formulae assignment with corresponding charge-states (a singly (or doubly) charged $^{13}C^{12}C_{n-1}$ ion will be higher in m/z by 1 (or 0.5) than the corresponding $^{12}C_n$ nuclide). Therefore the application of such a combination of methods to resolve and describe individual humic constituents is preferable. Despite of ultra-high resolution, any kind of non-adequate experimental settings might mislead the general result of the characterization[150, 162, 166].

Since the occurrences of poly-hydroxyl, -carboxylic acids and their relative high abundances had been shown in these type of mixtures[89, 91, 251], the formation of multiply charged negative ions in the ESI experiments would have been expected. Though it should be noted, that the denoted properties of large molecules might change during their transformation from polyelectrolyte state in solution to the detected ions in the gas phase. On the other hand, until now, the presence of probable multiple charged constituents were only assumed, moreover sometimes depicted as “bumps”, but without further details[159, 162].

This chapter was prepared, based on the article *” Combined utilization of Ion Mobility- and ultra high resolution-MS to identify multiple charged constituents in natural organic matter”* ***[III]***

2.3.2. Methods and Experimental Settings

The samples, SRFA and SRNOM standards were dissolved in methanol directly before the analysis and analyzed at different concentration (1000, 100, 10, 1, 0.1 μg/mL) and at two different pH (3 and 9). Ultra-high resolution mass spectra of these samples, were acquired at the Helmholtz Zentrum München with a Bruker APEX Qe Fourier transform mass spectrometer (FT-ICR/MS) equipped with a 12 Tesla superconducting magnet and an Apollo II electrospray source. The samples were injected with direct infusion with the flow rate of 2 μL/min. The spectra were obtained in negative mode with the number of data points per measurements of 4 MW(time domain size) with the typical resolution of $5 * 10^5$. The number of scans (512 for sample concentration 1000 and 100μg/mL, 1000 for 10μg/mL, 11000 for 1μg/mL and 45000 scans for 0.1μg/mL sample concentration) were increased in order to compensate the dilution effect and to obtain comparable datasets. The spectra were externally calibrated on arginin clusters and then internally recalibrated with fatty acids. Once the exact masses of the molecules had been determined, their molecular formulae were batch-calculated by a software tool, written in-house (E.V. Kunenkov). Following chemical constrains were applied: the maximum number of elements C(70)H(140)O(50)N(1)S(2), tolerance of mass error by ^{13}C isotope search ≤ 0.3ppm, and by direct formula assignment≤ 0.6ppm. For figure 31 and 32, elemental compositions were computed with the Data Analysis software, version 3.4 (Bruker) using following restriction: C,H,O unlimited; N, S 0-2; H/C ratio < 3, mass error ≤ 0.5ppm; observance of the N-rule. The molecular formula of given mass was considered only if the correspondent $^{12}C_{n-1}{}^{13}C_1$ peak was found. Generally the observed error were ≤ 90 ppb and in both charge-states the composition of the assigned formulae occurred in CHO>CHOS>>CHON,CHONS order.

High efficiency ion mobility based measurements were performed using a Synapt™ High Definition MS™ system (Waters Corporation) [252]. This hybrid quadrupole orthogonal acceleration Time-of- Flight (oa-ToF) mass spectrometer combines high resolution tandem mass spectrometry with high efficiency ion mobility (IMS) based gas-phase separations, capable of distinguishing isobaric molecules based on their mobility (combination of size, shape and charge). Measurements were made using a Waters Synapt High Definition MS system in the Waters European Application Laboratory (Manchester). The instrument was operated using argon as a collision gas for collision induced dissociation (CID) fragmentation experiments and with nitrogen for the IMS based measurements. The nitrogen pressure was 0.5 mBar. For measurements up to m/z 1000 the pusher frequency approximate 20,000 pushes

sec^{-1} . Each IMS based measurement required 200 pushes, therefore the each measurement takes approximately 10 msec. Duty cycle across the IMS region is approaching 100% due to ions being trapped prior to and released in packets into the IMS region. Furthermore rf confinement of ions within the trap, IMS, and transfer T-wave devices ensure that there are no diffusive loss of ions.

2.3.3. IM/MS & ICR/FT-MS

Herein, the obtained high resolution mass spectra of SRNOM (Suwannee river dissolved organic matter) and SRFA (Suwannee river fulvic acid) revealed beside the usually characterized single charged constituents further multiple charged species, and were described for the first time. A parallel series of measurements were conducted at a different concentration (Table 7), in order to confirm (i) the discussed multiple charged compounds are not only due to the measurements settings but might be originated from the sample itself; and (ii) the necessity of carefully chosen experimental settings (like the applied concentration of analytes, avoiding internal standards and additional ions (salt), which might suppress the ion-yield of the sample).

Number of scans	***Applied conc.(ppm)***	*Assigned Mol. Formulas(1-)*		*Assigned Mol. Formulas(2-)*		*Applied pH*
		SRNOM	***SRFA***	***SRNOM***	***SRFA***	
45000	0.1	-	1868	-	180	*3-4*
11000	1	3142	3162	3213	1839	
1024	10	2199	1539	2174	1862	
512	100	2794	2375	1629	1201	
512	1000	2900	-	1825	-	
11000	1	2462	2379	87	176	*9-9.2*
1024	10	1632	1496	77	17	
512	100	1497	1722	182	2444	
512	1000	1732	2523	356	2073	

Table 7. Observed numbers of assigned molecular formulae of SRNOM and SRFA at different settings.

The general outcome of these optimized measurements indicated the benefit the use of lower concentration (1-10 µg/mL) with longer acquisition time than the generally suggested and applied (up to 5 mg/mL) [147, 150]. However, if ammonium hydroxide was added, significant signals of doubly charged species were only observed above 100µg/mL. An other

important outcome of the systematic measurement of dilution rows indicates that the occurred multiple charged species are not aggregates[249], since these constituents exist even in diluted samples, at low concentrations.

A FT-ICR/MS mass spectrum of 1µg/mL SRNOM (experimental settings were detailed in experimental section) is shown in Figure 30. In the FT-ICR/MS spectrum, beside the regular pattern of singly charged constituents, where the most abundant isotopes (^{12}C) and their relevant $^{13}C^{12}C_{n-1}$ isotopes located 1 Da mass width from each other (see above), a second series of masses with 0.5 Da mass distances, between 250-560 m/z mass range is visible. The observed signals, with significantly lower intensities, denote the $^{13}C^{12}C_{n-1}$ isotopes of doubly charged species. Similar results were obtained from IMS/MS spectrum of SRDOM, where two groups, with a shorter and a longer drift time were observed (respectively also 1 Da and 0.5 Da mass distances in their simulated mass spectra (Figure 30)). The masses obtained from FT-ICR/MS spectrum of SRNOM, were converted into molecular formulae (indicated in figure description) with a software tool, written in-house. The elemental ratios, of each constituents were plotted in van Krevelen diagram separately, based on their denoted charge-state. The peculiar presentation of assigned molecular formulas, enables to individually describe certain structural properties of the observed constituents within this supermixtures[151]. Although we have to note that, in several cases, differentiation between charge states were not possible since constituents with $C_xH_yO_z^-$ and $C_{2x}H_{2y}O_{2z}^{2-}$ elemental composition, denote the same position in the van Krevelen diagram. But still, one of the most remarkable difference between charge states is that, molecules assigned as doubly charged, are densely situated in higher O/C field than the single charged ones (Figure 30.), thus related to higher contents in hydroxyl and carboxyl groups.

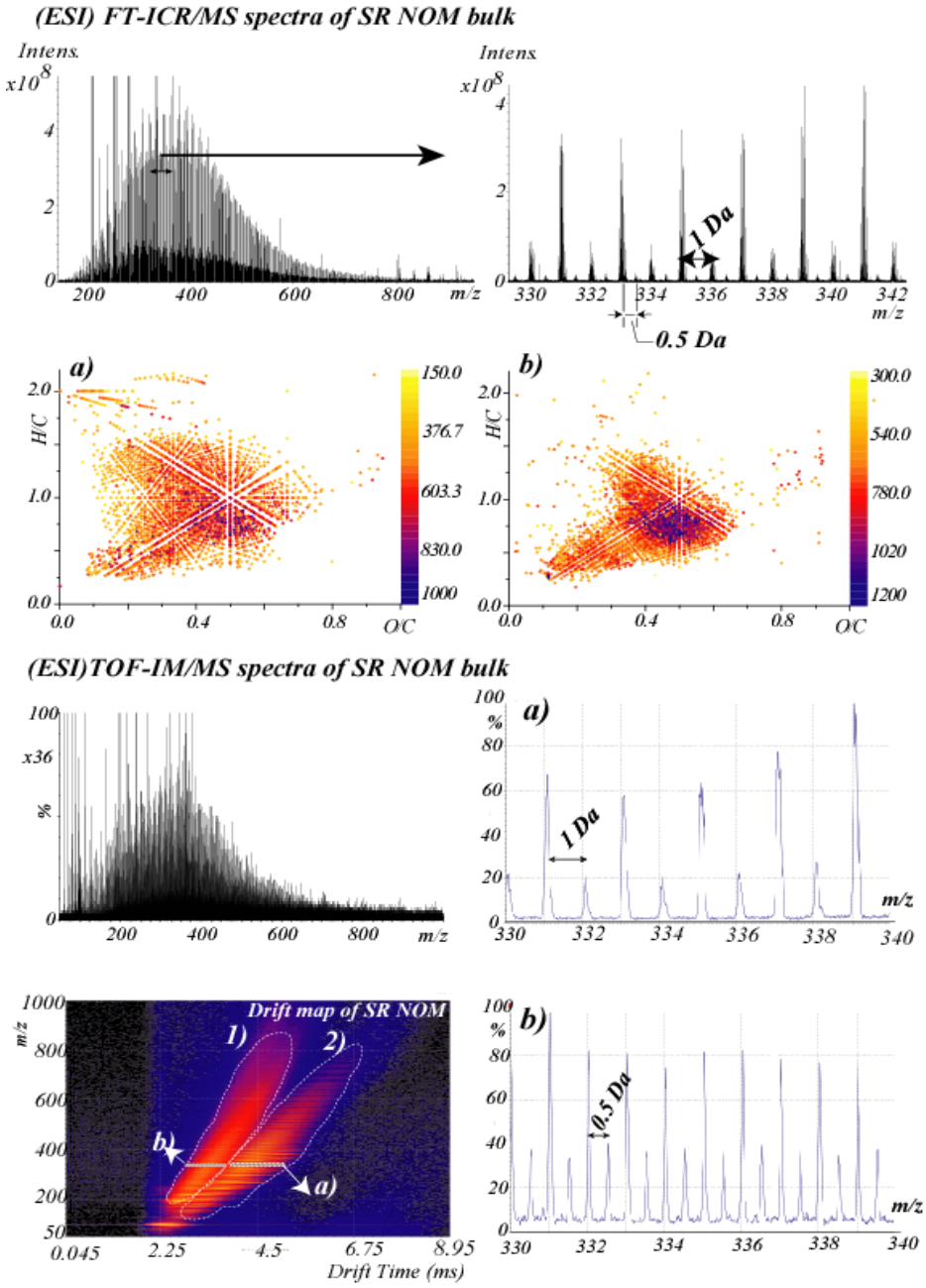

Figure 30. ESI negative ion 12 Tesla FT-ICR mass spectra of SRNOM (1µg/mL) ***(uppermost left)*** *with selected expanded section* ***(uppermost right)****, is given to demonstrate* ***(i)*** *the very high resolution in this spectra (120.000 resolved peaks, with the average resolution of ≥ 300.000) and* ***(ii)*** *the most significant mass differences between $C_cH_hO_oN_nS_s$ and $^{13}CC_{c-1}H_hO_oN_nS_s$ (Δm = 1 Da (singly charged), 0.5 Da (doubly charged)). Beneath the ICR-FT spectra, charge sorted (****(a)*** *only single charged-,* ***(b)*** *only doubly charged constituents) van Krevelen diagrams denote over 6000 assigned molecular formulae, plotted based on their H/C and O/C elemental ratios and color-coded according to detected masses. ESI negative ion TOF-Ion Mobility mass spectra and drift time vs. m/z distribution* ***(bottommost left)*** *of SRNOM was obtained on Synapt HDMS system (Waters, Manchester, England). In the drift map, at least two distribution of ions were denoted: 1) doubly charged constituents with shorter drift time and 2) singly charged molecules with longer drift time.* ***Inset a) and b) (right panel)*** *show an expanded view of the m/z region 330-340.* ***Inset a)*** *denote only singly-, while* ***inset b)*** *only doubly charged ions, as species containing one or more ^{13}C will appear 1/z above the m/z of the corresponding monoisotopic ions.*

Since formula assignment within a complex spectrum obtained from organic matters, without an automated approach is hardly possible, application of such a tool is needed. On the other hand, a revision of the reliability of these applications is evitable, therefore within the mass range of 348-350 m/z, the molecular formulae, obtained from the manual (Figure 32) and the automated assignments were confronted, with approximately 75% common hits. This result points to the fact that the application of this software tool describe possible constituents realistically (Figure 31).

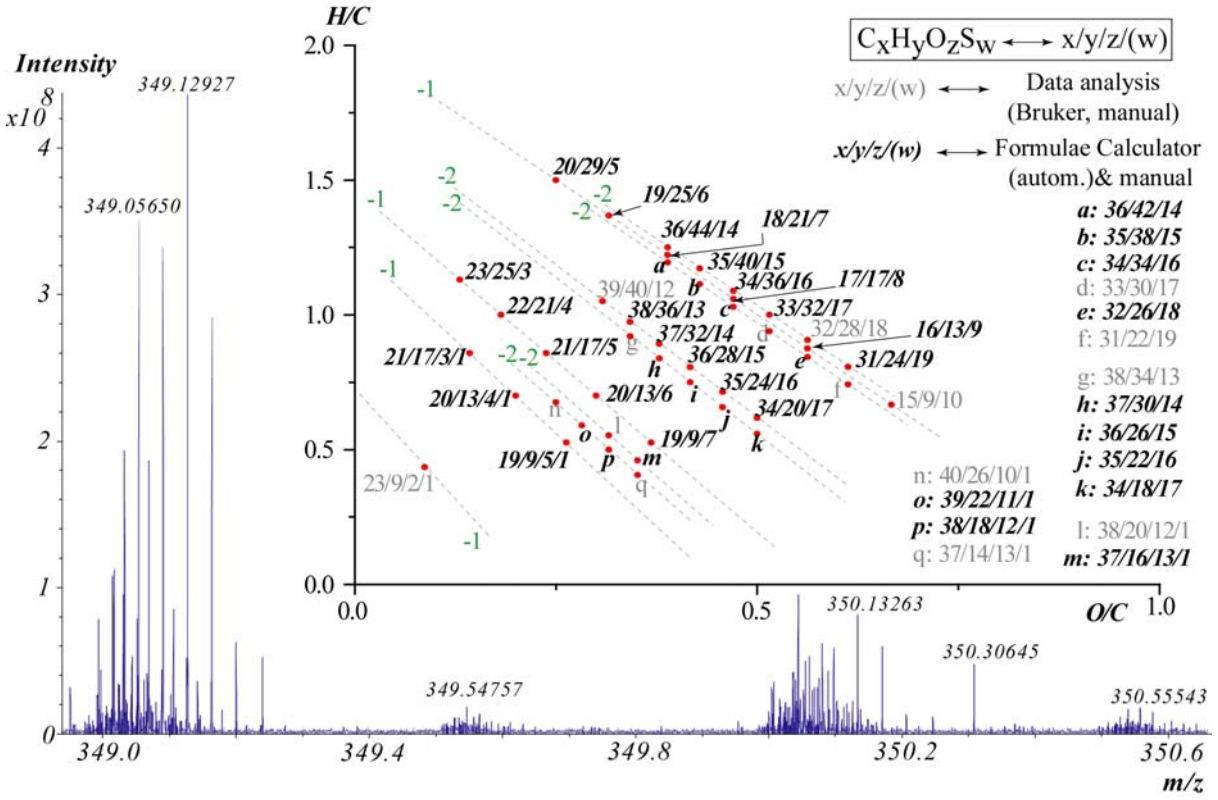

Figure 31. FT-ICR mass spectra of the expanded m/z region 348.8-350.6 and its feasible $C_xH_yO_zS_w$ compositional space (insert). 10 different series, with 44 constituents (see legend uppermost right) were manual identified, with isotope pattern recognition. Mass accuracy for all assignments were ≤ 90 ppb. Charge states for each members of series were highlighted with green. The automated formula assignment with specific chemical constrains (see experimental section), developed by E. V. Kunenkov, was also used, and the common hits were distinguished by the bold, italic labels.

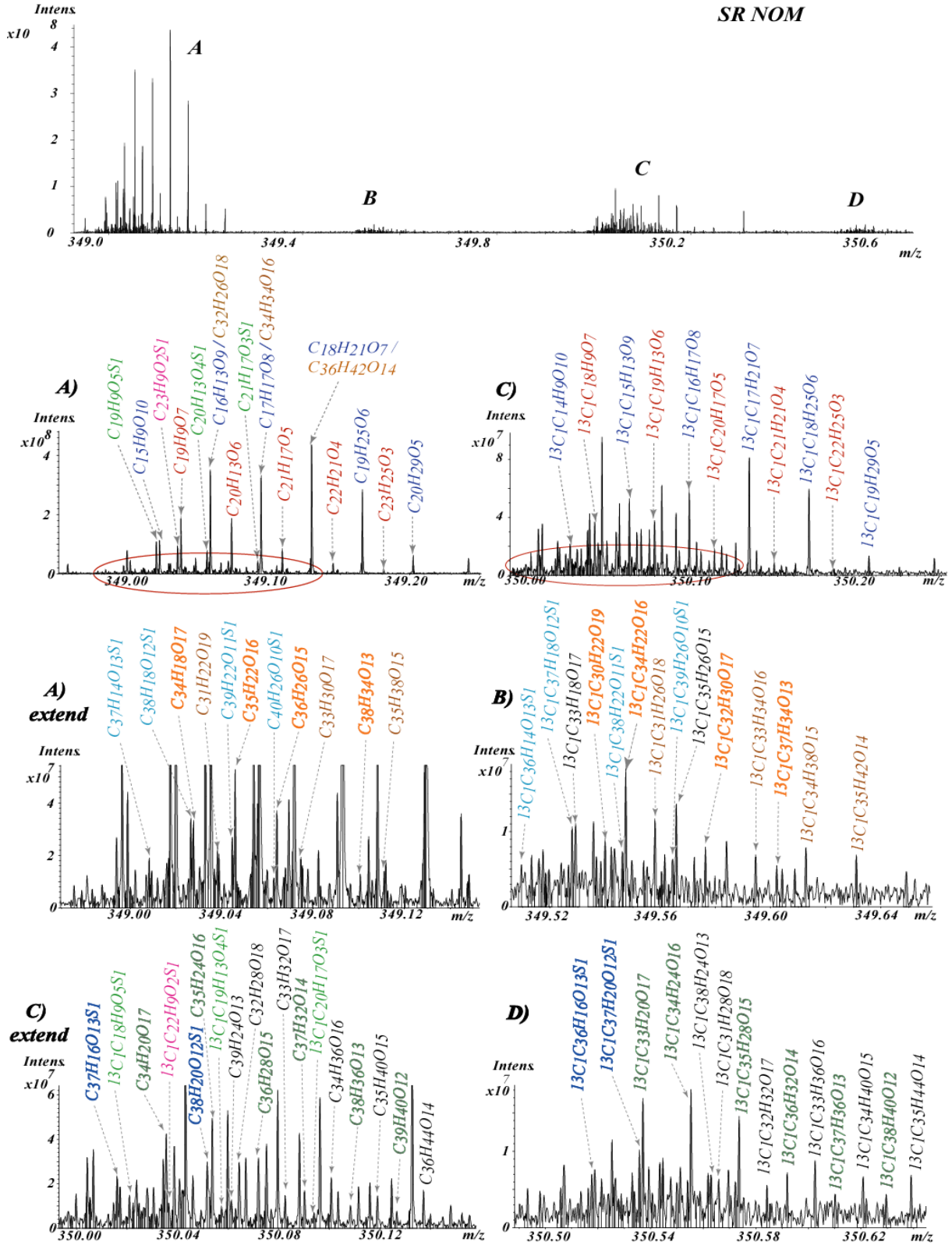

Figure 32. enlarged FT-ICR mass spectrum section of SRNOM sample (349-350.5 m/z) and their feasible molecular formulae assigned manually with <90 ppb error. Masses with relatively high intensities in region A and C are referring to single charged molecules and their $^{13}C_1{}^{12}C_{c-1}$ isotopes, respectively. A-extend (circled area in A), B and C-extend, D sections are referring to double charged species.

Enlargement of the same mass range in the mass spectra, obtained from IMS/MS (Figure 33) indicate similar intensity pattern like in the spectra obtained from FT-ICR/MS (Figure 31). Despite of lower resolution, the presented ion mobility distribution enables to visualize in a different way the existences of doubly charged constituents beside the single charged ones.

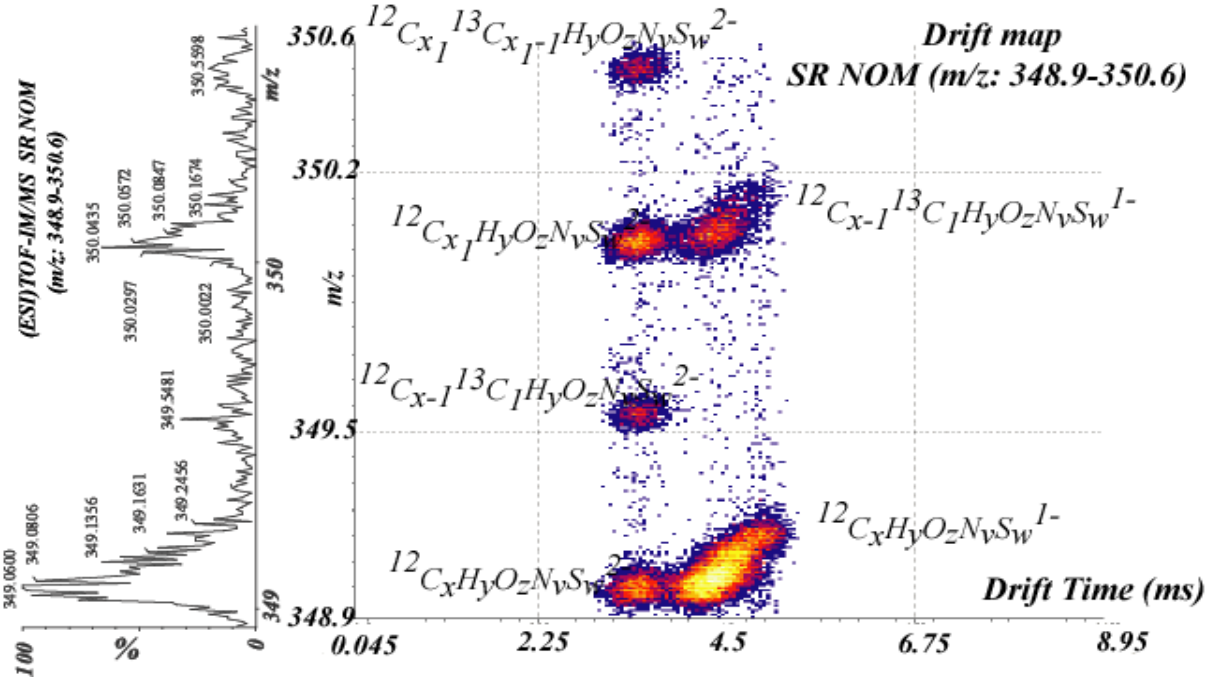

Figure 33. The expanded mass spectrum ***(left)*** *and the corresponding drift map selection* ***(right)*** *of m/z region 348.8-350.6, obtained from (ESI)TOF-IM/MS. The observed drift time distributions are labelled by their matching general elemental composition (obtained from FT-ICR/MS) and their charge-state (in agreement with Figure 30).*

IM/MS was also applied for the fractionated SRNOM samples, obtained from FFE separation. The comparison of the drift plots and their correspondent enlarged sections, denotes a visible increase in the intensities of the doubly charged species (indicated with dashed arrow) and parallel a decrease in the intensities and the occupied areas of the single charged species (regular arrow) (Figure 34. and 35.). The visible density changes of the doubly vs. singly charged species are in direct correlation with the observed electrophoretic mobilities. Species within the fraction 6, assigned with higher mobilities (see in Chapter 3), denote densely doubly charged species, with higher ion mobilities, while fraction 8 and 9 depleted in those.

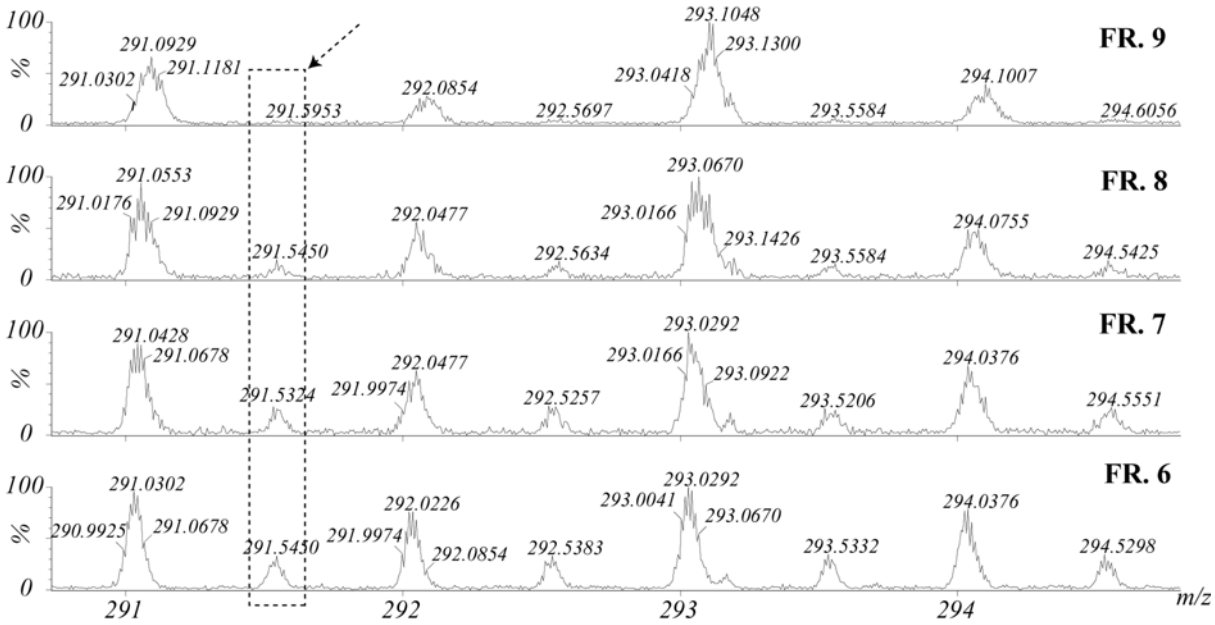

Figure 34. Enlarged section of SRNOM fractions spectra, obtained from IM/MS. The highlighted field indicates the correspondent group of $^{13}C_1{}^{12}C_{c-1}$ isotopes of the doubly charged species that are situated at the 291 nominal mass.

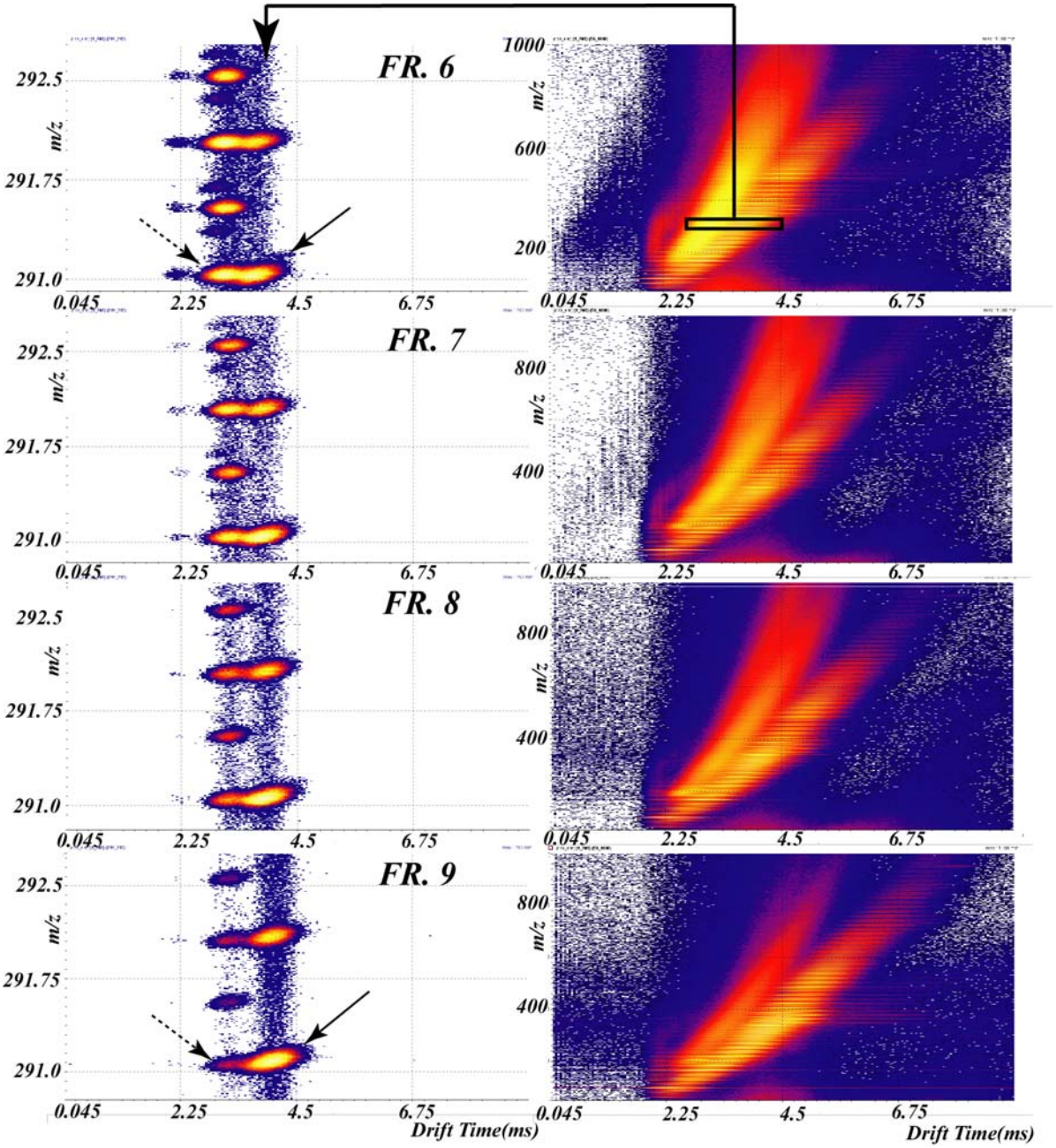

Figure 35. Drift time vs. m/z distribution ***(right)*** *of the FFE SRNOM samples and their enlarged sections* ***(left)****. Dashed and normal arrows indicate in the enlarged section, the doubly and the singly charged groups of species respectively.*

2.3.4. Conclusion

Overall, it can be stated that, the combined utilization of methods with different principles has the major wealth to complement the weak points of each others. For instance, a FT-ICR/MS equipped with 12 Tesla magnet could provide sufficient resolving power, however could not differentiate between the isomers of the constituents. Parallel, IMS/MS has not the necessary resolution to assign individual molecular formulas, but with its unique feature it is capable to distinguish isobaric molecules based on their ion-mobility, which depends on the size, shape and charge of the specific molecules. Therefore such a combination of these advanced mass spectrometric tools eventuated the extension of the existing knowledge on molecular level understanding of such supermixtures like natural organic matter. A good example for a possible benefit of the combination of these approaches, was shown when the SRNOM fractions, obtained from FFE separation, were analyzed. The results were able to visualize and support that general theoretical idea that the indicated higher electrophoretic mobilities, a result of not only compounds with small molecular weight, but even heavier constituents. Those bear multiple charges and since these species occupy the oxygen-rich region in the elemental ratio plot (see in section SRNOM), therefore we might deduct that fact that molecules with relatively higher density of functional groups (hydroxyl, carboxyl) can also denote high electrophoretic mobilities even with higher masses.[89, 91, 251].

3. Characterization of B complexation with NOM

3.1. Using immobilized Boronic acid polymers to study B-binding to NOM

Commercially available polymers with immobilized Boronic acid were tested, in order to describe the polyol content of different NOMs. B-functionalized polymers have the advantage to retain specifically molecules containing 1,2- or 1,3 cis-diol functional groups. Polymers with non-specific retention behaviour were eliminated based on experiments with model compounds. The selected polymer, with specific retention behaviour was tested with complex organic matter (peat).

3.1.1. Introduction

Natural soils contain multiple adsorption sites associated with inorganic and organic coatings that are characterized by different adsorption capacity and affinity for B [253, 254]. Numerous B adsorption studies conducted with various soils indicate that adsorption-desorption of B is the most significant process influencing B distribution between the liquid and solid phases in soils. Although the organic matter content in soil is commonly relatively low, its presence may significantly affect B adsorption/desorption behaviour. For instance, Marzadori et al. (1991) [255] have found that the amount of B adsorbed was considerably greater after the organic matter had been removed from the soil. On contrary, Yermiyahu et al. (1995) [56] and Ermiyahy et al.(1988)[55] have presented data where B adsorption increased as the content of the fresh organic matter in the soil was increased.

Although NOM is the most active component in soils, only a few studies of B-NOM interaction have been conducted so far. Humus was found to exhibit chemical affinity for B, which has been assigned an important role in the retention of B by soils [256]. Boron sorption on NOM originating from reclaimed wastewater has been found to be 3 to 5 times stronger as compared to smectite clays. Additions of NOM to soil resulted in a decline of B concentration in the soil solution and inhibited its uptake by plants.

Natural organic sorbents are rather complex materials consisting of OM in various stages of decomposition and with lignin and cellulose as major constituents. The humified constituents contain polar functional groups, such as alcohols, aldehydes, ketones, carboxylic acids, phenolic hydroxides and ethers that can be involved in chemical bonding.

Although several boron selective resins are available (Amberlite IRA-743, PuroliteS-108, Lewatit MK-51), cost-effective B removal/immobilization at the very spot of water processing, has to be developed. Small microfiltration (MF), ultrafiltration (UF) and RO systems, which have otherwise become an attractive option to farmers or farming communities to process saline or wastewater, do not satisfactory remove boron. Hence boron is one of the major obstacles in the use of these waters and therefore its removal is of great practical importance. Materials, derived from natural organic matter (NOM), which is an abundant and cheap resource, show strong boron binding and therefore exhibit great potential to act as a possible boron sorbents.

However a proper description of an organic matter, with specific boron retention potentials, is rather difficult, and time consuming[253,254]. A possible fast analytical approach might be CZE separation, since the effect of boron was already presented and the average analysis times are less than 20 minutes[19, 28]. The primer utilization of polymers, with immobilized Boronic acid on their surfaces, enables the necessary selectivity, before the CZE analysis and the observed ratios of the retained/remained organic matter indicate the abundances of the potential B-specific sites.

Boronic acid–functionalized polymers have attracted significant attention in the affinity chromatography of various biological agents. Affinity chromatography applications have been developed based on the complex formation between boronic acid and the cis–glycol groups of the biological agent [257]. Reversible nucleotide adsorption-desorption behaviours on boronate functionalized gel beads with different surface characteristics were prepared and their potential application for nucleotide isolation were investigated. m-aminophenyl Boronic acid was covalently attached onto different gel bead particles and their specific cis diol binding properties were tested with β-nicotinamide adenine dinucleotide with the prosperous future aspect as a stationary phase in liquid chromatography [258, 259]. The adsorption behaviour of mixed yeast RNA on agarose-immobilized *m*-aminophenylboronic acid was also tested[260]. The versatile application beside the regular affinity utilization were also showed in numerous cases over the decade. Functionalized polymers for sensoring saccharides [261], ultra-thin gel grafted on the tip of atomic force microscope[262] [263] electrochemical sensing of sugars [264, 265] nucleotide isolation [266, 267], glucose in tear fluids [268], a real-time glucose sensing holographic sensors for monitoring bacterial growth, using 3-acrylamidophenlylboronic acid [269].

In order to be able to describe a possible boron binding on different organic matter, a reverse approach was tested with commercially available polymers. Those polymers, which had different immobilized Boronic acid-based ligands, might have the capability to fish out specific boron active polyols from the vastly complex pool of organic matter constituents (Figure 36). Furthermore this reverse approach opens possibilities for direct characterization the B retention capabilities of different candidates. First and most important that this approach offers a non-invasive characterisation, therefore the possible organic sorbents could be investigated in their original conditions. Second, since the approach is relatively fast and straightforward, a possible application as a screening tool could be also conceivable.

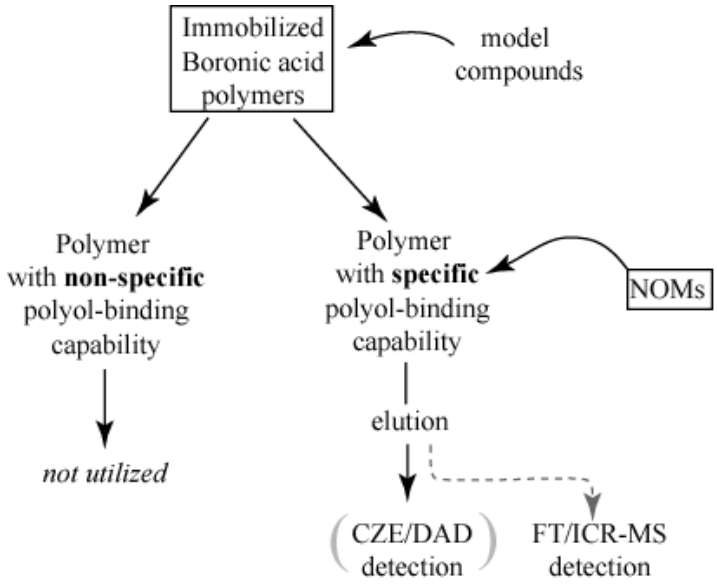

Figure 36: Potential work-flow of the utilization of commercially available polymers with immobilized Boronic acid. Model compounds, with or without 1,2-; 1,3-cis diol functional groups were used to test the specific retention of the polymers. Afterwards the selected polymer is used further for binding studies of NOM samples combined with capillary electrophoretic and mass spectrometry methods.

3.1.2. Commercially available immobilized Boronic acid polymers

For the column experiments five different polymers with immobilized Boronic acid on their surfaces were tested with model compounds. Seven out of the eleven model compounds have specific 1,2 or 1,3 diol functional groups, which in high pH able to bind specifically with the immobilized form. This first phase of the experiment was necessary in order to describe and furthermore exclude the polymers that either shows non-specific interaction or not able to retain all of the compounds with specific diol groups. After this characterization, those polymer(s), that shows an effective selective retention, were applied for the characterization of the different organic matters.

The five polymers were:

- *Pierce immobilized boronic acid,*
- *Sigma m-aminophenylboronic acid(A-8312),*
- *Bio-Rad Affigel boronate gel (153-6103),*
- *Aldrich Boric acid gel partical size 0,1-0,4mm(18445-4),*
- *Aldrich Boronic acid polymer bound 50-100 mesh (632627-1g);*

Immobilized boronic acid obtained from Pierce (Part of Thermo Fisher Scientific, Rockford, IL, USA) was supplied as 50% aqueous slurry with 0.02% sodium azide (Figure 37). The applied support was a beaded spherical polyacrylamide with m-aminophenyl group spacer with 1,800 MW exclusion limit.

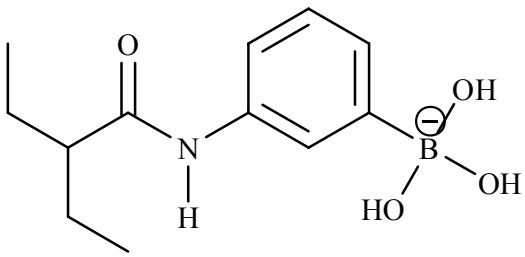

Figure 37. Pierce immobilized boronic acid gel

m-aminophenylboronic acid(A-8312), obtained from Sigma-Aldrich (Seelze, Germany) was beaded on 6% agarose matrix with attachment through amino group with a 9-atom spacer.

Affi-Gel boronate gel (153-6103) was a boronate-derivatized polyacrylamide gel, obtained from Bio-Rad (Bio-Rad Laboratories, Hercules, CA, USA) (Figure 38).

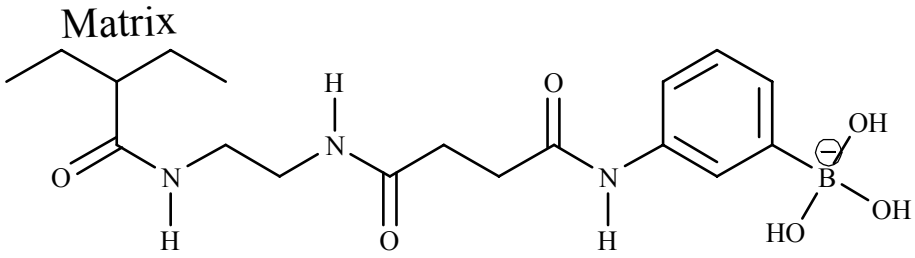

Figure 38. Affi-Gel boronate gel

Boric acid gel **(**particle size 0,1-0,4mm), obtained from Sigma-Aldrich (Seelze, Germany) is a cross-linked polymer insoluble in water and all organic solvents. It is prepared by the cross-linking copolymerization of dihydroxyborylanilino-substituted methacrylic acid with 1,4-butanediol dimethacrylate (Figure 39).

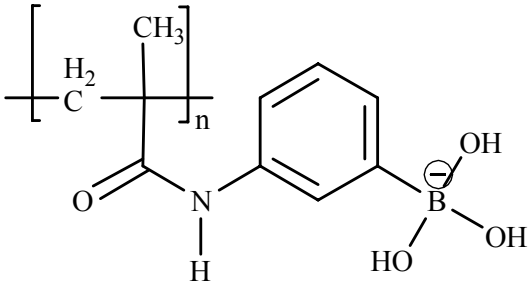

Figure 39. 3-Aminophenylboronic acid, boric acid gel

Boronic acid polymer bound (50-100 mesh) was obtained from Sigma-Aldrich (Seelze, Germany) (Figure 40).

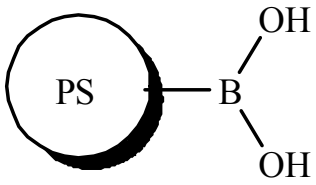

Figure 40. Boronic acid, polymer bound

3.1.3. Materials

3.1.3.1. Analytes

Pyrocatechol, benzoic acid and riboflavin were purchased from Merck (Darmstadt, Germany), cholic acid, quercetin dihydrate, rutin trihydrate, salicylic acid and 3-hydroxybenzoic acid were obtained from Fluka (Buchs, Germany), gallic acid and caffeic acid, 3,4-dihiydroxy phenylalanine (L-dopa), L-tyrosine was purchased from Sigma (Germany). All the chemicals used without further purification. The Suwannee Humic acid (SRHA), Summit Hill Humic acid and the Peat Humic acid were obtained from the International Humic Substances Society (IHSS). Organic matter obtained from peat sample (PHF-T598, unfractionated) was kindly provided by I. Perminova (Univ. Lomonosov, Moscow, Russia). For all experiment LC-MS grade methanol and water (Sigma-Aldrich, Seelze, Germany) were used.

3.1.3.1.1. Buffers and separation media

For the CZE separation borate and ammonium bicarbonate buffer was used as a separation media. The concentrations were in each run 12.5 mM of sodium borate. The pH of the buffers were adjusted to 9.2. For the column experiments the elution media was 20-200 mM ammonium bicarbonate (puriss. obtained from Riedel-de Haen) adjusted to pH 9.2 with ammonium hydroxide. Boric acid and the Borax were purchased from Merck (Darmstadt, Germany).

3.1.3.1.2. Methods and experimental settings

The electrophoretic separations were done on Beckman P/ACE 5510 system coupled with DAD detector. The applied capillary, conventional silica tube with 50 μm inner diameter, was obtained from Polymicro. The applied length was 50/57 cm. 30kV separation Voltage was applied in all cases.

3.1.4. Characterization of the specific retention behaviour by CE

Polymers with immobilized boronic acid enables theoretically the retention of compounds with 1,2- and 1,3-cis diol functional groups, however non-specific retention might also contribute to the total retention. Hence, prior the utilization of the polymers for NOMs, the boron specific retention were tested. Model compounds with and without 1,2- and 1,3-diol functional groups were used to characterize the retention properties of the polymers (Figure 41). For the characterization, a test-mixture was applied, with 11 model compounds solved in 10 mM ammonium bicarbonate buffer (pH 9.2). The final concentrations for individual compounds were 25-25 ppm.

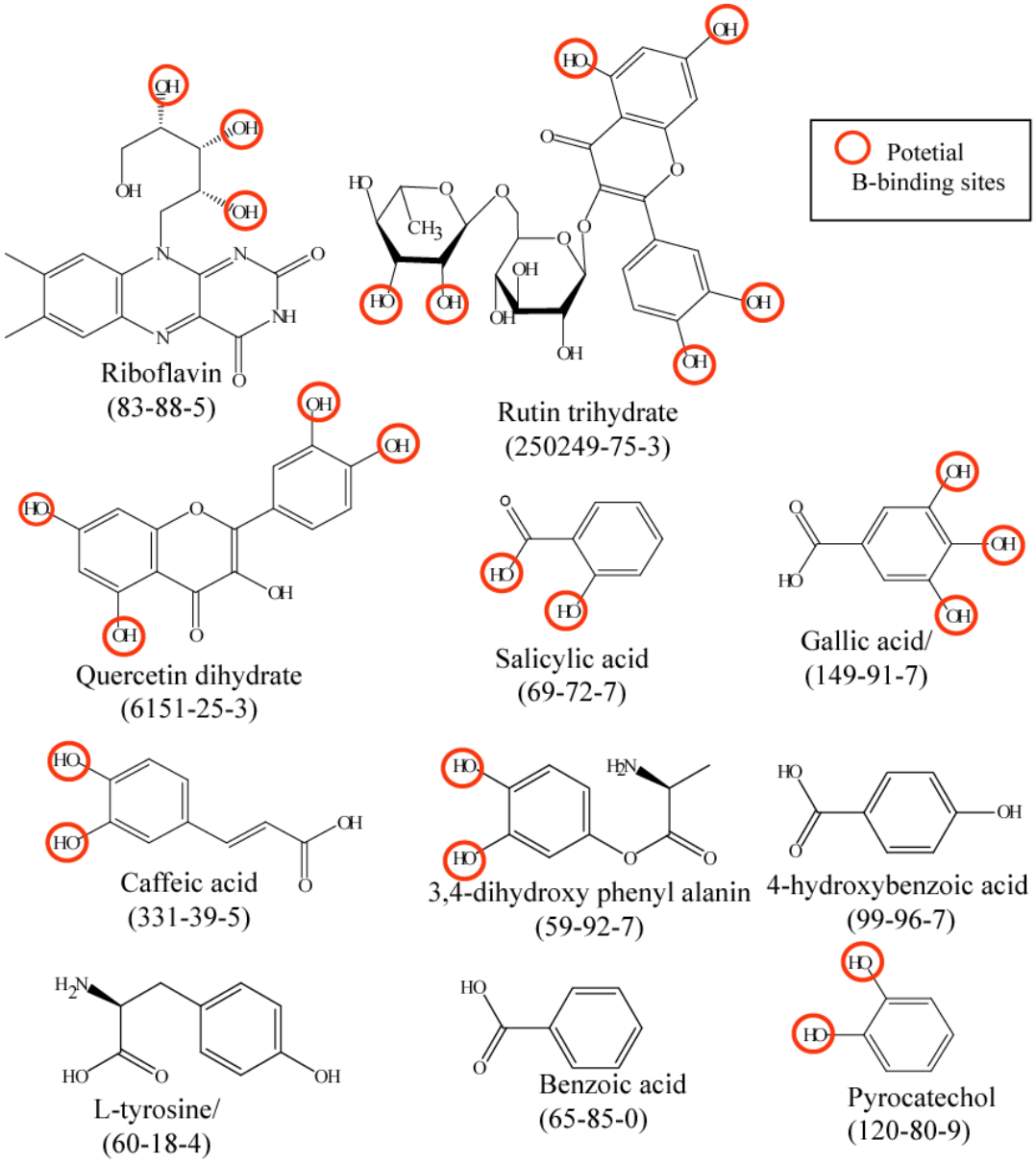

Figure 41: Applied model compounds (and their CAS numbers) with or without 1,2- or 1,3-cis diol functional groups

Equal weights of polymers were packed in plastic tubes in order to study the retention behaviour in conditions similar to affinity chromatography.

To follow the retention study, samples, obtained from wash out were analyzed by CZE measurement.

Prior to the column experiment, the electrophoretic separation conditions were optimized for the text mixture. Once the model compounds were visible separated and the compounds were individually identified (Figure 42), calibration was done for quantitative assessment. The obtained time domain electropherogram was converted into mobility scale.

The separation method was optimized to visualize each model compounds, the mixture were applied onto the conditioned polymers. The polymers were filled into empty SPE

columns ($V_{Polymer}$: 0.5mL) , with 7.5 mm inner diameter and conditioned with 200, 100, 50 and 25 mM ammonium bicarbonate buffer, in sequence. Afterwards 100-100 µL of mixture was applied onto each columns and were left to penetrate. The mixture, applied before the column and the wash-out was directly analyzed by CZE.

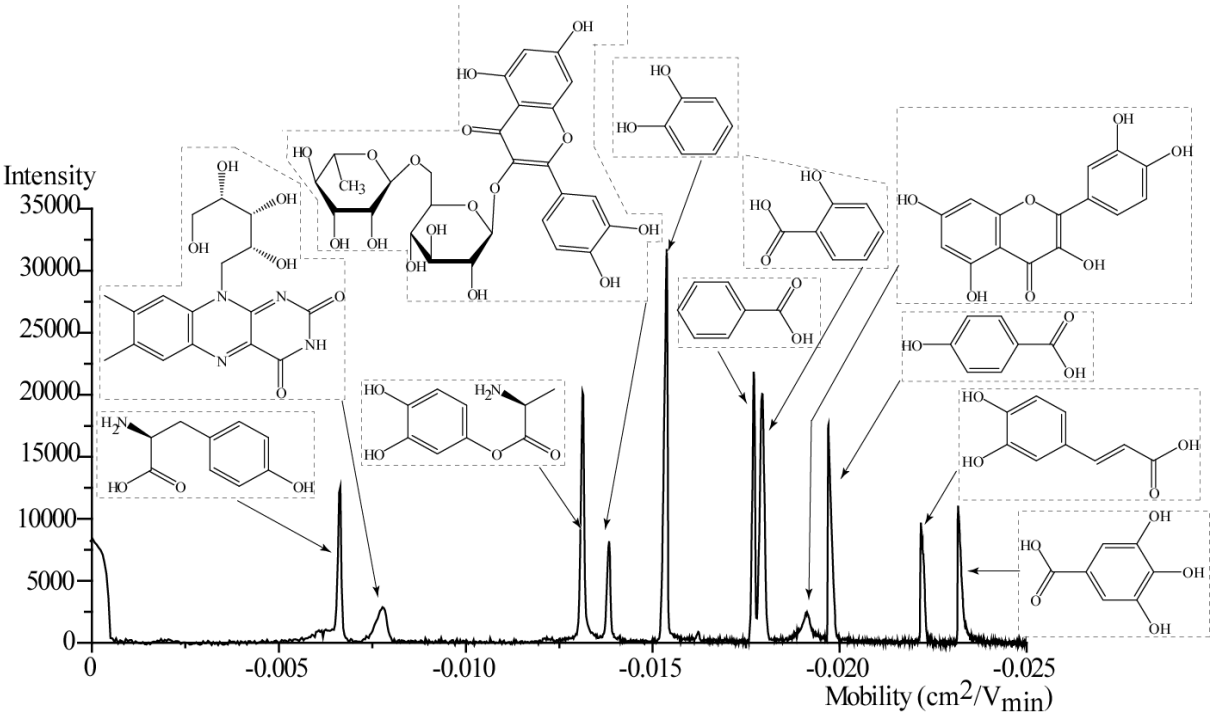

Figure 42. Electrophoretic separation of the 11 model compounds in sodium borate buffer(12.5 mM, pH 9.2). The compounds were ***(from left to right)****: L-tyrosine, riboflavin, 3,4-diOH-L-phenyl-Alanin, rutin trihydrate, pyrocatechol, benzoic acid, salicylic acid, quercetin dehydrate, 4-OH benzoic acid, caffeic acid, gallic acid.*

Based on their structure benzoic acid, L-tyrosine, salicylic acid and 4-OH benzoic acid were expected not to remain any of the polymers, if only specific retention is desired. The other compounds, contain 1,2-cis diol ligands, therefore complex formation with hydroxyl groups of the immobilized boronic acid, might take place at pH 9.2.

During the column experiment the eluting and the final conditioning buffers were the same. The wash-out were collected in 0.5 mL wise, consecutively, that were analyzed by CZE. The results were converted into mobility scales and confronted with the electropherogram of the untreated mixture.

To follow quantitatively the emerged changes for each model compounds, primary calibrations were done within the concentration range of 1-25 ppm (25, 10, 5, 1ppm).

When changes were observed, the peak areas were calculated and subtracted from the original signals of the relevant compounds. After the balance of the retention were calculated based on the calibration results. The calibrations were done individually for each component.

The proper polymer for further application by the complex samples, was selected based on the observed retention behaviours (Figure 43 and 44).

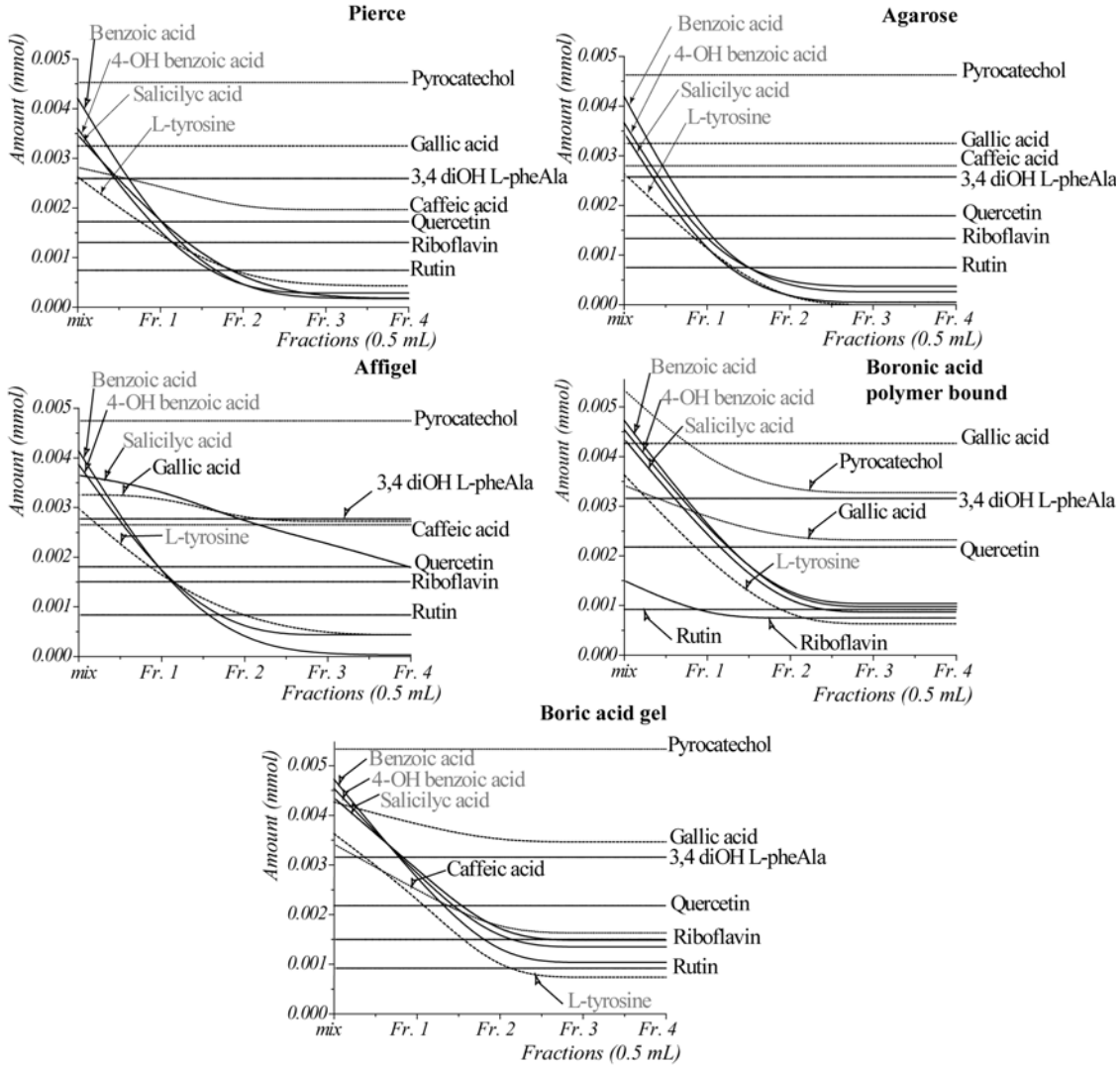

Figure 43. Retention behaviour of the 11 model compounds on five different polymers with immobilized Boronic acid ligands. The calculated amounts denote the retained amounts of each compound, therefore constant level of amount represent a complete retention of the specific compound on the polymer.

Affi-Gel boronate gel (Bio-Rad) showed the expected retention properties, since the original application of this gel was developed for mainly small molecules such as nucleotides, catecholamines, coenzymes and sugars however slightly decrease in the retained amount of gallic acid was observed. On the other hand, all compounds that had no 1,2 or 1,3 cis diol

functional groups were not retained on the column. Salicylic acid was also mobile, though with higher residence time. Polymer m-aminophenylboronic acid on agarose bed (Sigma-Aldrich), named as Agarose, denoted only specific retention properties. Immobilized boronic acid., obtained from Pierce, showed also the expected retentions, however in case of caffeic acid was not as expected.

The polymers, Boronic acid polymer bound and boric acid gel (Aldrich) showed parallel non-specific retention properties, since model compounds with diol groups were not retained on the polymers. Out of the eleven model compounds, four (benzoic acid, L-tyrosine, salicylic acid, and 4-OH benzoic acid) supposed not to remain on any of these columns. Theoretically those which have adjacent hydroxyl groups, at this pH, can form complex with the immobilized boric acid, therefore might be retained. The Pierce gel and the Agarose polymer show the closest behaviour to the ideal case. Although both retain some amount of molecules with non specific binding, they retain all of the expected compounds. In the other cases wash-out were observed in case of diol containing molecules (Figure 43). Considering these facts and assumed that the bindings were B-specific, the Agarose gel was chosen for further applications.

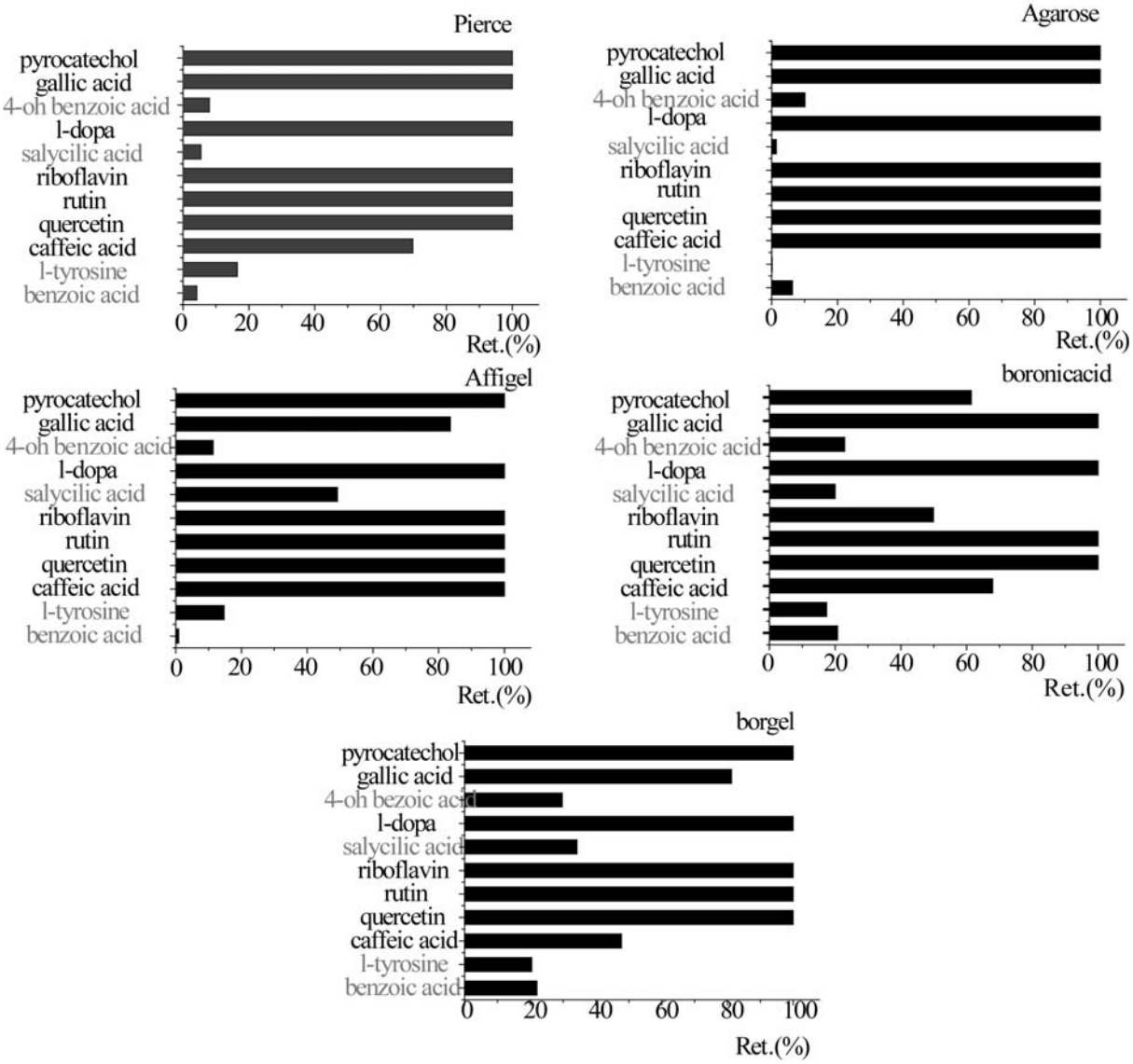

Figure 44. Summarize of the characterization of the five commercially available boric acid immobilized polymers.

3.1.5. Applying organic matter onto the selected polymer

Complex organic samples, like Peat, SRHA and Summit Hill HA, were tested with Agarose gel after the characterization process.

First, the unfractionated samples were measured in ammonium bicarbonate and sodium borate electrode buffer with similar experimental settings, in order to locate possible borate complexes (Figure 45). If ammonium bicarbonate was applied as separation buffer, homogenous humic humps were observed, while with borate buffer in each cases a salient peak appeared. This type of phenomena was described formally by Schmitt-Kopplin et al. [19, 28], hence the salient peaks, in case of borate separation buffer, were assigned as B complex containing polyols. 100-100 µL samples with 1 mg/mL concentrations were added onto the conditioned (100mM ammonium bicarbonate, pH9.2) columns and were left to penetrate.

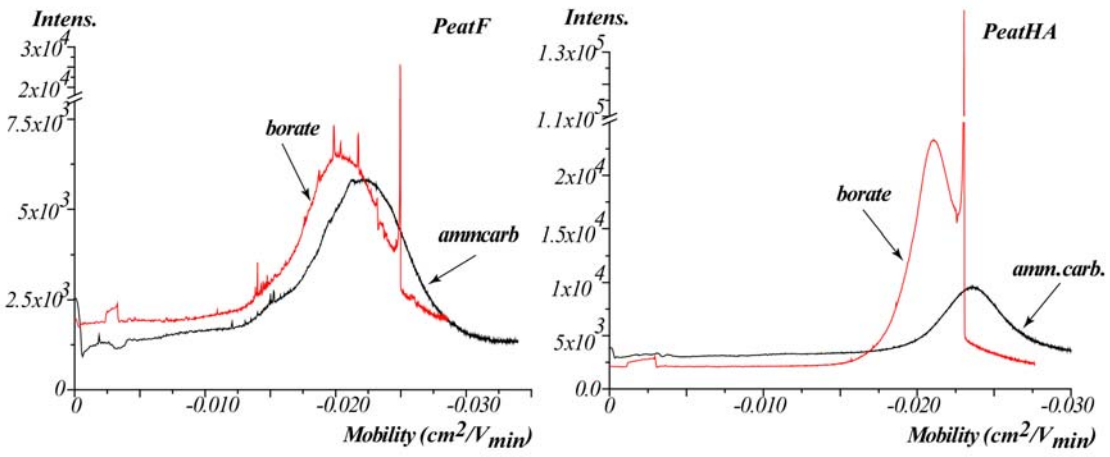

Figure 45. obtained electropherograms of Peat Organic Matter (PeatF) and IHSS standard Peat Humic acid (PeatHA) converted into mobility scales. The applied electrode buffers were ammonium bi carbonate (25mM pH 9.2) (black) and sodium borate (25mM pH 9.2) (red).

Afterwards, samples were applied onto the columns and eluted with the same buffer, that was applied for conditioning, in order to wash out the non-bounded part of the sample. Visible parts were remained on the columns, formed bands on the top of the columns. Therefore between the eluent and the untreated samples, a clear difference in the electropherograms was expected. However in each case only a significant peak, with different mobilities, was observed (Figure 46).

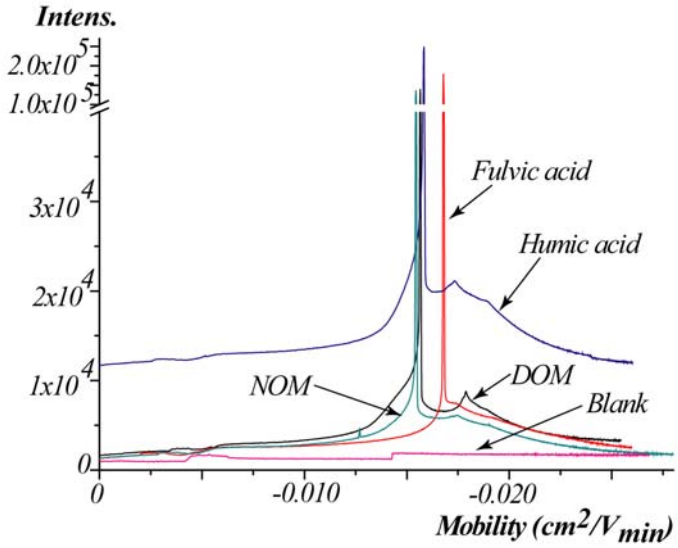

Figure 46. electropherograms of different IHSS standards and blank, obtained from CZE separations. In each case 100 mM ammonium carbonate buffer was used as elution media, and 12.5 mM sodium borate for CE separation buffer. The observed intense peaks in each sample were due to the ionic strength difference between the sample and the applied CE separation media.

This artefact was due to the large concentration difference between the buffer of the injected sample and the electrode buffer. The so called ”salt plug” was observed in the separation if the applied concentration of elution buffer was 100 mM. Therefore the concentration of the buffer, used for conditioning and elution, was decreased stepwise to 25 mM. The so obtained results has shown in Figure 45. During the column wash process fractions were taken (0.5-0.5mL) and directly analyzed without further changes with CZE, where 12.5 mM borate solution was used as separation buffer.

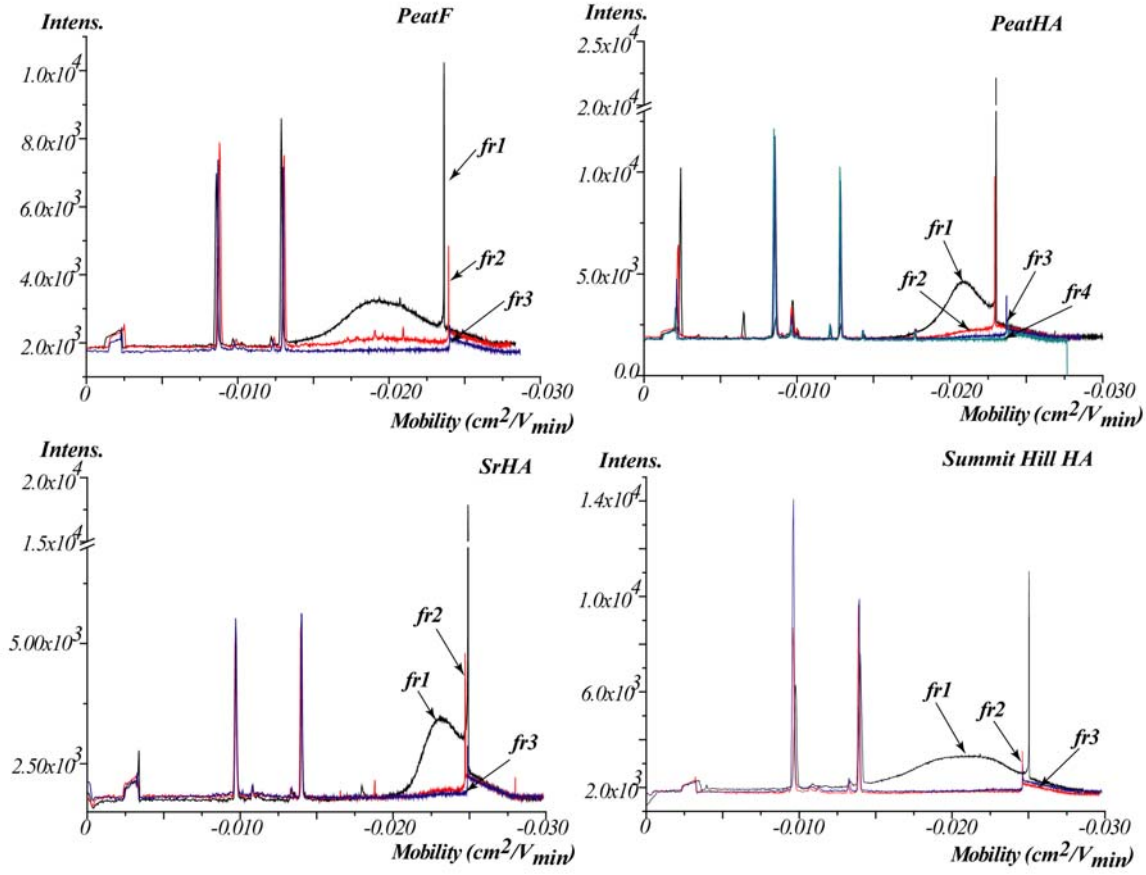

Figure 47. electropherograms of the obtained fractions of Peat F, Peat HA, SRHA and Summit Hill HA. Beside the unexpected distributions, several unidentified peaks were appeared, that might be originated from the samples, since the former measured blank sample (elution without sample) did not contain any of these. The intensities of these peaks were also decreased as the posterior fractions were analyzed.

The disappearance of intense and sharp peaks (Figure 47), denoted as B-polyol complexes, were expected since a visible retention was observed in each runs, however same electrophoretic distributions were obtained with decreased intensities, in the fractions as in the unfractionated samples. The phenomena, of the similar electrophoretic distribution, could be explain either with no specific retention on the column or with possible artefacts, derived from the applied ionic strengths.

Though with the model compounds, with less complexity, the specific retention was confirmed, and furthermore, a visibly part of the different organic matter remained on the columns, that were not eluted even with extended elution process (increased elution flow rate and volume). On the other hand, samples with extended chemical compositional space, like humic substances, offer various B specific polyols, with diverse masses and structure. This

fact allows to expect more complex electropherogram, with several peaks, with different mobilities, denoting complexes.

Hence, CZE/DAD approach was substituted with FT/ICR-MS method. FT-ICR mass spectrometry, with its ultra high resolution capability, enables, through advanced mathematical tools, a direct visualization and therefore the observed changes in the column experiments could be followed.

Peat organic matter were tested for this purpose with the similar experimental settings, that were applied before (mentioned above). Peat sample, because its peculiar natural condition, beside the other common alicyclic and aromatic structures with carboxylic and hydroxyl groups, rich in sugar and sugar derivatives. The occurred anaerobic conditions in peat lands hinder the possible degradation of these molecule species. Due to their structures, sugars are able to form stable complexes in presence of boron and therefore in this approach these materials are extremely good indicators of the complexation. The calculated elemental ratios from their assigned molecular formulae will be situated in the upper right corner in van Krevelen diagram. This observed pattern (Figure 48) specific for peat samples compared to other samples like SRNOM (see above), where aerobic conditions exist.

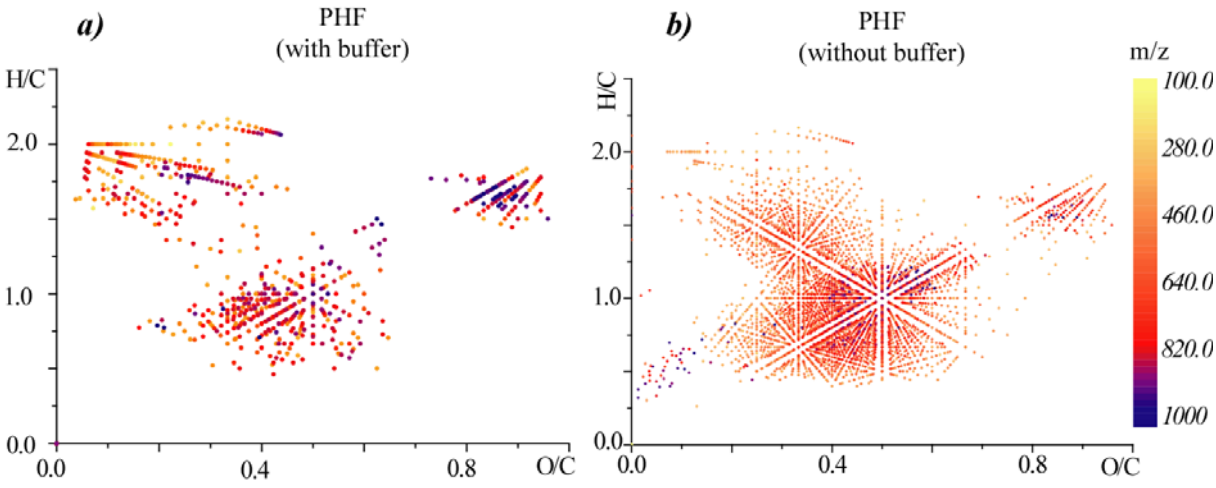

Figure 48. van Krevelen plot of the non-fractionated organic matter (Peat), derived from FT-ICR analysis. The sample was injected in methanol with ***(a)*** *and without* ***(b)*** *ammonium bicarbonate buffer.*

Fractions, obtained from column experiment were analysed by FT/MS without further modification. The obtained mass lists were converted to elemental formulae and were plotted in van Krevelen diagrams. The results were shown in Figure 48. However the same number of scans were applied for the analysis of the fractionated and the untreated peat samples, the obtained plots show difference in the number of assigned formulae. This phenomena is due to the occurred ionic suppression, when the samples were analyzed, since these samples were

buffered with the column elution buffer, since the non-treated peat sample (Figure 48/b) denote more complex van Krevelen diagram. Despite of the less assigned formulae, significant changes were observed, that occurred during the column experiment. In the region denoted with high O/C and high H/C ratios (0.8-1; 1.5-2), defined as probable sugar-type constituents, a clear disappearance was observed. Furthermore in the region (O/C: 0.2-0.4;H/C:0.5-1) with higher aromaticity[144] the density of the assigned formulae were also decreased. The third region (O/C;H/C: 0.2-0.3;1.5-2) occupied by aliphatic compounds, such as hydroxylated fatty acids, appeared also among the compounds that are possibly involved in B-complexation. These changes originated directly to the retention of the B-functionalized polymer. Preliminary studies with the model compounds and the changes in the specific location in the van Krevelen suggest, that these constituents retained on the column since they carry 1,2- or 1,3-cis diol functional groups (Figure 49/b). Differential molecular formulae list were calculated in order to visualize compounds that retained on the column.

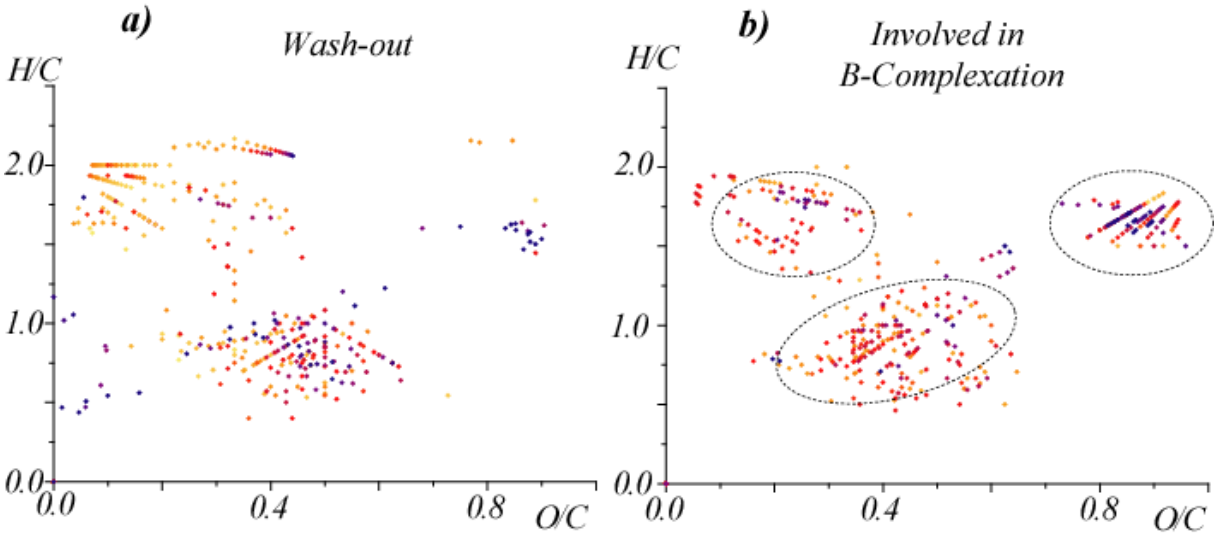

Figure 49. Elemental ratios plots of peat sample (from I. Perminova). ***(a)*** *assigned molecular formulae of the collected wash-out fraction (0.5 mL) and differential plot****(b)*** *obtained from the subtraction of the molecular formulae from molecular formulae of the original Peat sample (Figure 46/a). Samples contained 25mM of ammonium bicarbonate buffer (pH 9.2)*

3.1.6. Conclusion

A reversed approach to study boron complexation with NOM was presented. Different commercially available Boronic acid functionalized polymers were tested with model compounds in order to ensure the boron-polyol specificity of these polymers. Capillary electrophoresis was used after the column experiments to follow the retention behaviour on the polymers. Model compounds with and without 1,2- or 1,3-cis diol functional groups were used to characterize and exclude non specific retention. Based on the obtained results, m-aminophenylboronic acid on agarose gel was chosen for further applications with organic matter samples. NOM samples were applied onto the packed column, expecting that B-specific compounds will remain on the column. As expected, a visible part of the sample remained on the column, which was retained during the washing process. The sample, which was loaded onto the column and the wash-out were also measured with CZE/DAD with borate electrode buffer. The typical electropherogram was obtained with borate electrode buffer. Beside the "humic hump" a sharp peak, denoted earlier as B-complexes revealed in the electropherogram of the unfractionated sample.

This type of plot also appeared with less intensity also by the wash-out samples, however based on the denoted specific polyol retention, this was not expected. This type of phenomena can be originated a possible overload or an influence of the experimental settings, such as elution buffer concentration, electrode buffer concentration.

Although the column experiment had shown the expected results, the selected analytical method provided a result which interpretation needs further discussion. Therefore CZE/DAD method was substituted with FT-ICR/MS. Although the obtained mass spectra results suffered from a serious reduction of information, which was due to the applied ammonium bicarbonate buffer. Due to the applied buffer system, the obtained mass spectra contained less ionized species of the organic matter, since the ions of the elution buffer obstructed that, through ion suppression. Nevertheless the results showed that specific B-polyol complexation takes places on the applied polymer. Regions in the van Krevelen plot suggested polyols that are involved in complexation, are either phenolic type molecules with higher aromaticity and oxygen rich saturated constituents, such as carbohydrates.

3.2. Polyborate analysis with (ESI) FT-ICR/MS

Since Boron in aqueous condition tends to form polyborate structures, prior to the complexation studies, boric acid in solution was investigated by FT-ICR/MS. The observed results were considered for the further complexation studies.

3.2.1. Introduction

Mass spectrometry has been used in numerous studies of boric acid complexes of polyols and carbohydrates using ESI[41,270-272], matrix-assisted laser desorption[39, 273], though these analytical approaches described possible B-complex formation only with a borate-boric acid system, where the complex formation was simplified to mono- and bidundate complexes.

The existence of borate and polyborate anions in the principal sedimentary minerals and refined commercial borates has been already described. The hydrosphere, essentially the oceans, the outer crust or lithosphere and the inner mantle are important reservoirs for boron as minerals, with polyborate structures, (Borax ($Na_2B_4O_7$ x 10 H_2O), ulexite ($NaCaB_5O_9$ x $8H_2O$), kernite ($Na_2B_4O_7$ x 4 H_2O), colemanite ($Ca_2B_6O_{11}$ x 5 H_2O), etc.). Furthermore the existence of the complex equilibrium between borate/boric acid and polyborates in solution had been also shown in several studies[273]. NMR[274-276] and temperature jump studies[277], electrometric titrations[278] or by Raman spectroscopy[279] were applied to examine borate-boric acid-polyborate equilibrium and identify possible structures, that were already assumed[280]. The existence of polyborate anions and also their positively charged gaseous forms were also observed and studied with FT-ICR/MS[281-283] extended with additional information on the structures and energetic. Hence, the presumption of a multiple-partner complex formation with different, parallel existed, polyborate species aroused. In order to obtain later properly described complexes, in this chapter, boric acid solution with the generally utilized and less concentration was characterized by FT-ICR/MS.

3.2.2. Chemical reagent

Regular Boric acid (>99.8% purity) was purchased from Merck (Darmstadt, Germany), while ^{11}B enriched boric acid was obtained from Sigma-Aldrich. For all

experiment LC-MS grade a water and methanol (Sigma-Aldrich, Seelze, Germany) were used.

3.2.3. Sample preparation for ESI-MS analysis

100 mM stock solutions of boric acids were prepared fresh in LC-MS grade water. The pHs of the solutions were adjusted with 25 V/V% ammonium hydroxide solution to pH 9. Directly before the FT/MS measurement the stock solutions were diluted with methanol to 20 and 1mM final concentration Polyborate formation was followed by FT-ICR/MS in negative modus.

3.2.4. Methods and experimental setting

3.2.4.1. FT-ICR MS

High-resolution mass spectra were acquired on a Bruker (Bremen, Germany) APEX Qe Fourier transform ion cyclotron resonance mass spectrometer, equipped with a 12 Tesla superconducting magnet and an Apollo II ESI source. Samples were introduced into the micro-electrospray source at a flow rate of 120 µl/h with a nebulizer gas pressure of 20 psi, and a drying gas pressure of 15 psi (@ 250 °C). Spectra were externally calibrated on clusters of arginine (10 mg/l in methanol); calibration errors in the relevant mass range were always below 0.1 ppm. In the mass range of 150 –1500 m/z 4 MW time domain was applied in order to enhance resolution. The spectra were zero filled to a processing size of 4 megawords. Before Fourier transformation of the time-domain transient, a sine apodization was performed. The ion accumulation time in the ion source was set to 2 s for 125 scans were accumulated for samples. To gain further structural information on the complexes, collision-induced dissociation (CID) was carried out. The mass window of 1 Da of the parent ions was selected between the ion source and the analyzer cell with the quadrupole and were fragmented by varying the excitation power in the collision cell (CID). Argon, as a collision gas was pulsed into the chamber at a pressure of 1 x 10^{-8} Torr, with 50 ms gas pulse duration. On resonance CID provided abundant structural information. The ion accumulation time in the ion source was set to 0.2 s for 256 scans were accumulated for samples

3.2.5. FT-ICR/MS analysis of boric acid solution

Boric acid solutions (normal and enriched) were injected without further modification in order to observe the occurred polyborate formation (Figure 50). Isotope clusters, containing up to 19 boron atoms were discussed here which have intensities significantly higher intensities than the background and the correct isotope ratios, that were expected and simulated for the corresponding B_n multiplet, however the spectrum showed further clusters with lower intensities. Using the built-in formula calculator, several, formally not described polyborate complexes were revealed [281-283]. Formulae were assigned and confirmed based on their denoted isotope patterns, since compounds, incorporating only B, O, H atoms show specific isotope pattern, that is determined by the specific isotope distribution of boron. Therefore and because of the high mass accuracy, provided by the instrument, the proposed structures are tend to be realistic.

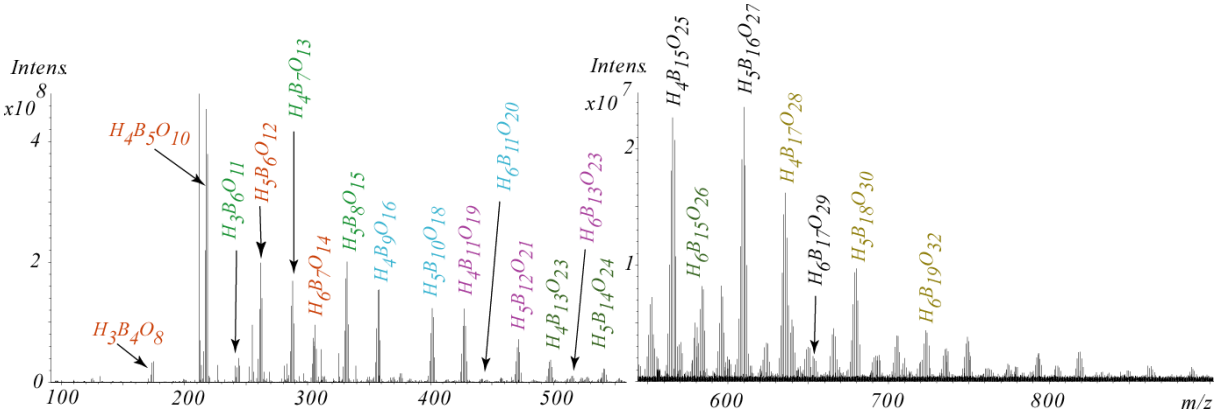

Figure 50. Mass spectrum of 25 mM Boric acid, obtained from FT-ICR/MS. The assigned molecular formulae were sorted as potential members of possible series.

To assign the main isotope peaks within these clusters ^{11}B enriched boric acid was also measured (Figure 51 and 52). In order to assign the main isotope peaks out of the cluster of isotopes, the spectra from normal and ^{11}B enriched boric acid were confronted and confirmed those specific isotope peaks of the complexes, that was later highlighted with asterisks. Figure 50 stands as an example for the confronted mass spectra. The ^{11}B enriched boric acid solution denoted the similar, formally also observed polyborate ions, however in this case only one dominant peak was presented per ion. Since the used boric acid contained >99% of ^{11}B in some cases the other isotopes could be also observed, however with significantly lower intensities. Assignment of the main isotope peak was not only necessary to assign molecular formulae, but also for the following fragmentation experiments, where the selected isotopes were isolated by the Quadrupole and fragmentized.

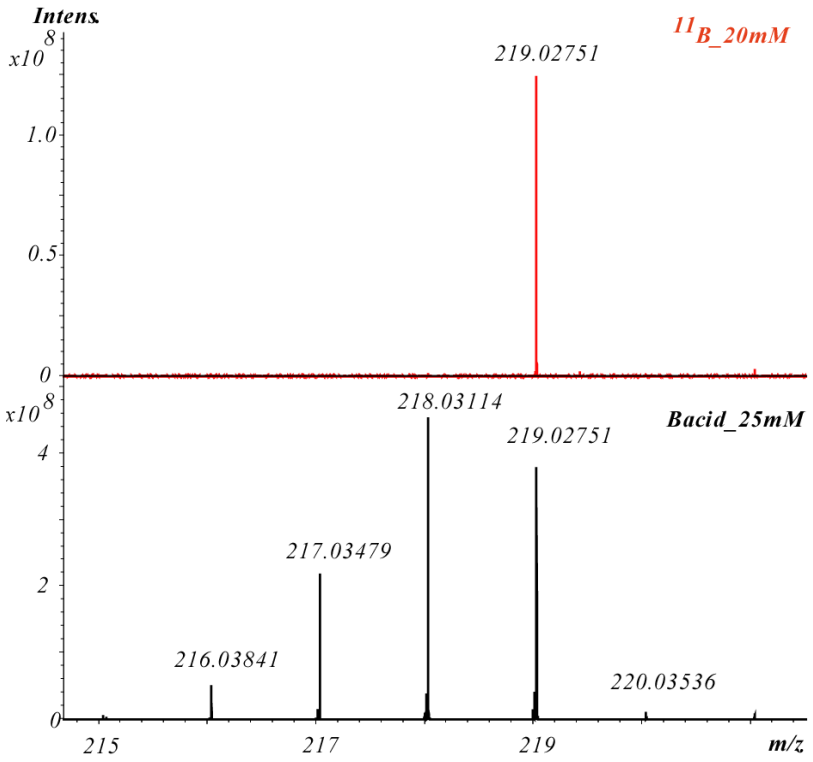

Figure 51. compared spectra of the similar m/z range derived from FT/MS analysis of ^{11}B enriched and normal boric acid.

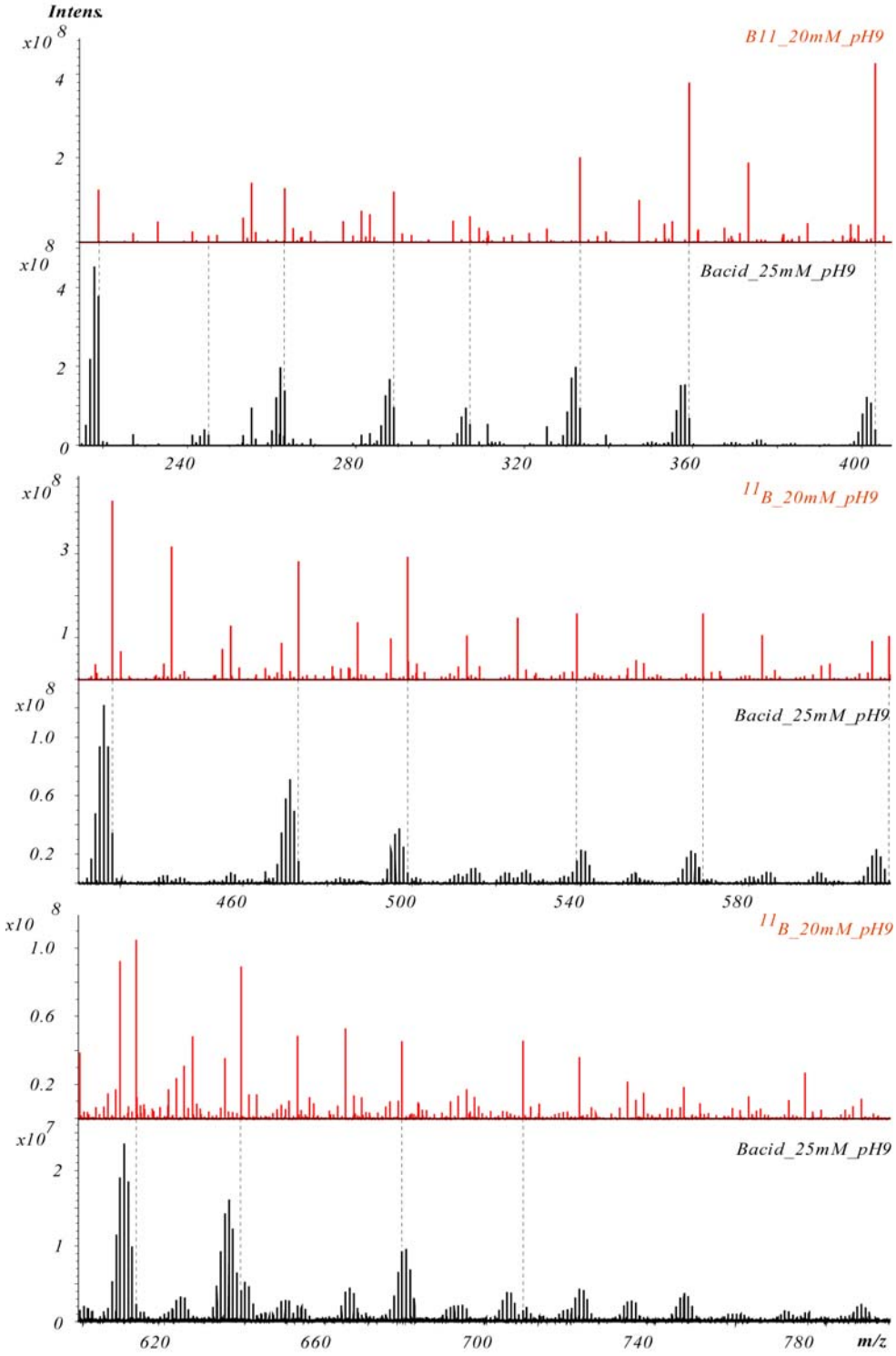

Figure 52. confronted broadband mass spectra of ^{11}B enriched and normal boric acid.

Since the denoted isotope pattern changes proportionally with the number of incorporated boron, the isotope pattern of the polyborate is getting more and more complex. To describe and follow the incorporation, theoretical isotope patterns were simulated of boric acid and different polyborates, with stepwise increased boron atoms (Figure 53). The simulation clearly visualize the changes of the observed isotope ratios of $^{10}B/^{11}B$, when the

number of boron atoms were increased in the molecule. Here it has to be noticed, that the isotopes ^{18}O and ^{2}H were disregarded by the simulations, since they denote isotopes with low abundances relative to ^{10}B.

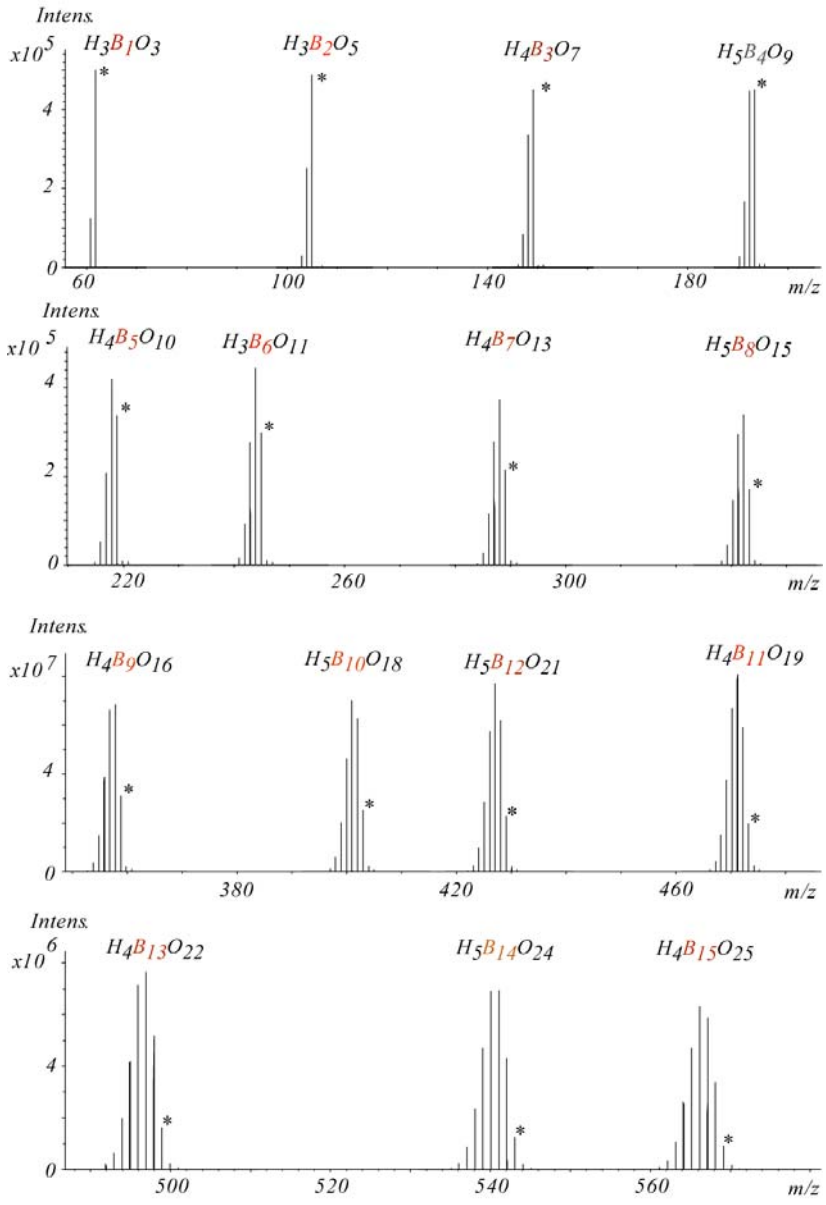

Figure 53. Simulated isotope patterns of different polyborates up to 15 boron atoms incorporated. The peaks highlighted with asterisk denote the main isotope (^{11}B).

3.2.6. Collusion induced fragmentation of polyborates

The result of the fragmentation of polyborates, up to 15 incorporated boron atoms were showed here enable to verify the proposed molecular formulae and possible relation between the observed species. Formal studies[281-283], where with stepwise boric acid additions in gas phase the authors were able to build up a series of polyborate ions, might suggest similar behaviour of ions formation in aqueous phase. In this case the initial experimental conditions, like ionic strength, boric acid concentration and pH might also effect the evolution of the different polyborate ions, that were later observed in the gaseous phase.

For the most abundant polyborates, observed in FT mass spectrum, collusion induced fragmentations were conducted in order to describe potential relationship between the species of the observed polyborate ions and establish the parent-daughter relationships illustrated in figure x. The main isotopes, formally denoted with asterisks, were isolated and fragmented. Out of fifteen different species that were isolated and fragmented, one with the mass 263 denoted as $H_5B_6O_{12}^-$ was show here as an example (Figure 54).

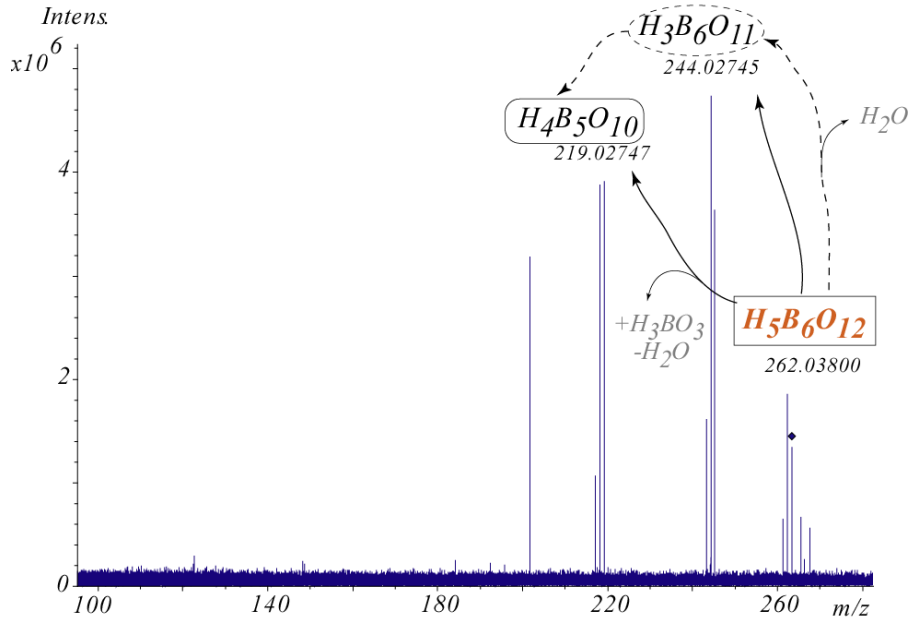

Figure 54. example for CID fragmentation, species $H_5B_6O_{12}$ as an abundant peak were isolated in quadrupole and fragmented with argon.

The obtained spectrum revealed two fragment species with fairly similar intensities, that might allow to deduct that these are direct fragments of the parent ion and not consecutive ones, due to a further fragmentation of an observed daughter ion. As shown in Figure 54. the fragmentation of the parental ion ($H_5B_6O_{12}$) yields, through a loss of water, a daughter ion ($H_3B_6O_{11}$), which might be a consequence of cyclic structure formation (Figure

55/b). The mass difference between the parental ion and the other observed fragment at mass 220 m/z, refers to a complete loss of boric acid, that might originally was only bounded over only one hydroxyl group to the main structure (Figure 55/a).

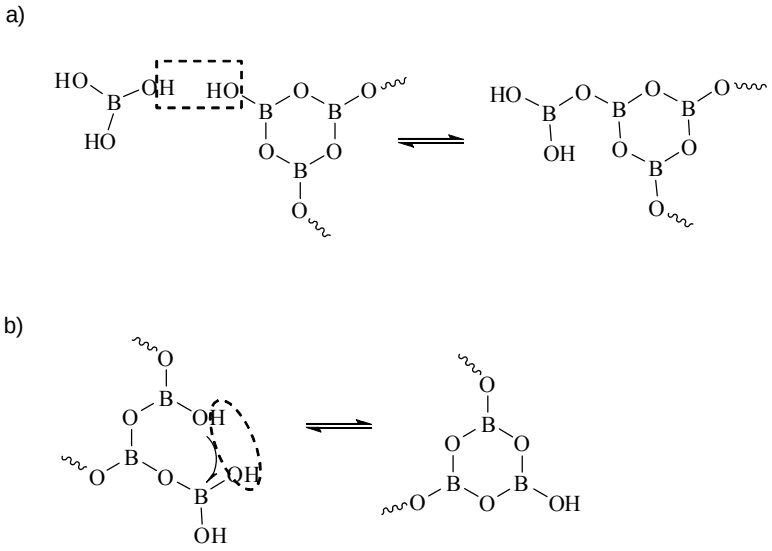

*Figure 55. Possible boric acid incorporation **(a)** resulting an open structure, where two trigonal BO_3 sharing an oxygen atom and ring formation **(b)** resulting a basic structure of polyborates with a six-atom ring with alternate boron and oxygen atoms.*

Initially, (Figure 50) the different polyborate clusters of ions were ordered into different series, based on their denoted specific mass differences. The observed differences might refer to a further boric acid (H_3BO_3) incorporation followed by a water elimination, which is denoted with HBO_2 changes in the following. To examine the relations of the possible members, similar principle could be interpreted as showed in the presented example above. In Figure 56, the first denoted series (coloured with red) might contain four polyborate ions with relative high abundances.

Separate fragmentation of $H_6B_7O_{14}$ yielded a fragment at mass 263 m/z that might refer to $H_5B_6O_{12}$. If the polyborate at 263 m/z was fragmented, daughter ion at 219 m/z ($H_4B_5O_{10}$) was also appeared. Further fragmentation of this species revealed clusters of ions at 175 m/z, which was assigned as $H_3B_4O_8$. Beside the highlighted daughter ions, in cases of parental ions 307 m/z and 263 m/z, further fragments were observed, which were results of a water elimination. These phenomena could be explained with a possible ring formation, which was mentioned above. Follow the similar principles, fragmentation studies confirmed in most cases that the assumed connection between the polyborate species might be correct.

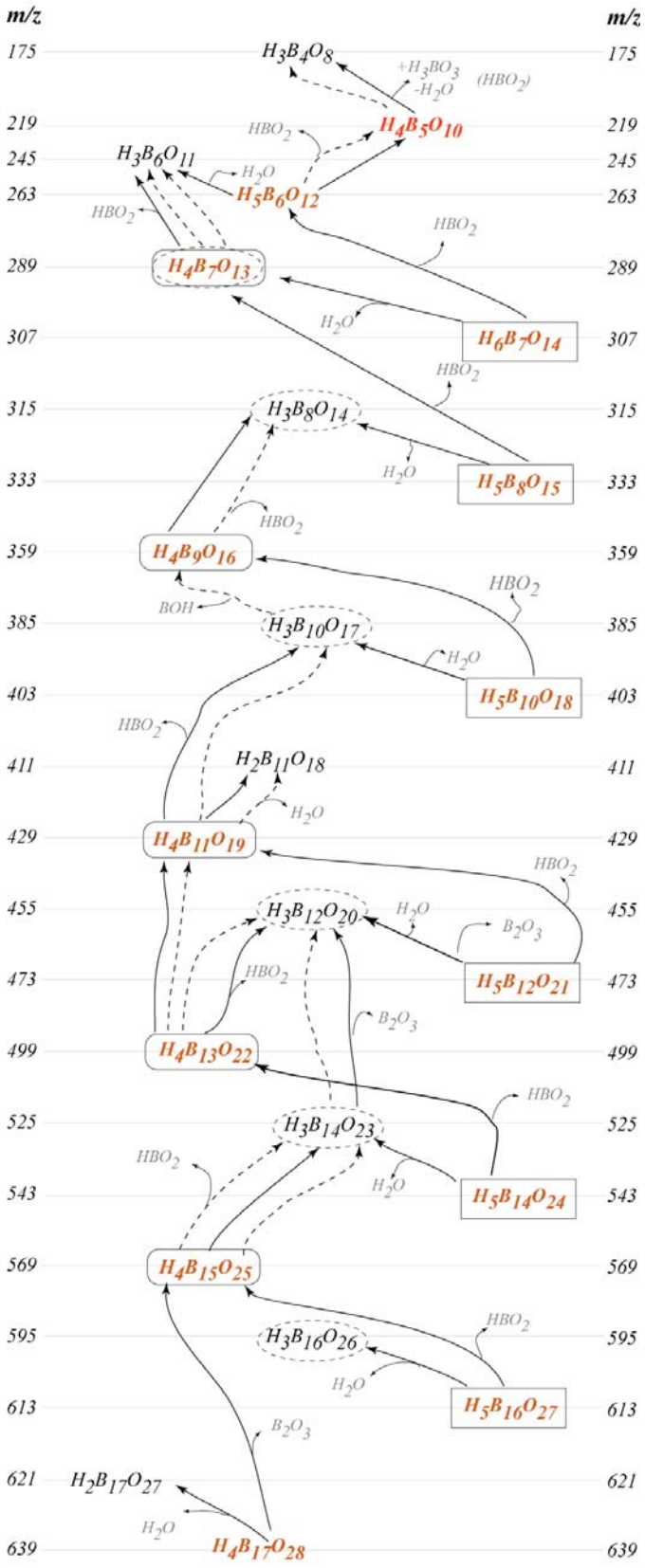

Figure 56. Proposed fragmentation pathways of polyborate species, derived from the CID fragmentation studies. Species coloured with red were selected for fragmentation as parental ions. Normal lines symbolize the directly observed daughter ions, derived from the fragmentations. Dashed lines denote possible fragments of the daughter ions and possible correlation between the different species.

3.2.7. Conclusion

The broad-band spectrum of boric acid, obtained from FT-ICR/MS, revealed unexpected clusters of ions with specific isotope pattern distributions, hence further description was necessary. The spectrum with ultra high resolution and mass accuracy enabled the molecular formula assignment based on the mass and the denoted isotope distribution. The obtained formulae were ordered in series, with regular mass differences (HBO_2), corresponding to an incorporated boric acid into the existing structure, with a loss of a water. To examine this phenomena collusion induced fragmentation was used. The fragmentation also revealed the suggested relationships among the polyborate species. Up to now polyborates only with lower number of boron atoms were reported with mass spectrometric approaches. Here, molecules with up to 19 B-atoms were assigned and confirmed. The here presented and confirmed polyborate ions represent a further step to a fully described polyborate system. Furthermore the observed polymerization should be considered in the following studies, and complex formation with boron should not exclude polyborates as potential reaction partners.

3.3. Study of B-complexation with monomolecular models

Fourier transform ion cyclotron resonance mass spectrometry (FT-ICR/MS), was applied to identify boric acid(B°)/borate(B^-) complexes in a monomolecular model system, containing caffeic acid and boric acid/borate solution in various concentration ratios at pH 9.2. Using electrospray ionization operated in negative mode as a "soft" ionization technique, clusters of polyborate were detected beside the well known B°L, B^-L and B^-L_2 complexes.

3.3.1. Introduction

The main goal of this chapter is to identify the type of molecules that are playing a key role in boron complex formation in natural environmental conditions. Within this study the goal was to use high magnetic field Fourier transform ion-cyclotron resonance mass spectrometry (FT-ICR/MS), with its ultra-high mass resolution and mass accuracy over a sizeable mass range, to identify the borate complexes with caffeic acid as a model diol containing aromatic acid, based on exact mass and isotopic ratios. This approach will define an experimental basis with a monomolecular model system that can be further extended to describe B-complex formation in natural polyols such as present in natural organic matter. This contribution presents the first mass-based experimental evidence of polyborate and multiple-ligand complex formation, exemplified with caffeic acid and analyzed with electrospray ionization FT-ICR/MS.

This chapter was prepared, based on the article " *Targeted borate complex formation as followed with electrospray Fourier transform ion cyclotron mass spectrometry: monomolecular model system and polyborate formation"* **[IV]**

3.3.2. Chemicals

Caffeic acid and ferulic acid, ammonium bicarbonate (used as a volatile buffer) and acetonitrile (as the volatile organic solvent for the mass spectrometry) were obtained from Sigma-Aldrich; boric acid was purchased from Merck (Darmstadt, Germany). All chemicals were used without further purification. Ultra pure water was produced with a MilliQ system (Millipore, Billerica, MA, USA). For all ICR-FT/MS experiment LC-MS grade acetonitrile and water (Sigma-Aldrich, Seelze, Germany) were used.

3.3.3. Sample preparation for ESI-MS analysis

The boric acid concentration dependency experiments were all conducted on pH 9.2. The injected samples were prepared identically; differ only in the concentrations of the added boric acid, which were 1, 2.5, 5, 10, 25 and 50 mM. The pH dependency experiments were conducted on pH 4.3 and 9.2 with the boric acid concentrations of 10 mM (620µg/mL) and 25µg/mL of model compound (caffeic acid). For further fragmentation study, the mixture of 25 ppm (final concentration) caffeic acid and 10 mM boric acid solution was adjusted with 10 mM ammonium bicarbonate buffer. All aqueous samples were prepared fresh in ultra pure water. The samples were diluted 4-fold with acetonitrile to stabilize the electrospray current, directly before the injection.

3.3.4. Methods and Experimental Settings

3.3.4.1. FT-ICR /MS

High-resolution mass spectra were acquired on a Bruker (Bremen, Germany) APEX Qe Fourier transform ion cyclotron resonance mass spectrometer, equipped with a 12 Tesla superconducting magnet and an APOLLO I and more recently APOLLO II electrospray source. For negative electrospray, acetonitrile was used. Samples were introduced into the micro-electrospray source at a flow rate of 120 µl/h with a nebulizer gas pressure of 20 psi, and a drying gas pressure of 15 psi (@ 250 °C). Spectra were externally calibrated on clusters of arginine (10 mg/l in methanol); calibration errors in the relevant mass range were always below 0.1 ppm. The spectra were acquired with a time domain of 1 megaword with a mass range of 150 –1000 m/z. The spectra were zero filled to a processing size of 2 megawords. Before Fourier transformation of the time-domain transient, a sine apodization was performed. To gain further structural information on the complexes, collision-induced dissociation (CID) was carried out. The mass window of 1 Da of the parent ions was selected between the ion source and the analyzer cell with the quadrupole and were fragmented by varying the excitation power in the collision cell (CID). Argon, as a collision gas was pulsed into the chamber at a pressure of 1 x 10^{-8} Torr, with 50 ms gas pulse duration. On resonance CID provided abundant structural information. The ion accumulation time in the ion source was set to 0.2 s for 256 scans were accumulated for samples

3.3.5. Concentration and pH dependency

As the applied analytical system contains electrospray ionization, which is clearly sensitive to its operational settings and depends on the measured samples, certain limitations of the set up might be minimized with the carefully chosen parameters. Hence before the fragmentation experiments, samples with different boric acid concentrations were analyzed, in order to investigate possible ion suppression. These experiments were conducted with Apollo I ion source which is less sensitive as the second version, therefore minor complexes did not showed up, though focusing on the most abundant and intensive masses, the obtained information are also representative. The monitored masses were the borate-caffeic acid (at m/z 223), borate-bidundate (at m/z 367) (combination of ^{11}B and the ^{12}C isotopes) complexes and the ^{12}C isotopes of the two model compounds, caffeic acid (at m/z 179) and ferulic acid (at m/z 193). Alone the correlation between the signal intensity of the caffeic acid and its complexes, and the applied boric acid concentration might not be consistent, while certain artefacts, like ion suppression, could interfere. Therefore ferulic acid was used in this system as a general marker for possible ion suppression, while its structure hinders the specific complexation with boric acid, hence the decreased signal intensity of its representative mass might only due to the occurred suppression in electrospray. The injected samples were containing 1; 2.5; 5; 10; 25 and 50 mM of boric acid respectively. The results show negative gradient in case of caffeic acid and an increasing intensity of the complexes (Figure 57). Beside the caffeic acid, the signal intensity of the ferulic acid was also decreasing, indicating slightly the effect of the applied boric acid concentration. This and the fact that the complexes reached their maximum intensity, suggest not exceeding the 10 mM boric acid concentration level, in further measurements.

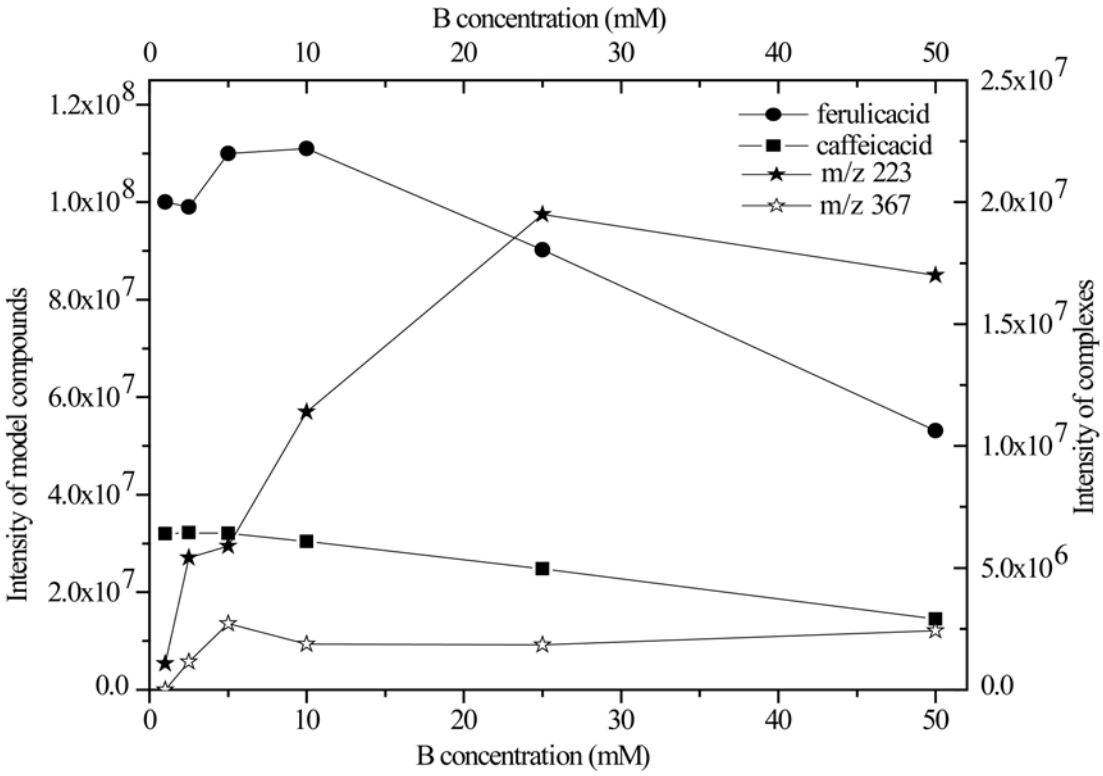

Figure 57. Boric acid concentration dependency experiment. Increasing of the boric acid concentration at constant concentration of the ferulic and caffeic acid, respectively, resulted in an MS peak intensity increase for both borate complexes, and a concomitant decrease in both model compounds peak intensity. Since the signal intensity of the ferulic acid has a negative slope, the negative gradient of the caffeic acid might represent not only the use of it as a substrate, but the effect of the ion suppression.

Two experiments were conducted, to investigate the possible effect of the pH. The pH of 9.2 was adjusted with 10 mM ammonium bicarbonate buffer. In case of the pH 4.3, buffer was not applied, the solution of boric acid and the model compounds resulting alone the certain pH. Obtaining spectra with similar number of scans, the intensity of 11 complexes were divided by the intensity of the caffeic acid obtained from each run. The result is summarized in Figure 58. In each case the observed relative intensities were higher if the pH were increased of the sample up to 9.2. This distribution might correlate with the fact that boric acid in diluted solutions at pH 9.2 has equally number of boric acid and borate molecules; therefore none of them limit the possible formation of the polyborate and polyborate-polyol complexes.

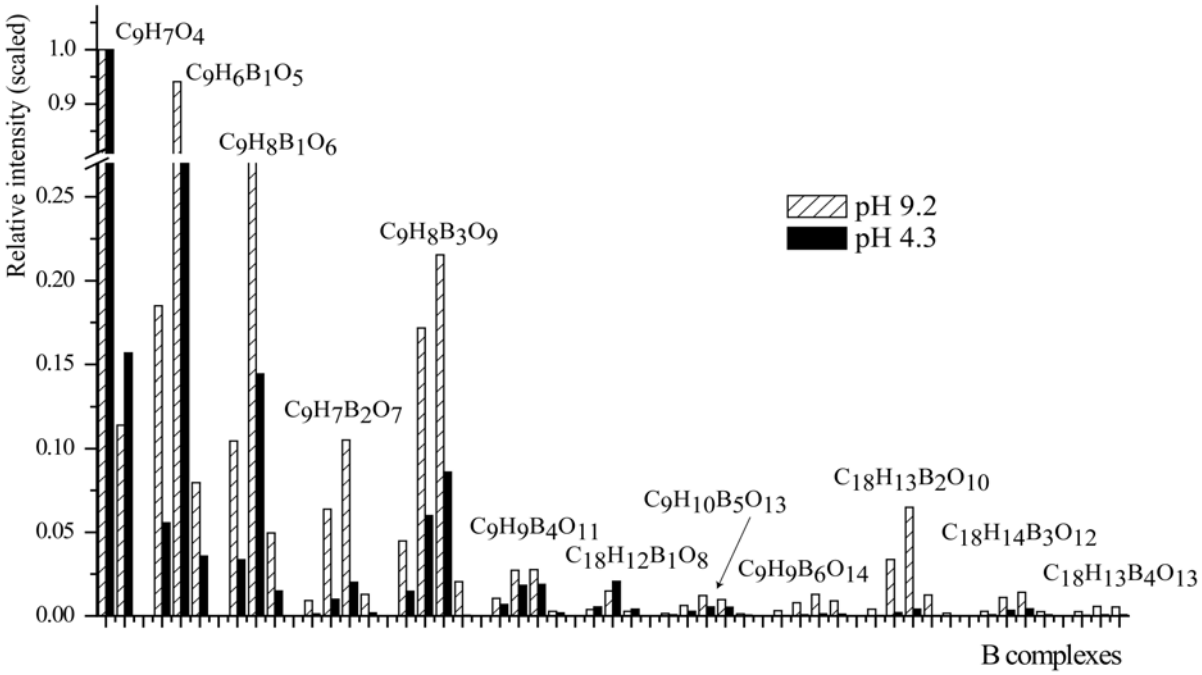

Figure 58. pH dependency experiment.

3.3.6. ESI/FTMS of caffeic acid-boric acid/borate complexes

Negative ion ESI-mass spectra of 25 ppm of caffeic acid in 10 mM ammonium bicarbonate buffer at pH 9.2, revealed the prominent molecular anion for the singly charged molecule $[M-H]^-$ at m/z 179.03497 (calculated 179.03498 Da). Since caffeic acid containing 1,2-cis diol group on its aromatic backbone, the possibility of the complexation with boric acid/borate system is given. At this pH the carboxylic group of the caffeic acid deprotonated, providing the negative charge of the whole molecule. This pH equals the pK_a of the boric acid, allowing the coexistence of both $B(OH)_3$ and $B(OH)_4^-$, and hence the observation of the three different kinds of boric acid/borate complexes, like $C_9H_6O_5B_1^-$, $C_9H_8O_6B_1^-$, $C_{18}H_{12}O_8B_1^-$ (Figure 61) in accordance with previous studies of borate complexes of 1,2-cis-diol-containing molecules[284]. Earlier studies focused, independently of the methods employed, primarily on the formation of complexes containing single boron atoms such as illustrated in Figure 61[33, 39, 43]; However Penn et al. [43] observed a maltotriose-derived complex $B_2L_2H^-$samples containing 10 mM maltotriose and 10 mM boric acid by MALDI FT mass spectrometry and suggested the existence of oligosaccharide complexes containing multiple

boron atoms. Thevenon et al. [276]carried out ^{11}B NMR studies to determine the boron species present in protein borate wood preservatives. At acidic pH only the undissociated $B(OH)_3$ at $\delta(^{11}B)$ = 20 ppm occurred, while at alkaline pH NMR resonances of the charged and uncharged boron atoms at $\delta(^{11}B)$ = 16 ppm and 12.6-13.7 ppm, attributed to the three ion species $[B(OH)_4]^-$, $[B_3O_3(OH)_4]^-$, $[B_3O_3(OH)_5]^{2-}$ occurred. A third signal with much lower intensity at $\delta(^{11}B)$ = 1.7-1.8 ppm was assigned to a reaction product of polyborate with the protein.

Isotope patterns in mass spectra allow to unambiguously confirm the number of boron atoms in each complex. Boron has two stable isotopes, ^{10}B and ^{11}B, with average relative abundances near 20% and 80%, respectively. This unusual feature (the higher mass isotope shows the larger abundance) results in unique isotope-patterns of boron-containing molecules (Figure 59) which allow an unambiguous assignment based on intensity ratios and mass differences. Owing to the uniqueness of this signature, this analysis even works with mass spectra obtained with mass spectrometers of lower resolution[43]. However, unambiguous assignment of $C_nH_mO_qB_z$ mass peaks required higher resolution, as provided by the 12 T magnetic field (Figure 59). The ultra-high resolution and mass accuracy of FT-ICR/MS allows identifying and distinguishing even the isotopes of lower abundance, like ^{18}O, providing key information in the complete and unambiguous molecular formula assignment.

The distinctive isotope patterns of CHOB-molecules depict the probable mixture of the naturally occurred ^{12}C, ^{13}C, ^{1}H, ^{16}O, ^{18}O, isotopes and the ^{10}B, ^{11}B isotopes. Caffeic acid in the presence of 10mM (final concentration) boric acid at pH 9.2 produced mass spectra representing boron-containing molecules in addition to the initial caffeic acid signal (Figure 60). The peak list containing only the caffeic acid-B complexes, has been shown in Table 8.

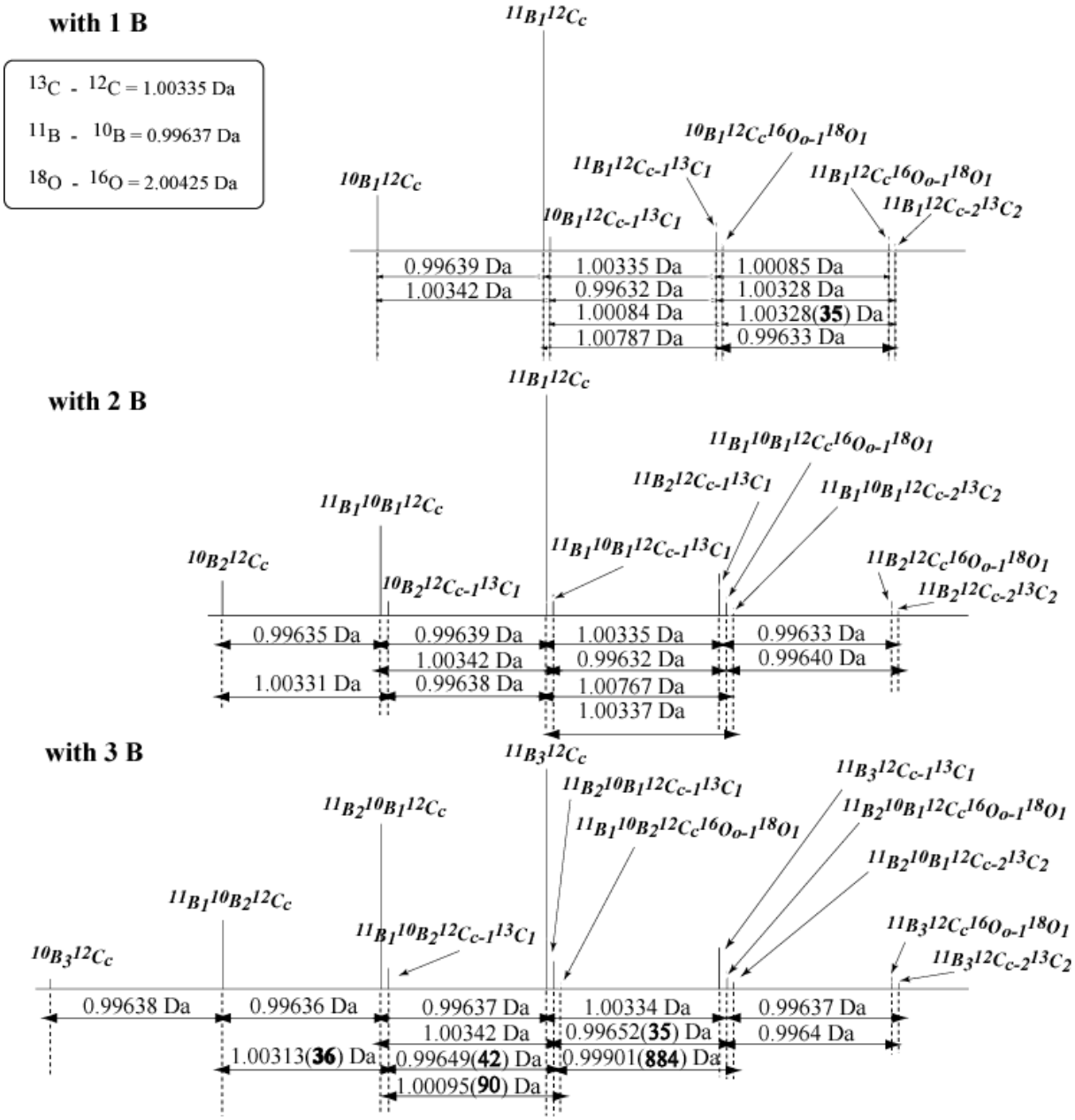

Figure 59. Theoretical isotope patterns (C,H,O containing parent molecules only) in case of one, two and three involved boron. The denoted isotope abundances are not reflecting the natural ratios. The mass differences (last digits (bolded) in bracket denote the theoretical values) between the most abundant isotopes (^{12}C, ^{11}B, ^{16}O,^{1}H) were utilized for the complex characterization.

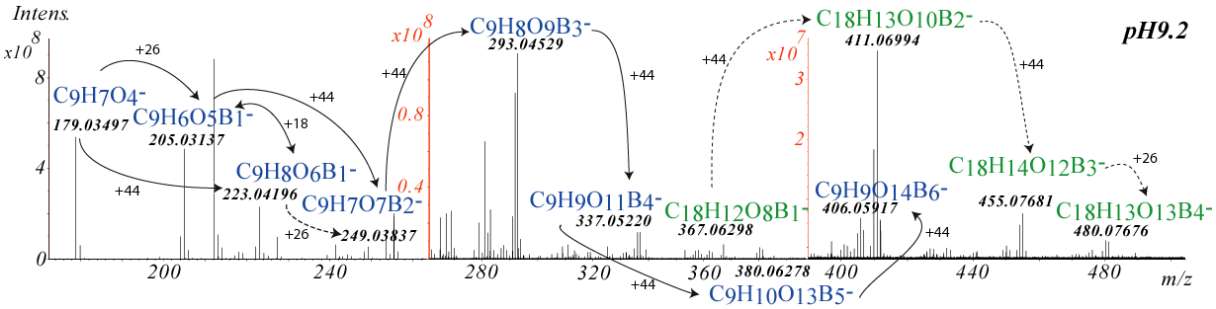

Figure 60. Scaled and superimposed FT/MS spectra of the detected and assigned boron containing caffeic acid complexes at pH 9.2. The marked mass differences occurred by every incorporation of a boric acid molecule. FT/MS spectra of high signal-to-noise ratio (256 scans) allowed to identify complexes with up to 6 boron atoms, which could be assigned based on their isotope pattern. Further complexes of lower abundance might be detected in case of longer acquisition time.

Identified Molecular Formula	Detected mass (m/z)	Theoretical mass (m/z)	Error (mDa)	Error (ppm)
$C_9H_7O_4^-$	179.03497	179.03498	+0.02	0.1
$C_9H_6O_5B_1^-$	205.03137	205.03138	+0.00	0.0
$C_9H_8O_6B_1^-$	223.04196	223.04194	-0.01	0.1
$C_9H_7O_7B_2^-$	249.03837	249.03834	-0.03	0.1
$C_9H_8O_9B_3^-$	293.04529	293.04530	+0.01	0.0
$C_9H_9O_{11}B_4^-$	337.05220	337.05226	+0.06	0.2
$C_{18}H_{12}O_8B_1^-$	367.06298	367.06307	+0.10	0.3
$C_9H_{10}O_{13}B_5^-$	381.05915	381.05922	+0.06	0.2
$C_9H_9O_{14}B_6^-$	407.05554	407.05561	+0.07	0.2
$C_{18}H_{13}O_{10}B_2^-$	411.06994	411.07003	+0.09	0.2
$C_{18}H_{14}O_{12}B_3^-$	455.07681	455.07699	+0.18	0.4
$C_{18}H_{13}O_{13}B_4$	481.07316	481.07339	+0.22	0.5

Table 8. Assigned molecular formulas from the obtained FT/MS spectra of the interaction of boric acid and caffeic acid at pH 9.2. Only formulae which referring to most probable complexes are shown.

Boric acid was also injected under the same conditions and the obtained spectral peaks were subtracted from the original mass list, leaving only (caffeic acid)-boric acid/borate complexes. Although the obtained masses coincided with the simulated masses within an error margin below 0.6 ppm three different B containing complexes (at m/z 223.04195, assigned as $[C_9H_6BO_6]^-$; at m/z 249.03836 as $[C_9H_7B_2O_7]^-$; and at m/z 293.04529 as $[C_9H_8B_3O_9]^-$) were subject to a detailed isotopomer analysis to verify the proposed/calculated formulas (Figure 61.).

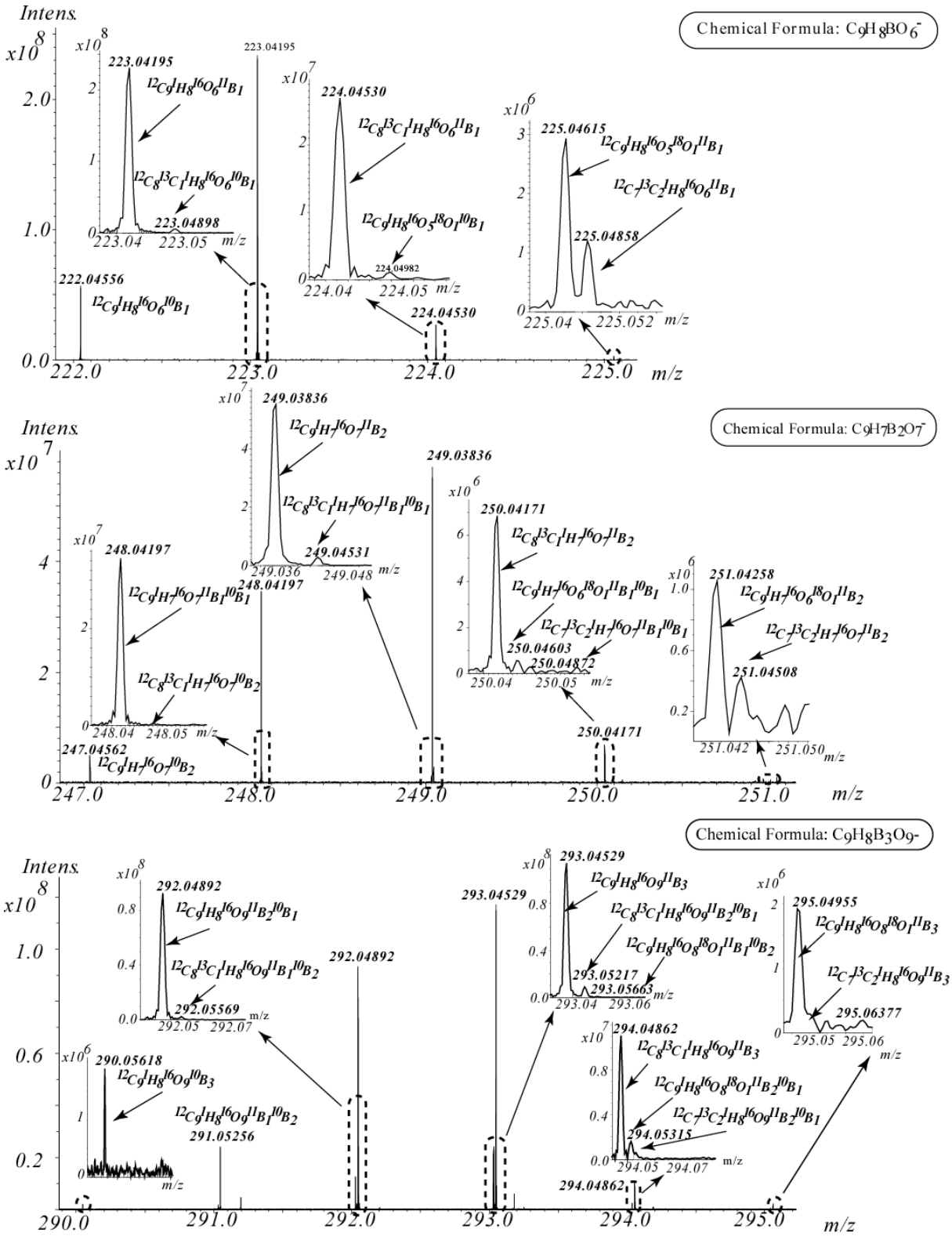

Figure 61. Isotope pattern distribution in FT-ICR mass spectra of boron complexes at m/z 223. 04195 assigned as $[C_9H_6BO_6]^-$, 249.03836 as $[C_9H_7B_2O_7]^-$, and 293.04529 as $[C_9H_8B_3O_9]^-$.

The exact accordance of the experimental and theoretical isotope patterns enabled to assign the mass ranges given in Figure 61 (222-225 Da, 247-251 Da, 290-295 Da) from 222

to 225 Da to unique CHOB-molecular ions, containing a single, two and three boron atoms, respectively. Furthermore, the proposed formulae and observed mass peaks indicated the occurrence of singly charged molecules in the spectra. At pH 9.2, the carboxylic group of the caffeic acid is fully deprotonated, and the tetragonal form of the borate also bears negative charge, which would make an occurrence of doubly charged ions conceivable, however only single charged ions were observed under the given experimental conditions.

This disagreement can be partly explained by variance of boric acid solution phase acidity (solely Lewis acidity of $B(OH)_3$) and gas phase acidity (Brönsted acidity with conjugate pairs H_3BO_3 and $H_2BO_3^-$) that enable ion-molecule reactions not feasible in solution [282]; in addition, the charges of the ions generated by ESI may not reflect the charge state of solution state compounds, but rather the results of both charge accumulation in the droplets and charge modification by electrochemical process at the probe tip[285]. For the first sight, the molecular formulae of the observed complexes were in excellent accordance with the theoretical calculations, however, collision induced fragmentation revealed additional structural assignments.

3.3.7. Collision induced dissociation of the caffeic acid- B complexes

To gain supplementary structural information on the observed complexes, collision induced dissociation (CID) was carried out. The utilization of this technique was necessary to verify our assumption that certain mass peaks were referring to specific covalently bound polyborate-caffeic acid complexes. The presence of polyborate anions in solution has been established by NMR, pH titration, temperature jump techniques, Raman spectroscopy and even with FT/MS[277-279, 282, 286]. The proportions of these polyborate ions are governed by the solution pH and the initial concentration of boric acid [277]. However the given concentration level of the polyborate formation varies among the different publications; generally, these ions formed only when the concentration of the boric acid was in excess of 10 mM. We should emphasise here, that lower value may also represent the anion formation limit, depend on the sensitivity of the different applied method. At first, the "common" single-boron incorporating caffeic acid complexes like $C_9H_6O_5B_1^-$, $C_9H_8O_6B_1^-$, $C_{18}H_{12}O_8B_1^-$ (Figure 62) were fragmented in order to demonstrate real covalent complexation in the aqueous phase rather than downstream cluster formation of ions in the gas phase. The parental ion at m/z 205.03118 ($C_9H_6B_1O_5^-$) representing a trigonal coordinated boron complex

produced only one fragment at 161.04143, resulting from the loss of CO_2, equivalent to the carboxylic acid group of the caffeic acid.

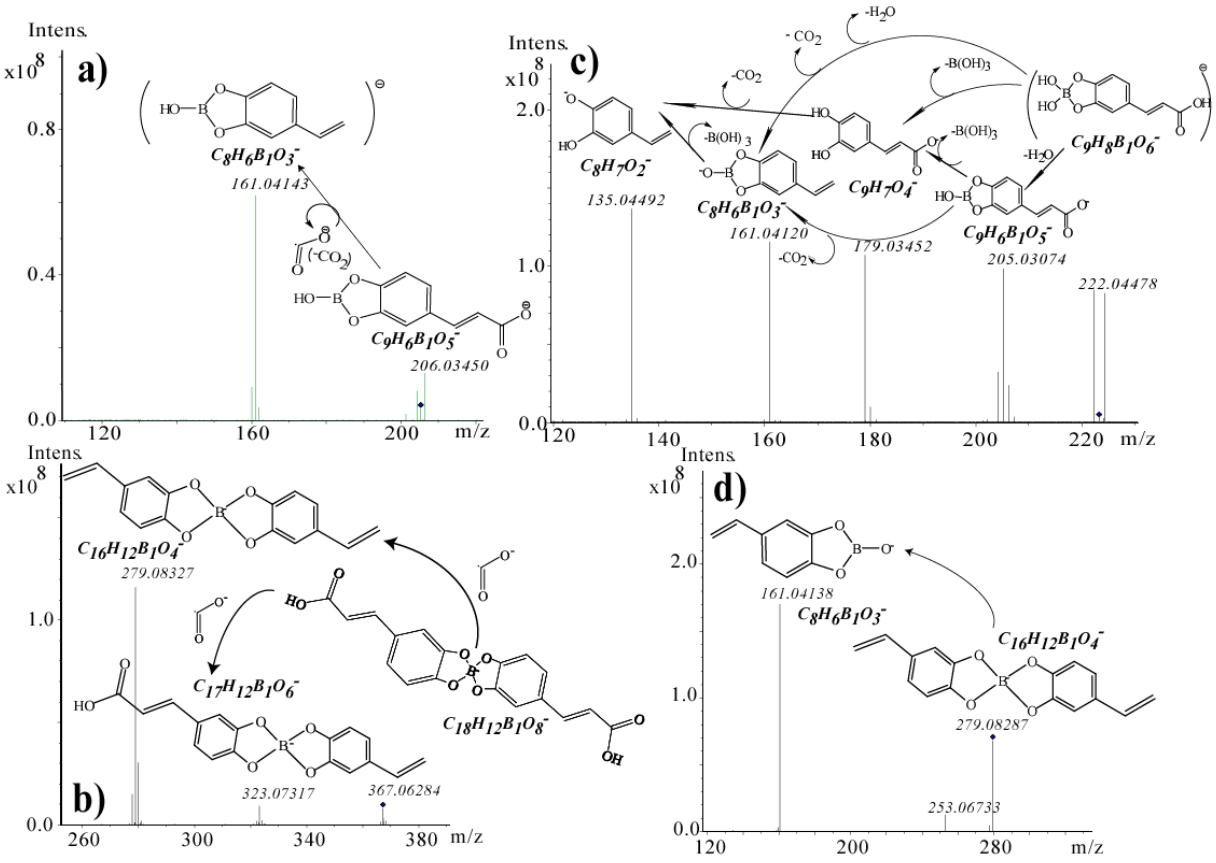

Figure 62. Proposed fragmentation pathways of mono- and bidundate boron esters with caffeic acid.

Since it was not possible in some of the experiments to cleanly isolate the given parental ion, only the other isotopomers such as $^{12}C_8{}^{13}C_1H_6{}^{11}B_1O_5^-$ at m/z 206.03450 and $^{12}C_9H_6{}^{10}B_1O_5^-$ at m/z 204.03482 were also inevitably fragmented, resulting in the corresponding fragments of the isotopomers (Table 9). The fragmentation pathway of the tetrahedral complex contained more numerous fragments than that of the trigonal form, which might be a consequence of a lesser stability (Table 9). in line with the observation that a lesser applied collision voltage than in case complexes. Among the fragmented and showed complexes this was the only case when the original caffeic acid (peak at m/z 179.03488) was obtained under the condition of the fragmentation. The lack of the direct formation of the free and the decarboxylated forms of caffeic acid from the trigonal boron complex allows us to disregard several of the proposed pathways in the fragmentation of $^{12}C_9H_6{}^{10}B_1O_5$. The BL_2^- complex of caffeic acid observed at m/z = 367.06298 and was fragmented (Table 9) in the quadrupole and one of the obtained fragments at m/z = 279.08287 was fragmented further in

the collision cell, which proves that the relatively easy CO_2 loss was followed by a break of the bidundate, resulting the trigonal boron complex at m/z = 161.04138 (Figure 62).

Fragment (m/z)	Assignment	Mass of assigned formula (m/z)	Error (ppm)	Loss of fragment
160.04507	$^{12}C_8H_6{}^{10}B_1O_3^-$	160.04518	0.7	CO_2
161.04143	$^{12}C_8H_6{}^{11}B_1O_3^-$	161.04155	0.7	
162.04476	$^{12}C_7{}^{13}C_1H_6{}^{11}B_1O_5^-$	162.04490	0.9	
204.03482	$^{12}C_9H_6{}^{10}B_1O_5^-$	204.03501	0.9	-
205.03118	$^{12}C_9H_6{}^{11}B_1O_5^-$	205.03118	0.9	-
206.03450	$\mathbf{^{12}C_8{}^{13}C_1H_6{}^{11}B_1O_5^-}$	206.03473	1.1	-

135.04510	$^{12}C_8H_7O_2^-$	135.04515	0.4	$-H_2O$; $-CO_2$; $-B(OH)_3$
160.04512	$^{12}C_8H_6{}^{10}B_1O_3^-$	160.04518	0.4	$-H_2O$; $-CO_2$
161.04148	$^{12}C_8H_6{}^{11}B_1O_3^-$	161.04155	0.4	
179.03488	$^{12}C_9H_7O_4^-$	179.03498	0.6	$-B(OH)_3$
180.03824	$^{12}C_8{}^{13}C_1H_7O_4^-$	180.03834	0.6	
204.03488	$^{12}C_9H_6{}^{10}B_1O_5^-$	204.03501	0.6	$-H_2O$
205.03125	$^{12}C_9H_6{}^{11}B_1O_5^-$	205.03138	0.6	
206.03460	$^{12}C_8{}^{13}C_1H_6{}^{11}B_1O_5^-$	204.03501	0.9	
222.04540	$^{12}C_9H_8{}^{10}B_1O_6^-$	206.03473	0.7	-
223.04117	$^{12}C_9H_8{}^{11}B_1O_6^-$	223.04194	1.1	
224.04509	$\mathbf{^{12}C_8{}^{13}C_1H_8{}^{11}B_1O_6^-}$	224.04530	0.9	

279.08327	$^{12}C_{16}H_{12}{}^{11}B_1O_4^-$	279.08341	0.5	$-2\ CO_2$
323.07317	$^{12}C_{17}H_{12}{}^{11}B_1O_6^-$	323.07324	0.2	$-CO_2$
367.06284	$\mathbf{^{12}C_{18}H_{12}{}^{11}B_1O_8^-}$	367.06307	0.6	-

161.04138	$^{12}C_8H_6{}^{11}B_1O_3^-$	161.04155	1.0	break
279.08287	$\mathbf{^{12}C_{16}H_{12}{}^{11}B_1O_4^-}$	279.08341	1.9	-

Table 9. Observed peaks and the assigned formulae of collision induced dissociation (CID) fragmentation of parental ions $\mathbf{^{12}C_8{}^{13}C_1H_6{}^{11}B_1O_5^-}$ *at m/z* ***206.03450***, $\mathbf{^{12}C_8{}^{13}C_1H_8{}^{11}B_1O_6^-}$ *at m/z* ***224.04509*** *and* $\mathbf{^{12}C_{18}H_{12}{}^{11}B_1O_8^-}$ *m/z* ***367.06284***. *The observed masses were compared with the theoretical masses of the assigned formulas and the differences between these were given in ppm. Isolation of the parental ions was done in the quadrupole, than were fragmented in the collision chamber, but in case of the bidundate molecule, the parental ion was fragmented already in the quadrupole, and the fragment at m/z* ***279.08287*** *was fragmented again in the collision chamber. The losses of fragments are not representing the exact loss of mass, but the theoretical loss of the certain group.*

The peak at 249.03837 Da, was identified based on the isotope pattern as containing two boron atoms and provided the molecular formula of $C_9H_7O_7B_2^-$, based on the fragmentation of this molecule, finally the complex which contains the tetrahedral and the trigonal B atom form is seemed to be reasonable (Figure 63).

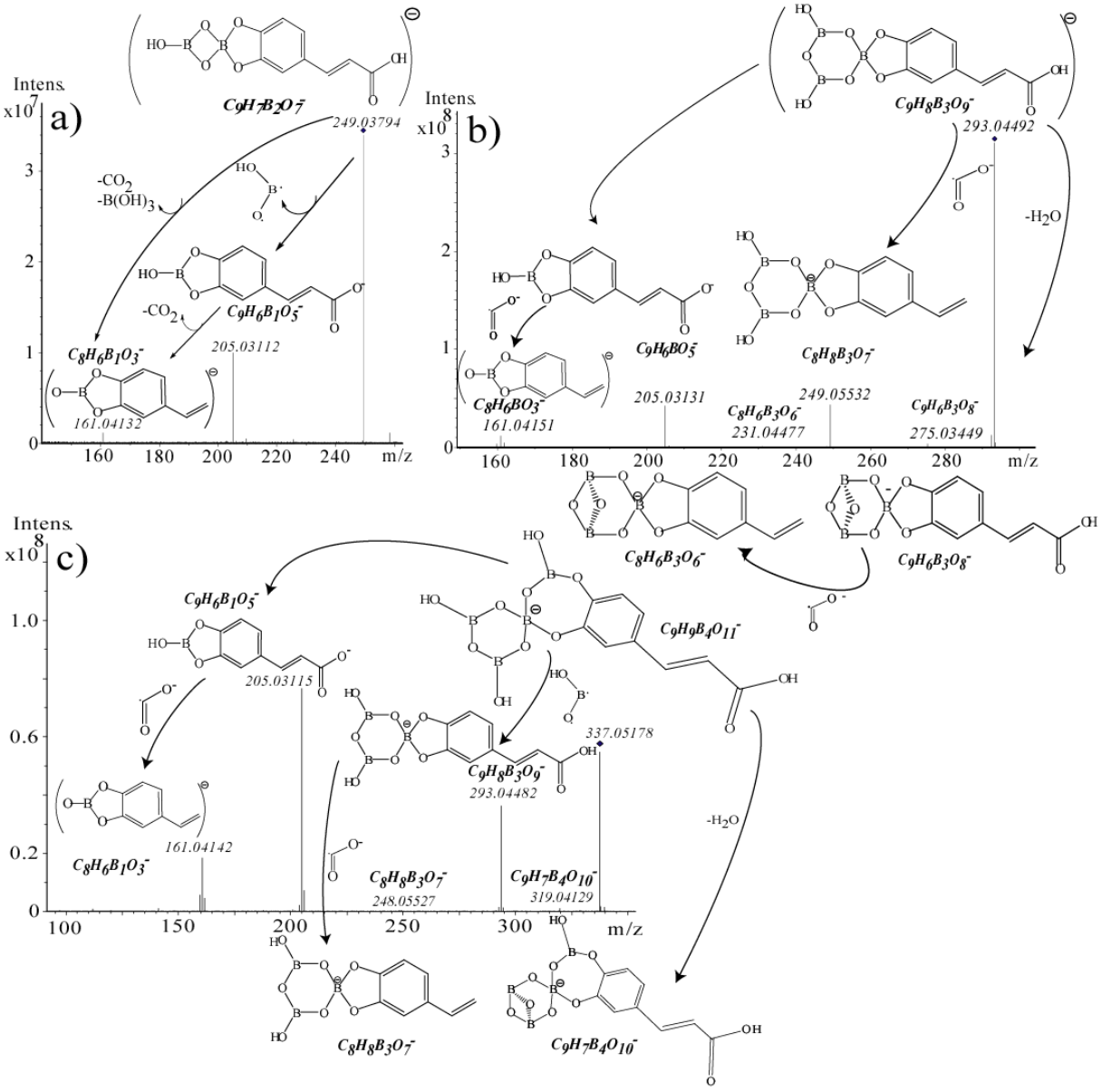

Figure 63. Complexes, containing 3 B atoms and their possible structures, confirmed by fragmentation study.

The observed peak at 293 m/z ($C_9H_8O_9B_3^-$), represented dominantly (beside the mononuclear borate/boric acid complexes), the fragmentation of the isolated parental ion at m/z 293.04371 (referring to the most abundant $^{12}C_9{}^{11}B_3$ isotopomer), necessitated an elevated collision voltage, pointing toward the $B_3O_3(OH)_4^-$ anion as the complexing polyborate, which is fused to the diol by its tetrahedral B atom (Figure 63). This anion with its six-atom ring of alternate boron and oxygen atoms represents a fundamental structural unit of the polyborates and the stability of this anion is conferred by a four-coordinated B atom in a cyclic structure and by the relative ease of charge delocalization[26]. Since the proposed six-membered ring is relatively stable compared with the mono borate-complexes, the fragmentation yielded only

peaks of low abundance (Table 10). One of the peaks at m/z 249.05443 Da was assigned as $^{12}C_8H_8{}^{11}B_3O_7^-$ and originated from a loss of CO_2. The observed fragment could be the $C_9H_7O_7B_2^-$ (m/z = 249.03837 Da), but thanks to the mass accuracy, the mentioned formula can be excluded, which also a clue for the formally proposed structure.

Fragment (m/z)	Assignment	Mass of assigned formula (m/z)	Error (ppm)	Loss of Fragment
161.04132	$^{12}C_8H_6{}^{11}B_1O_3^-$	161.04155	1.4	$-B(OH)_3$; $-CO_2$
205.03112	$^{12}C_9H_6{}^{11}B_1O_5^-$	205.03138	1.3	$-B(OH)_3$
249.03794	**$^{12}C_9H_7{}^{11}B_2O_7^-$**	249.03834	1.6	-
161.04151	$^{12}C_8H_6{}^{11}B_1O_3^-$	161.04155	0.2	$-CO_2$
205.03131	$^{12}C_9H_6{}^{11}B_1O_5^-$	205.31380	0.3	- 2 $B(OH)_3$
231.04477	$^{12}C_8H_6{}^{11}B_3O_6^-$	231.04477	0.6	$-H_2O$; $-CO_2$
249.05532	$^{12}C_8H_8{}^{11}B_3O_7^-$	249.05547	0.6	$-CO_2$
275.03449	$^{12}C_9H_6{}^{11}B_3O_8^-$	275.03473	0.9	$-H_2O$
293.04492	**$^{12}C_9H_8{}^{11}B_3O_9^-$**	293.04530	1.3	-
161.04142	$^{12}C_8H_6{}^{11}B_1O_3^-$	161.04155	0.8	$-CO_2$
205.03115	$^{12}C_9H_6{}^{11}B_1O_5^-$	205.31380	1.1	- 3 $B(OH)_3$
249.05527	$^{12}C_8H_8{}^{11}B_3O_7^-$	249.05547	0.8	$-B(OH)_3$; $-CO_2$
293.04482	$^{12}C_9H_8{}^{11}B_3O_9^-$	293.04530	1.6	$-B(OH)_3$
319.04129	$^{12}C_9H_7{}^{11}B_4O_{10}^-$	319.04169	1.3	$-H_2O$
337.05178	**$^{12}C_9H_9{}^{11}B_4O_{11}^-$**	337.05226	1.4	-

Table 10. Beside the boric acid and borate mono- and bidundate complexes with caffeic acid, further complexes were identified with their fragmented.

Two of the low abundance fragments, present polyborate structure, which was similar to the naturally occurred borax ions, where also two share B atoms are bent about a common oxygen atom [279]. In case of B_4 atoms complexes, observed at m/z 337.05220, the applied collision voltage was again lower than in case of $C_9H_7O_7B_2^-$, and the fragmentation patterns are shown in Figure 62. The proposed structure differed from the cyclic $B_3O_3(OH)_4^-$ derived complex, only by an additional boric acid on the tetrahedral B part of the polymer. However the existence of singly charged $H_5B_4O_9^-$ has not been reported, only by Attina et al., in aqueous solution, since the tetraborate anion $H_5B_4O_9^{2-}$ identified in natural and synthetic borates has been doubly charged (Figure 64). The proposed structure of the parental ion is characterized by two perpendicular rings fused by a common tetrahedral B atom, where one of the rings is built up with the diol and formed a seven-membered ring alternating B and O atoms and two adjacent C atoms contributing to facile extrusion of HO-B-O, forming five-

membered cyclic structures (Table 10). It is interesting to note that water and the carboxyl group loss from the caffeic acid unit are dominant fragmentation pathways in nearly all these ions. Generally, the observed water loss is either a result of the alteration between tetragonal and trigonal boron coordination or caused by formation of an oxygen bridge (B-O-B) in the polyborate ring. Additional peaks as given in Figure 60 were identified as boron containing complexes with one (at m/z 381.05915 referring to $C_9H_{10}O_{13}B_5^-$ and at m/z 407.05554 indicated as $C_9H_9O_{14}B_6^-$) and with two caffeic acid ligands ($C_{18}H_{13}O_{10}B_2^-$, formulae were assigned to m/z= 411.06994, at m/z 455.07681, and 481.07316, $C_{18}H_{14}O_{12}B_3^-$ and $C_{18}H_{13}O_{13}B_4^-$ respectively (Figure 64).

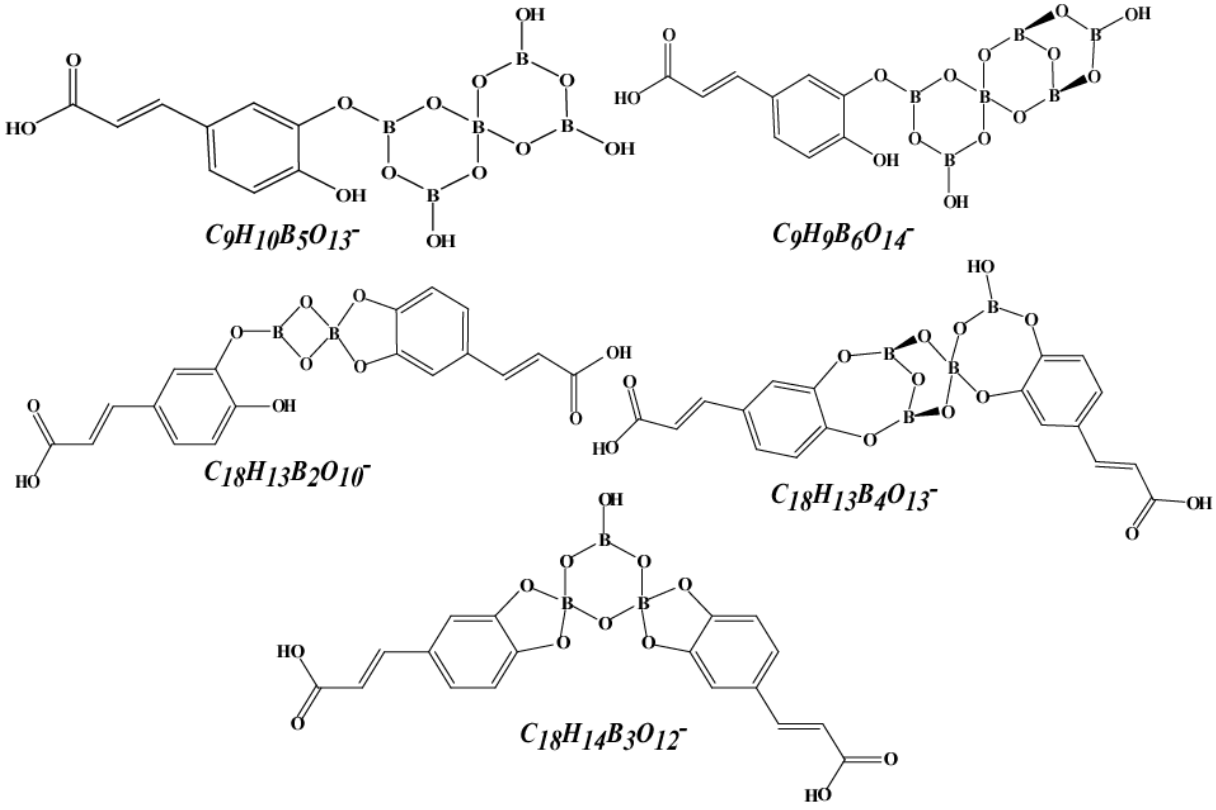

Figure 64. Proposed structures of the non- fragmented but confirmed(by mass accuracy) molecular formulae. These assumptions are based on feasible polyborate structures and a possible linkage over a single hydroxyl group between these ions and the model compound[273, 282, 287].

The presence of these ions might indicate polyborate-polyhydroxyl complexes of lower abundance especially at longer acquisition times. In case of $C_{18}H_{13}O_{10}B_2^-$ and $C_9H_{10}O_{13}B_5^-$, the suggested complexes are bounded only via one hydroxyl group. Polyborate ions are composed of planar trigonal (BO_3) and tetrahedral coordinated (BO_4) boron. At higher concentration and increased pH, polynuclear ions such as $B_2O(OH)_6^{2-}$ or those incorporating B_3O_3 rings such as $B_3O_3(OH)_4^-$, $B_4O_5(OH)_4^{2-}$ (borax anion) and $B_5O_6(OH)_4^-$ etc.

were formed; however, above pH 10 the $B(OH)_4^-$ ion produced exclusively. These groups might connect via common oxygen atoms to form isolated rings and cages or polymerize into infinite chains, sheets, and networks [273, 278, 282, 288], a type of binding also suggested by Revilla et al. [287].

3.3.8. Conclusion

In conclusion, we described through the example of the model system, caffeic acid a high resolution mass spectrometric method for identification of its borate and polyborate complexes. The high resolving power and mass accuracy of FT-ICR/MS were needed to assign the elementary formulae; and CID fragmentation of these supposed molecular ions was employed to propose structural assignments. The clear evidence of polyborate complexes is important to complement the common knowledge about reactions between boric acid/borate system and polyols. Although the current chapter mainly refers to the (poly)borate complexes of the model compound, caffeic acid, these findings will be applied to characterize more complex samples. The necessity of recognizing polyborate complexes in borate containing mixtures is demonstrated, since the conditions, such as intermediate pH, employed in this study may occur in real environments[277]. Which makes an extended boric acid/borate system as partner in complex formation rather plausible. In the future, the proposed findings will contribute to describe more appropriately the specific boron complex formation in more intricate samples, for instance in humic substances and natural organic matter.

3.4. Study of borate complexes with natural organic matter

Boron ester formation was investigated in peat soluble humified materials with molecular-level description of the boron-organic interactions. The boron complexing organic matter structure classes present in the complex organic mixtures could be described: classes which denote diol functional groups such as carbohydrate and phenolic derivatives. In addition, an algorithm was described, which effectively enabled us to distinguish and filter these complexes from the original signals, derived from natural organic matter.

3.4.1. Introduction

Fundamental characteristics of borate –cis-diol containing biomolecules complex were shown for different purposes[38, 39]. Mass spectrometry, as a superior method based on its ability was also used for examining borate complexation 16 different nucleotides, where the authors demonstrated the stability of the borate-nucleotide complex in different charge and phosphorilation state[40, 41]. MS has been also used in studies of boric acid complexes of polyols and carbohydrates using thermospray mass spectrometry (TSP-MS) [42] and MALDI[43] and coordination-ionspray MS[44]. Negative thermal ionization mass spectrometry (NTIMS) was applied to analyze the boron isotopic composition of natural waters[45]. How an ESI-MS can become an alternative technique to ICP-MS and TIMS was showed by of Moraes M.C.B. et al[46]. Although they converted all boron species to BF_4^-, the isotope patter of those is equivalent to the isotope pattern of the boron atom, with relatively free-off interference spectrum.

However direct and fast molecular-level characterisation of boron interaction with immensely complex mixtures, like organic matter, can only be implemented if sufficient mass accuracy and resolution are available. High magnetic field FT/ICR-MS, with its unsurpassed resolution in broad band, combined with soft ionization technique, such as electrospray, enables ten thousands of baseline resolved peaks in a single run. Within this enormous dataset distinguish between boron and non-boron containing molecules relatively difficult and time consuming, though generally isotope patterns of the molecules are well defined and enabling postulate exact molecular formulae. The aims of the chapter are to combine ICR-FT/MS with an adapted data handling software that enables to filter out the B-containing constituents from the organic matter signals. Therefore only organic matters without boron “contamination” and with potential binding sites were considered, where the complex formation could be followed.

Distinguishing between already existed and directly formed complexes might be extremely difficult. A tool developed for this purpose and its possible applications are presented herein with model components and selected dissolved organic matter.

This chapter was prepared, based on the article " *Targeted and non-targeted borate complex formation as followed with electrospray Fourier transform ion cyclotron mass spectrometry: Novel approach for identifying borate complexes with natural organic matter"***[V]**

3.4.2. Chemical reagent

Boric acid (>99.8% purity) like pyrocatechol, benzoic acid and riboflavin were purchased from Merck (Darmstadt, Germany), cholic acid, quercetin dihydrate, rutin trihydrate, salicylic acid and 3-hydroxybenzoic acid were obtained from Fluka (Buchs, Germany), gallic acid and caffeic acid, 3,4-dihiydroxy phenylalanine (L-dopa), L-tyrosine and ammonium bicarbonate, used as a buffer, were purchased from Sigma (Germany) and ferulic acid and 4-Hydroxybenzoic acid were obtained from Serva (Heidelberg, Germany). All the chemicals used without further purification. The Suwannee river fulvic acid (SRFA) was obtained from the International Humic Substances Society (IHSS). Organic matter obtained from peat sample (PHF-T598, unfractionated) was provided by I. Perminova (Univ. Lomonosov, Moscow, Russia). For all experiment LC-MS grade acetonitrile and water (Sigma-Aldrich, Seelze, Germany) were used.

3.4.3. Sample preparation for ESI-MS analysis

All aqueous stock solutions of the model compounds (0.2 mg/mL) were prepared fresh in LC-MS grade water. The pHs of the solutions were adjusted with 10 mM ammonium bicarbonate to pH 9. The borate complexes (esters) were prepared by mixing the stock solution of boric acid (6.2 mg/mL) and stocks of the compounds, respectively after the mixtures were diluted with LC-MS grade acetonitrile, yielding final concentrations of 1μg/mL of compounds and 310 μg/mL of boric acid. In case of the peat sample, the final concentration was 100 μg/mL of peat and 620 μg/mL of boric acid. The sample was solved in 10 μL of 10 V/V% ammonium hydroxide and diluted with water/acetonitrile (1:9) to the desired concentration. The concentration settings were only considered to avoid the possible ion

suppression during the measurements; however the effect of the applied concentrations were investigated in the first chapter of this study.

3.4.4. Methods and experimental setting

3.4.4.1. FT-ICR MS

High-resolution mass spectra were acquired on a Bruker (Bremen, Germany) APEX Qe Fourier transform ion cyclotron resonance mass spectrometer, equipped with a 12 Tesla superconducting magnet and an Apollo II ESI source. Samples were introduced into the micro-electrospray source at a flow rate of 120 µl/h with a nebulizer gas pressure of 20 psi, and a drying gas pressure of 15 psi (@ 250 °C). Spectra were externally calibrated on clusters of arginine (10 mg/l in methanol); calibration errors in the relevant mass range were always below 0.1 ppm. In the mass range of 150 –1000 m/z 4 MW time domain was applied in order to enhance resolution. The spectra were zero filled to a processing size of 4 megawords. Before Fourier transformation of the time-domain transient, a sine apodization was performed. The ion accumulation time in the ion source was set to 2 s for 256 scans were accumulated for samples.

3.4.4.1.1. Calculations

The obtained mass spectra were calibrated internally with the generally occurred fatty acids and the calibrated spectra were converted to mass list. The possible candidates were selected from the list of peak values using a software tool developed for this purpose. The selection criterion is based on the difference of masses requiring to be confined within an interval having the extreme values of 0.99633 and 0.99644 Da. The values between these extremes are referring to the specific mass differences between the ^{10}B and ^{11}B isotope containing species (Figure 65). Theoretically, only 0.99636 Da is representative for the difference of ^{10}B and ^{11}B isotopes, though the application of only this discrete value without certain tolerance is not plausible, as the observed isotope differences might slightly vary over the mass range. Boron, from its origin, represent in environment not only in mono-boron, but polyborate forms, incorporating more than one boron atom, and those could also participate in complex formation with polyols. Depend on the number of the incorporated boron atom the polyborate-polyol complex denote various isotope pattern, however the isotope mass

differences remain the same. Therefore an isotope abundance check, might exclude potential complexes from the list.

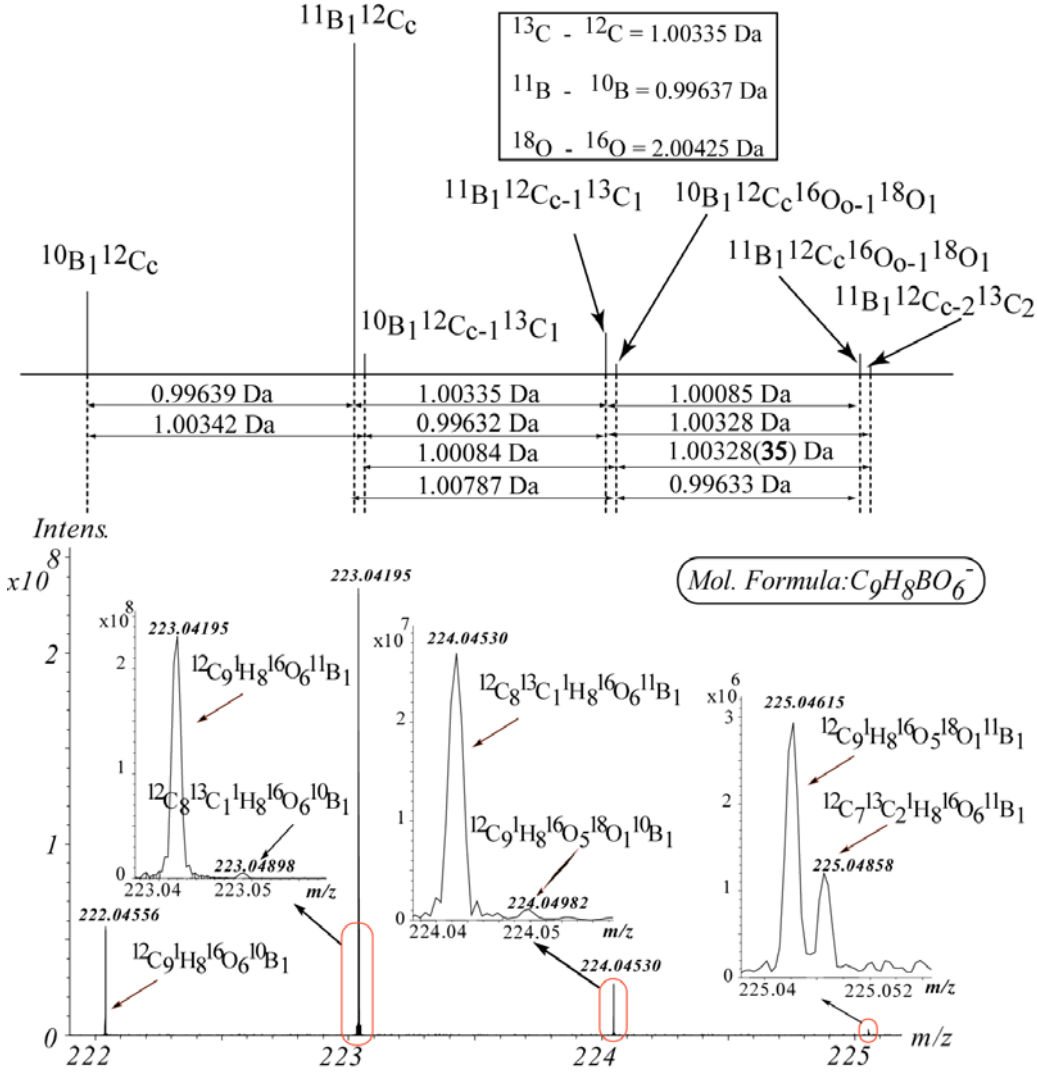

Figure 65. Theoretical and obtained isotope pattern of a feasible boron complex (caffeic acid-borate) Based on the high mass accuracy and unsurpassed resolution not only molecular formulas can be proposed but the revealed isotopes and their differences can be used for further data analysis. The observed differences in Da were assigned to each isotope. The specific differences between the ^{10}B and ^{11}B containing species allow its application as a search tool for boron incorporated molecules.

This effect is increasing proportionally with the general mass value, therefore certain flexibility of the searching tool, which is indicated by the given interval (see above) is necessary. Although the mannered mass difference is not exactly the theoretical value any more, still not interfere with the values of differences of any other common isotope (C,H,O,N,S,P) or medley of these isotope. All these masses are saved in a new file for further successive analysis. Same filtering were conducted on the mass list of boric acid, obtained

from 25 mM boric acid spectrum. Afterwards, the common masses (of sample and B acid) were eliminated, since these might be considered as "background" complexes, that were originated from possible polyborates, formed under the used conditions[282]. The filtered mass list in case of model compounds were crosschecked manually and only the common boric acid/borate complexes were taken into account (Figure 67.).

The identified complexes by the search program were confronted with the expected and manually identified complexes to characterize the efficiency of the developed tool. Finally the program was used to identify possible complexes with Suwannee river fulvic acid and peat, where the obtained peak list was converted into molecular formulas. FT-ICR spectra were exported to peak lists at a signal to noise S/N=2. From the exact masses, possible elemental formulas were calculated for each peak in batch mode by a software tool (*Formulae*) written by M. Frommberger in-house [79, 289]. The generated formulas were validated by setting sensible chemical constraints (N rule, O/C ratio ≤ 1, H/C ratio ≤ 2n + 2, element counts: C ≤ 80, H unlimited, O ≤ 60) in conjunction with an automated theoretical isotope pattern comparison. The flow chart of the method is shown in Figure 66.

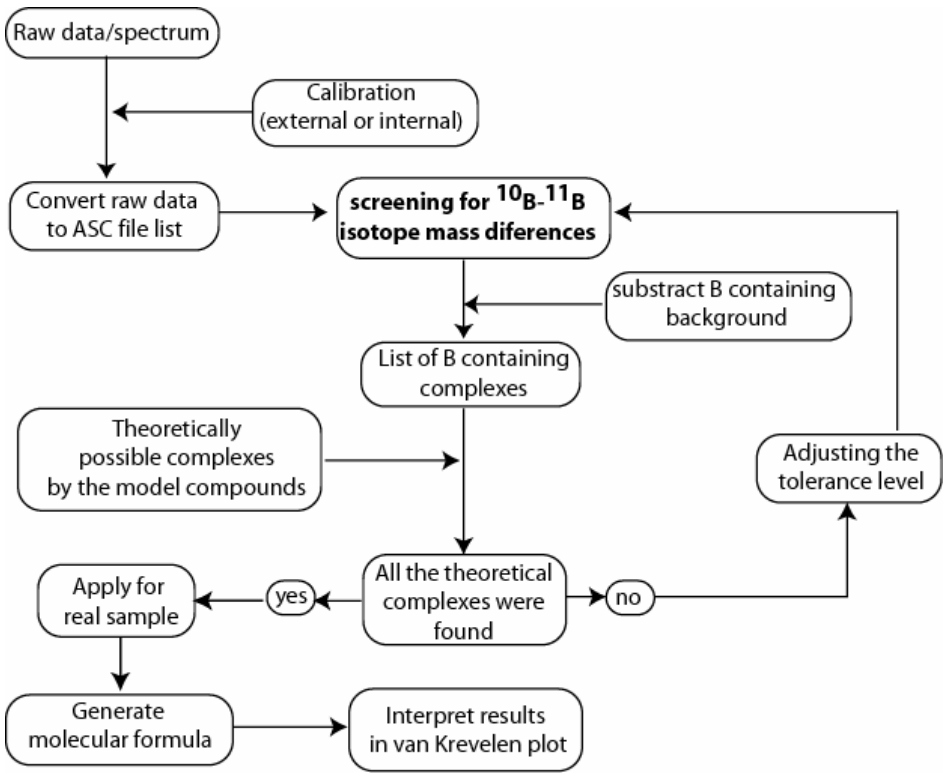

Figure 66. Flow chart of the proposed search algorithm to distinguish boron complexes among ten-thousands of peaks derived from mass spectra obtained by FTICR MS.

3.4.5. ESI/FTMS of model compounds-boric acid/borate complexes

The preliminary aim of this experiment was to examine systematically boron specific interaction with model compounds (with or without suitable binding sites for boron complexation), in order to deduct generalized rules on the formation of B-complex, which might be applicable in case of unknown samples. Therefore, model compounds were analyzed individually, the borate-polyol, boric acid-polyol and polyol-borate-polyol structures and their representative masses and isotope patterns were identified manually in each obtained spectra (Table 11).

Compound	Mol. Formula	Detected mass	Observed with the software tool
Gallic acid	$C_7H_5O_5$	169.01433	
Gallic acid-boric acid	$C_7H_4O_6B_1$	195.01071	+
Gallic acid-borate	$C_7H_6O_7B_1$	213.02127	+
Gallic acid bidundate	$C_{14}H_8O_{10}B_1$	347.02175	+
Ferulic acid	$C_{10}H_9O_4$	193.05065	
Cholic acid	$C_{24}H_{39}O_5$	407.2803	
Caffeic acid	$C_9H_7O_4$	179.03477	
Caffeic acid-boric acid	$C_9H_6O_5B_1$	205.03129	+
Caffeic acid-borate	$C_9H_8O_6B_1$	223.04185	+
Caffeic acid bidundate	$C_{18}H_{12}O_8B_1$	367.06269	-
Pyrocatechol	$C_6H_5O_2$	n.d.	
Pyrocatechol-boric acid		n.d.	
Pyrocatechol-borate	$C_6H_6O_4B_1$	153.03635	+
Pyrocatechol bidundate	$C_{12}H_8O_4B_1$	227.05213	+
Rutin	$C_{27}H_{29}O_{16}$	609.14597	
Rutin-boric acid	$C_{27}H_{28}O_{17}B_1$	635.14157	+
Rutin-borate	$C_{27}H_{30}O_{18}B_1$	653.15194	+
Rutin bidundate		n.d.	
Quercetin	$C_{15}H_9O_7$	301.03526	
Quercetin-boric acid	$C_{15}H_8O_8B_1$	327.03163	+
Quercetin-borate	$C_{15}H_{10}O_9B_1$	345.0421	+
Quercetin bidundate	$C_{30}H_{16}O_{14}B_1$	611.06302	+
Riboflavin	$C_{17}H_{19}N_4O_6$	375.13099	
Riboflavin-boric acid	$C_{17}H_{18}O_7N_4B_1$	401.12711	+
Riboflavin-borate	$C_{17}H_{20}O_8N_4B_1$	n. d.	-
Riboflavin bidundate	$C_{34}H_{36}O_{12}N_8B_1$	759.25475	+
4-OH Benzoic acid	$C_7H_5O_3$	137.02431	
3-OH Benzoic acid	$C_7H_5O_3$	n.d.	
Benzoic acid	$C_7H_5O_2$	n.d.	
L-Dopa	$C_9H_{10}N_1O_4$	196.0616	
L-Dopa-boric acid	$C_9H_9O_5N_1B_1$	222.05787	+
L-Dopa-borate	$C_9H_{11}O_7N_1B_1$	240.06844	+
L-Dopa bidundate	$C_{18}H_{18}O_8N_2B_1$	401.11623	-
L-Tyrosine	$C_9H_{10}O_3N_1$	180.06676	
Salicilyc acid	$C_7H_5O_3$	137.02439	
Salicilyc acid-boric acid	$C_7H_4O_4B_1$	163.02077	+
Salicilyc acid-borate	$C_7H_6O_5B_1$	181.03136	+
Salicilic acid bidundate		n.d.	

Table 11. List of applied model compounds and their restrained boron complexes

The molecular formulas of the complexes were assigned based on their probable structures proposed by Figure 2 and were aligned with their spectra. The mass lists of the obtained spectra were screened with the developed algorithm for boron containing complexes. The generated mass lists were confronted with the masses of the manually confirmed complexes. Where matches could confirmed, were highlighted with "+". The efficiency of the

search algorithm could be considered as the ratio of the existing and assigned versus existing complexes but not assigned.

In case of ferulic acid, cholic acid, 3-OH-benzoic acid, 4-OH-benzoic acid, benzoic acid and L-tyrosine, in absences of cis-diol reaction site, no complexes were observed. It is interest to note that salicylic acid showed complexes with boric acid and borate, although the applied pH was 9.2 and at this pH the carboxylic acid functional group supposed to be deprotonated, obstructing complex formation due to electrostatic repulsion. FTICR spectra of the other 8 model compounds showed the expected complexes, as detailed in Figure 2.
For better visualisation the observed masses of the model compounds and their complexes, were converted to molecular formulas with *Formulae*, and plotted in van Krevelen diagram where the x and y axes referring to elemental ratios of O/C and H/C respectively (Figure 67).

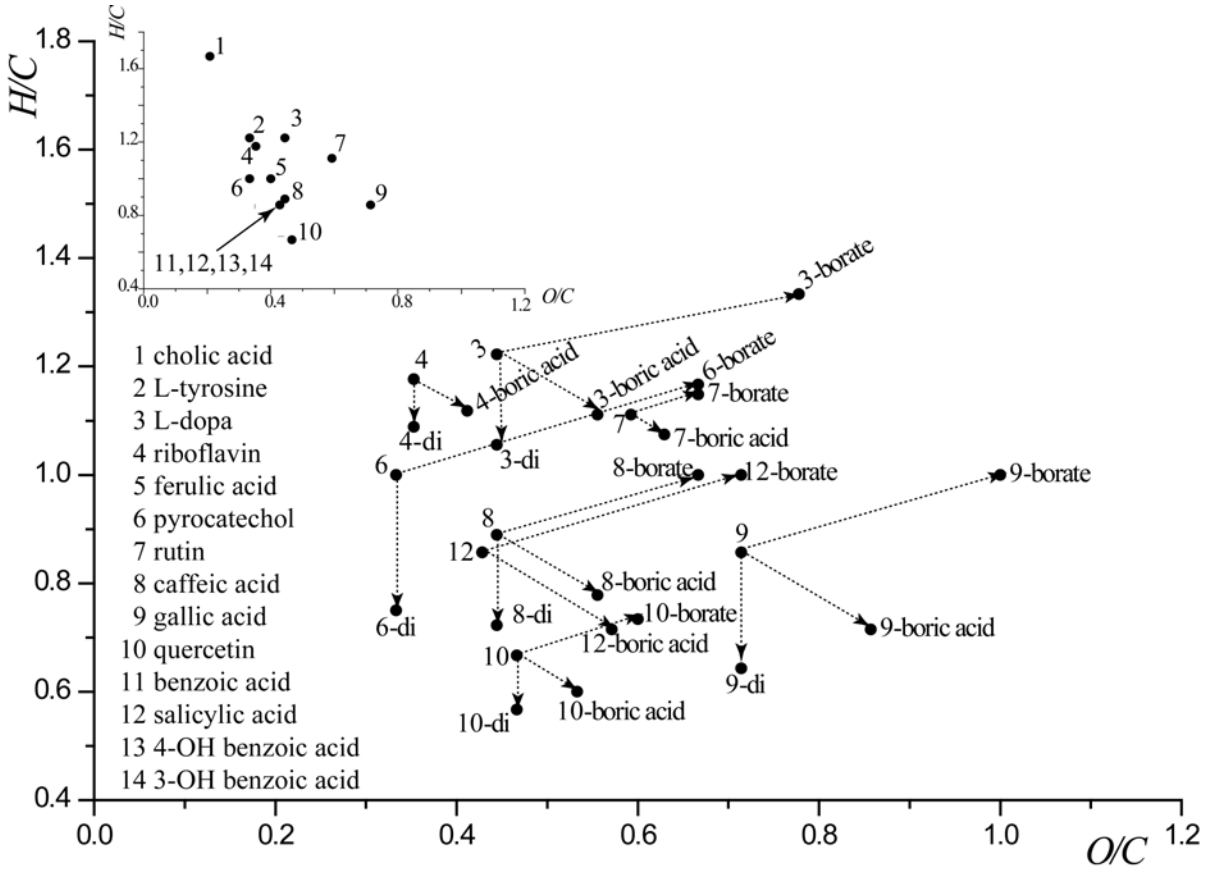

Figure 67. van Krevelen plot of the applied model compounds and their proposed assigned complexes. The inset plot present the H/C, O/C elemental ratios of all the applied model compounds, while the main plot only the selected model compounds which denote possible binding sites (diols). The coherent molecules were connected with arrows, which indicated similar gradients in case of borate and boric acid complexes, respectively. However this type of generalization of the complexation is not fulfilled since the length of these connectors varied by the mass of the compound.

The inset van Krevelen plot contains all the observed and calculated (**6**, **11**) model compounds molecular formulas without boric acid addition. In the main diagram only the compounds, which were participated in complex formation, namely **3**, **4**, **6**, **7**, **8**, **9**, **10** and **12** and their detected borate, boric acid or bidundate forms were plotted. The coherent complexes and model compounds were connected with arrows. The connection lines, between the original compounds and their derivatives, denoted the same gradient and their lengths are proportional of the change in O/C relative to the O/C and showed correlation with the mass of the model compound. Therefore this is directly not applicable for mixtures, if the original complexing compound needs to be described. Hence and because of the increasing number of the false molecular formula assignments at high m/z values up to 1000 m/z, Kendrick Mass Defect might be more suitable for this purpose. The Kendrick mass defect (KMD) plot acquits the obtained masses into homologous series of compounds within a sample. A homologous series is a series of m/z values that differ only by the exact mass of a certain functional group, such as a CH_2 or OH group. As in this study during the complex formation hydroxyl group(s) is (are) replaced (Figure 2), Kendrick mass and its defect of a hydroxyl group is more relevant (KMD(OH)). The calculation shown by the equation below:

Kendrick Mass (OH) = exact m/z of peak *(17/17.00274)

Then, the KMD (OH) is calculated by subtracting the Kendrick mass from the observed nominal mass:

KMD (OH) = Observed nominal mass – Kendrick mass (OH)

Therefore, ions differing by only an OH group (i.e. loss of water) will have the same KMD (OH). As the KMD (OH) plot is not as descriptive as the van Krevelen, KMD could be also used, in combination with the van Krevelen, as a safety filter. In our approach 0.5 ppm was given as an error window and as the m/z values proceeding to the upper mass field, within the given error window might more than one formula be extracted. As a result of the usage of the KMD, if there are multiple formulas for one m/z value, the one that falls within a homologous series is chosen as the correct assignment. After the observed and manually assigned peaks of the relevant molecules were converted into KM and KMD, the difference of the KMD of the model compound and the boric acid, borate and bidundate complex were calculated and plotted as a function of KM and the number of carbon atoms. The results indicate that, the

KMD(OH) difference is a function of the m/z in case of the bidundate forms, but no correlations were observed neither in case of boric acid, nor borate complexes. The KMD difference values were, independently from the mass of the compound, 0.00418 and 0.00708 respectively (Figure 68).

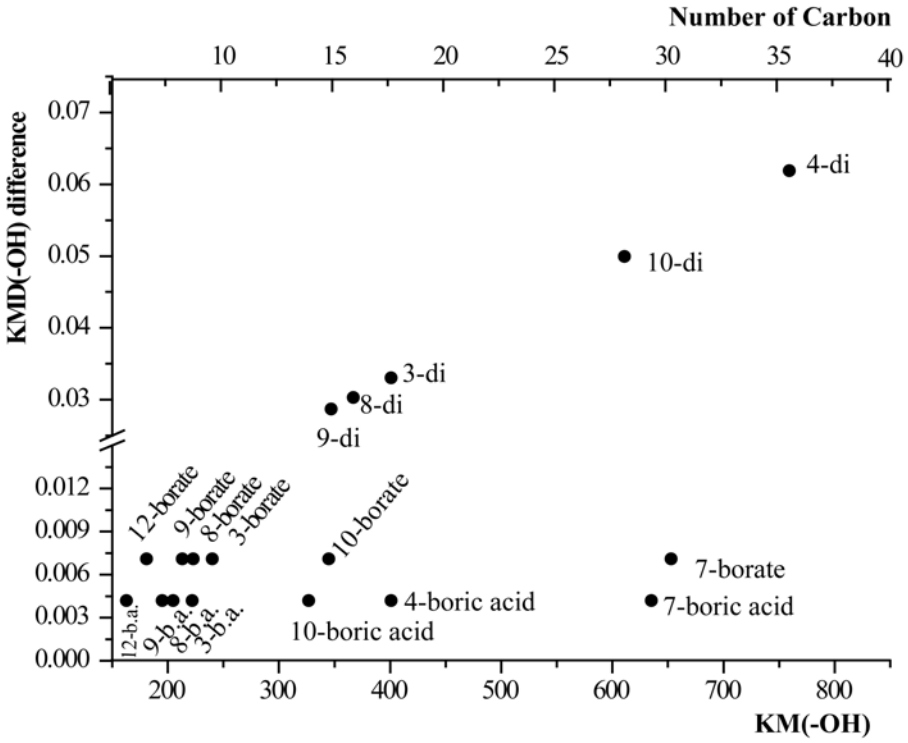

Figure 68. Plot of differences in Kendrick mass defects is presented. The applied OH Kendrick mass defect was used since during the complex formation hydroxyl groups were changed to boric acid or borate tag.

This phenomena and the fact of the additional masses of complexing partners (+26 Da and +43 Da) (Figure 2) under the complexation reaction, might allow us to describe in detail the obtained mass list with the novel approach (discussed above in calculation section).

The results from the detected and manually identified complexes were confronted with the search tool to test its efficiency. The outcome is presented in Table 11. All the significant complexes were pointed out with the search engine except the caffeic acid and the L-dopa bidundate and the rutin-boric acid and rutin-borate complexes, as the occurred difference between the $^{10}B^{12}C$ and the $^{11}B^{12}C$ isotope were exceeded the set up interval.

3.4.6. ESI/FTMS of natural organic matter-boric acid/borate complexes

After validation, the search tool was tested with the SRFA reference material of the International Humic Substances Society and the organic matter obtained from peat. The samples was measured with and without additional boric acid. From the obtained spectra (without boron) list of molecular formulas were generated and plotted in van Krevelen diagram, in order to discern the types of molecules, present in the sample. For further investigation, organic matter from peat, was selected, since as a complex mixture, compared with surface water originated materials (SRFA (results are not shown here)), contains carbohydrate derivatives (with the O/C ratio ≥0.8 and H/C ration≥1.3in the van Krevelen), carboxylic rich and phenolic type compounds. These might preserved due to the anaerobic conditions, which prevents microbial activities and these structures could provide highly probable binding sites for boron (1,2- or 1,3-cis diols) (Figure 69).

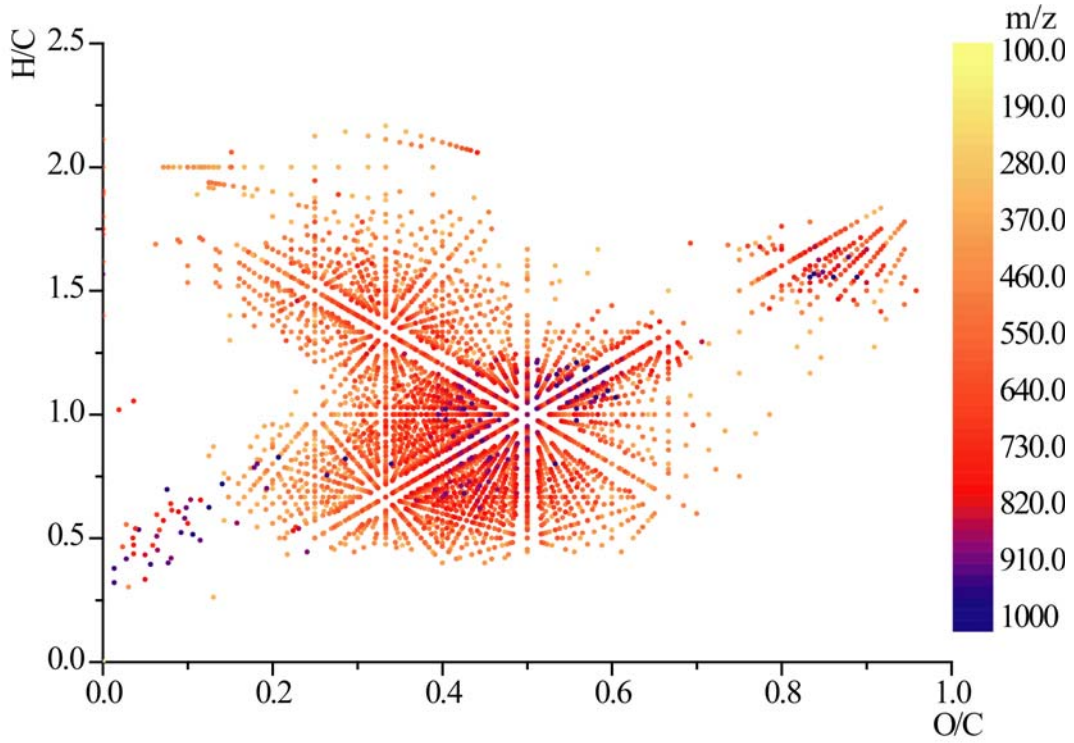

Figure 69. van Krevelen diagram of the Peat Fulvic acid, color-coded according to the mass.

Peat sample was measured, and after the boric acid background masses were subtracted, the developed software tool was used to filter out the boron containing pair of masses. From the peat sample with additional boric acid, a list, with pairs of isotopes with $^{10}B^{12}C$ and $^{11}B^{12}C$, was obtained by the software tool and afterwards molecular formulas were assigned. For the formula calculation, elements C,H,O and B were considered and for

validation, isotope pattern check with $^{13}C_1{}^{12}C_{n-1}$ isotopes were done. Van Krevelen diagram was created from the obtained molecular formulas (Figure 70), where the molar H/C ratio was plotted on the *y*-axis and the molar O/C ratios on the *x*-axis.

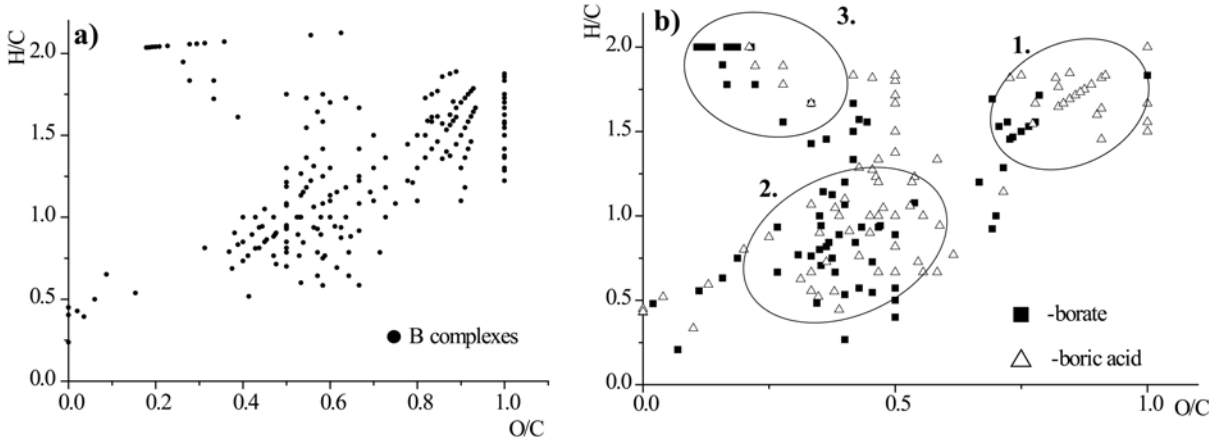

Figure 70. van Krevelen plot of the boron containing molecules, derived from the search program and assigned with isotope pattern recognition ***(a)*** *and plot of molecular formulas obtained with the subtraction of masses related to complexation* ***(b)****. Those molecules which are tend to form complexes with boron cover basically two main region in the van Krevelen plot: 1) high O/C and H/C elemental ratios referring to carbohydrate and cellulose derivatives 2) relatively low H/C and higher O/C ratios might refer to partly aromatic, condensed aromatic structures with carboxyl and hydroxyl functional groups. 3)aliphatic region with possible hydroxylated fatty acids. The diagram (b) is coded based on the subtracted masses applied by the mass list, which were obtained by the search engine.*

The result showed that the boron containing molecules are rather situated the oxygen-rich region, which also include the region of carbohydrates. Since the general goal of this study was to develop a relatively fast and reliable analytical approach which enabling the characterization of possible new materials for specific boron retention, describing only the complexes is not sufficient. Therefore the next step was to find those constituents in the peat sample, that formed complexes with boron. As detailed above, during boron complex formation, generally three main types of complexes were distinguished. In all cases the net growth of the original masses can be calculated as a result of a loss of one or two water molecules and the incorporation of the boric acid/borate molecule (Figure 2). From the masses, obtained by the search software, Kendrick masses were calculated and two separate lists (boric acid/borate) were generated parallel by subtracting the Kendrick masses of the occurred additional masses. By boric acid complex this value was 25.9922 Da and by the borate complex was 43.9998 Da. The obtained lists were aligned with the Kendrick transformed mass list of the original Peat sample. The alignments of the spectra were done by house-made software taking a 2 ppm error window. The common masses of the original peat

sample and the generated subtraction list were selected, considered as masses of existing constituents, which might form complexes with different boron species, verified by their presence in the mass list of the original peat sample. As a next step the masses of the obtained mass lists were converted back to nominal masses and each mass was amended with its theoretical ^{13}C isotope mass, added 1.003355 Da to each nominal mass. Finally, the molecular formulas were calculated from the two separated mass list, distinguishing between constituents that from complexes either with boric acid or borate. For theoretical isotope pattern comparison, during the formula calculation ^{13}C was considered as the most abundant isotope. Figure 69/b shows van Krevelen diagram created from the formula assignments of the aligned and with ^{13}C isotopes completed mass lists. As expected, general shift was observed in the loci of the average H/C, O/C ratios toward the oxygen-depleted region (relative to the boron complexes), when the original molecules are plotted, that are tend to form complexes with boron. Two main regions in the van Krevelen were identified as their members were mainly contributors to the complex formation. Constituents in region 1, could be described as carbohydrate derivatives, since they bear relatively high oxygen and hydrogen content, due to their high hydroxyl group density. This result also correlates with theoretical expectation, that sugar derivatives, through their peculiar hydroxyl groups, might play an important role in boron-complex formation[36, 147, 290, 291]. However the second region compiles many types of compounds and covers a wider range of elemental ratios. The O/C and H/C ratios cluster between 0.3 and 0.6 and between 0.3 and 1.3, respectively. In the range for substituted aromatic compounds such as lignin and its derivatives[284, 292] are also expected as alicyclic and aliphatic (hydroxyl-) polycarboxylates [289]. Tannin like molecules in its upper region and hydrogen-poor structures consisting of condensed aromatic rings having sufficient oxygen functional groups (most probable carboxylic and some hydroxyl groups) to render them complexing agent for boron in the lower elemental ratios region[151]. Aliphatic region, with possible hydroxylated fatty acids, also appeared as B-complexing compounds.

To distinguish between peat constituents which form preferentially complexes with the boric acid or borate, two separate mass lists were generated and plotted (Figure 70/b). Constituents which form complexes with boric acid or borate form of boron, equally contribute to each region.

The molecular formulas of the calculated original masses (respectively to their probable reverse-pathway) and the boron containing complexes were overlaid in van Krevelen diagram (Figure 71). The elemental ratios of molecular formulas, presented as outcome of the

reverse-pathway approach and by the model compounds observed general gradients of the connector lines, might describe possible paths of complex formation in vast mixtures also. Hence in the model system, the exact lengths of the connectors varied, therefore the arrows only represent as possible pathways of the complex formation.

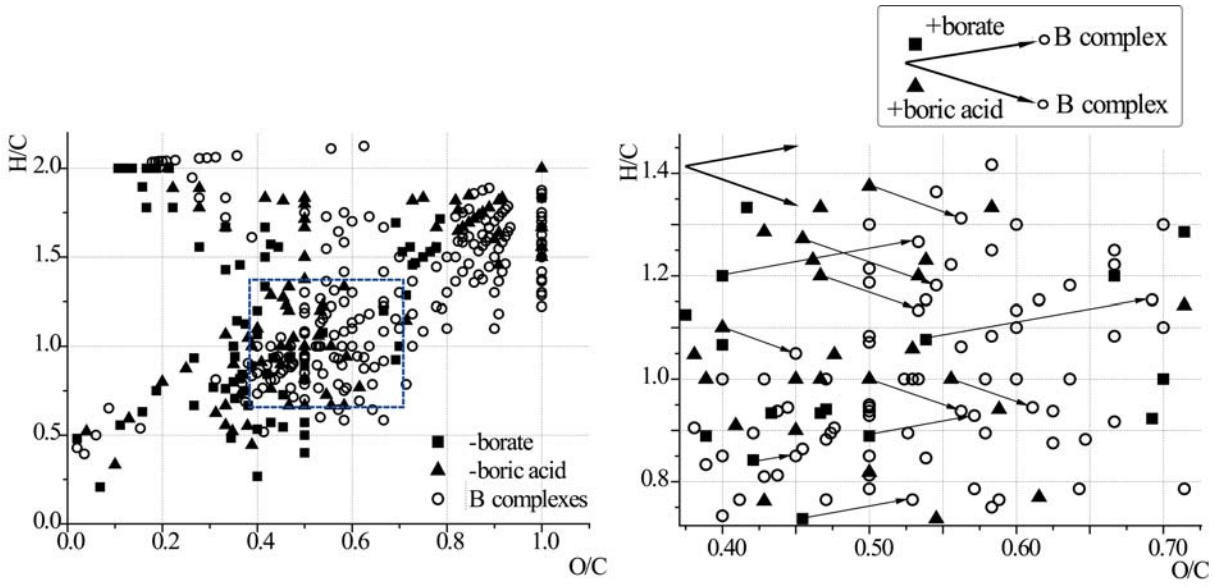

Figure 71. Apply the observed gradients for origination of boron complexes. The enlarged section (showed right) presents possible pairs of initial molecules and their complex forms based on the assumption that, the gradient of the connector line is given by the type of complex. However note that application as a vector is not plausible since the length is not defined.

3.4.7. Conclusion

Since natural organic matter (NOM) is a highly complex mixture, advanced spectroscopy and mathematical data analysis and data sorting are required for a detailed description of boron complexation. ICR-FT/MS with its ultra-high resolution enables several thousand to ten-thousands of resolved signals with (sub)milli-mass spacing (mDalton) which vast information obstruct of a molecular level understanding of boron complex formation without data sorting approaches. To follow the complex formation and describe molecules that are involved in this reaction, specific search software tool was developed and tested. The identification of borate and boric acid complexes is enabled by their isotope pattern recognition; especially with their given distance between the different boron isotopes. To describe the general outcome of the program, van Krevelen plots were applied, which are derived from high-quality ICR-FT/MS mass spectra and efficiently expose compositional characteristics of the concerned molecules. The results, were presented here, confirm those

initial expectations that presume diol-rich constituents, basically carbohydrate derivatives and phenolic-like compounds are binding partner of boron.

Hereby it has to be highlighted, that the similar results were obtained if m-aminophenylboronic acid polymer was used in combination with FT-ICR/MS (Chapter 3.1). There, in spite of ion suppression, originated from the applied buffer, similar regions in the van Krevelen were affected.

The selective identification of susceptible molecules with this method has denoted its competence therefore this approach is useful in ongoing projects for the characterization of complexes with other elements of specific isotopic signatures in complex systems (*non targeted ligand fishing*).

4. Conclusion and Outlook

Boron and its forms, considered as contaminants, might be discharged either from natural or anthropogenic sources. Beside the rare volcanic activities, the usage of seawaters, with the elevated B content, represent a common threat for plantation in arid countries, where water sources are limited. Unfortunately the elimination of B during the desalination process is rather challenging than plausible. Further problem is a continuous discharge of elevated B content from industrial and domestic processed water sources. These general contributors might increase the level of B in soil and produce a toxic environment for the vegetation.

If natural organic matter is not considered as an emerging contaminant but an inexhaustible and exploitable material that might react with and adsorb Boron, than the generally existing low cost-effective adsorbents could be replaced. For instance cheap composted materials with significant organic matter content, could be a possibility.

However the first step to find a proper organic matter, and beside the adsorption behaviour, is to understand on molecular level the mechanism of boron complexation with such a complex material. And based on the obtained results, the expected properties, that might preferentially favourable for B complexation, could be exploited by the screening of the adequate NOM.

Therefore in this thesis different type of analytical approaches were tested and introduced, either alone or in combination. Since the potentially applicable organic matters denote such a complexity, it was necessary to pay attention and describe the NOM constituents in detail. Hence almost half of the thesis was dealing with the characterization of a standard NOM, that draw some attention on the necessity and the benefit of multiple analytical approaches. Since the complexity of these materials often hinders the analysis of a complex array of structures, prior, an electrophoretic separation was introduced. The application of such separation, is originated from the generally observed attribute of B complexation mechanism. B and its forms are tend to complex with hydroxyl and carboxyl groups in adequate forms and positions. And whilst electrophoretic separation is capable, to separate constituents based on functional groups, that are in negative operation modus, within these materials are mainly hydroxyl and carboxyl groups. Beside the expected separation phenomena, further benefit was also experienced. Due to the separated constituents a wider range of constituents were revealed under the analysis, extending the number of the visualized molecules that were limited by the analytical method itself.

As a next step based on the gained information about the potential binding sites and their abundances and former B-complex identification via capillary electrophoresis, a reverse approach was tried out, as a possible fast and descriptive method to characterize the B binding capacity of different NOMs with different origins. Polymers with immobilized Boronic acid on their surfaces were utilized in order to enable a fast and in a first row a qualitative method to differentiate between boron affinity of the different organic matters. However, by closer examination of the B-complex detection methodology, the obtained responses were difficult to interpret, hence capillary electrophoresis as a detection method was replaced with a direct and more informative detection method, namely mass spectrometry.

FT-ICR/MS with its mass accuracy and ultra high resolution enabled to identify dozens of complexes in a single run, however the observed number and abundances of the complexes were greatly depended from the instrumental and experimental settings. However one of the major drawback of such an analysis, that during the ionization the analyte might undergoes changes that could influence the results and might mislead the conclusion about the complexation properties. Nevertheless the utilization of such a mass accuracy and resolution enabled to identify and assign molecular formulae of B complexes in batch experiments. Not only with model compounds and in designed experiments, but also with natural organic matter were tested successfully. Based on the observed regularity by model compounds and B, which were derived from the properties of the B complex formation, general rules were set up to follow and assign complexes among thousands of constituents. With the developed search tool boron complexation tendencies could be revealed among the analyzed organic matters and therefore effective candidates with potential B retention can be assigned. The observed molecules and their position in van Krevelen plot are in good agreement with the observed results, derived from the polymer utilization. Therefore, this search engine in combination with FT/MS might help in the near future to select and advise potential organic matter or even organic matter containing material that will be used for boron elimination from irrigation water not only in laboratory scale. Beside the routine applicability further test will follow these results, where the distribution of the B-complexes within the characterized free-flow fractions of SRNOM, with relative changing in the number of oxygen-depleted constituents, will be screened.

References

[1] Hall D. G., *Boronic acids*, WIley-VHC, Weinheim 2005.

[2] Park H., Schlesinger W. H. *Global biogeochemical cycle of boron,* Global Biogeochemical Cycles 2002, **16**, 1072.

[3] Smith R A. *Basic geology and chemistry of borate,* American Ceramic Society Bulettin 2002, **81**.

[4] Barr R D, Clarke W B, Clarke R M, Venturelli J, Norman G R, Dowing R G. *Regulation of lithium and boron levels in normal human blood: environmental and genetic factors.,* J. Lab. Clin. Med. 1993, **121**, 614.

[5] Kobayashi M, Matoh T, Azuma J-I. *Two chains of rhamnogalacturonan II are cross-linked by borate-diol ester bonds in higher plant cell walls,* Plant Physiology 1996, **110**, 1017.

[6] Pellerin P, Doco T, Vida S, Williams P, Brillouet J-M, O'Neill M A. *Structural characterization of red wine rhamnogalacturonan II,* Carbohydrate Research 1996, **290**, 183.

[7] Warrington K. *The effect of boric acid and borax on the broad bean and certain other plants,* Ann. Bot. 1923, 629.

[8] Power P. P., Woods W. G. *The chemistry of boron and its speciation in plants,* Plant and Soil 1997, **193**, 1.

[9] Dembitsky V. M., Smoum R., Al-Quntar A. A., Abu Ali H., Pergament I., Srebnik M. *Natural occurrence of boron-containing compounds in plants, algae and microorganisms,* Plant Science 2002, **163**, 931.

[10] Lee S, Aronoff S. *Boron in Plants: A Biochemical Role,* Science 1967, **158**, 798.

[11] Smyth D A, Dugger W M. *Cellular changes during boron deficient culture of the diatom Cylindrotheca fusiformis,* Plant Physiology 1981, **51**, 111.

[12] WHO, *ENVIRONMENTAL HEALTH CRITERIA 204: Boron*, World Health Organization, Geneva 1998.

[13] Miwa K., Takano J., Omori H., Seki M., Shinozaki K., Fujiwara T. *Plants tolerant of high boron levels,* Science 2007, **318**, 1417.

[14] Yermiyahu U., Tal A., Ben-Gal A., Bar-Tal A., Tarchitzky J., Lahav O. *Environmental science - Rethinking desalinated water quality and agriculture,* Science 2007, **318**, 920.

[15] Yermiyahu U., Ben-Gal A., Sarig P. *Boron toxicity in grapevine,* Hortscience 2006, **41**, 1698.

[16] Yilmaz A. E., Boncukcuoglu R., Yilmaz M. T., Kocakerim M. M. *Adsorption of boron from boron-containing wastewaters by ion exchange in a continuous reactor,* Journal of Hazardous Materials 2005, **117**, 221.

[17] Baek K. W., Song S. H., Kang S. H., Rhee Y. W., Lee C. S., Lee B. J., Hudson S., Hwang T. S. *Adsorption kinetics of boron by anion exchange resin in packed column bed,* Journal of Industrial and Engineering Chemistry 2007, **13**, 452.

[18] Simonnot M. O., Castel C., Nicolai M., Rosin C., Sardin M., Jauffret H. *Boron removal from drinking water with a boron selective resin: Is the treatment really selective?,* Water Research 2000, **34**, 109.

[19] Schmitt-Kopplin P., Hertkorn N., Garrison A. W., Freitag D., Kettrup A. *Influence of borate buffers on the electrophoretic behavior of humic substances in capillary zone electrophoresis,* Analytical Chemistry 1998, **70**, 3798.

[20] Wolf B. *Improvements in the azomethine-H method for the determination of boron,* Comm. Soil Sci. Plant Anal. 1974, **5**, 39.

[21] Fang Z. *Nonequilibrated sample manipulation—The essence of flow-injection analysis* Microchem. J. 1992, **45**, 137.

[22] Kaplan D I A. D. C., Mills G, Burkman W,. Soil Sci. Soc. Am. J. 1990, **54**, 708.

[23] Chen D , Lázaro F, Luque De Castro M D , Valcárel M. *Direct spectrophotometric determination of total boron in soils with ultrasonic leaching in automatic flow systems,* Analytica Chimica Acta 1989, **222**, 221.

[24] Sah R N, Brown P. H. *Boron determination-A review of analytical methods,* Microchem. J. 1997, **56**, 285.

[25] Evans S, Krahenbuhl U. *Boron analysis in biological material: microwave digestion procedure and determination by different methods* Fresenius Z. Anal. Chem. 1994, **349**, 454.

[26] van Duin M, Peters J A, Kieboom A P G, van Bekkum H. *Studies on borate esters I,* Tetrahedron 1984, **40**, 2901.

[27] Schmitt-Kopplin P., Fischer K., Freitag D., Kettrup A. *Capillary electrophoresis for the simultaneous separation of selected carboxylated carbohydrates and their related 1,4-lactones,* Journal of Chromatography A 1998, **807**, 89.

[28] Schmitt-Kopplin P., Garrison A. W., Perdue E. M., Freitag D., Kettrup A. *Capillary electrophoresis in the analysis of humic substances - Facts and artifacts,* Journal of Chromatography A 1998, **807**, 101.

[29] Van Duin M, Peters J A, Kieboom A P G, Van Bekkum H. *Studies on borate esters II,* Tetrahedron 1985, **41**, 3411.

[30] Pizer R. D., Ricatto P. J., A. T. C. *Thermodynamics of several boron acid complexation reactions studied by variable-temperature 1H and 11B NMR spectroscopy,* Polyhedron 1993, **12**, 2137.

[31] van den Berg R, Peters J A, H V. B. *The structure and (local) stability constants of borate esters of mono- and di-saccharides as studied by 11B and 13C NMR spectroscopy,* Carbohydrate Research 1994, **253**, 1.

[32] Yoshimura K, Miyazaki Y, Sawada S, Waki H. *11B NMR studies on complexation of borate with linear and crosslinked polysaccharides,* Journal of the Chemical Society, Faraday Transactions 1996, **92**, 651.

[33] Taylor M. J., Grigg J. A., Laban I. H. *Triol borates and aminoalcohol derivatives of boric acid: their formation and hydrolysis,* Polyhedron 1996, **15**, 3261.

[34] Dawber J. G, Green S I. E. . *An 11B nuclear magnetic resonance study of the reaction of the tetrahydroxyborate ion with polyhydroxy compounds,* Journal of the Chemical Society, Faraday Transactions 1: Physical Chemistry in Condensed Phases 1986, **82**, 3407.

[35] How M. J., Kennedy G. R., Mooney E. F. *The pH dependence of the boron-11 chemical-shift of borate–boric acid solutions,* Journal of the Chemical Society D: Chemical Communications 1969, 267.

[36] Böeseken J. *The use of boric acid for determination of the configuration of carbohydrates,* Advances in Carbohydrate Chemistry 1949, **4**, 189.

[37] Smith J. T., Rassi Z. *Micellar electrokinetic capillary chromatography with in situ charged micelles : IV. Influence of the nature of the alkylglycoside surfactant,* Journal of Chromatography A 1994, **685**, 131.

[38] Kim D H, Marbois B N, Faull K F, D E. C. *Esterification of borate with NAD+ and NADH as studied by electrospray ionization mass spectrometry and 11B NMR spectroscopy,* Journal of Mass Spectrometry 2003, **38**, 632.

[39] Hu H., Penn S. G., Lebrilla C. B. , Brown P. H. *Isolation and Characterization of Soluble Boron Complexes in Higher Plants (The Mechanism of Phloem Mobility of Boron),* Plant Physiology 1997, **113**, 649.

[40] Kim D H, Faull K F, Norris A J, Eckhert C D. *Borate-nucleotide complex formation depends on charge and phosphorylation state,* Journal of Mass Spectrometry 2004, **39**, 743.

[41] Ackloo S Z, Burgers P C, McCarry B E, Terlouw J K. *Structural Analysis of Diols by Electrospray Mass Spectrometer on Boric Acid Complexes,* Rapid Communication in Mass Spectrometry 1999, **13**, 2406.

[42] Lipták M, Dinya Z, Herczegh P, J J. *Studies on the complexation of polyols and carbohydrates with excess borate using thermospray mass spectrometry* Organic Mass Spectrometry 1993, **28**, 780.

[43] Penn S G, Hu H, Brown P H, Lebrilla C B. *Direct analysis of sugar alcohol borate complexes in plant extracts by matrix-assisted laser desorption/ionization Fourier transform mass spectrometry,* Analytical Chemistry 1997, **69**, 2471.

[44] Bayer E, Gfrörer P, C R. *Coordination-Ionspray-MS (CIS-MS), a Universal Detection and Characterization Method for Direct Coupling with Separation Techniques,* Angewandte Chemie International Edition 1999, **38**, 992.

[45] Barth S. *Boron isotopic analysis of natural fresh and saline waters by negative thermal ionization mass spectrometry,* Chemical Geology 1997, **143**, 255.

[46] Moraes M C. B., Brito NetoJ G. A, C L. d. L. *Boron isotopic ratio by electrospray mass spectra of tetrafluoroborate Part 1. Instrumental conditions, data acquisition, memory effect, and ion stability* Journal of Analytical Atomic Spectrometry 2001, **16**, 1259.

[47] Keren R., Bingham F. T., Rhoades J. D. *Plant Uptake of Boron as Affected by Boron Distribution Between Liquid and Solid Phases in Soil* Soil Science Society of America Journal 1985, **49**, 297.

[48] Keren R., Bingham F. T., Rhoades J. D. *Effect of Clay Content in Soil on Boron Uptake and Yield of Wheat* Soil Science Society of America Journal 1985, **49**, 1466.

[49] Wear J. I., Patterson R. M. *Effect of Soil pH and Texture on the Availability of Water-Soluble Boron in the Soil,* Soil Science Society of America Journal 1962.

[50] Fleming G. A., Essential micronutrients. I: Boron and molybdenum in: Davis, B. E. (Ed.), *Soil Trace Elements*, John Wiley and Sons, New York 1980, pp. 155.

[51] Goldberg S., Forster H. S. *Boron sorption on calcareous soils and refence calcites,* Soil Science 1991, **152**, 304.

[52] Goldberg S., Forster H. S., Heick E. L. *Boron adsorption mechanism on oxides, clay minerals and soils inferred from ionic strength effects,* Soil Science Society of America Journal 1993, **57**, 704.

[53] Toner C. V., Sparks D. L. *Chemical relaxation and double layer model analysis of boron adsorption on alumina,* Soil Science Society of America Journal 1995, **59**, 395.

[54] Evans L. J. *Retention of Boron by agricultural soils from Ontario,* Canadian Journal of Soil Science 1987, **67**, 33.

[55] Yermiyaho U., Keren R. *Boron Sorption on Composted Organic Matter,* Soil Science Society of America 1988, **52**, 1309.

[56] Yermiyahu U., Keren R. *Boron Sorption by Soil in the Presence of Composted Organic Matter,* Soil Science Society of America 1995, **59**, 405.

[57] Hedges J. I., Oades J. M. *Comparative organic geochemistries of soils and marine sediments,* Organic Geochemistry 1997, **27**, 319.

[58] Vandenbroucke M., Largeau C. *Kerogen origin, evolution and structure,* Organic Geochemistry 2007, **38**, 719.

[59] Hedges I. J., Keil R. G. *Sedimentary organic matter preservation: an assessment and speculative synthesis,* Marine Chemistry 1995, **49**, 81.

[60] Graber E. R., Borisover M. *Exploring organic compound interactions with organic matter: The thermodynamic cycle approach,* Colloids and Surfaces a-Physicochemical and Engineering Aspects 2005, **265**, 11.

[61] Borisover M. D., Graber E. R. *Specific interactions of organic compounds with soil organic carbon,* Chemosphere 1997, **34**, 1761.

[62] Kalinichev A. G., Kirkpatrick R. J. *Molecular dynamics simulation of cationic complexation with natural organic matter,* European Journal of Soil Science 2007, **58**, 909.

[63] Perdue E. M., Ritchie J. D., Dissolved Organic Matter in Fresh Waters in: Holland, H. D., Turekian, K. K. (Eds.), *In Treatise on Geochemistry Volume 5: Surface and ground Water, Weathering, Erosion and Soils*, Elsevier-Pergamon, Oxford 2003, pp. 273.

[64] Mopper K., Stubbins A., Ritchie J. D., Bialk H. M., Hatcher P. G. *Advanced instrumental approaches for characterization of marine dissolved organic matter: Extraction techniques, mass spectrometry, and nuclear magnetic resonance spectroscopy,* Chemical Reviews 2007, **107**, 419.

[65] Koprivnjak J. F., Perdue E. M., Pfromm P. H. *Coupling reverse osmosis with electrodialysis to isolate natural organic matter from fresh waters,* Water Research 2006, **40**, 3385.

[66] Koprivnjak J. F., Pfromm P. H., Ingall E., Vetter T. A., Schmitt-Kopplin P., Hertkorn N., Frommberger M., Knicker H., Perdue E. M. *Isolation and characterization of marine dissolved organic matter using the coupled reverse osmosis-electrodialysis,* Submitted to Geochimica Et Cosmochimica Acta 2008.

[67] Vetter T. A., Perdue E. A., Ingall E., Koprivnjak J. F., Pfromm P. H. *Combining reverse osmosis and electrodialysis for more complete recovery of dissolved organic matter from seawater,* Separation and Purification Technology 2007, **56**, 383.

[68] Skoog A., Benner R. *Aldoses in various size fractions of marine organic matter: Implications for carbon cycling,* Limnology and Oceanography 1997, **42**, 1803.

[69] Benner R., Pakulski J. D., McCarthy M., Hedges I. J., Hatcher P. G. *Bulk chemical characteristics of dissolved organic matter in the ocean.,* Science 1992, **255**, 1561.

[70] McCarthy M., Hedges J., Benner R. *Major biochemical composition of dissolved high molecular weight organic matter in seawater,* Marine Chemistry 1996, **55**, 281.

[71] Thurman E. M., Malcolm R. L. *Preparative isolation of aquatic humic substances,* Environmental Science & Technology 1981, **15**, 463.

[72] Abbt-Braun G., Lankes U., Frimmel F. H. *Structural characterization of aquatic humic substances - The need for a multiple method approach,* Aquatic Sciences 2004, **66**, 151.

[73] Hedges J. I., Eglinton G., Hatcher P. G., Kirchman D. L., Arnosti C., Derenne S., Evershed R. P., Kogel-Knabner I., de Leeuw J. W., Littke R., Michaelis W., Rullkotter J. *The molecularly-uncharacterized component of nonliving organic matter in natural environments,* Organic Geochemistry 2000, **31**, 945.

[74] Frimmel F. H., Abbt-Braun G. *Basic characterization of*
reference NOM from central Europe – similarities and differences., Environment International 1999, **25**, 191.

[75] Hayes M. H. B., in: Malcolm, R. L., Swift, R. S. (Eds.), *Humic substances II: in search of structure.*, John Wiley & Sons., New York 1989.

[76] Benner R., Biddanda B., Black B., McCarthy M. *Abundance, size distribution, and stable carbon and nitrogen isotopic compositions of marine organic matter isolated by tangential-flow ultrafiltration,* Marine Chemistry 1997, **57**, 243.

[77] Davis J., Benner R. *Seasonal trends in the abundance, composition and bioavailability of particulate and dissolved organic matter in the Chukchi/Beaufort Seas and western Canada Basin,* Deep-Sea Research Part Ii-Topical Studies in Oceanography 2005, **52**, 3396.

[78] Dittmar T., Koch B. P., Hertkorn N., Kattner G. *A simple and efficient method for the solid-phase extraction of dissolved organic matter (SPE-DOM) from seawater,* Limnology and Oceanography 2008, **6**, 230.

[79] Hertkorn N., Ruecker C., Meringer M., Gugisch R., Frommberger M., Perdue E. M., Witt M., Schmitt-Kopplin P. *High-precision frequency measurements: indispensable*

tools at the core of molecular-level analysis of complex systems, Analytical Bioanalytical Chemistry 2007, **389**, 1311.

[80] Einsiedl F., Hertkorn N., Wolf M., Frommberger M., Schmitt-Kopplin P., Koch B. P. *Rapid biotic molecular transformation of fulvic acids in a karst aquifer,* Geochimica Et Cosmochimica Acta 2007, **71**, 5474.

[81] Huffman E. W. D., Stuber H. A., Analytical methodology for elemental analysis of humic substances. in: Aiken, G. R., McKnight, D. M., Wershaw, R. L., MacCarthy, P. (Eds.), *Humic substances in soil, sediment and water*, John Wiley

& Sons, New York 1985, pp. 433.

[82] Rice J., MacCarthy P. *Statistical evaluation of the elemental composition of humic substances,* Organic Geochemistry 1991, **17**, 635.

[83] van Krevelen D. W. *Graphical-statistical method for the study of structure and reaction processes of coal.,* Fuel 1961, **29**, 269.

[84] Perdue E. M. *Analytical constraints on the structural features of humic substances,* Geochimica Et Cosmochimica Acta 1984, **48**, 1435.

[85] Abbt-Braun G., Frimmel F. H. *Basic characterization of Norwegian NOM samples - Similarities and differences,* Environment International 1999, **25**, 161.

[86] Perdue E. T., Chemical composition, structure and metal

binding properties. in: Hessen, D. O., Tranvik, L. J. (Eds.), *Aquatic humic substances.*, Springer-Verlag, Berlin 1998, pp. 41.

[87] Barak P., Chen Y. *Equivalent radii of humic macromolecules from acid-base titration.,* Soil Science 1992, **154**, 184.

[88] Abbt-Braun G., Lankes U., Jahnel J. B., Lambert J., Lüdemann H.-D., Frimmel F. H., Chemical and spectroscopic

data of the reference samples – comparison and evaluation. in: Frimmel, F. H., Abbt-Braun, G., Heumann, K. G., Hock, B., Lüdemann, H.-D., Spiteller, M. (Eds.), *Refractory organic substances*

(ROS) in the environment, Wiley – VCH, Weinheim 2002, pp. 302.

[89] Ritchie J. D., Perdue E. M. *Proton-binding study of standard and reference fulvic acids, humic acids, and natural organic matter,* Geochimica Et Cosmochimica Acta 2003, **67**, 85.

[90] Ritchie J. D., Perdue E. M. *Analytical constraints on acidic functional groups in humic substances,* Organic Geochemistry 2008, **39**, 783.

[91] Perdue E. M., Acidic functional groups of humic substances. in: Aiken, G. R., McKnight, D. M., Wershaw, R. L., MacCarthy, P. (Eds.), *Humic substances in soil sediment and water. Geochemistry, isolation and characterisation*, Wiley-Interscience, New York 1985, pp. 493.

[92] Korshin G. V., Li C. W., Benjamin M. M. *Monitoring the properties of natural organic matter through UV spectroscopy: A consistent theory,* Water Research 1997, **31**, 1787.

[93] Uyguner C. S., Bekbolet M. *Implementation of spectroscopic parameters for practical monitoring of natural organic matter,* Desalination 2005, **176**, 47.

[94] Langhals H., Abbt-Braun G., Frimmel F. H. *Association of humic substances: Verification of Lambert-Beer's law.,* Acta hydrochimica et hydrobiologica 2000, **28**, 329.

[95] Chen Y., Senesi N., Schnitzer M. *Information provided on humic substances by E4/E6 ratios,* Soil Science Society of America Journal 1977, **41**, 352.

[96] Chen J., Gu B. H., LeBoeuf E. J., Pan H. J., Dai S. *Spectroscopic characterization of the structural and functional properties of natural organic matter fractions,* Chemosphere 2002, **48**, 59.

[97] Hay M. B., Myneni S. C. B. *Structural environments of carboxyl groups in natural organic molecules from terrestrial systems. Part 1: Infrared spectroscopy,* Geochimica Et Cosmochimica Acta 2007, **71**, 3518.

[98] Niemeyer J., Chen Y., Bollag J. M. *Characterization of humic acids, composts, and peat by diffuse reflectance Fourier transform infrared spectroscopy.,* Soil Science Society of America Journal 1992, **56**, 135.

[99] Bloom P. R., Leenheer J. A., Vibrational, electronic, and high-energy spectroscopic methods for characterizing humic substances in: Hayes, M. H. B., MacCarthy, P., Malcolm, R. L., Swift, R. S. (Eds.), *Humic substances II: in search of structure.*, John Wiley & Sons, New York 1989, pp. 409.

[100] Peuravuori J., Monteiro A., Eglite L., Pihlaja K. *Comparative study for separation of aquatic humic-type organic constituents by DAX-8, PVP and DEAE sorbing solids and tangential ultrafiltration: elemental composition, size-exclusion chromatography, UV-vis and FT-IR,* Talanta 2005, **65**, 408.

[101] Preston C. M. *Application of NMR to soil organic matter analysis: History and prospects.,* Soil Science 1996, **161**, 144.

[102] Gonzalez-Perez J. A., Gonzalez-Vila F. J., Almendros G., Knicker H. *The effect of fire on soil organic matter - a review,* Environment International 2004, **30**, 855.

[103] Chen Y. N. *Nuclear magnetic resonance, infra-red and pyrolysis: Application of spectroscopic methodologies to maturity determination of composts,* Compost Science & Utilization 2003, **11**, 152.

[104] Hatcher P. G., Dria K. J., Kim S., Frazier S. W. *Modern analytical studies of humic substances,* Soil Science 2001, **166**, 770.

[105] Kogel-Knabner I. *C-13 and N-15 NMR spectroscopy as a tool in soil organic matter studies,* Geoderma 1997, **80**, 243.

[106] Hertkorn N., Permin A., Perminova I., Kovalevskii D., Yudov M., Petrosyan V., Kettrup A. *Comparative analysis of partial structures of a peat humic and fulvic acid using one- and two-dimensional nuclear magnetic resonance spectroscopy,* Journal of Environmental Quality 2002, **31**, 375.

[107] Haiber S., Herzog H., Buddrus J., Burba P., Lambert J., Quantification of substructures of refractory organic substances by means of nuclear magnetic resonance. in: Frimmel, F. H., Abbt-Braun, G., Heumann, K. G., Hock, B., Lüdemann, H.-D., Spiteller, M. (Eds.), *Refractory organic substances (ROS) in the environment.*, Wiley – VCH, Weinheim 2002, pp. 115.

[108] Lambert J., Lankes U., Application of nuclear magnetic resonance spectroscopy to structural investigations of refractory organic substances: principles and definitions. in: Frimmel, F. H., Abbt-Braun, G., Heumann, K. G., Hock, B., Lüdemann, H.-D., Spiteller, M. (Eds.), *Refractory organic substances (ROS) in the environment.*, Wiley – VCH, Weinheim 2002, pp. 89.

[109] Newman T. H., Tate K. R. *Soil phosphorous characterisation by 31P nuclear magnetic resonance.,* Communication in Soil Science and Plant Analysis 1980, 835.

[110] Knicker H., Almendros G., GonzalezVila F. J., Ludemann H. D., Martin F. *C-13 and N-15 NMR analysis of some fungal melanins in comparison with soil organic matter,* Organic Geochemistry 1995, **23**, 1023.

[111] Knicker H., Scaroni A. W., Hatcher P. G. *N-15 NMR spectroscopy - A promising technique for the examination of organic nitrogen in geomacromolecules.,* Abstracts of Papers of the American Chemical Society 1996, **212**, 8.

[112] Knicker H., Scaroni A. W., Hatcher P. G. *C-13 and N-15 NMR spectroscopic investigation on the formation of fossil algal residues,* Organic Geochemistry 1996, **24**, 661.

[113] Knicker H., Hatcher P. G. *Survival of protein in an organic-rich sediment: Possible protection by encapsulation in organic matter,* Naturwissenschaften 1997, **84**, 231.

[114] Zang X., van Heemst J. D. H., Dria K. J., Hatcher P. G. *Encapsulation of protein in humic acid from a histosol as an explanation for the occurrence of organic nitrogen in soil and sediment,* Organic Geochemistry 2000, **31**, 679.

[115] Xu X., Kalinichev A. G., Kirkpatrick R. J. *133Cs and Cl-35 NMR spectroscopy and molecular dynamics modeling of Cs+ and Cl- complexation with natural organic matter,* Geochimica Et Cosmochimica Acta 2006, **70**, 4319.

[116] Kogel-Knabner I. *Analytical approaches for characterizing soil organic matter,* Organic Geochemistry 2000, **31**, 609.

[117] Mahieu N., Powlson D. S., Randall E. W. *Statistical analysis of published carbon-13 CPMAS NMR spectra of soil organic matter,* Soil Science Society of America Journal 1999, **63**, 307.

[118] Simpson A. *Multidimensional solution state NMR of humic substances: A practical guide and review,* Soil Science 2001, **166**, 795.

[119] Deshmukh A. P., Pacheco C., Hay M. B., Myneni S. C. B. *Structural environments of carboxyl groups in natural organic molecules from terrestrial systems. Part 2: 2D NMR spectroscopy,* Geochimica Et Cosmochimica Acta 2007, **71**, 3533.

[120] Simpson A. J., Lefebvre B., Moser A., Williams A., Larin N., Kvasha M., Kingery W. L., Kelleher B. *Identifying residues in natural organic matter through spectral prediction and pattern matching of 2D NMR datasets,* Magnetic Resonance in Chemistry 2004, **42**, 14.

[121] Haiber S., Herzog H., Burba P., Gosciniak B., Lambert J. *Two-dimensional NMR studies of size fractionated Suwannee River Fulvic and Humic Acid Reference,* Environmental Science & Technology 2001, **35**, 4289.

[122] Haiber S., Herzog H., Burba P., Gosciniak B., Lambert J. *Quantification of carbohydrate structures in size fractionated aquatic humic substances by two-dimensional nuclear magnetic resonance,* Fresenius Journal of Analytical Chemistry 2001, **369**, 457.

[123] Simpson A. J., Kingery W. L., Hatcher P. G. *The identification of plant derived structures in humic materials using three-dimensional NMR spectroscopy,* Environmental Science & Technology 2003, **37**, 337.

[124] Donard O. F. X., Lamotte M., Belin C., Ewald M. *High-Sensitivity Fluorescence Spectroscopy of Mediterranean Waters Using a Conventional or a Pulsed Laser Excitation Source,* Marine Chemistry 1989, **27**, 117.

[125] Coble P. G., Green S. A., Blough N. V., Gagosian R. B. *Characterization of dissolved organic matter in the Black Sea by fluorescence spectroscopy* Nature 1989, **348**, 432.

[126] Sharpless C. M., McGown L. B. *Effects of Aluminum-Induced Aggregation on the Fluorescence of Humic Substances,* Environmental Science and Technology 1999, **33**, 3264.

[127] Kim H.-C., Yu M. J., Han I. *Multi-method study of the characteristic chemical nature of aquatic humic substances isolated from the Han River, Korea,* Applied Geochemistry 2006, **21**, 1226.

[128] Kumke M. U., Frimmel F. H., Stationary and time-resolved fluorescence for refractory organic substances characterization. in: Frimmel, F. H., Abbt-Braun, G., Heumann, K. G., Hock, B., Lüdemann, H.-D., Spiteller, M. (Eds.), *Refractory organic substances (ROS) in the environment.*, Wiley– VCH, Weinheim 2002, pp. 215.

[129] Löhmannsröben H.-G., Schultze U., Skrivanek T., Investigation of the interaction between polycyclic aromatic compounds and refractory organic substances with stationary and absorption spectroscopy. in: Frimmel, F. H., Abbt-Braun, G., Heumann, K. G., Hock, B., Lüdemann, H.-D., Spiteller, M. (Eds.), *Refractory organic substances (ROS) in the environment.*, Wiley – VCH, Weinheim 2002, pp. 516–534.

[130] Zhang T., Lu J., Ma J., Qiang Z. *Fluorescence spectroscopic characterization of DOM fractions isolated from a filtered river water after ozonation and catalytic ozonation,* Chemosphere 2008, **71**, 911.

[131] Chen J., LeBoeuf E. J., Dai S., Gu B. *Fluorescence spectroscopic studies of natural organic matter fractions,* Chemosphere 2003, **50**, 639.

[132] McIntyre C., Batts B. D., Jardine D. R. *Electrospray mass spectrometry of groundwater organic acids,* Journal of Mass Spectrometry 1997, **32**, 328.

[133] Gaskell S. J. *Electrospray: Principles and practice,* Journal of Mass Spectrometry 1997, **32**, 677.

[134] Gamero-Castano M., de la Mora J. F. *Kinetics of small ion evaporation from the charge and mass distribution of multiply charged clusters in electrosprays,* Journal of Mass Spectrometry 2000, **35**, 790.

[135] Kebarle P. *A brief overview of the present status of the mechanisms involved in electrospray mass spectrometry,* Journal of Mass Spectrometry 2000, **35**, 804.

[136] Kebarle P., Peschke M. *On the mechanisms by which the charged droplets produced by electrospray lead to gas phase ions,* Analytica Chimica Acta 2000, **406**, 11.

[137] Leenheer J. A., Rostad C. E., Gates P. M., Furlong E. T., Ferrer I. *Molecular resolution and fragmentation of fulvic acid by electrospray ionization/multistage tandem mass spectrometry,* Analytical Chemistry 2001, **73**, 1461.

[138] Kujawinski E. B., Freitas M. A., Zang X., Hatcher P. G., Green-Church K. B., Jones R. B. *The application of electrospray ionization mass spectrometry (ESI MS) to the structural characterization of natural organic matter,* Organic Geochemistry 2002, **33**, 171.

[139] Comisarow M. B., Marshall A. G. *Fourier transformn Ion Cyclotron Resonance Spectroscopy,* Chemical Physics Letter 1974, **25**, 282.

[140] Marshall A. G., Hendrickson C. L., Jackson G. S. *Fourier transform ion cyclotron resonance mass spectrometry: A primer,* Mass Spectrometry Reviews 1998, **17**, 1.

[141] Makarov A. *Electrostatic axially harmonic orbital trapping: A high-performance technique of mass analysis,* Analytical Chemistry 2000, **72**, 1156.

[142] Makarov A., Denisov E., Lange O., Horning S. *Dynamic range of mass accuracy in LTQ Orbitrap hybrid mass spectrometer,* Journal of the American Society for Mass Spectrometry 2006, **17**, 977.

[143] Marshall A. G., Guan S. H. *Advantages of high magnetic field for Fourier transform ion cyclotron resonance mass spectrometry,* Rapid Communications in Mass Spectrometry 1996, **10**, 1819.

[144] Koch B. P., Dittmar T. *From mass to structure: an aromaticity index for high-resolution mass data of natural organic matter,* Rapid Communications in Mass Spectrometry 2006, **20**, 926.

[145] Koch B. P., Dittmar T., Witt M., Kattner G. *Fundamentals of molecular formula assignment to ultrahigh resolution mass data of natural organic matter,* Analytical Chemistry 2007, **79**, 1758.

[146] Kind T., Fiehn O. *Seven Golden Rules for heuristic filtering of molecular formulas obtained by accurate mass spectrometry,* Bmc Bioinformatics 2007, **8**.

[147] Stenson A. C., Marshall A. G., Cooper W. T. *Exact masses and chemical formulas of individual Suwannee River fulvic acids from ultrahigh resolution electrospray ionization Fourier transform ion cyclotron resonance mass spectra,* Analytical Chemistry 2003, **75**, 1275.

[148] Sleighter R. L., Hatcher P. G. *The application of electrospray ionization coupled to ultrahigh resolution mass spectrometry for the molecular characterization of natural organic matter,* Journal of Mass Spectrometry 2007, **42**, 559.

[149] Hughey C. A., Hendrickson C. L., Rodgers R. P., Marshall A. G., Qian K. N. *Kendrick mass defect spectrum: A compact visual analysis for ultrahigh-resolution broadband mass spectra,* Analytical Chemistry 2001, **73**, 4676.

[150] Kujawinski E. B., Hatcher P. G., Freitas M. A. *High-resolution Fourier transform ion cyclotron resonance mass spectrometry (FT-ICR MS) of humic and fulvic acids: Improvements and comparisons,* Analytical Chemistry 2002, **74**, 413.

[151] Kim S., Kramer R. W., Hatcher P. G. *Graphical method for analysis of ultrahigh-resolution broadband mass spectra of natural organic matter, the van Krevelen diagram,* Analytical Chemistry 2003, **75**, 5336.

[152] Kunenkov E. V., Kononikhin A. S., Perminova I. V., Gaspar A., Schmitt-Kopplin P., Hertkorn N., Popov I. A., Garmash A., Nikolaev E. N. *New Approach to Interpretation of High Resolution Mass Spectra of Natural and Synthetic Macromolecular Compounds: Total Mass Difference Spectroscopy,* submitted to Anal.Chem. 2008.

[153] Fievre A., Solouki T., Marshall A. G., Cooper W. T. *High-resolution Fourier transform ion cyclotron resonance mass spectrometry of humic and fulvic acids by laser desorption/ionization and electrospray ionization,* Energy & Fuels 1997, **11**, 554.

[154] Schmitt-Kopplin P., Englmann M., Rosello-Mora R., Schiewek R., Brockmann K. J., Benter T., Schmitz O. J. *Combining chip-ESI with APLI (cESILI) as a multimode source for analysis of complex mixtures with ultrahigh-resolution mass spectrometry,* Analytical Bioanalytical Chemistry 2008, DOI 10.1007/s00216.

[155] Freitas M. A., Kujawinski E., Zang X., Hatcher P. G. *High resolution Fourier transform ion cyclotron resonance mass spectrometry for the analysis of complex humic and fulvic acids.,* Abstracts of Papers of the American Chemical Society 2001, **221**, U465.

[156] Koch B. P., Witt M. R., Engbrodt R., Dittmar T., Kattner G. *Molecular formulae of marine and terrigenous dissolved organic matter detected by electrospray ionization Fourier transform ion cyclotron resonance mass spectrometry,* Geochimica Et Cosmochimica Acta 2005, **69**, 3299.

[157] Kramer R. W., Kujawinski E. B., Hatcher P. G. *Identification of black carbon derived structures in a volcanic ash soil humic acid by Fourier transform ion cyclotron resonance mass spectrometry,* Environmental Science & Technology 2004, **38**, 3387.

[158] Kujawinski E. B. *Electrospray ionization Fourier transform ion cyclotron resonance mass spectrometry (ESI FT-ICR MS): characterization of complex environmental mixtures,* Environmental Forensics 2002, **3**, 207.

[159] Stenson A., Landing W. M., Marshall A. G., Cooper W. T. *Ionization and fragmentation of humic substances in Electrospray Ionization Fourier Transform-Ion Cyclotron Resonance Mass Spectrometry,* Analytical Chemistry 2002, **75**, 1275.

[160] Remmler M., Georgi A., Kopinke F. D. *Evaluation of matrix-assisted laser-desorption ionization (MALDI) time-of-flight (TOF) massspectrometry as a method for the determination of the molecular-mass distributions of humic acids.,* European Journal of Mass Spectrometry 1995, **1**, 403.

[161] Reemtsma T., These A., Linscheid M., Leenheer J., Spitzy A. *Molecular and structural characterization of dissolved organic matter from the deep ocean by FTICR-MS, including hydrophilic nitrogenous organic molecules,* Environmental Science & Technology 2008, **42**, 1430.

[162] Brown T. L., Rice J. A. *Effect of experimental parameters on the ESI FT-ICR mass spectrum of fulvic acid,* Analytical Chemistry 2000, **72**, 384.

[163] Novotny F. J., Rice J. A. *Characterization of Fulvic Acid by Laser-Desorption Mass Spectrometry,* Envionmental Science and Technology 1995, **29**, 2464.

[164] Chilom G., Chilom O., Rice J. A. *Exploring the high-mass components of humic acid by laser desorption ionization mass spectrometry,* Rapid Communications in Mass Spectrometry 2008, **22**, 1528.

[165] McIntyre C., McRae C., Jardine D., Batts B. D. *Self-esterification of fulvic acid model compounds in methanolic solvents as observed by electrospray ionization mass spectrometry,* Rapid Communications in Mass Spectrometry 2002, **16**, 785.

[166] McIntyre C., McRae C. *Proposed guidelines for sample preparation and ESI-MS analysis of humic substances to avoid self-esterification,* Organic Geochemistry 2005, **36**, 543.

[167] Smith D. L., Deng Y. Z., Zhang Z. Q. *Probing the non-covalent structure of proteins by amide hydrogen exchange and mass spectrometry,* Journal of Mass Spectrometry 1997, **32**, 135.

[168] Solouki T., Freitas M. A., Alomary A. *Gas-phase hydrogen/deuterium exchange reactions of fulvic acids: An electrospray ionization Fourier transform ion cyclotron resonance mass spectral study,* Analytical Chemistry 1999, **71**, 4719.

[169] Alomary A., Solouki T., Patterson H. H., Cronan C. S. *Elucidation of aluminum-fulvic acid interactions by gas-phase hydrogen/deuterium (H/D) exchange and electrospray Fourier transform ion cyclotron resonance mass spectrometry (ESI FT-ICR),* Environmental Science & Technology 2000, **34**, 2830.

[170] McCarthy M. D., Hedges J. I., Benner R. *Major bacterial contribution to marine dissolved organic nitrogen,* Science 1998, **281**, 231.

[171] Wu F. C., Evans R. D., Dillon P. J. *High-performance liquid chromatographic fractionation and characterization of fulvic acid,* Analytica Chimica Acta 2002, **464**, 47.

[172] McDonald S., Bishop A. G., Prenzler P. D., Robards K. *Analytical chemistry of freshwater humic substances,* Analytica Chimica Acta 2004, **527**, 105.

[173] Jahnel J. B., Brinkmann T., Abbt-Braun G., Frimmel F. H., Occurence of amino acids, carbohydrates, and low-molecular-weight organic acids in refractory organic substances. in: Frimmel, F. H., Abbt-Braun, G., Heumann, K. G., Hock, B., Lüdemann, H.-D., Spiteller, M. (Eds.), *Refractory organic substances*

(ROS) in the environment., Wiley – VCH, Weinheim 2002, pp. 264.

[174] Kaiser K., Benner R. *Determination of amino sugars in environmental samples with high salt content by high performance anion exchange chromatography and pulsed amperometric detection,* Analytical Chemistry 2000, **72**, 2566.

[175] Skoog A., Biddanda B., Benner R. *Bacterial utilization of dissolved glucose in the upper water column of the Gulf of Mexico,* Limnology and Oceanography 1999, **44**, 1625.

[176] Munster U. *Amino acid profiling in natural organic matter isolated by reverse osmosis from eight different boreal freshwaters,* Environment International 1999, **25**, 209.

[177] Benner R., Molecular indicators of the bioavailability of dissolved organic matter. in: Findlay, S. E. G., Sinsabaugh, R. L. (Eds.), *Aquatic Ecosystems: Interactivity of Dissolved Organic Matter*, Elsevier Science. 2003, pp. 97

[178] Kaiser K., Benner R. *Hydrolysis-induced racemization of amino acids,* Limnology and Oceanography-Methods 2005, **3**, 318.

[179] Stevenson F. J., van Winkle Q., Martin W. P. *Physicochemical investigations of clay absorbed organic colloids,* Soil Science Society American Proceeding 1953, **17**, 31.

[180] Deyl Z., Everaerts F. M., Prusik Z., Svendsen P. J., *Electrophoresis: a survey of techniques and applications*, Elsevier, Amsterdam 1979.

[181] Khaledi M. G., Theory Techniques, and Applications, *High-performance Capillary Electrophoresis*, John Wiley and Sons, Chichester 1998.

[182] Kuhn R., Hoffstetter-Kuhn S., *Capillary electrophoresis: principles and practise*, Springer-Verlag, Berlin Heidelberg 1993.

[183] Schmitt-Kopplin P., *Capillary electrophoresis; from small ions to macromolecules*, Humana Press 2005.

[184] Schmitt-Kopplin P., Frommberger M. *Capillary electrophoresis - mass spectrometry: 15 years of developments and applications,* Electrophoresis 2003, **24**, 3837.

[185] Duxbury J. M., *In Search of Structure*, John Wiley and Sons, New York 1989, pp. 594.

[186] Schmitt-Kopplin P., Junkers J. *Capillary zone electrophoresis of natural organic matter,* Journal of Chromatography A 2003, **998**, 1.

[187] Henry D. C. Proceeding Royal Society London 1931, **133**, 106.

[188] Offord R. E. *Electrophoretic mobilities of peptides on paper and their use in the determination of amide groups.,* Nature 1966, **211**, 591.

[189] Jalali-Heravi M., Shen Y., Hassanisadi M., Khaledi M. G. *Prediction of electrophoretic mobilities of peptides in capillary zone electrophoresis by quantitative structure-mobility relationships using the Offord model and artificial neural networks.,* Electrophoresis 2005, **26**, 1874.

[190] Carbeck J. D., Negin R. S. *Measuring the size and charge of proteins using protein charge ladders, capillary electrophoresis, and electrokinetic models of colloids.,* Journal of American Chemical Society 2001, **123**, 1252.

[191] Stokes J. C., and Johnson, M.J. *Resolution in sub-micrometer particle separations by capillary electrophoresis.,* Microchemical Journal 2004, **76**, 121.

[192] Avena M. J., Koopal L. K., van Riemsdijk W. H. J. *Proton binding to humic acids: electrostatic and intrinsic interactions,* Colloid Interface Sciences 1999, **217**, 37.

[193] Benedetti M. F., Van Riemsdijk W. H., Koopal L. K. *Humic substances considered as a heterogeneous Donnan gel phase,* Environmental Science and Technology 1996, **30**, 1805.

[194] Carballeira J. L., Antelo J. M., Rey F., Arce F. *Modeling the effects of ionic strength on ionization parameters for a soil fulvic acid at low concentrations,* Analytica Chimica Acta 1999, **401**, 243.

[195] De Wit J. C., van Riemsdijk W. H., Koopal L. K. *Proton binding to humic substances. 1. Electrostatic effects,* Environmental Science and Technology 1993, **27**, 2005.

[196] Ephraim J. H., Alegret S., Mathuthu A., Bicking M., Malcom R. L., Marinsky J. A. *A unified physicochemical description of the protonationandmetal ion complexation equilibria of natural organic acids (humic and fulvic acids). 2. Influence of polyelectrolyte properties and functional group heterogeneity on the protonation equilibria of fulvic acid,* Environmental Science and Technology 1986, **20**, 354.

[197] Marinsky J. A., Ephraim J. *A unified physicochemical description of the protonation and metal ion complexation equilibria of natural organic acids (humic and fulvic acids).*

1. Analysis of the influence of polyelectrolyte properties on protonation equilibria in ionic media: Fundamental concepts., Environmental Science and Technology 1986, **20**, 349.

[198] Klein Wolterink J., Leermakers F. A. M., Fleer G. J., Koopal L. K., Zhulina E. B., Borisov O. V. *Screening in solutions of starbranched polyelectrolytes,* Macromolecules 1999, **32**, 2365.

[199] Gosh K., Schnitzer M. *Macromolecular structures of humic substances,* Soil Science 1980, **129**, 266.

[200] Kinniburgh D. G., Milne C. J., Benedetti M. F., Pinheiro J. P., Filius J., Koopal L. K., van Riemsdijk W. H. *Metal ion binding by humic acid: application of the NICA model.,* Environmental Science and Technology 1996, **30**, 1687.

[201] Duval J., Wilkinson K. J., van Leeuwen H., Buffle J. *Humic substances are soft and permeable: evidence from their electrophoretic mobilities,* Environmental Science and Technology 2005, **39**, 6435.

[202] Schmitt-Kopplin P., Menzinger F., Freitag D., Kettrup A. *Improving the use of CE in a chromatographer's world,* LC-GC Europe 2001, **14**, 284.

[203] Schmitt P., Poiger T., Simon R., Garrison A. W., Freitag D., Kettrup A. *Simultaneous ionization constants and isoelectric points determination of 12 hydroxy-s-triazines by capillary zone electrophoresis (CZE) and capillary electrophoresis isoelectric focusing (CIEF),* Analytical Chemistry 1997, **69**, 2559.

[204] Bianco G., Schmitt-Kopplin P., De Benedetto G., Kettrup A., Cataldi T. R. *Determination of glycoalkaloids and relative aglycones by non-aqueous capillary electrophoresis coupled with electrospray ionization-ion trap mass spectrometry,* Electrophoresis 2002, **23**, 2904.

[205] Righetti P. G., Brown R. P., Stone A. L. *Aggregation of ampholine on heparin and other acidic polysaccharides in isoelectric focussing,* Biochimica et Biophysica Acta 1978, **542**, 232.

[206] Govi M., Bonoretti G., Ciavata C., Sequi P. *Characterization of soil organic matter using isoelectric focusing: a comparison of six commercial carrier ampholytes,* Soil Science 1994, **157**, 91.

[207] Kutsch H., Schumacher B. *Isoelectric focusing of humic substances on ultrathin polyacrylamide gels: evidence of fingerprint performance,* Biology and Fertility of Soils 1994, **18**, 163.

[208] Ciavatta C., Govi M., Bonoretti G., Gess C. *Identification of peat and leonardite using humification parameters and isoelectric focusing (IEF): A first approach.,* Fertilizer Research 1996, **44**, 225.

[209] De Nobili M. *Electrophoretic evidence of the integrity of humic substances separated by means of electrofocusing,* Journal of Soil Science 1988, **39**, 437.

[210] Ceccanti B., Bertolucci M. T., Rustighi G., Calcinai M. *Isoelectric focusing of soil humic substances in the presence of 8M urea,* Biology and Fertility of Soils 1986, **2**, 71.

[211] Ciavatta C., Govi M., Sitti L., Gessa C. *Influence of blood meal organic fertilizer on soil organic matter,* Journal of Plant Nutrition 1997, **20**, 1573.

[212] Garcia C., Hernandez T., Ceccanti B. *Characterization by isoelectric focusing of the organic matter of a regenerated soil,* Soil Science and Plant Analysis 1995.

[213] Govi M., Francisco O., Ciavatta C., Sequi P. *Influence of long-term residue and fertilizer applications on soil humic substances: A study by electrofocusing,* Soil Science and Plant Analysis 1992, **154**, 8.

[214] Petrussi F., De Nobili M., Viotto M., Sequi P. *Characterization of organic matter from animal manures after digestion by earthworms,* Plant and Soil 1988, **105**, 41.

[215] Schmitt P., Garrison A. W., Freitag D., Kettrup A. *Capillary isoelectric focusing (CIEF) for the characterization of humic substances,* Water Research 1997, **31**, 2037.

[216] Trubetskoj O. A., Trubetskaya O. E., Afanaseva G. V., Reznikova O. I., Saiz-Jimenez C. *Polyacrylamide gel electrophoresis of soil humic acid fractionated by size-exclusion chromatography and ultrafiltration,* Journal of Chromatography A 1997, **767**, 285.

[217] Trubetskoj O. A., Trubetskaya O. E., Afanasieva G. V., Reznikova O. I., Hermosin B., Saiz-Jimenez C. *Tandem size exclusion chromatography polyacrylamide gel electrophoresis of humic acids,* Journal of Plant Nutrition and Soil Science 1998, **161**, 619.

[218] Trubetskaya O. E., Trubetskoj O. A., Saiz-Jimenez C. *Polyacrylamide gel electrophoresis of humic and fulvic acids after acid hydrolysis,* Fresenius Environmental Bulletin 2001, **10**, 635.

[219] Trubetskaya O. E., Trubetskoj O., Guyot G., Andreux F., Richard C. *Fluorescence of soil humic acids and their fractions obtained by tandem size exclusion chromatography-polyacrylamide gel electrophoresis,* Organic Geochemistry 2002, **33**, 213.

[220] Richard C., Trubetskaya O. E., Trubetskoj O., Reznikova O., Afanaseva G. V., Aguer J. P., Guyot G. *Key role of the low molecular size fraction of soil humic acids for*

fluorescence and photoinductive activity, Environmental Science and Technology 2004, **38**, 2052.

[221] De Nobili M., Bragato G., Mori A. *Capillary electrophoretic behaviour of humic substances in physical gels,* Journal of Chromatography A 1999, **863**, 195.

[222] Phillips S. L., Olesik S. V. *Initial characterization of humic acids using liquid chromatography at the critical condition followed by Size-Exclusion Chromatography and Electrospray Ionization Mass Spectrometry,* Analytical Chemistry 2003, **75**, 5544.

[223] Reemtsma T., These A. *Comparative investigation of low-molecular-weight fulvic acids of different origin by SEC-Q-TOF-MS: New insights into structure and formation,* Environmental Science and Technology 2005, **39**, 3507.

[224] Reemtsma T., These A. *On-line coupling of Size Exclusion Chromatography with Electrospray Ionization-Tandem Mass Spectrometry for the analysis of aquatic fulvic and humic acids,* Analytical Chemistry 2003, **75**, 1500.

[225] Reemtsma T., These A., Springer A., Linscheid M. *Differences in the molecular composition of fulvic acid size fractions detected by size-exclusion chromatography-on line Fourier transform ion cyclotron resonance (FTICR-) mass spectrometry,* Water Research 2008, **42**, 63.

[226] Persson L., Alsberg T., Kiss G., Odham G. *On-line size-exclusion chromatography / electrospray ionisation mass spectrometry of aquatic humic and fulvic acids,* Rapid Communication in Mass Spectrometry 2000, **14**, 286.

[227] Richardson S. D. *Water analysis: emerging contaminants and current issues,* Analytical Chemistry 2003, **75**, 2831.

[228] Simpson A. J., Tseng L. H., Simpson M. J., Spraul M., Braumann U., Kingery W. L., Kelleher B. P., Hayes M. H. B. *The application of LC-NMR and LC-SPE-NMR to compositional studies of natural organic matter,* Analyst 2004, **129**, 1216.

[229] Saiz-Jimenez C. *Analytical pyrolysis of humic substances: pitfalls, limitations, and possible solutions,* Environmental Science and Technology 1994, **28**, 1773.

[230] van Bergen P., Flannery M. B., Poulton P. R., Evershed R. P., Fate of N-Containing Macro- molecules in the Biosphere and Geosphere in: Stankiewicz, B. A., van Bergen, P. F. (Eds.), American Chemical Society 1998, pp. 321.

[231] Martın F., Gonzalez-Vila F. J., del Rıo J. C., Verdejo T. *Pyrolysis derivatization of humic substances 1. Pyrolysis of fulvic acids in the presence of tetramethylammonium hydroxide,* Journal of Analytical and Applied Pyrolysis 1994, **28**, 71.

[232] de Leeuw J. W., Baas M. *The behaviour of esters in the presence of tetramethylammonium salts at elevated temperatures; flash pyrolysis or flash chemolysis,* Journal of Analytical and Applied Pyrolysis 1993, **26**, 175.

[233] Dai X. Y., Ping C. L., Michaelson G. J. *Characterizing soil organic matter in Arctic tundra soils by different analytical approaches,* Organic Geochemistry 2002, **33**, 407.

[234] Mercier F., Moulin V., Guittet M. J., Barre N., Gautier-Soyer M., Trocellier P., Toulhoat P. *Applications of new surface analysis techniques (NMA and XPS) to humic substances,* Organic Geochemistry 2002, **33**, 247.

[235] von Brocke A., Nicholson G., Bayer E. *Recent advances in capillary electrophoresis / electrospray-mass spectrometry,* Electrophoresis 2001, **22**, 1251.

[236] Schmitt-Kopplin P., Kettrup A. *Capillary electrophoresis – electrospray ionization – mass spectrometry for the characterization of natural organic matter: An evaluation with free flow electrophoresis-off-line flow injection electrospray ionization mass spectrometry,* Electrophoresis 2003, **24**, 3057.

[237] Whelan T. J., Shalliker R. A., McIntyre C., Wilson M. A. *Development of a multidimensional high-performance liquid chromatography (HPLC) separation for bayer humic substances,* Industial and Engineering Chemistry Research 2005, **44**, 3229.

[238] Woelki G., Friedrich S., Hanschmann G., Salzer R. *HPLC fractionation and structural dynamics of humic acids,* Fresenius Journal of Analytical Chemistry 1997, **357**, 548.

[239] Wu F. C., Evans D., Dillon P., Schiff S. *Molecular size distribution characteristics of the metal-DOM complexes in stream waters by high-performance size-exclusion chromatography (HPSEC) and high-resolution inductively coupled plasma mass spectrometry (ICP-MS),* Journal of Analytical Atomic Spectrometry 2004, **19**, 979.

[240] Perminova I. V. *Size exclusion chromatography of humic substances: Complexities of data interpretation attributable to non-size exclusion effects,* Soil Science 1999, **164**, 834.

[241] Kudryavtsev A. V., Perminova I. V., Petrosyan V. S. *Size-exclusion chromatographic descriptors of humic substances,* Analytica Chimica Acta 2000, **407**, 193.

[242] Perminova I. V., Frimmel F. H., Kudryavtsev A. V., Kulikova N. A., Abbt-Braun G., Hesse S., Petrosyan V. S. *Molecular weight characteristics of humic substances from different environments as determined by size exclusion chromatography and their statistical evaluation,* Environmental Science & Technology 2003, **37**, 2477.

[243] Schmitt-Kopplin P., Englmann M. *Capillary electrophoresis-mass spectrometry: Survey on developments and applications 2003-2004,* Electrophoresis 2005, **26**, 1209.

[244] Gaspar A., Englmann M., Fekete A., Harir M., Schmitt-Kopplin P. *Trends in CE-MS 2005-2006,* Electrophoresis 2008, **29**, 66.

[245] Keuth U., Leinenbach A., Beck H. P., Wagner H. *Separation and characterization of humic acids and metal humates by electrophoretic methods,* Electrophoresis 1998, **19**, 1091.

[246] Krivankova L., Bocek P. *Continuous free-flow electrophoresis,* Canadian Journal of Chemistry-Revue Canadienne De Chimie 1998, **19**, 1064.

[247] Junkers J., Schmitt-Kopplin P., Munch J. C., Kettrup A. *Up-scaling capillary zone electrophoresis separations of polydisperse anionic polyelectrolytes with preparative free-flow electrophoresis exemplified with a soil fulvic acid,* Electrophoresis 2002, **23**, 2872.

[248] Schmitt-Kopplin P., Garmash A. V., Kudryavtsev A. V., Menzinger F., Perminova I. V., Hertkorn N., Freitag D., Petrosyan V. S., Kettrup A. *Quantitative and qualitative precision improvements by effective mobility-.scale data transformation in capillary electrophoresis analysis,* Electrophoresis 2001, **22**, 77.

[249] Hughey C. A., Hendrickson C. L., Rodgers R. P., Marshall A. G. *Elemental composition analysis of processed and unprocessed diesel fuel by electrospray ionization fourier transform ion cyclotron resonance mass spectrometry,* Energy & Fuels 2001, **15**, 1186.

[250] Kim S., Rodgers R. P., Marshall A. G. *Truly "exact" mass: Elemental composition can be determined uniquely from molecular mass measurement at similar to 0.1 mDa accuracy for molecules up to similar to 500 Da,* International Journal of Mass Spectrometry 2006, **251**, 260.

[251] Hertkorn N., Benner R., Frommberger M., Schmitt-Kopplin P., Witt M., Kaiser K., Kettrup A., Hedges J. I. *Characterization of a major refractory component of marine dissolved organic matter,* Geochimica Et Cosmochimica Acta 2006, **70**, 2990.

[252] Pringle S. D., Giles K., Wildgoose J. L., Williams J. P., Slade S. E., Thalassinos K., Bateman R. H., Bowers M. T., Scrivens J. H. *An investigation of the mobility separation of some peptide and protein ions using a new hybrid quadrupole/travelling wave IMS/oa-ToF instrument,* International Journal of Mass Spectrometry 2007, **261**, 1.

[253] Goldberg S. *Reactions of boron with soils,* Plant and Soil 1997, **193**, 35.

[254] Keren R., Bingham F. T., *Boron in water, soils, and plants*, 1985, pp. 229.

[255] Marzadori C., Vittori Antisari L., Ciavatta C., Sequi P. *Soil Organic Matter Influence on Adsorption and Desorption of Boron,* Soil Science Society of America 1991, **55**, 1582.

[256] Gu B., Lowe L. E. *Studies on the adsorption of boron on humic acid.,* Canadian Journal of Soil Science 1990, **70**, 305.

[257] Koyama T., Terauchi K. *Synthesis and application of boronic acid-immobilized porous polymer particles: A novel packing for high-performance liquid affinity chromatography,* Journal of Chromatography B-Biomedical Applications 1996, **679**, 31.

[258] Tuncel A., Ozdemir A. *Boronic acid-functionalized HEMA-based gels for nucleotide adsorption,* Journal of Applied Polymer Science 2000, **78**, 268.

[259] Tuncel A., Ozdemir A. *Thermally reversible VPBA-NIPAM copolymer gels for nucleotide adsorption* Journal of Biomaterials Science-Polymer Edition 2000, **11**, 817.

[260] Singh N., Willson R. C. *Boronate affinity adsorption of RNA: possible role of conformational changes,* Journal of Chromatography A 1999, **840**, 205.

[261] Arimori S., Bell M. L., Oh C. S., Frimat K. A., James T. D. *Modular fluorescence sensors for saccharides,* Chemical Communications 2001, 1836.

[262] Sano M., Okamura J., Kanekiyo Y., Shinkai S. *Nucleotide-responsive gel tips for atomic force microscopy,* Colloids and Surfaces a-Physicochemical and Engineering Aspects 2000, **169**, 131.

[263] Dukler A., Freeman A. *In situ product removal of ketoses by immobilized 3-amino phenyl boronic acid: Effect of immobilization method on pH profile,* Biotechnology and Bioengineering 2001, **75**, 25.

[264] Nicolas M., Fabre B., Simonet J. *Electrochemical sensing of fluoride and sugars with a boronic acid-substituted bipyridine Fe(II) complex in solution and attached onto an electrode surface,* Electrochimica Acta 2001, **46**, 1179.

[265] Asher S. A., Alexeev V. L., Goponenko A. V., Sharma A. C., Lednev I. K., Wilcox C. S., Finegold D. N. *Photonic crystal carbohydrate sensors: Low ionic strength sugar sensing,* Journal of the American Chemical Society 2003, **125**, 3322.

[266] Camli S. T., Senel S., Tuncel A. *Nucleotide isolation by boronic acid functionalized hydrophilic supports,* Colloids and Surfaces a-Physicochemical and Engineering Aspects 2002, **207**, 127.

[267] Cicek H. *Nucleotide isolation by boronic acid functionalized hydrogel beads,* Journal of Bioactive and Compatible Polymers 2005, **20**, 245.

[268] Alexeev V. L., Das S., Finegold D. N., Asher S. A. *Photonic crystal glucose-sensing material for noninvasive monitoring of glucose in tear fluid,* Clinical Chemistry 2004, **50**, 2353.

[269] Lee M. C., Kabilan S., Hussain A., Yang X. P., Blyth J., Lowe C. R. *Glucose-sensitive holographic sensors for monitoring bacterial growth,* Analytical Chemistry 2004, **76**, 5748.

[270] Kim D. H., Faull K. F., Norris A. J., Eckhert C. D. *Borate-nucleotide complex formation depends on charge and phosphorylation state,* Journal of Mass Spectrometry 2004, **39**, 743.

[271] Kim D. H., Hee S. Q., Norris A. J., Faull K. F., Eckhert C. D. *Boric acid inhibits adenosine diphosphate-ribosyl cyclase non-competitively,* Journal of Chromatography A 2006, **1115**, 246.

[272] Kim D. H., Marbois B. N., Faull K. F., Eckhert C. D. *Esterification of borate with NAD(+) and NADH as studied by electrospray ionization mass spectrometry and B-11 NMR spectroscopy,* Journal of Mass Spectrometry 2003, **38**, 632.

[273] Edwards J. O., Ross V. *Structural principles of the hydrated polyborates,* Journal of Inorganic Nuclear Chemistry 1960, **15**, 329.

[274] Momii R. K., Nachtrieb N. H. *Nuclear magnetic resonance study of borate- polyborate equilibria in aqueous solution,* Inorganic Chemistry 1967, **6**, 1189.

[275] Smith H. D., Wiersema R. J. *Boron-11 nuclear magnetic resonance study of polyborate ions in solution,* Inorganic Chemistry 1972, **11**, 1152.

[276] Thevenon M. F., Pizzi A. *Polyborate ions' influence on the durability of wood treated with non-toxic protein borate preservatives,* Holz Als Roh-Und Werkstoff 2003, **61**, 457.

[277] Anderson J. L., Eyring E. M., Whittaker M. P. *Temperature jump rate studies of polyborate formation in aqueous boric acid,* Journal of Physical Chemistry 1964, **68**, 1128.

[278] Mesmer R. E., Baes C. F., Sweeton F. H. *Acidity measurements at elevated temperatures. VI. Boric acid equilibria,* Inorganic Chemistry 1972, **11**, 537.

[279] Maya L. *Identification of polyborate and fluoroborate ions in solution by Raman spectroscopy,* Inorganic Chemistry 1976, **15**, 2179.

[280] Ingri N., Lagerström G., Frydman M., Sillen L. G. *Equilibrium Studies of Polyanions. II. Polyborates in NaClO4 Medium,* Acta Chemica Scandinavica 1957, **11**, 1034.

[281] Attinà M., Cacace F., Grandinetti F., Occhiucci G., Ricci A. *Positive ion chemistry of gaseous boric and polyboric acids,* International Journal of Mass Spectrometry and Ion Processes 1992, **117**, 47.

[282] Attina M., Cacace F., Occhiucci G., Ricci A. *Gaseous borate and polyborate anions,* Inorganic Chemistry 1992, **31**, 3114.

[283] Attinà M., Cacace F., Ricci A., Grandinetti F., Occhiucci G. *Gas-phase ion chemistry of H3BO3. Protonated orthoboric, metaboric and polyboric acids, and their anions in the gas phase,* Journal of the Chemical Society, Chemical Communications 1991, 66.

[284] Bell C. F., Gallagher B. C., Lott K. A. K., Short E. L., Walton L. *Boric acid complexes of phenolic acids,* Polyhedron 1991, **10**, 613.

[285] Hoffmann E., Stroobant V. *Mass spectrometry, principles and applications 2nd edition,* Wiley: New York 2003.

[286] Tsuyumoto I., Oshio T., Katayama K. *Preparation of highly concentrated aqueous solution of sodium borate,* Inorganic Chemistry Communications 2007, **10**, 20.

[287] Revilla A. L., Havel J., Jandik P. *Peak splitting observed during capillary electrophoresis of alpha- and beta-naphthols in borate buffer,* Journal of Chromatography A 1996, **745**, 225.

[288] Wang G. M., Pan C. Y., Zheng S. T., Yang G. Y. *Poly[ethylenediammonium hydroxydec-mu(2)-oxo-pentaborate,* Acta Crystallographica Section E-Structure Reports Online 2007, **63**, o1101.

[289] Hertkorn N., Benner R., Witt M., Frommberger M., Schmitt-Kopplin P., Kaiser K., Kettrup A., Hedges I. J. *An integrated NMR and FTCIR mass spectroscopic study to characterize a new and major refractory component of (marine) natural organic matter (NOM) at the molecular level, CRAM: Carboxyl-rich alicyclic molecules,* Geochimica Et Cosmochimica Acta 2007, **71**, A399.

[290] Verchere J. F., Hlaibi M. *Stability constants of borate complexes of oligosaccharides,* Tetrahedron 1987, **6**, 1415.

[291] Ricardo A., Carrigan M. A., Olcott A. N., Benner S. A. *Borate minerals stabilize ribose,* Science 2004, **303**, 196.

[292] Whetten R., Sederoff R. *Lignin biosynthesis,* The Plant Cell 1995, **7**, 1001.

Lebenslauf

Angaben zur Person

Nachname(n) / Vorname(n)	Gàspàr Andràs
Adresse(n)	Am Schaeferanger str. 13/138, 85764-Oberschleißheim
Telefon	+49 89 31873775 Mobil: +36203235471
Fax	+498931873313
E-mail	andras.gaspar@helmholtz-muenchen.de
Staatsangehörigkeit	Ungarisch
Geburtsdatum	02.03.1980
Geschlecht	Männlich

Berufserfahrung

Zeitraum	9. April 2007- 20. May 2007
Beruf oder Funktion	DAAD Kurzaufenthalt
Wichtigste Tätigkeiten und Zuständigkeiten	Analysis von natürlichen organischen Substanzen im molekularen Bereich: Zucker- und Aminosäuren-Analysis, und Elementaranalysen (CHON) von Suwannee River „natural organic matter"-Proben
Name und Adresse des Arbeitgebers	Prof. R. Benner, University of South Carolina, Columbia, USA
Tätigkeitsbereich oder Branche	Wissenschaftliche Forschung

Schul- und Hochschulbildung

Zeitraum	Mai 2005 bis August 2008
Angestrebter Titel	Dr. rer. nat.
Forschungsgebiet	Titel der Doktorarbeit: Unravelling the interactions of Boron with natural organic matter (NOM) on a molecular level
Hochschule bzw. Forschunseinrichtung	Wissenschaftszentrum in Weihenstephan für Ernährung, Landnutzung und Umwelt; Fakultät der Technischen Universität in München, Deutschland Institut für Ökologische Chemie im Helmholtz Zentrum München - Deutsches Forschungszentrum für Gesundheit und Umwelt (GmbH), Neuherberg
Forschungsaktivitäten	Molekulare Charakterisation von Bor- und borhaltigen Komponenten mit natürlichen organischen Substanzen (NOM) mit kombinierten Analytischen Methoden: CE; FFE; FT-ICR MS; CE-ESI/MS; NMR;
Zeitraum	März 2004 bis Februar 2005
Angestrebter Titel	Dipl.-Bioingenieur
Forschungsgebiet	Titel der Diplomarbeit: Automation of foaming extraction method, development of an on-site TPH analytical tool (Automatisierung einer Schaum-Extraktionsmethode, Entwicklung einer Feld-Extraktions-Methode für die „Total-Petroleum-Hydrocarbon"-Bestimmung)

Hochschule bzw. Forschunseinrichtung	Budapest University of Technology and Economics; MOL Rt. KTD Mining Laboratories, Division of Research and Production, Budapest, Hungary
Forschungsaktivitäten	Genormte Analyse von „TPH“ (Gesamt-Erdöl-Kohlenwasserrstoff), Entwicklung und Automatisierung einer Feld-Extraktions-Methode
Zeitraum	1999-2005
Angestrebter Titel	Studium für Dipl. Bioingenieur
Hochschule	Budapest University of Technology and Economics: Fakultät für Chemieingenieurwesen und Fakultät für Bioingenieurwesen im Institut für Umweltschutz in der „Budapest Universität für Technologie und Wirtschaft“, Ungarn;
Forschungsaktivitäten	Umweltanalytische Chemie, Biotechnologie, Verfahrens- und Applikation in Bioingenieurswesen,

Veröffentlichungen

A. Gaspar, M. Englmann, A. Fekete, M. Harir and Ph. Schmitt-Kopplin. *Trends in Capillary Electrophoresis-Mass Spectrometry 2005 - 2006. Review* Electrophoresis. 29, 66-79, 2008

A. Gaspar, M. Harir, M. Lucio, Ph. Schmitt-Kopplin. *Preparative Free-flow electrophoretic separation and off-line ESI-FTICR/MS analysis of Suwannee River Fulvic Acid.* Electrophoresis *(submitted)*

A. Gaspar, E. V. Kunenkov, R. Lock, M. Desor, I. Perminova, Ph. Schmitt-Kopplin. *Combined utilization of Ion Mobility- and ultra high resolution-MS to identify multiple charged constituents in natural organic matter.* Rapid Communication in Mass Spectrometry (accepted)

A. Gaspar, M. Harir, M. Lucio, Ph. Schmitt-Kopplin. *Targeted borate complex formation as followed with electrospray Fourier transform ion cyclotron mass spectrometry: monomolecular model system and polyborate formation.* Rapid Communication in Mass Spectrometry 22, 3119-3129, 2008

A. Gaspar, M. Lucio, M. Harir, Ph. Schmitt-Kopplin. *Targeted and non-targeted borate complex formation as followed with electrospray Fourier transform ion cyclotron mass spectrometry: Novel approach for identifying borate complexes with natural organic matter* Analytical Chemistry (under revision)

M. Harir, M. Frommberger, A. Gaspar, D. Martens, A. Kettrup, M. El Azzouzi, Ph. Schmitt-Kopplin. *Characterization of imazamox degradation by-products by using liquid chromatography mass spectrometry and high-resolution Fourier transform ion cyclotron resonance mass spectrometry*. Anal. Bioanal. Chem. 389, 1459-1467 (2007)

M. Harir, A. Gaspar, M. Frommberger, M. Lucio, D. Martens, A. Kettrup, M. El Azzouzi, Ph. Schmitt-Kopplin. *Photolysis pathway of Imazapic in aqueous solution: ultrahigh resolution mass spectrometry analysis of intermediates*. J. Agric. Food. Chem. 55(24), 9936-9943 (2007)

M. Harir, A. Gaspar, M. Frommberger, D. Martens, A. Kettrup, M. El Azzouzi, Ph. Schmitt-Kopplin. *Photocatalytic reactions of imazamox at TiO2, H2O2 and TiO2/H2O2 in water interfaces: Kinetic and photoproducts study*. Appl. Catal. B-Environ. (in press)

Poster und Vorträge

A. Gaspar, E.Kunenkov, R. Lock, M. Desor, I. Perminova, Ph. Schmitt-Kopplin: *Multiple charged constituents in Suwannee river natural organic matter,* 14th IHSS Conference, Sept. 15 - 19, 2008, Moscow (Presentation)

A. Gaspar, E.Kunenkov, R. Lock, M. Desor, I. Perminova, Ph. Schmitt-Kopplin: *Evidences of the existence of multiple charged constituents in Suwannee river dissolved organic matter,* 56th ASMS Conference, June 1 - 5, 2008 in Denver (Poster)

Kovács K., Sajgó Cs., Brukner-Wein A., Kárpáti Z., Gáspár A., Tombácz E., Schmitt-Kopplin Ph.: *Preliminary results on molecular characterization of humic substances from thermal waters as an unexplored biogeosystem*, P32. 9th Conference on Colloid Chemistry (9CCC), October 3-5. 2007. Siofok, Hungary, Book of Abstracts p. 120 (Poster)

A. Gaspar, E. Belyaeva, M. Meuller, I. V. Perminova, F. Frimmel, M. Frommberger, N. Hertkorn, Ph. Schmitt-Kopplin: *Analysis of Suwannee river fulvic acid with ESI-ICR/FTMS after fractionation with free-flow electrophoresis and size exclusion chromatography*, First International Symposium on Ultrahigh Resolution Mass Spectrometry for the Molecular Level Analysis of Complex(BioGeo)Systems, 6-7 November, 2006, Neuherberg, Germany (Poster)

E. V. Kunenkov, A. S. Kononikhin, A. Gaspar, Ph. Schmitt-Kopplin, I. V. Perminova, A. V. Garmash, N. Hertkorn, I. A. Popov, E. N. Nikolaev: C*omparison of FTICR Data on the Suwannee river humic and fulvic acid*, First International Symposium on Ultrahigh Resolution Mass Spectrometry for the Molecular Level Analysis of Complex(BioGeo)Systems, 6-7 November, 2006, Neuherberg, Germany (Poster)

A. Gaspar, J. Junkers, Ph. Schmitt-Kopplin, N. Hertkorn: *ESI ICR FTMS and NMR analysis of Free-Flow Electrophoresis fractions of Suwannee river NOM*, 17th International Mass Spectrometry Conference, 27 Aug.- 1 Sept., 2006, Prague, Czech Republic (Poster)

A. Gaspar, M. Frommberger, J. Junkers, Ph. Schmitt-Kopplin, N. Hertkorn; *Molecular-level analysis of Suwannee river NOM derived from organic structural spectroscopy and fractionation studies*, 3rd Symposium on NMR spectroscopy in soil and geo sciences, 6-9 August, 2006 Freising, Germany, (Poster)